

# For Reference

---

TAKEN FROM THIS ROOM



# For Reference

NOT TO BE TAKEN FROM THIS ROOM

Ex LIBRIS  
UNIVERSITATIS  
ALBERTAENSIS











Digitized by the Internet Archive  
in 2017 with funding from  
University of Alberta Libraries

<https://archive.org/details/lee1958>





Thesis  
1958  
# 36

THE UNIVERSITY OF ALBERTA

FOUNDATION SETTLEMENT PROBLEMS  
AT THE  
ALUMINUM COMPANY OF CANADA SMELTER  
KITIMAT, BRITISH COLUMBIA

A DISSERTATION  
SUBMITTED TO THE FACULTY OF GRADUATE STUDIES  
IN PARTIAL FULFILMENT OF THE REQUIREMENTS FOR THE DEGREE  
OF MASTER OF SCIENCE

DEPARTMENT OF CIVIL ENGINEERING

by

KENNETH L. LEE

EDMONTON, ALBERTA

APRIL, 1958









## SYNOPSIS

The Aluminum Smelter at Kitimat is underlain by compressible sediments to a maximum depth of 350 feet. These sediments consist mainly of three principal strata, gravel, silt and clay. The buildings are founded on a thick, dense fill placed on top of these compressible soils. Settlement due to the fill and building loads have been continuously recorded at numerous points over the area since the first fill was placed in 1952. At the time of writing the magnitude of settlement had exceeded five feet in some areas and was continuing at the rate of one half foot per year. Some structural damage to the long Potroom buildings appeared to be the result of differential settlement and accompanying horizontal movement at the ground surface.

Theoretical time curves which match the observed settlements were obtained by computing a time curve for each of the three principal layers. From these time curves future settlements were predicted. Coefficients of consolidation and compressive indices were computed from the matching theoretical curves. These coefficients differed appreciably from those obtained by conventional laboratory tests, but agreed with values which could be expected in nature.

Measurements indicated horizontal movement of the ground surface toward the zone of maximum settlement. The cause of this movement was shown to be the deflecting beam action of a thick surface layer of relatively incompressible soil modified somewhat by the effect of consolidation in the direction of the major principal stress within a deep compressible stratum.





## ACKNOWLEDGEMENTS

Dean R. M. Hardy, University of Alberta, and Mr. C. F. Ripley, Consulting Engineer, Vancouver, have been retained by the Aluminum Company of Canada Ltd., as foundation consultants on the Kitimat Project since the first beachhead was established in 1951. They have maintained a field engineering staff on the site to supervise drilling and sampling, inspect foundation preparations and take all readings and observations in relation to the settlement problem. Laboratory testing and processing the data has been done in Edmonton and Vancouver.

For one year commencing September, 1956 the Author served on the Consultant's engineering staff at Kitimat. Here he gained much valuable first hand information and experience with this very interesting and unique problem of building on fill which overlies highly compressible material.

The data for this study came entirely from the private files of Dean R. M. Hardy and Mr. C. F. Ripley. This data was in the form of drill hole logs, laboratory test results, letters and reports.

The author wishes to express his gratitude to the following people whose helpful assistance has been greatly appreciated:

Dean R. M. Hardy, for suggesting the thesis topic, for providing much of the original data, and for helpful suggestions throughout the preparation of this report; Mr. C. F. Ripley for providing original data and other personal assistance; Mr. W. E. Jubien of Ripley and





Associates, Vancouver, for his helpful criticism of many of the assumptions and calculations; Mr. S. R. Sinclair, University of Alberta, for many helpful suggestions and criticisms; Mrs. E. Noble, for typing the numerous rough drafts of the manuscript; to Mrs. P. Huffman for typing the final manuscript, and to the author's wife, Mrs. Shirley Lee, for her patience and cooperation throughout the trying times during which this thesis was written.



## TABLE OF CONTENTS

CHAPTER	PAGE
I. INTRODUCTION . . . . .	1
The Problem . . . . .	1
Geology . . . . .	2
Site Development . . . . .	5
Settlement . . . . .	6
The Smelter Buildings . . . . .	8
Settlement During Construction . . . . .	9
Structural Damage Due to Settlement . . . . .	10
II. MATCHING THEORETICAL TIME CURVES TO OBSERVED SETTLEMENTS .	13
Consolidation Theory . . . . .	13
Observed Time Curves . . . . .	18
Pressure-Void Ratio Curves . . . . .	19
Soil Samples . . . . .	21
Load Application at the Smeltersite . . . . .	23
Settlement Observation . . . . .	26
Settlement Gauge Time Curves . . . . .	27
Matching Theoretical Time Curves to Observed Settlement.	27
Identifying Time Curves for each Layer . . . . .	32
Coefficient of Consolidation . . . . .	33
Compressive Index . . . . .	34
Most Probable Curve . . . . .	38
Significant Figures . . . . .	40



CHAPTER	PAGE
Consolidation Factors for the Gravel Stratum . . . . .	41
Initial and Secondary Compression . . . . .	42
Predicted Future Settlements . . . . .	42
Theoretical Time Curves Compared . . . . .	45
Coefficient of Consolidation and Compressive Index . . .	46
Conclusions . . . . .	49
III. CONSOLIDATION AND HORIZONTAL DISPLACEMENT . . . . .	50
Theory . . . . .	50
Stress Computations . . . . .	51
Boussinesq Equations . . . . .	51
Westergaard Solution . . . . .	54
Burmister Solution . . . . .	55
Equations Used . . . . .	55
Calculations . . . . .	57
Discussion of Results . . . . .	61
Conclusions . . . . .	64
IV MODEL STUDY . . . . .	67
Introduction . . . . .	67
Description of Model . . . . .	67
Operation of the Model . . . . .	69
Observations . . . . .	69
Conclusions . . . . .	70



CHAPTER	PAGE
V. GEOMETRY OF SUBSIDENCE . . . . .	71
Description of Measurements . . . . .	71
Interpretation of Measurements . . . . .	75
Surface Geometry . . . . .	77
Similar Problems From Other Sources . . . . .	77
Description of the Subsidence Curve . . . . .	80
Horizontal Displacement Caused by Soil Consolidation . .	83
Basic Assumptions . . . . .	83
Mechanism of Movements . . . . .	84
Application to the Kitimat Problem . . . . .	85
Discussion of Results . . . . .	87
Gravel as a Beam . . . . .	89
Comparison to Movement From Stress Computations . . . .	90
General Summary . . . . .	93
Conclusions . . . . .	95
Future Movement . . . . .	96
Damage to Superstructure . . . . .	96
BIBLIOGRAPHY . . . . .	97
APPENDIX A - Time Factor Values . . . . .	100
APPENDIX B - Notation . . . . .	101
APPENDIX C - Tables	
APPENDIX D - Figures	





## LIST OF TABLES

### TABLE

- I. Computation of  $c_v$  Coefficient of Consolidation
- II. Computation of Initial Stress  $P_0$
- III. Series A, Computation of  $C_c$  Compressive Index
- IV. Series B, Computation of  $C_c$  Compressive Index
- V. Gravel, Computation of  $C_c$  Compressive Index
- VI. Summary of Theoretical Time Curves
- VII. Summary of Consolidation Factors
- VIII. Results of Stress Computation and Horizontal Movement
- IX. Measured and Computed Horizontal Distances
- X. Column Line G - Horizontal Displacement
- XI. Column Line H - Horizontal Displacement



## LIST OF FIGURES

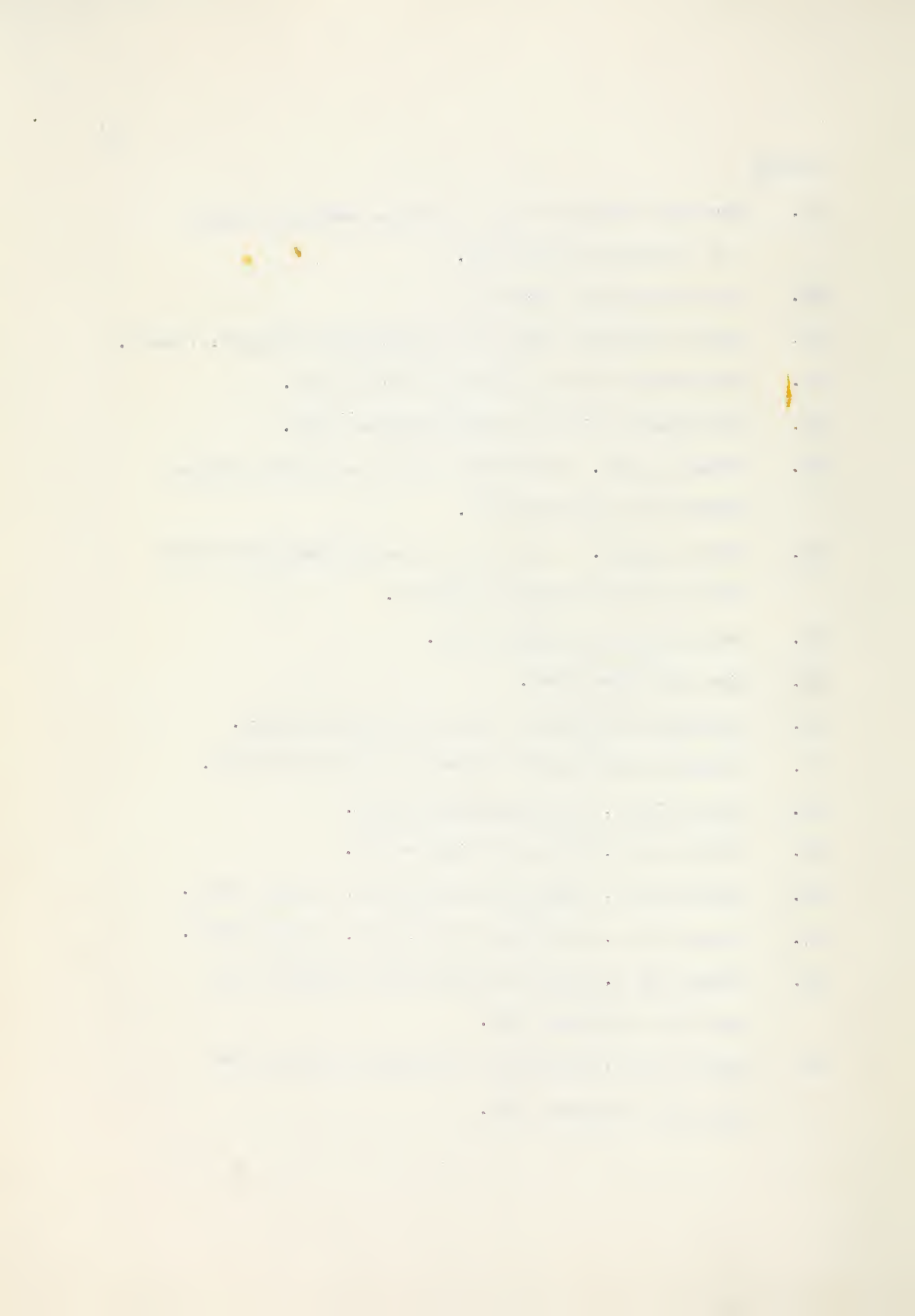
### FIGURE

1. Map of the Kitimat Municipality.
2. Potlines 1 to 5, Subsoil Profiles and Net Applied Load.
3. Potlines 3 to 5, General Building Arrangement. Potlines 1 and 2. Location of Settlement Observation Points.
4. Potlines 1 and 2, Contours of Total Foundation Settlement to June 28, 1957.
5. Typical Potroom, Longitudinal Section.
6. Typical Potroom, Sectional View.
7. Potlines 1 and 2, Contours of Total Equal Settlement From Start of Construction to June 28, 1957.
- 8, 9. Ground Water Elevations at Settlement Gauges.
10. Legend for Plates 11 to 40. Theoretical Time Curve Fitting for Settlement Gauges 1 to 15.
- 11 to 25. Settlement Gauges 1 to 15, Most Probable Fit.
- 26 to 40. Settlement Gauges 1 to 15, Alternate Fit.
- 41 to 48. Settlement Gauges 1 to 15, Time Curves Compared.
49. Coefficient of Consolidation versus Applied Load From Laboratory Consolidation Tests.
50. Pressure-Void Ratio Curves from Silt Soil Samples.
51. Pressure-Void Ratio Curves from Clay Soil Samples.
52. Initial Void Ratio versus Depth from Consolidation Tests.



## FIGURE

53. Increased Vertical Stress  $\Delta p$ , Below Settlement Gauges 1 to 15 Caused by Fill Load.
54. Three Dimensional Stresses
55. Stress Components Below Fill at Settlement Gauges 6, 7 and 8.
56. Theoretical Horizontal Movement versus Depth.
57. Theoretical Horizontal Movement versus Depth.
58. Vector Diagram. Horizontal Movement as Percent Vertical Movement for Depth 150 Feet.
59. Vector Diagram. Theoretical Horizontal Movement at Depth 150 Feet Since Buildings Completed.
60. Model Study with Elastic Bands.
61. Mine Subsidence Curve.
62. Horizontal Displacement Caused by Mine Subsidence.
63. Horizontal Displacement Caused by Soil Consolidation.
64. Column Line G, Horizontal Displacement.
65. Column Line H, Horizontal Displacement.
66. Column Line G, Horizontal Displacement, Average Values.
67. Column Line H, Horizontal Displacement, Average Values.
68. Column Line G, Horizontal and Vertical Movement From May 1953 to December 1957.
69. Column Line H, Horizontal and Vertical Movement From May 1953 to December 1957.





THE KITIMAT SMELTER, 1954

Potlines 1 and 2, looking Northwest.





## CHAPTER I

### INTRODUCTION

#### The Problem

The smeltersite at Kitimat is underlain by sedimentary deposits of a complex nature including sand, gravel, silt and marine clay. These sediments are normally loaded and vary in thickness to a maximum of 350 feet. Fill, varying in depth to a maximum of 30 feet, was placed over an area of approximately 1800 feet by 1200 feet to bring the working site to a suitable elevation. This original area has since been considerably enlarged. Settlement due to the fill load on the underlying compressible soil has been continuously recorded at numerous points since the first fill was placed in 1952.

On June 28, 1957, the last date for which complete records are available, the total maximum settlement had amounted to  $5\frac{1}{2}$  feet. Of this, 3 feet had taken place after the buildings were constructed. The rate of settlement was proceeding at approximately one half foot per year with no indication of any change in the immediate future. Two phases of the settlement problem are considered, estimation of rate and magnitude of future settlements from past records and the effect of settlement on the buildings.

The plot of observed settlement versus time does not completely resemble the theoretical time curve for a one-layered consolidating system, and previous attempts to explain the observed settlement on this basis have not been entirely successful. This study attempts



to explain the shape of the observed settlement-time curve by considering the effect of each of the three major soil types contributing to the settlement. Using the assumptions which agree with the past records, the future settlements are predicted.

Until very recently structural damage due to settlement was not a serious problem despite the fact that the magnitude of vertical movement had not been uniform from point to point over the area. During the summer of 1957 however, many building columns had developed a distinct tilt. Some were out of plumb by as much as  $1\frac{1}{2}$  inches in 10 feet of height while others remained vertical. This was accompanied in some cases by cracking of the concrete pedestals which supported the steel columns. A portion of this study is an inquiry into the role settlement has played in the movement of these columns.

### Geology

The geology and early history of Kitimat has been adequately described in a recent paper by R. M. Hardy and Charles F. Ripley (9).<sup>\*</sup> The geological conditions are typical of the coastline of British Columbia at the head of the many inlets or fjord channels. The smeltersite is located at the head of the Kitimat arm of Douglas Channel. At this place the valley is approximately 2 miles wide. The mountain slopes rise steeply from the valley sides. It is thought that this valley was filled with sediments during the glacial and interglacial periods of the Pleistocene age. The Kitimat River is

---

\* Numbers refer to bibliography at the end of the text.



entrenched in these sediments and flows southward emptying into Douglas Channel at Kitimat. A high ridge approximately 3 miles upstream from the smelter seems to mark the terminus of one glacial period. Northward from this ridge the land is from 300 to 500 feet above present sea level. Southward from the ridge the land slopes gently from approximate elevation 50 to the sea. The colored map, Figure 1\*, is a plan of the Kitimat Municipality, and shows the location of the smeltersite with respect to the main topographic features.

Beneath the portion of the smeltersite considered in this report the thickness of sediments above bedrock varies to a known maximum of 350 feet. The geology of the sediments is complex because they include alluvial fan deposits of sand and gravel laid down by the Kitimat River running south, and Moore and Anderson Creeks which are two streams running from mountains eastward across the smeltersite. Deltaic sand, silt, and marine clays are all interlaid in an irregular manner. In the upper 20 feet numerous buried logs, stumps, peat and organic silt layers have been found indicating considerable forest growth as sediment from the River and Creeks was being deposited. Most of the logs were remarkably well preserved. Before construction commenced in 1951, the entire area was covered with a dense forest growth. An upper layer of from about 3 to 15 feet thick was composed chiefly of peat and organic silt.

---

\* Figures and tables are grouped together following the written text.





From a grid of widely spaced deep drill holes an average generalized soil profile was obtained. This is shown in Figure 2. The subsoil is generally composed of three principal layers of varying thickness. The upper layer is chiefly sand and gravel with silt and organic matter irregularly distributed throughout. The middle layer is chiefly nonplastic silt but again contains stratifications of fine sand and organic matter throughout. The lower layer is lean clay stratified with silt. The water table was very near the ground surface.

Conventional laboratory tests indicated the following properties for the silt and clay layers.\*

Silt - Specific Gravity 2.72

Natural moisture content 33 percent

Generally non plastic

Slope of e-log P curve at the anticipated  
applied load 0.14

Clay - Specific Gravity 2.72

Natural moisture content 33 percent generally  
close to or above the liquid limit

Liquid limit 28

Plastic limit 18

Plasticity index 10

Slope of e-log P curve at the anticipated  
applied load 0.25

---

\* Descriptions of conventional laboratory soil mechanics tests can be found in Reference 15.





### Site Development

To raise the working surface above the high water tides and to be safe from flooding by mountain freshets from Moore and Anderson Creeks, a fill of up to 30 feet in depth was required over the entire smeltersite. Prior to placing the fill, the upper layer of the organic overburden was removed from the site. The depth of stripping varied from approximately 3 to 15 feet. Fill was placed on the site immediately following the stripping operation. This material which consisted of a clean sandy gravel, was placed in thin lifts and compacted with a cat-drawn 50-ton pneumatic tired roller. This gave an excellent foundation material which was free draining and dense.

The initial area filled, and the one of concern in this report, was located immediately north of high tide mark and adjacent to the west side of the valley. The filling operation commenced in June 1952, and was completed to elevation 45.5 above sea level between September and November, 1952. Figure 2 shows the net applied load on this area. It was here that the first buildings, Potlines 1 and 2, were constructed during 1953.

South of this area fill was placed on the tidal flats to provide a storage area for the raw materials unloaded from the ships. This fill consisted of sandy gravel obtained from dredging a shipping channel in the harbour and was completed to elevation 28.5. This fill was placed between May and November 1952.



North of Potlines 1 and 2, other areas of similar size have been stripped and filled in a similar manner. The fill at the site of Potlines 3 to 5 was placed between November 1953 and October 1954. North of Moore Creek the site is prepared for three additional potlines which when completed will extend a total distance of about one half a mile north from Potline 1.

### Settlement

To determine the settlement pattern caused by the fill load, 15 settlement gauges were placed in the fill area and read periodically. Each gauge consisted of a 3 by 3 foot square timber base to which a standard 2 inch diameter pipe was attached. The timber base was set at the base of stripping prior to the placement of any fill, and the 2 inch pipe was carried through the fill to the surface. The settlement was measured by running a line of levels to the gauge from a permanent bench mark on bedrock adjacent to the site. The level was a precise tilting level and the rod was read to the nearest 0.005 feet. Short circuits and frequent checks on turning points resulted in very exact work considering the number of settlement gauges, the distances, and the frequency they were read. It is felt that the settlement readings are accurate to within 0.01 feet.

The bottom one foot of settlement gauge pipe was perforated, and care was taken to insure the pipe did not plug. Since the completion of the fill these gauges have also been used to record the water table.



This is done by lowering a bomb carrying two bare wire ends into the gauge pipe. A small battery feeds current into the wires at the surface while an ohmmeter records the instant the bare ends make contact with the water in the pipe.

After the buildings were constructed, settlement observations were made at approximately 200 points on the buildings. The observation points are specially prepared brass plugs set in the concrete columns and are placed around every building at approximately 100 foot spacing. Readings are made periodically using the same method and with the same care and precision as for reading the gauges. Figure 3 shows a plan of the buildings and the location of all settlement observation points in this area.

The magnitude of settlement has varied considerably over the smelter area as shown by Figure 4 which is a plan of contours of equal total settlement to June, 1957. Plots of settlement versus time for any particular settlement gauge show important differences from the general shape of a theoretical time curve. This is especially true for the early stages of settlement. The observed curve plotted to both arithmetic and logarithmic time scale shows no indication of any immediate reduction in the rate of settlement. A previous attempt to predict the amount of total settlement was done by fitting a theoretical time curve to the observed points assuming the initial irregularities were similar to the initial settlement from a conventional laboratory consolidation test.





To attempt to gain a better understanding of the nature of consolidation within the compressible soil below the smeltersite, theoretical time curves for each of the three principal layers were fitted in such a way that the sum of the settlement from each individual curve was equal to the total observed settlement.

### The Smelter Buildings

A complete unit of the smeltersite buildings at Kitimat is shown in Figure 3. The first to be constructed were Potlines 1 and 2, and the auxiliary buildings in the central courtyard. These buildings covered the initial fill area. Construction commenced in the fall of 1952 and was completed by August 1954 when the first part of the smelter went into production. Fill for Potlines 3 to 5 was placed in 1953 and the buildings were not fully completed until the fall of 1956. The only serious structural damage which had developed thus far, which could be attributed to settlement occurred in Potlines 1 and 2. These buildings were the subject of this study.

Typical longitudinal and cross sections of a potroom are shown in Figures 5 and 6. Each Potroom building of Potlines 1 and 2 are essentially structurally similar. They are long relatively flexible buildings of steel frame construction. A 9 foot concrete column rises from a spread footing founded in the gravel fill and supports the steel superstructure. The only moving equipment within the potrooms is a 20 ton electric crane which spans the width of the building and runs





the entire length on a steel beam 22 feet above the working floor, this floor is approximately at the ground surface. Rigid electrical connections, the operation of the crane, and the operation of each individual pot makes differential settlement undesirable, but these limitations have not as yet proved to be as serious a factor as actual damage to the superstructure.

#### Settlement During Construction

The first footings were poured almost immediately following completion of the fill, and were set at their design elevation. It was soon realized however that the magnitude of settlement would exceed the original estimate, and would require longer to complete than originally planned. Accordingly all footings not already in place were set at an elevation so adjusted that all footings would settle to a level position by January 1, 1955. It was estimated that settlement occurring after this date would not cause intolerable differential movement.

Between pouring of the concrete footings and erecting the steel a revised estimate indicated still more expected settlement. To account for this, and to still provide for all steel columns to be level by January 1, 1955, the concrete columns were extended. This double field adjustment resulted in deviation from design length and elevations by up to one foot for some columns. No changes were made in the horizontal directions. A complete record was kept of all deviations from design procedure. Unfortunately the records only



contain recommended changes. Only a few accurate independent checks were made in the field to determine the exact setting of each column, from these checks it is assumed that they were set precisely as recommended. Other work in the field has shown that departures from the recommended settings, if any, were small.

#### Structural Damage Due to Settlement

Following construction of the buildings, settlement continued at almost a uniform rate until the summer of 1957.\* Figure 7 shows contours of total settlement since construction. Settlement previous to this time would have no bearing on any structural damage. Until 1957 only minor signs of damage were evident. A few cracks appeared in the concrete block walls, and a few diagonal braces were slightly buckled. This in no way contributed to structural damage or unsightliness.

By the summer of 1957 however a serious problem had arisen. Many potroom columns, especially on the west end had developed a distinctly noticeable lean. The column tops were out of plumb to the west by as much as  $1\frac{1}{2}$  inches. On the east end some columns leaned eastward but to a lesser extent. This was accompanied by cracking of the concrete columns. These cracks appeared more severe at columns joined

---

\* June 28, 1957, the last date for which a complete set of readings was available at the time of writing. Later readings, where available, were included in this report.



by diagonal bracing, but were evident at other columns as well. Many of the diagonal bracing members had buckled relieving the excess stress, but the opposite member being in tension and having no way to relieve the stress had in some cases appeared to have caused the bottom of the steel column to shift and crack its concrete support.

Examination of the expansion joints on the crane rail beam showed that all except a very few on the east end appeared closed which indicated the crane rail beam was in compression.

Some of the more severe damage was repaired immediately. This was accomplished by replacing the diagonal bracing, jacking the steel column, and chipping out and replacing the damaged concrete. The new diagonal braces were fabricated with bolts and slotted holes so that stress could be periodically relieved. Less severe damage was left untouched pending the results of an investigation to determine the primary cause of damage and the best way of coping with the problem.

The structural damage appeared to be the result of horizontal movements caused either by movement of the ground surface, or movement of the superstructure due to some external force. It was suggested that perhaps the rapid acceleration and stopping of the electric crane developed sufficient horizontal thrust to shift the network of steel columns. Other factors indicated that the source of movement was within the soil which supported the footings.





Three methods of approach were used to attempt to ascertain and explain any horizontal movements within the soil. These were, theoretical computation of horizontal movement due to consolidation, model analysis, and comparison to the problem of mining subsidence.





## CHAPTER II

### MATCHING THEORETICAL TIME CURVES TO OBSERVED SETTLEMENTS

#### Consolidation Theory

The term consolidation, as used in soil mechanics explains the settlement which occurs within a mass of soil subject to a static load. It is not to be confused with mechanical compaction of soil under dynamic loads, or to solidification, sometimes called consolidation by geologists. The first rigorous mathematical solution to this problem was published by Terzaghi in 1923 and is found summarized in most text books on Soil Mechanics.\* Stated briefly, the Terzaghi theory of Consolidation explains the settlement which occurs due to an applied load on a layer of soil as being a result of the soil grains squeezing closer together. This reduces the void spaces, and hence the volume of the soil, resulting in settlement at the surface.

The Terzaghi theory assumes a saturated claylike soil. At the instant the load is applied it is entirely carried by the water within the voids and the pressure of this water immediately exceeds hydrostatic pressure by the amount of the applied load. Under this hydrostatic excess the water is gradually driven from the void spaces,

---

\* See for example Reference 24.



the soil grains move closer together to take up the volume once occupied by the water, the load is gradually transferred from the water to the soil, the hydrostatic excess pressure becomes zero, and the load carried by the soil grains increases by an amount equal to the load applied. Thus equilibrium is reached under this new loading condition, and the process of consolidation is complete. Any additional load change would cause the process to be repeated.

At any intermediate time the degree of consolidation can be expressed as a ratio of the reduction in hydrostatic excess pressure to the initial excess. Since reduction in hydrostatic excess pressure is accompanied by volume reduction in the soil, the degree of consolidation can also be expressed as the ratio of settlement at any time to the total settlement which will occur under the particular loading conditions. Because settlements are generally easier to observe than pore water pressure the latter is the more common way of expressing degree of consolidation. The mathematical solution to the problem expresses the degree of consolidation  $U$ , as a function of dimensionless number  $T$ , called a time factor. This time factor depends on the drainage conditions of the soil, and plots of time factor versus degree of consolidation are available for several drainage conditions. (24 and 27)

The plot of time factor versus the average degree of consolidation within a layer of soil is called a theoretical time curve. A normal curve begins at the origin and ends as an asymptote to the 100% consolidation line. It has been found that when the time factor scale



is changed from arithmetic to a log or square root scale a large portion of the curve is a straight line. It also has the advantage of showing the entire curve without an extremely long time factor scale. The use of a semi log plot is preferred in Western Canada, and is the form adopted for this study.

The actual time  $t$ , required for a consolidating stratum of soil to reach any particular degree of consolidation is determined by the equation:

$$T = \frac{c_v t}{H^2} \quad (1)$$

where  $H$  is the length of the path a particle of water must travel to the nearest drainage face from the farthest point from this face. If the stratum is drained on one side  $H$  is the thickness of the stratum. If drained on both sides  $H$  is one half the thickness. The term  $c_v$  and  $H$  are essentially constant over a loading increment of usual magnitude.

If  $c_v$  and  $H$  are known, the time for the soil to reach any degree of consolidation under an applied load can be computed by equation 1. On many jobs these values are not accurately known. If records of the settlement at any time are available they can be plotted, and by successive approximations using the above formula a theoretical curve can

---

\* Subscripts are used to denote a particular degree of consolidation. Thus  $t_{90}$  and  $T_{90}$  refer to the time at which 90% of the consolidation has been completed.





be obtained which will match the plot of observed values. This process is called time curve fitting or matching. Both  $c_v$  and  $H$  are assumed to be constant. Also by this method a theoretical curve can be fitted to the observed values before the process of consolidation is fully complete. When a theoretical curve is found which fits the observed settlement it can then be extended over the full cycle of consolidation. Future settlement can then be predicted on the basis that it follows the fitted theoretical curve.

The first problem in fitting time curves is to choose time factors for the various degrees of consolidation. Taylor (24) and others have published time factor values for different drainage conditions and initial excess hydrostatic pressures. When these values are plotted together it is observed that all curves are similar. The choice of which set of time factors to use is difficult because the type of drainage and initial excess hydrostatic pressure are usually not accurately known. Taylor gives one particular theoretical time curve which he states is generally accepted as an adequate representation of typical cases in nature. It is for one dimensional drainage and uniform initial excess hydrostatic pressure. Whether or not a case satisfies all the assumptions in the derivation of this specific theoretical curve, especially that of one dimensional drainage, is open to question. Unless there is strong evidence to support the use of a particular theoretical time curve then, the preferred one given by Taylor should be used.\*

---

\* Time factor values for this case are given in the Appendix.





The Terzaghi theory of consolidation assumes the load to be applied instantaneously, and time factors are computed on this basis. In practise this simplification is seldom realized. The load is usually applied over a considerable length of time called the loading period. A method of correcting theoretical time curves for this loading period has been advanced by Terzaghi (25). This method assumes that the settlement, or degree of consolidation at the end of the period of uniformly increasing load would be the same as if the total load were applied suddenly after one half the loading period had elapsed.

It follows that if  $P$  is the total applied load,  $P_1$  the total load applied at some intermediate time within the loading period and  $U_1$  the degree of consolidation at time  $t/2$  after the sudden application of  $P_1$ , then the total degree of consolidation at time  $t$  is equal to

$$U = U_1 \frac{P_1}{P} \quad (2)$$

where  $t$  is the time measured from the start of the loading period, and  $U$  is the amount of final settlement due to consolidation of the soil under the load  $P_1$ . At any time following completion of the loading period the theoretical settlement can be computed from the basic equations assuming the total load was applied instantaneously at one half the loading period.



### Observed Time Curves

A test frequently run on soils for which the consolidation characteristics are desired is called the Consolidation Test.\* This test is designed to duplicate the basic assumptions of the Terzaghi theory of consolidation. In the laboratory a small sample of soil is placed in a suitable mold where it is free to drain from only the upper and lower surfaces. A load is applied to the drainage faces and the deformation or settlement of the surface of the soil is measured at regular time intervals.

Time curves from a laboratory test resemble the theoretical time curve in all respects except at the very beginning, and at the end. Settlement at the beginning of the test proceeds at a much faster rate than expected from a theoretical time curve. In fact it appears that some settlement occurs almost instantly. This initial compression is not explained by the Terzaghi theory. The usual explanation for the occurrence of initial settlement is that it is partly due to the compression of any air entrapped in the soil. (24) After the load has remained on the soil for a considerable length of time the laboratory settlement curve does not become asymptotic at any particular amount of compression, but continues at a slow rate even though the excess

---

\* See Reference 15 for a complete description of this and other laboratory soil mechanics tests.



hydrostatic pressure appears to be zero. This phenomenon is also not explained by Terzaghi's theory of consolidation, and is called secondary compression. It is probably due to plastic flow or gradual adjustment of the soil structure under the new load (24 and 26). For most inorganic soils both initial and secondary compression are usually small compared to the primary compression which is explained by the Terzaghi theory. No proven theory exists to explain the magnitude or rate of settlement to be expected from initial or secondary compression. The question of whether they exist in the field to the same degree as in the laboratory test has not yet been satisfactorily answered. Graphical constructions are outlined by Taylor (24) to determine the theoretical zero and 100 percent consolidation from a laboratory time curve.

#### Pressure - Void ratio Curves

The maximum consolidation pressure to which a soil has ever been subjected in nature is called its preconsolidation load. When this load equals the present overburden pressure the soil is said to be normally consolidated. When the present pressure on the soil is less than it has been in previous geological time the soil is said to be precompressed or preconsolidated.

When a consolidation test is performed on a sample of soil it is usually loaded in small increments and allowed to completely consolidate under each increment of load before the next load is applied.





The void ratio at each stage of the test can be calculated from the observed compression of the sample. These void ratios are then plotted against the log of applied pressure and the resulting curve is called an e-log P curve, or a pressure void ratio curve. For pressures in excess of the preconsolidation pressure the e-log P curve is usually a straight line. This portion of the curve is called the virgin branch. The virgin branch of the consolidation curve for some extra sensitive soils is slightly concave.

The slope of the virgin branch of the e-log P curve is called the compressive index ( $C_c$ ) of the soil. Below the preconsolidation load, or where the e-log P curve is not a straight line settlement is computed on the basis of the average slope of the curve between the pressures of interest.

Knowing the compressive index, initial void ratio ( $e_0$ ) and pressure ( $p_0$ ) of a soil, the void ratio ( $e$ ) after any pressure change ( $P$ ), can be computed from the expression

$$e = e_0 - C_c \log_{10} \frac{P_0 + P}{P_0} \quad (3)$$

The total settlement ( $S$ ) of a stratum of thickness ( $H$ ) can be computed from

$$S = \frac{e - e_0}{1 - e_0} H^* \quad (4)$$

---

\* The derivation of these equations can be found in any text book on soil mechanics, for example see Reference 27.





combining these two equations it follows that

$$C_c = \frac{S (1 + e_0)}{H \log_{10} \frac{P_0 + \Delta P}{P_0}} \quad (5)$$

### Soil Samples

In a paper entitled Undisturbed Clay Samples and Undisturbed Clays (26) Terzaghi compares laboratory consolidation tests to the actual field behaviour of a normally loaded clay soil. In the field, the clay has been deposited by sedimentation at an estimated rate of 0.04 grams per square centimeter per day. This rate of load increase on the previously deposited soil is so slow that certain bond stresses can build up between the soil grains. These bond stresses tend to maintain the soil in a state similar to that at which it was deposited. The gradually increasing pressure from overlying soil, is not fast or great enough to destroy these bond stresses or cause the amount of compression expected from laboratory tests. This explains why the void ratio or moisture content in such a deposit does not usually show any marked decrease with increasing depth.

When a sample of soil is removed from the ground, the total stress on it is decreased to atmospheric pressure. Capillary forces however tend to resist any volume change. When tested in a consolidation machine the load is reapplied at a rate of up to several tons per square centimeter per day. This greatly exceeds the rate of loading from material deposition, and is rapid enough to destroy the bond stress



between the individual soil grains. With these bond stresses destroyed the soil sample will compress to a smaller volume than that at which it existed in the field under the same consolidation pressure. This explains why the void ratio at a pressure equal to the preconsolidation load determined from the pressure void ratio curve is smaller than the void ratio at the beginning of the test. Theoretically capillary forces should hold the soil from expanding when removed from the ground, and if no destruction of the internal structure of the soil occurred on reloading there should be no change in void ratio for loads less than the preconsolidation load. Terzaghi, as just stated, attributes this change in void ratio to destruction of the internal structure by rapid loading. Any rough handling, or change of orientation of the soil grains when sampling would tend to further aggravate the situation.

The rate of loading in the field from man made sources will approach the rate of loading of conventional laboratory tests. It is highly probable that this rate of field loading is sufficient to at least partially destroy the internal bond stress of clay-like soil. For this reason compressive index values from laboratory tests may not be indicative of the field compressive index under similar loading conditions. A method of determining the field compressive index for a normally loaded clay soil is suggested by Terzaghi and Peck (27).



It has been found from the results of consolidation tests on soils from the same geological area that all of the virgin compression branches, if extended, intersect at approximately the zero void ratio axis. Terzaghi and Peck suggest that the field compression curve if extrapolated, would also intersect these laboratory curves at a void ratio of zero. This then is one point on the field virgin compression branch. The existing void ratio and overburden pressure can be computed from a few relatively undisturbed samples and this defines another point on the field compression curve. Assuming the field virgin branch to be a straight line, or if an extra sensitive soil, slightly concave, the field virgin compression curve can be drawn and the field compressive index determined.

#### Load Application at the Smeltersite

To prepare the site of Potlines 1 and 2, approximately 3 to 15 feet of organic soil was stripped from the surface. Stripping was followed almost immediately by placing of the fill. This fill consisted of clean sand and gravel and varied in final thickness to a maximum of 30 feet. Shortly after completion of the fill to its nominal elevation of 45.5 feet, construction of the buildings commenced. A few footings were poured late in 1952, but the major construction occurred in 1953. Following completion of the buildings additional fill was added for the purpose of site grading and landscaping. Figure 2 shows a plan of net applied load. This load consists of the





weight of the fill plus buildings minus the weight of the soil stripped from the site. The weight of the buildings alone amounted to only about 500 pounds per square foot.

From the records which were kept at the time the following is known regarding the time and rate of application of these loads.

1. The date each settlement gauge was installed which was the approximate date of placing the first fill in the vicinity of the gauge.
2. The date the fill was completed in the vicinity of each settlement gauge.
3. The date the site grading load was applied.
4. The amount of the site grading load expressed as a percent of the previously applied load.

These dates and magnitudes are shown on the loading diagram of Figures 10 to 25.

Each settlement gauge was installed prior to placing any fill at the particular site and it can be reasonably assumed that the total settlement has been recorded by each gauge. The actual rate of load application could possibly be determined from daily progress reports. These reports were not readily available, and furthermore the loading period was so short compared to the total settlement period that it was felt precise determination of the loading curve was not warranted. Examination of the time versus settlement plots showed very little settlement for quite some time following installation of the gauge.





This was followed by a period of very rapid settlement which reduced rapidly after the fill was completed. The time settlement curve for each gauge was examined and the approximate date at which the rapid settlement commenced was taken as the start of the loading period. This date is shown on the theoretical time curves, Figures 10 to 25. The load was assumed to increase at a uniform rate from this date until the fill operation in the vicinity of the gauge was completed.

No further load was assumed to be added from completion of the fill until the completion of the site grading load. It is known however, that during this time the buildings were constructed, but their weight was small in comparison to the weight of the fill. It probably took between 30 to 60 days for the building load to be added. The site grading load was assumed to be instantly applied. In reality it probably took less than one week.

As with any large construction operation the practise is seldom to concentrate on one specific area and complete it before starting on the next. Most likely there were periods of comparative inactivity within each assumed loading period, these would probably be followed by periods of very intensive loadings. On this assumption, and based on the results of theoretical time curve fitting yet to be described, a probable loading diagram at each gauge was shown superimposed over the loading diagram just described. This probable loading diagram was not essentially different from the first assumed loading, and was not used to change or modify any of the computations or results.



Another load which should be mentioned is increase in effective stress resulting from a lowering of the ground water table. Figures 8 and 9 show the variation of the ground water table at each settlement gauge since 1952. Some gauges had become plugged and only early readings were available. Readings between 1955 and early 1957 were not available at the time of writing. The water table at each gauge has lowered considerably since the fill was completed. Most of this lowering however, appears to have taken place within the first two years. The amount of lowering since 1954 appears to have been generally less than 5 feet, and may be within the range of seasonal variation. In such a case the effect on settlement may not be as large as if the lowering were permanent.

#### Settlement Observation

Total settlement since the first fill was placed has been continuously recorded by means of 15 settlement gauges spread over the area. One piezometer was installed adjacent to the area for the purpose of observing pore water pressures within the consolidating soil. This installation has never worked properly and no use was made of any of the readings. The 15 settlement gauges record settlement at the base of the fill. Settlement observations taken simultaneously on buildings adjacent to these gauges have shown there is no measurable settlement within the fill itself.



### Settlement Gauge Time Curves

To facilitate the computation of matching theoretical time curves the observed settlement was plotted to a log time scale. The settlement at each gauge was plotted on a separate page and is shown on Figures 10 to 25, Figure 10 being a legend for these settlement time curves.

### Matching Theoretical Time Curves to Observed Settlement

It has been shown that the theoretical time curve for a single layer of soil can be expressed by the equation

$$T = \frac{c_v t}{H^2} \quad (1)$$

Assuming  $c_v$  and  $H$  to be constant over the loading range it is a simple matter to compute any theoretical time curve. By trial and error a theoretical curve may be found which will match settlement observations providing the consolidation is proceeding according to the Terzaghi theory.

The sub soil profile beneath the Kitimat smelter differs considerably from the ideal assumptions of the basic consolidation theory. The most important difference is that instead of a one layer consolidating system there are three principal layers, each having different consolidation properties. Besides the three principal layers there are countless stratifications and differences in soil properties within each stratum.





Since it was impossible to account for the differences within each stratum the assumption was made that each layer was in itself homogenous, isotropic, and in all respects agreed with Terzaghi's basic assumptions for this theory of consolidation. This of course introduces an unknown error, but it is the only known way of dealing with consolidation problems, and is the method nearly always used when predicting settlements from consolidation tests.

To extend the Terzaghi theory for a one layered system to the three consolidating layers at Kitimat a theoretical time curve was computed for each layer: The first problem was to choose a proper set of time factors. It was decided to use the theoretical time curve published by Taylor (24) for linear variation of initial excess hydrostatic stress. The basis for this choice was that all theoretical curves are quite similar and as Taylor states, "the approximate nature of the assumptions in the Terzaghi theory generally lead to the accepted conclusion that this curve is an adequate representation of typical cases in nature." Time factor values for this condition are found in the appendix.

Having chosen the theoretical time curve it was a straight forward matter to compute a specific theoretical curve and compare it to the observed plot. This was done by means of equation 1.



To begin, a certain degree of consolidation was assumed to correspond to a particular time and settlement. This assumption fixed the entire time curve which was then easily computed. Equation 2 was used to correct the computed theoretical curve for the settlement during the loading period. The time for the entire curve however, was reckoned from the beginning rather than the middle of the loading period. The reasons for this were threefold. First, the beginning of the assumed loading period was generally quite some time after the gauge was installed and no doubt some fill had been placed prior to the beginning of the assumed loading period. The second reason was that the loading period was always less than 60 and generally less than 30 days. One half of this time would not make any appreciable difference in the log time plot after the completion of the loading period. These two reasons coupled with the fact that the load was assumed to be applied linearly when in reality it may have been applied at some other rate lead to the conclusion that it mattered little whether the curve was computed on the basis of load suddenly applied at the beginning, or middle of the loading period.

The site grading load was accounted for by assuming that the settlement of a theoretical time curve for any increment of load would be proportional at any time to the settlement caused by any other increment of applied load. Knowing this increase in load compared to the initial load, and the time this increase was applied, the theoretical settlement at any later time due to this increased load



was computed and added to the settlement curve for the initial load. Since the computed times for the site grading load did not generally coincide with the computed times for the initial curve, the addition of settlement was done by plotting the theoretical curve for one load, and then graphically adding the increased settlement due to the site grading load at the proper elapsed time.

By this method a theoretical time settlement curve for each of the three principal layers was computed. The theoretical total settlement of the entire system at any time was the sum of the settlements of each individual layer. Again it was found convenient to plot the three time curves together, and add the settlements at each time graphically. The resulting curve joining points of total settlement for different times was the theoretical time curve for the entire system. If the assumption for the individual curves was correct then this curve matched the observed settlement time plot. If the curves did not agree then new assumptions were made for each individual layer and the process was repeated. Finally by trial and error a best fit theoretical curve was obtained.

The number of possible combinations is countless. It can be appreciated that this process was tedious and time consuming. However with practice it was found that a good fit could usually be obtained with comparative





ease. It required approximately three quarters of an hour to make one complete trial and seldom was a good fit obtained in less than ten trials.

The best fit theoretical time curve so obtained was not necessarily a unique solution. Other assumptions for individual layers, when combined could also give a time curve which agreed equally well with the observed plot. For this reason two different matching theoretical time curves were found for the observed settlement plot at each gauge. To identify the two fitted curves they were called Series A and Series B. Series A was the fit first obtained and Series B was the second. The results are shown on Figures 10 to 40 inclusive.

After Series A was completed it was noticed that the assumed curve for the gravel layer was probably almost unique. The very short period of consolidation, and the difference between this curve and the other two suggested that no major changes should be attempted for this curve. The curves for the silt and clay layers were often quite similar. However, at many of the gauges one of the curves had a considerably shorter consolidation period than the other. It was decided to commence the fitting for Series B by assuming the same settlement for each layer, but interchanging the times. The gravel layer was generally left as for Series A. In this way it was hoped to get a band of possible future settlements rather than just one theoretical time settlement curve which might not be correct.





In some cases this interchange of times had no effect on the final total theoretical curve. This was especially true in cases where the assumed times for each layer were not greatly different. At other gauges however, the mere interchange of times did not result in a matching curve. In these cases the trial and error procedure was again employed to furnish a curve which agreed with the observed one and yet was composed of individual curves different from Series A.

The results of these two separate matchings are shown compared on Figures 41 to 48. From these comparison curves it can be seen that the only significant difference between the two methods is for gauges 11, 13 and 14. At these gauges the final total settlements from the two fittings differ by from 0.5 to 0.8 feet or by approximately 10 percent of the total settlement. The difference in theoretical final total settlement at all other gauges was less than 0.20 feet.

#### Identifying Time Curves for Each Layer

Having completed two separate fittings for each gauge there still remained the question of which single curve represented the settlement within each layer. Gravel soil is much more permeable than silt or clay, even if it does contain considerable organic matter and other foreign material. It should therefore consolidate at a much faster rate than either the silt or clay. On this basis the single curve showing the most rapid rate of consolidation was assumed to represent the settlement within the gravel layer. There was no question about



which curve to choose because there was always one curve which reached approximately 90 percent consolidation about the time the loading period was completed. Obviously this was the curve for the gravel layer.

The silt and clay curves were more difficult to determine since they were often not greatly different. The fact that a good match could also be obtained by interchanging the times, giving Series A and Series B fits further complicated the matter. For each series either individual layer curve could possibly represent the consolidation of either the silt or the clay. There existed four possibilities: Series A with the middle curve representing the silt and lower curve the clay, Series A with the middle being clay and the lower being silt, and Series B with the same two combinations. The choice of which of the four represented the most probable combination was made after the coefficient of consolidation and compressive index were computed for each possible combination. These coefficients were based on results from the theoretical time curves and were compared to values from laboratory tests.

#### Coefficient of Consolidation

From the results of several laboratory consolidation tests the coefficient of consolidation was computed for both the silt and clay soil samples. This was done by means of equation 1. These coefficients were plotted against applied load as shown on Figure 49. It can be seen that the coefficient of consolidation for silt is approximately 4 to 6 times greater than for clay. The range of values for silt is



shown to be from approximately 1 to 3 ft.<sup>2</sup> per day while the range for clay is between about 0.3 and 0.8 ft.<sup>2</sup> per day. These values were all computed from samples which were loaded and drained on horizontal surfaces, that is, the drainage was all in a vertical direction. It was appreciated that field drainage would probably tend to follow any horizontal lenses of high permeability, and not be entirely vertical. However it was felt that these laboratory test results would at least give some indication of field conditions, and relative magnitudes of  $c_v$  for silt compared to  $c_v$  for clay.

Equation 5 was used to compute the field coefficient of consolidation. Values for  $t$  and  $T$  were arbitrarily chosen for the condition of 90 percent consolidation. The value for  $H$  was taken as the full thickness of the stratum. This assumed drainage occurred from only one face which seemed a reasonable assumption considering that the lower boundary of the clay is bedrock and the upper boundary of the silt is gravel. Certainly the silt would not drain into the clay, but it could be expected that the clay would have to drain into the silt, and the silt into the gravel.

Table I shows the data and results of the computation for coefficient of consolidation.

#### Compressive Index

The laboratory compressive index or average slope of the  $e$ -log  $P$  curve within the range of overburden pressure and applied load







averaged 0.14 for the silt samples and 0.25 for the clays. The shape of the e-log P curves were generally quite curved indicating that the samples had suffered some disturbance. Because the natural moisture content was close to and generally above the liquid limit it was felt that these samples probably behaved as normally loaded clays described in Reference 26. It was therefore decided to attempt to obtain a field consolidation curve for the silt and clay layers by the method outlined by Terzaghi and Peck (27). As previously described this method consisted of extending the laboratory consolidation curve to the zero void ratio axis and joining this point to the point of initial void ratio and pressure.

Accordingly, a number of e-log P curves were plotted on the same sheet. When these curves were extrapolated to the zero void ratio axis it was found that they all intersected very close to the same point. By joining this point to the two outside limits of initial condition a band of probable field virgin compression curves were obtained. These curves are shown on Figures 50 and 51. The field compressive indices for the silt ranged from 0.25 to 0.44 and for the clay from 0.34 to 0.60.

The compressive index from the results of the theoretical time curves were computed by equation 5. Before this equation could be applied several factors had to be evaluated. The settlement (S) was taken directly from the theoretical time curves. The thickness of the consolidating stratum (H) was taken as the thickness of the layer



as shown on Figure 2. To obtain the initial void ratio ( $e_0$ ) an examination was made from the available laboratory test results. Figure 52 shows initial void ratios computed from consolidation tests plotted against depth below the surface. Terzaghi (26) explains that removing a clay like sample from the ground does not appreciably alter the void ratio. It was therefore assumed that the initial void ratio computed from these relatively undisturbed samples was probably representative of the initial void ratio existing in the field.

The void ratio from the e-log P curve at the overburden pressure was always approximately 0.1 less than the computed initial void ratio. This again agrees with Terzaghi's hypothesis for normally loaded clays (26).

Figure 50 shows that the initial void ratios are quite scattered and range from 0.6 to 1.2. The majority of the points however fall within a narrow band between 0.8 and 1.0 and show a slight decrease with depth. There is no apparent difference between silt and clay soils. A best fit straight line was arbitrarily drawn through the plotted points and all initial void ratios for future calculations were assumed to fall on this line.

The unit weight of the soil in each layer was also required in order to compute the overburden pressure ( $P_0$ ). The average specific gravity ( $G_s$ ) and initial void ratio of both the silt and clay was 2.72 and 0.90 respectively. From the fundamental equation

$$\gamma_b = \frac{G_s - 1}{1 + e} \gamma_w \quad (6)$$



where  $\gamma_w$  = the unit weight of water, the buoyant or submerged unit weight ( $\gamma_b$ ) of the soil was computed to be 57 pounds per cubic foot. This unit weight was used in computing the initial stress within the soil.

The soil within the gravel layer was generally a coarse dense gravel. However there is considerable organic matter both within the voids and in pockets and layers throughout the entire stratum. The buoyant unit weight of the gravel was arbitrarily chosen to be 5 pounds per cubic foot heavier than the silt or the clay making  $\gamma_b$  for the gravel equal to 62 pounds per cubic foot. Assuming  $G_s$  for this material to be equal to 2.65 the initial void ratio was calculated by equation 6 to be 0.66. This is a rather low unit weight and high void ratio for gravel soil, but when the existence of organic material within the stratum was considered these values seemed reasonable. Using these unit weight values the initial stress was computed at the mid height of each principal layer. The pertinent data and results are shown on Table II.

The original settlement computation done by the engineering consultants assumed an initial void ratio of all materials to be equal to 1.0 at a pressure of 1 ton per square foot. The submerged unit weight was assumed to be 60 pounds per cubic foot for all materials.

Boussinesq equations and Newmarks influence chart (19) were used to compute the increase in vertical stress at the mid height of each layer. A detailed discussion of calculation of stresses within a soil





due to a load applied at the surface is given in Chapter III. Suffice it to say here that of the many mathematical solutions to this type of problem, the Boussinesq solution gives the largest stresses, and his assumptions probably are in greater disagreement with actual soil conditions than any other solution. His equations were used however because they were far easier to apply to the irregular loading conditions than any other, and they are commonly used by others in the field of soil mechanics. The results of this stress computation are shown plotted against depth on Figure 53.

Having decided upon values for all the factors the compressive index was then computed from equation 5. The data and results of this computation for all the combinations are shown on Tables III and IV.

#### Most Probable Curve

With values of  $c_v$  and  $C_c$  computed for the four possible combinations using theoretical fitting curves Series A and Series B the most probable theoretical curve could then be determined. This was done by comparison of the computed values with results from laboratory consolidation tests. For example, the possible combinations for Settlement Gauge 1 were as follows:





	SILT	CLAY
<u>Series A, middle curve</u>	$t_{90} = 4400$	$t_{90} = 4000$
Assumed to be silt,	$c_v = 5.55$	$c_v = 0.90$
Bottom curve assumed	$S = 1.60$	$S = 1.25$
to be clay.	$C_c = .221$	$C_c = .766$
	$t_{90} = 4000$	$t_{90} = 4400$
<u>Series A, middle curve</u>	$c_v = 6.10$	$c_v = 0.82$
Assumed to be clay	$S = 1.25$	$S = 1.60$
bottom curve assumed	$C_c = .172$	$C_c = .98$
to be silt		
	$t_{90} = 4000$	$t_{90} = 4400$
<u>Series B, middle curve</u>	$c_v = 6.10$	$c_v = 0.82$
assumed to be silt,	$S = 1.60$	$S = 1.25$
bottom curve assumed	$C_c = .221$	$C_c = .766$
to be clay.		
	$t_{90} = 4400$	$t_{90} = 4000$
<u>Series B, middle curve</u>	$c_v = 5.55$	$c_v = 0.90$
assumed to be clay,	$S = 1.25$	$S = 1.60$
bottom curve assumed	$C_c = .172$	$C_c = 0.98$
to be silt.		

The units were  $t_{90}$  in days,  $S$  in feet and  $c_v$  in  $\text{ft.}^2/\text{day}$ .

The first of these four possible combinations was assumed to represent the most probable field condition.



In this case  $c_v$  and  $C_c$  for the silt was 5.55 and 0.221 and for the clay 0.90 and .766 respectively. The values of  $c_v$  for silt is somewhat higher than computed from the laboratory tests. The silt compressive index, although being considerably higher than that obtained from the laboratory tests, was only slightly lower than the lower limit of the range of field compressive indices shown on Figure 50. The coefficient of consolidation for the clay agreed with the results of laboratory tests. The compressive index was however slightly higher than the highest field compressive index shown on Figure 51. The results of other possible combinations showed even greater disagreement with laboratory test results and were therefore rejected.

In a similar manner the most probable set of time curves was chosen for each settlement gauge. These most probable values for  $c_v$  and  $C_c$  are shown underlined in Tables I, III and IV. They are also recorded on the plot of the most probable fitting curve, Figures 10 to 25. A summary of the results of theoretical curve matching is shown on Tables VI and VII.

### Significant Figures

All of the computations were done to three figure accuracy. The final results were also recorded using three significant figures. It was realized however, that the use of three significant figures in computations or results does not in any way mean that these coefficients were known to this accuracy. In consideration of the



uncertainty of the many assumptions involved, the values for  $c_v$  and  $C_c$  are probably not even accurate to one significant figure. Three figures are required to insure accuracy in the mathematical calculations, and for this reason only are three significant figures shown in the calculations and results. These physical soil properties were of secondary importance in this study, being used mainly to identify the most probable correct time curve. Their use does not warrant further discussion on the accuracy in their determination.

#### Consolidation Factors for the Gravel Stratum

The theoretical time curve for the gravel stratum was essentially the same for both Series A and Series B fits. Values for  $c_v$  and  $C_c$  were not needed to assist in the determination of which curve would be the most probable representation of field conditions. Computed values were used only to obtain an indication of the field consolidation characteristics. It was appreciated that settlement within the gravel layer was probably mostly a result of decrease in volume of the organic matter contained in the voids, layers and pockets of this stratum. Clean dense gravel would have very little settlement.

The field compressive index of the gravel stratum was computed from equation 5. The factors for this equation were obtained in a manner similar to the method used for the silt and clay. The settlement data was taken from the most probable fitting theoretical curve, and no alternative values were computed. These compressive indices





are shown computed on Table V and are summarized on Figures 11 to 25, and Table VII.

No attempt was made to compute any coefficients of consolidation for the gravel layer. It was felt that because of the complex nature of these surface sediments any computed  $c_v$  would be meaningless if not misleading.

#### Initial and Secondary Compression

The theoretical time curves which were found to match the observed settlements were all computed on the basis of the Terzaghi theory of consolidation. As previously mentioned, practical experience has found that the total settlement of a soil is made up not only of primary settlement, which follows the theory of consolidation, but also of initial and secondary compressions. These latter compressions do not follow the theory of consolidation and no proven theory exists to predict the rate or magnitude of settlement from either cause. No corrections were applied to the matching theoretical curves to account for any initial or secondary compression.

#### Predicted Future Settlements

The purpose of obtaining a theoretical time curve to match the observed settlement was to explain the shape of the observed settlement curve, and predict future settlement at each gauge. The matching Theoretical curves, Figures 11 to 40, show very close agreement with the observed settlement. Any deviation from the



theoretical curve of a one layered system consolidating under an instantaneously applied load is due to the gradual application of the fill load coupled with very rapid consolidation within the gravel layer. This accounts for the rapid initial settlement. For a period following the completion of the fill, very little load was applied, and the settlement began to level off on the log time plot. Increase in settlement on the log time plot coincided with the application of the site grading load just at the completion of building construction. Within a very few days following the application of this load settlement within the gravel layer had reached very nearly theoretical 100 percent completion. Small differences of up to approximately 0.3 feet between the theoretical and observed curves occur before this time. These differences are probably due to deviations from the assumed actual loading conditions. A more probable loading diagram is shown superimposed on the assumed diagram of Figures 11 to 40.

Following placing of site grading fill, the seat of settlement was almost entirely within the lower silt and clay layers. This settlement appears to be following basic consolidation theory very nicely. If the applied load remains unchanged future settlements should follow the fitted theoretical time curve. At the time of the latest set of readings, September 1957, the total settlement varied from 60 to 85 percent completed, (Table VI). The settlement within the silt and clay layers was between 50 and 70 percent completed. According to these fitted time curves, this remaining settlement will



take place at a gradually decreasing rate. Most of this settlement will have been completed within the next ten years, and theoretical settlement beyond 1980 for all practical purposes will be zero. Table VI shows a summary of the matching theoretical time curves.

If however, there is an increase in applied load, the magnitude and rate of settlement will also be increased. One potential cause of increase in consolidation load is the increase in effective stress due to lowering of the ground water table. Figures 7 and 8 show the latest ground water table to be from approximate elevations 20 to 30. These elevations were referenced to the elevation of low tide water which is called elevation zero. Since high tides exceeding 20 feet are common in the ocean immediately adjacent to the smeltersite it is probable that there will be very little future lowering of the ground water table.

Another factor which could cause the settlement to exceed that predicted by the theoretical time curves is the effect of secondary compression.

How much secondary compression has taken place in the gravel stratum and how much more secondary compression will occur there as well as in the silt and clay layers is completely unknown. Furthermore there is no known method of estimating this settlement. Judging from laboratory tests on inorganic soils, any secondary settlement will probably occur at a very slow rate, and be small in comparison to the primary settlement.





### Theoretical Time Curves Compared

Approximately two years before this writing a different theoretical time curve was fitted to the observed settlement for gauges 1 to 15. This fitting was done by the conventional method of assuming only one layer of consolidating soil. The irregularities in the early part of the observed time settlement pattern were treated as if they were initial compression in an ordinary consolidation test. By this method a theoretical time curve was obtained which matched the later observed settlements as well as the theoretical curves obtained from consideration of a three layered system. Figures 41 to 48 show a comparison of the time curves obtained from this one layered fitting and the two curves from the three layered consideration. The agreement is remarkable. Generally the theoretical total settlement is within a few tenths of a foot. The only exceptions are gauges 5 and 14 which disagree in final total settlement by approximately one foot.

A study of the comparisons between theoretical time curves obtained from these different assumptions leads to the conclusion that a satisfactory fit can be obtained from the simple assumption of a one layered consolidating system. Certainly it is much faster and easier to match one curve to observed settlements than to match the combined sum of three separate theoretical curves. There is little to choose between the final end result. The one layered curve, however, reveals nothing of the behaviour of the individual soil layers. If this





information is required then the more tedious three layered procedure must be employed.

#### Coefficient of Consolidation, and Compressive Index

A by-product of the theoretical time curve fitting, was the determination of values for field coefficients of consolidation and compressive indices at each settlement gauge. The main assumptions and methods of computation have already been discussed. It should however be repeated that the value for these consolidation factors are no more accurate than the matching theoretical time curves, and the assumed soil properties. Although they are recorded to three figure accuracy for convenience in calculating and checking the mathematics they are probably not accurate to more than one significant figure.

A summary of  $c_v$  and  $C_c$  values is shown on Table VII.

These consolidation factors were found to vary widely from one gauge to the next. Although the values differed considerably from those obtained by conventional laboratory tests these differences can be explained by consideration of the physical conditions of the test compared to that in nature.

The coefficient of consolidation for both the silt and clay was often 3 and sometimes as much as 10 times that obtained by laboratory tests. The laboratory test however, permits drainage in only the vertical direction while in the field drainage will occur along the path of greatest permeability. A well known fact, which is supported



by sound theory (25) is that for a stratified soil the coefficient of permeability is always greater parallel to the stratifications than perpendicular to them. The coefficient of consolidation, being proportional to the coefficient of permeability would also be greatest in a direction parallel to the stratifications. It is expected that since the silts and clays below the Kitimat smelter were deposited as marine sediments, they would contain horizontal stratifications. This assumption is verified in part by the drill hole logs which record layers or pockets of fine sand and silt within these strata. It is expected that drainage of the silt and clay layers would at least partly follow these horizontal permeable layers and thus effectively increase the overall coefficient of consolidation from that of vertical drainage only.

In a study of the field consolidation characteristics of a uniform deposit of Boston blue clay which to visual inspection showed only a few fine sand strata, Gould (8) determined the horizontal permeability to be from 34 to 50 times the vertical. He also found for this material that the time rate of consolidation from three dimensional drainage was about 3 times that expected from basic theory of vertical drainage. The coefficients of consolidation for the Kitimat sediments computed from the matching time curves seem quite reasonable when considered in the light of probable field conditions.



Regarding the compressive indices it was noted that they were considerably larger than expected from laboratory test. Of course no tests were run on the soil within the gravel layer. When gravel is washed into place by a river or stream the deposit is usually quite dense and little settlement is expected from a dense gravel deposit. The presence of compressible material within the gravel contributes to increasing the settlement within the layer. The compressive indices computed from the matching theoretical time curves ranged from 0.01 to 0.12 with a general average of about 0.06. Since it is almost impossible to make laboratory consolidation tests on such a heterogeneous gravel deposit, about the only way of determining the consolidation characteristics is by field observations such as have been done here.

The laboratory compressive indices of the silts and clays were taken as the average slope of the  $e$ -log  $P$  curve within the range of field loading. These values were considerably lower than those computed as shown on Figures 50 and 51 which agreed quite well with the time curve computations. Some of the indices for silt were slightly low, and some values for clay were slightly high. The general agreement with the values from Figures 50 and 51, and the disagreement with the values from conventional laboratory tests appeared quite significant. It would seem that for a normally loaded soil of this type, the more realistic procedure for estimating settlement is that based on a field compressive index determined by the method outlined on Figures 50 and 51 rather than from the average slope of the  $e$ -log  $P$  curve over the range of





applied load. This conclusion is in agreement with Terzaghi's hypothesis concerning the effect of sampling a normally consolidated clay soil. (26)

### Conclusions

In conclusion it can be said that a theoretical time curve was found to match the observed settlement at each gauge. This curve was the summation of settlements from time curves for each of three principal layers. From time curves of each layer values of  $c_v$  and  $C_c$  were computed for each soil type. These consolidation factors were somewhat different from those expected from basic theory and conventional laboratory tests, but agreed quite well with that which should be expected in nature. A method of computing the field compressive index from several consolidation tests was verified for the Kitimat silts and clays.

The rate and magnitude of settlement was such that between 60 and 80 percent of the final total settlement had been completed by September 1957. Settlement within the gravel layer was completed very soon after the buildings were constructed. If the loading remains unchanged, all settlement after October 1957 will be within the lower silt and clay strata and will continue at an ever decreasing rate until after 1970.



## CHAPTER III

### CONSOLIDATION AND HORIZONTAL DISPLACEMENT

#### Theory

Any element of soil below a surface applied load is acted on by stresses in all directions. In the Cartesian system of coordinates six independent stresses are both necessary and sufficient to completely define the stress on any element. (28) In dealing with settlement problems the vertical component of stress is usually all that is of interest because the settlement or movement in a vertical direction is generally the only concern. Consolidation, being a direct function of applied excess stress will be a maximum in the direction of the maximum stress on the element which is called the major principal stress. Only directly under the center of a uniformly distributed load, or point load can the direction of the major principal stress be assumed vertical without detailed analysis. Since the applied load was large and irregular it was decided to determine the direction of the major principal stress at various points within the consolidating soil beneath Potlines 1 and 2. Knowing this stress the theoretical horizontal components of movement could then be calculated on the basis that the maximum movement was in the direction of the major principal stress. This information could then be compared to the actual observed movements.



### Stress Computations

A search of the pertinent literature showed that there were three distinctly separate methods of computing the stresses in an elastic system below a loaded area. These methods are named after the men who first advanced the theory; Boussinesq, Westergaard, and Burmister.

A brief review of the assumptions and theories of each of these solutions follows.

### Boussinesq Equations

The first adequate solution to the problem of stresses within an elastic medium acted on by a force at its surface was published by Boussinesq in 1885. His equations first appeared in Cartesian coordinates (30) but are quoted in most textbooks on soil mechanics using spherical coordinates (24). Boussinesq assumed a semi-infinite elastic medium which was homogeneous and isotropic. His equations define all components of stress on any element beneath a point load acting normal to the surface. The derivation of these equations is found in several places (18, 28). Later authors have extended his work by integrating the equations for point loading over an area, and so found stress equations due to various loading conditions. Other authors have modified his equations to account for departures from the original assumptions of a homogeneous, isotropic, semi-infinite





elastic solid. The list of such special considerations was long but a few however were worth special mention.

In 1924, Carothers published formulae for line and strip loads, for both a semi-infinite mass, and for the case of a smooth and rough rigid boundary at some finite depth below the surface. The solution of the case of a rough boundary at a finite depth contained an error which was objected to at the time in an oral discussion by Timmoshenko, but was not generally known until years later.\*

In 1934, Jurgenson (12) expanded Carothers' equations and published tables and charts to facilitate the computation. These charts and tables are for stresses caused by line, strip or symmetrical area loads. They give equations in one plane only. Carothers' error is inherent in Jurgenson's solution for the one particular case.\*

Biot (1) in 1935 derived formulae for stress at the rigid boundary due to a point load acting on the surface and showed that the stress so computed is different from that obtained by the Boussinesq solution. Cummings (5) expanded Biot's formula to apply to the case of a circular area and showed that the stress so obtained at the rigid boundary could be approximated by using a depth of 0.75 times the actual depth in the Boussinesq equations. He showed that the stress on the rigid boundary is greater than the stress obtained from

---

\* The reference for this is Pickett (21) Page 35. He refers to Carothers, S.D., Elastic Equivalence of Statically Equipollent loads, Proceedings of the International Mathematical Congress, Vol. 2. Toronto University Press.





Boussinesq's solution but suggests that by St. Venants Principal the stress concentration would be relieved a short distance from the rigid boundary and be the same as computed by Boussinesq.

In 1938, Pickett (21) published the necessary equations for determination of the stresses, vertical, horizontal, and shearing, at any point in a homogeneous, isotropic elastic solid bounded on the lower side by a rough rigid boundary and carrying a known normal load on the surface. This was complete with a description of how to solve the equations for special cases. The solution and application to a specific case however is quite involved. He states that for vertical stress the existing Newmark Charts (19) are satisfactory for Poisson's ratio between 0.25 and 0.5.

These and other papers on variations of the Boussinesq equations were generally unsuitable for this study because:

1. The equations were left in a purely mathematical form, not sufficiently simplified to be readily usable.
2. Where simplified formulae, tables or charts were published to facilitate the computations they dealt only with stress components in one plane, or with very simple loaded areas.
3. The charts and tables available for simplified computations applied only for the determination of the vertical stress. These charts are common and are found in most text books on Soil Mechanics.



A graphical solution, which proved to be the most useful was developed by Newmark (19). This method provides a graphical means of computing all six components of stress under any loading system regular or irregular for any desired value of Poisson's ratio. The method is based on the Boussinesq equations.

### Westergaard Solution

In 1938, Westergaard (31) published a solution based on assumptions which are more realistic for soil than those of Boussinesq. He assumes a semi-infinite material, loaded normal to the surface. The material is reinforced with numerous closely spaced horizontal sheets which retard lateral motion. His solution is valid for any Poisson's ratio, and is left in an integral form for expansion to suit the boundary conditions of a particular case.

Taylor (24) and Fadum (6) have simplified the Westergaard analysis to provide a quick means of computing the vertical stress under simple loading conditions for Poisson's ratio = 0. This is done by means of tables and charts which are similar to those published by these authors for solving Boussinesq equations. The vertical stress computed by these charts are approximately two thirds of the value computed by the Boussinesq equations.

There seems to be no simplified solutions for any but the vertical stress by the Westergaard analysis.



### Burmister Solution

The solution for the stress due to a load applied on the surface of a layered system was first published by Burmister in 1943 (2). He assumes a two layered system, each layer being homogeneous and isotropic but with different physical properties. His solution shows that the top layer acts as reinforcing and distributes the load over a wider area onto the lower layer. Thus the stresses in the lower layer computed by this method are lower than if computed by Boussinesq. Prior to this time Casagrande (3) had suggested that a sand and gravel layer above a softer clay layer would spread the load and distribute the stress over a wider area which would aid in smoothing out differential settlements.

### The Equations Used

The consolidating soil at the Kitimat Smelter is definitely a layered soil and for this reason the Westergaard or Burmister solution would probably be the most realistic. The compressible material also rests on solid rock at a depth of between 25 and 30 percent of the width of the applied load. This fact would suggest an approach similar to that of Pickett and others who have considered the effect of a rigid boundary beneath the compressible material. None of these methods were chosen however, because it was felt that the accuracy of the results did not warrant the time and effort to reduce the general equations into a form which could be applied to this particular case. It was therefore decided to use the Boussinesq solution.





Of the many available approaches using the Boussinesq method the following were considered and rejected.

1. Dividing the area into squares small enough to act as point loads and sum the stress produced by each "point loaded square". It can be easily shown that to be within an error of 10% the distance below a loaded square must be approximately three times the width of the square before the square can be replaced by an equivalent point load. Stresses were desired within the clay stratum, from about 150 to 300 feet below the applied load. Choosing the greater depth, the side of each square would have to be less than 100 feet, and the number of squares would be approximately 200. At a depth of 150 feet the number of point loaded squares would approach 1000. This number could be reduced somewhat because the contribution of the outer squares to the total stress would be insignificant compared to that of squares close to the point. It was felt however, that the required number of computations by this method was too large for practical consideration.
2. The use of Jurgenson's or Fadum's tables. These tables provided only the stress components in one plane due to a line or symmetrical load. They were rejected because a method to apply them to this case of an unsymmetrical load could not be found.



3. Integrate the Boussinesq equations as published by Way (30) over the boundary of the applied load and obtain by mathematical computation a rigorous solution to the equations at each desired point. By approximating the actual applied load by a wedge the equations were set up in integral form, but their complexity discouraged any further pursuit along this line.
4. The use of Newmark's Influence Charts. As previously stated, these charts provide a simple graphical method of obtaining the six necessary components of stress due to any normally applied load, and for any value of Poisson's ratio. As this was the most straight forward of all methods, and one which was most readily adaptable to this particular case it was adopted.

### Calculations

Newmarks influence charts are graphical solutions to the Boussinesq equations. There is a separate chart for each of the six components of stress (three normal and three shearing). These six charts are set up for Poisson's ratio of 0.5. Three other charts are provided to correct the applicable stress component to any other value of Poisson's ratio. The use of the charts involves drawing the loaded area on tracing paper to an appropriate scale and superimposing it over the chart. The load



of the area covering each square is multiplied by an influence value and the total stress is the summation of all the individual squares.

Having determined the six stress components from Newmarks charts the direction and magnitude of the major principal stress can then be found by standard equations of continuity for three dimensional stress system. These equations are derived in textbooks on the theory of elasticity (for example Reference 28) and are summarized in Figure 54. After the direction of the major principal stress has been determined its horizontal projection in the direction of the coordinate axes can be easily found by the method outlined in Figure 54. This expresses the horizontal projection of major principal stress as a fraction of the vertical stress.

The vertical settlement which has taken place over any period of time was accurately known. From this movement the horizontal components of the maximum movement were calculated. This involves the assumption that the vertical and maximum movements were parallel to and proportional to the vertical and major principal stresses. The consolidation characteristics in the horizontal direction were probably considerably different from those in the vertical direction, but lacking information on this subject the soil was assumed to have like properties in all directions.

As discussed in Chapter V a detailed set of observations was made for column lines G and H of Potroom 2A. Settlement gauges 6, 7 and 8 being adjacent to column line H, were chosen as the sites for the determination of theoretical horizontal stresses and displacements.





Stresses at depths of 50, 150 and 250 feet below these gauges were obtained for Poisson's ratio of 0.5. Numerical values for the stress components and resulting horizontal displacements are shown in Table VIII. To show the variation of the individual stress components with depth the normal and shearing stresses are plotted on Figure 55. The theoretical horizontal movement expressed as a percent of the vertical movement is plotted on Figure 56. From the total building settlement the horizontal movement was calculated and is shown on Figure 57.

It was shown in Chapter II that the settlement in the gravel layer was almost completed before the buildings were constructed. Settlement at any point within the gravel layer was assumed to be the same as the surface settlement. In Chapter II it was also shown that the settlement of the silt and clay is quite similar. The proportion of surface settlement assigned to any point within the silt and clay was assumed to be the same as the ratio of the depth below the top of this layer to the total thickness of these compressible soils.

An examination of the individual stress components shows that the major principal stress is only slightly greater than the vertical stress. The shearing stresses are very small and the direction of the major principal stress is close to being vertical. It is extremely difficult to make exact checks on the computations when working with three figure accuracy and small magnitude stresses and stress differences. When the questionable validity of assumptions involving





the use of the Boussinesq equations for this soil condition, and the method of graphical computation are considered, the required accuracy in calculations does not warrant the use of calculating machines and several places of decimal. The resulting curves of horizontal displacement are plotted as they were calculated. They show distinct breaks which are probably due to errors incurred from calculations involving differences of small numbers. This in no way invalidates the results. Sufficient computations were made to indicate the general magnitude and trend. None of the results showed significant disagreement from this average.

To show the general trend of horizontal movement at various other places over the Potline 1 and 2 area stresses and displacements were computed at a depth of 150 feet below each settlement gauge in this area. The results are shown plotted as a vector diagram on Figures 58 and 59.

All of the aforementioned calculations were made assuming Poisson's ratio equal to 0.5. This assumes no volume change occurs during elastic deformation which is the usual assumption for a saturated soil. Poisson's ratio does not appear in the Boussinesq equations for vertical normal stress or for shearing stress on vertical planes. In most settlement computations the vertical stress is the only component required. Since the Boussinesq equations are often used for this computation the choice of a value for Poisson's ratio for soil is often not important.



The Westergaard analysis contains Poisson's ratio in the expression for vertical stress. The value is usually chosen to be zero which represents no lateral expansion due to compression (6 and 24). This gives a maximum value for vertical normal stress. Although no applicable method of using the Westergaard equations was available it was decided to recompute the movement at a few points from the Boussinesq equations for a Poisson's ratio equal to zero. The solution for Poisson's ratio of 0.5 and zero would represent limiting values for the Boussinesq solution. It was felt that the solution for Poisson's ratio of zero would be an approximation to the Westergaard analysis. Stresses and horizontal displacements at a depth of 150 feet were computed for Poisson's ratio of zero at the site of settlement gauges 6, 7, 8, 9, 10 and 11. The results are shown on Table VIII and Figures 56 and 57. The horizontal movement for Poisson's ratio equal to zero was approximately one half the value computed for Poisson's ratio equal to 0.5.

#### Discussion of Results

At settlement gauges 6, 7 and 8 the calculated horizontal component of movement was within the range of 10 to 25 percent of the vertical movement for Poisson's ratio of 0.5. Using Poisson's ratio equal to zero reduced this horizontal movement by approximately one half. The calculated movements at other points over the smelter area showed the same general trend, (Figure 58). The direction of movement



in every case was away from the center of the loaded area and the magnitude of movement increased towards the edges of the load.

Jurgensen (12) has published a diagram showing the direction of the principal stresses at several points below and at some distance beyond the edge of a strip footing. The direction of principal stresses as shown herein agreed with Jurgensen's diagram. At increasing distance beyond the edges of the load Jurgensen's chart shows that the direction of the major principal stress becomes almost horizontal.

The actual horizontal movement at each point was computed on the basis of observed total settlement since construction of the buildings. The gravel layer was considered to contribute nothing to the vertical settlement. Thus all points lying within the depth of the gravel layer were assumed to settle the same as at the surface. Vertical settlement of points within the compressible silt and clay layers were reduced in proportion to their depth and the horizontal movement of these points was computed on the basis of this reduced vertical settlement. Within the depth of compressible material the magnitude of actual movements decrease from a maximum at the top of the silt to zero at the rock interface because zero vertical movement was assumed for this depth.

The magnitudes of horizontal movement in the upper layer ranged up to 0.5 feet at the edges of the buildings using Poisson's ratio equal to 0.5. This is true for gauges 6, 7 and 8, (Figure 57) as well as the other gauges over the smelter area (Figure 59). If Poisson's





ratio equal to zero were used it would be expected to reduce the computed horizontal movement by one half, or to approximately 0.25 feet at each end of the buildings.

Movements at the upper layer were based on calculation of stresses at a depth of 50 feet below the bottom of the fill. This is only 1/60th of the width of the loaded area. Theoretically the Boussinesq equations hold true for every point below the load except at the contact face. It can easily be shown that for simple loading conditions the induced stress changes rapidly toward the contact face. While the equations are theoretically correct it would be expected that at such a relatively shallow depth great care and precision would be required to obtain accurate results. As previously mentioned however, the general agreement of all points between depths of 50 and 250 feet would indicate that the results are sufficiently reliable.

The actual field conditions were in some respects considerably different from the basic assumptions inherent in the equations which were used to compute the stress below the fill.

1. The soil was not an isotropic and homogenous material.  
There were three principal layers of quite different elastic properties, and within each layer were numerous horizontal stratifications.
2. The rock surface at a relatively shallow depth below the load presented a discontinuity not assumed by Boussinesq.



3. The main movement within the soil was due to consolidation rather than elastic deformation, and theories of elasticity may not strictly apply.

Modified equations have been introduced by Westergaard and Burmister to attempt to account for horizontal stratification. While no computations were made for this particular case other investigators have suggested that these horizontal layers tend to reduce the stress within the soil below the value computed on the basis of a homogeneous and isotropic material.

Biot and Cummings have attempted to account for the effect of a rigid lower boundary. Cummings suggested that the stress at this boundary could be approximated by using Boussinesq equations and a modified depth of 0.75 times the actual depth. He also suggested that by St. Venant's principle the stress within the soil a short distance from the rigid boundary would be the same as computed assuming no discontinuity. The plots of stress and horizontal movements versus depth show little variation over the depth considered. Therefore using a somewhat smaller depth would have little effect on the computed stresses.

### Conclusions

The direction and magnitude of the major principal stress was found at several places below the smeltersite. The direction of this stress was found to be away from the center of the loaded area. It was approximately vertical at the center of the area and had an increasing



horizontal inclination toward the edges of the fill. The direction of the major principal stress did not vary significantly with depth within the compressible soil.

By assuming that movement in any direction due to consolidation was proportional to the component of the major principal stress in that direction horizontal movements were calculated at various places over the smeltersite. The vertical component of movement was taken as the vertical settlement of the buildings since they were constructed. This computed horizontal movement was away from the center of the loaded area. At the surface of the compressible soils it varied from zero at the middle of the area to a maximum of 0.5 feet at the edges of the potroom buildings.

It was shown in Chapter II that settlement since construction of the buildings has been almost entirely within the lower silt and clay layers. Therefore this computed maximum horizontal movement would occur at the gravel silt interface, which is 50 to 120 feet below the surface. How this outward movement is transmitted through the gravel layer is uncertain. Certain physical boundary conditions must be met. Some of these are:

1. A closed system - no cracks can form within the soil at depth.
2. The horizontal movement must be zero at the rock surface.



3. Since there was no significant settlement within the upper gravel layer, approximately 50 to 120 feet thick, the seat of all horizontal movement was within the silt and clay below.
4. There cannot be a discontinuity at the silt-gravel interface and the movement at each layer must be the same in magnitude and direction.

In Chapter V it will be shown that the ends of the potroom buildings appear to have moved closer together by approximately one half foot. This would represent a movement of  $\frac{1}{4}$  foot at each end of the potroom, or approximately one half of the movement computed on the basis of a non vertical major principal stress. The direction of the observed movement however was inward, and opposite to the outward movement calculated from the stress consideration. An explanation for this apparent contradiction is presented in Chapter V along with a discussion of other factors related to the problem of horizontal movements.





## CHAPTER IV

### MODEL STUDY

#### Introduction

To try to obtain a general picture of the behaviour of the soil surface as a result of settlement it was decided to construct a model. This was done by substituting elastic bands for the compressible soil, and inducing in them a tensile rather than a compressive stress. This would give results exactly opposite to the movement in the field.

#### Description of Model

The model study was made prior to receiving detailed information regarding the movements along column lines G and H. Column line A was chosen for the study. Along this column line the subsoil and settlement profiles were plotted. The settlement profile was plotted above the subsoil with settlements increasing upwards as shown in Figure 60. The same horizontal scale was used in each case, but to accentuate the results vertical scales were distorted. These scales were:

Subsoil:	Horizontal 1" = 50 feet.
	Vertical 1" = 30 feet.
Settlement Profile:	Horizontal 1" = 50 feet.
	Vertical 1" = 1 foot.



Since only qualitative results were expected from the test, great precision was not required in setting up the apparatus. For this reason the rubber bands which substituted for the soil were chosen on the basis of availability. Three sizes were used for each of the three subsoil layers.

$\frac{1}{4}$  inch wide for gravel

$\frac{3}{16}$  inch wide for silt

$\frac{1}{8}$  inch wide for clay.

All the bands were approximately  $\frac{1}{24}$ th inch thick. Within the range of strain applied the ratio of the strains was constant and equal to

$$\frac{1}{4}" \text{ (Gravel)} : \frac{3}{16}" \text{ (Silt)} : \frac{1}{8}" \text{ (Clay)} = 1 : 1.2 : 1.7$$

Using the appropriate size band in each soil layer a grid of 1.8 inch squares was formed with horizontal and vertical orientation. The vertical side of each square fell immediately below the column on which settlement observations were taken.\* The arrangement was such that the soil surface was replaced by a horizontal  $\frac{1}{4}$  inch band but the lower squares were sometimes not complete. Seven inch long wire connectors stretched from the line of zero settlement on the settlement pattern, to the line of zero deformation on the soil profile where they were joined to the rubber bands. The horizontal bands extended a variable distance beyond the end of the building. Figure 60 shows these distances to the same horizontal scale as the model. The entire model

---

\* See figure 3 for location of settlement observation points.



was constructed on a sheet of  $2\frac{1}{2}' \times 3' \times \frac{1}{4}$  inch plywood. The rubber bands were given an initial strain equal to 20 percent of their original length. They were then pinned to the boundaries as described. The corners of the squares were then attached by rubber cement.

#### Operation of the Model

When the cement had hardened the wire connectors were moved from the line of zero settlement to the line showing the total settlement of the building, and pinned in place. Thus the soil surface at each settlement observation point was given an induced vertical displacement corresponding to the actual conditions without introducing any horizontal fixity.

When the soil had been deformed as described the horizontal movement at the ground surface was observed at every settlement observation point. This process was repeated with the horizontal bands pinned at various distances beyond the edges of the building.

#### Observations

The results of the model study tests are summarized on Figure 60. The horizontal movements shown were measured to the scale of the model, but were really only a matter of one tenth inch and less. It can be seen that the movements which occurred in the model indicated the end column footings of the prototype moved together. The greatest movement was in the vicinity of maximum settlement.





Conclusion

The model was not constructed with great precision, and the results can only be considered of a qualitative nature. The results however do indicate a horizontal movement of the ground surface. This movement was generally toward the center of the potroom buildings.



## CHAPTER V

### GEOMETRY OF SUBSIDENCE

#### Description of Measurements

The first indication of serious structural damage in the Potroom buildings which could be attributed to settlement came in the summer of 1957. Many of the steel columns had developed a distinct tilt. It was first thought that the tendency was for the tops of the columns to tilt towards the west, and it seemed probable that they were being given a horizontal thrust in this direction at the height of the crane rail. The most serious effect was on the west one half of the buildings, but there was some evidence of an eastward thrust of the column tops on the east end as well. Associated with this apparent movement of the steel superstructure were buckled diagonal bracing members, and cracked concrete supports. Longitudinal and cross-sections of a typical Potroom are shown in Figures 5 and 6.

Since the cause of the damage was not manifest by general observations and measurements made at the time, a detailed set of measurements were taken during November and December 1957. Column lines G and H (Potroom 2A) were chosen for the detailed study because they were situated in an area of maximum differential settlement. The following measurements were taken on each column line.



1. Horizontal distance between Columns 1 and 48 at the elevation of the steel base plate, (i.e. top of the concrete columns) and at the elevation of the working floor.
2. Horizontal distance between the center line of each column at the elevation of the steel base plate.
3. Deviation from plumb taken:
  - (i) Between the top of the concrete column and 7.6 feet below.
  - (ii) Between steel base plate and 1 inch below the gusset plate on the crane beam web.
  - (iii) Between the steel base plate and the top of the steel column.
4. Elevation of the structural steel base plates.
5. Distance across expansion joints at the crane beam.

The end to end distances were each measured twice at the elevation of the base plates and once at the working floor. A further check was made by aligning the end columns by transit and noting the difference in length. A steel chain, calibrated to a standard chain was used and corrections for sag tension and temperature were applied. All measurements were taken inside the potroom where the radiant heat from the smoldering pots created variable temperatures along the room.

The first measurement was made November 25, 1957 at the elevation of the steel base plates. The temperature was recorded at the 23 and 73 foot marks of the 100 foot steel chain. On November 26



measurement was taken at the elevation of the working floor with temperatures similarly recorded. The end points of this measurement were vertically below that of the previous day, and the distance was between the center lines of the end steel columns.

On December 5, a further measurement was made at the elevation of the steel base plates and air temperatures were recorded at every column. These temperatures varied from 40 to 84° F with as much as 10° F difference between adjacent columns. A comparison of all measurements is shown in Table IX. The difference in length as measured by the transit alignment was assumed to be correct. On this basis the probable error in measuring the overall length varied from .060 feet on November 25 to .007 feet on November 26.

Measurement of the lean of the concrete columns was done by suspending a lead plumb bob from a wooden frame held to the side of the column. Allowance was made for any deviation in width of the column. Measurements were taken to the nearest 1/16 inch and are probably accurate to the nearest 1/8 inch. Lead and wood were chosen because they would not be effected by the extremely high electro-magnetic forces in the potroom.

Measurement of the tilt of the steel column was done by means of a transit and reading the intersection of the vertical cross hair on a steel tape held against the base of the column. Again measurements are probably accurate to the nearest 1/8 inch.





The elevation of the steel base plates were compared to the recommended setting elevation. In this way the total settlement of each column since construction was determined. The elevations are probably accurate to the nearest 0.01 feet but since no previous check was made of the exact setting elevation, and as all columns may not have been brought to their final position the day the recommended setting was given it is probable that some of the settlement values may be in error by a maximum of 0.05 feet.

The measurement across the expansion joints were mainly for the purpose of future comparisons and gave only an indication of whether the expansion was fully taken up or not. While an indication of the relative amount the joint is open or closed could be observed, it was not possible to tell by visual inspection whether the joints were fully closed. A power failure which occurred December 7, 1957 resulted in a lowering of the air temperatures inside the potrooms by an estimated 10 to 15° F. Measurement of the expansion joints before and after showed no significant change except at G30 and H30 which opened 3/8 and 7/16 inch respectively. A few measurements of the lean of steel columns before and after the power failure showed movement of up to  $\frac{1}{4}$  inch but insufficient readings were taken to establish a pattern. The results of all measurements are summarized on two large drawings, Figures 68 and 69 enclosed herewith.



### Interpretation of Measurements

The most significant fact emerging from the detailed measurements is that both column lines G and H appeared to have shortened approximately one half foot. Two explanations seemed possible.

1. The columns were initially set in error by this amount.
2. The settlement has drawn the columns closer together.

Only a few checks, independent of the contractors own work were made at the time of construction. These checks however indicated that the initial column setting was correct. An error of one half foot in 1100 feet (approximately .04 feet in a 100 foot chain) is rather large. It is improbable that an error in the chain of this magnitude would go unnoticed at the time of construction.

Other factors also indicate that the initial setting was correct, and the column bases have since moved to their present position. When the power was shut off and the temperatures lowered approximately 15° the 1100 foot crane beam would have tended to shorten approximately 0.10 feet.\* The fact that only the joint at column 30 showed any significant opening would indicate that a compressive force existed across the other joints which was not relieved by the temperature change. Movement of the steel column tops during this temperature

---

\* Coefficient of linear expansion of steel =  $6.7 \times 10^{-6}$  ft./ft./°F, Steel Construction, AISC, New York, 1949, p.348.



change may also indicate that a stress existed in the crane beam and was transferred across the expansion joints. An examination of the general lean of the steel columns showed that while the leans were very erratic, it appeared that the tops were being pushed away from the zone of maximum settlement. This movement of the steel columns and compression of the crane beam would probably only occur if the base of the columns moved together.

The horizontal thrust transferred to the crane beam when the crane stops and starts at the ends of the potroom has also been suggested as a possible explanation for some of the lateral movement of the steel column tops. While this may be a contributing factor to the distortion of the superstructure there are other more probable causes. A factor which will be discussed later in greater detail is that the major shortening and the greatest amount of column disturbance lies in the region of maximum differential settlement. This suggests a relationship between settlement, column distortion and horizontal movement.

From the above reasoning it appeared likely that the deviation from design spacing, and the distortion of the superstructure were related in part at least to settlement of the buildings. The problem was therefore to find an explanation for, or relationship between settlement, horizontal movement, and column disturbance. A theory is suggested to account for the horizontal movement of the ground surface, but a detailed study of the distortion of the superstructure was not made.





### Surface Geometry

The first attempt to explain the shortening of the column line was to consider the change in length due to simple geometry. The plot of total settlement of each column hereafter referred to as the subsidence curve, was approximated by two straight lines joining each end to the point of maximum settlement. The two triangles formed by these sloping lines, the common vertical and the original horizontal surface were considered. By the Pythagoras theorem the length of the horizontal side was computed assuming the sloping length remained constant during the settlement. It was found by this method that the combined shortening would be less than .005 feet. Obviously another explanation was required.

### Similar Problems from other Sources

Literature on the subject of settlement and subsidence of the ground contains many examples of similar movements and resulting structural damage.

For many years the mining industry has been concerned because of subsidence at the surface over a mining area. The concern in this case is generally because many mines go beneath important existing structures which are susceptible to damage when the earth subsides. It has been observed that horizontal movements of the earth's surface is usually associated with vertical subsidence, and it is these horizontal movements which are most damaging to existing structures. Unfortunately much of the literature on this subject was in European publications,



mostly English and German, and not generally available in this country. The reason was perhaps that with the European population being more dense than in America, especially over the mining area, the problem is more acute in that part of the world. Much of the literature contained only a general description of ground subsidence at a particular area. However, many theories and explanations have been advanced to attempt to explain the horizontal movements which often occur when the ground subsides (20). The fact that new theories are still being advanced would indicate that much is yet to be learned. A thorough understanding seemed to be hampered somewhat because of lack of reliable data. Almost all writers stressed the need of more precise measurements, both horizontal and vertical, over a subsiding area.

Vertical and horizontal movements of the ground surface have also been a serious problem in areas where the water table has been lowered, or where oil has been pumped from its reservoir in the sand beneath the surface. In fact one author states that he knows of no "older oil field where sufficient data will not show subsidence" (23).

To indicate the similarity of the problem at Kitimat with other subsiding areas a few examples will be cited. In a recent textbook Henry (10) has noted several cases of ground subsidence with resulting horizontal movement. In the Netherlands a building 420' long with columns every 40'-10" subsided approximately 11 feet and had a maximum differential settlement of 6 inches between the ends of the building. The maximum horizontal movement was 3 inches per column bay. When the



differential settlement was  $1\frac{1}{2}$  inches over the length of the building, horizontal movements of plus and minus one inch per bay were observed. The seat of settlement was the mining of a nearby coal seam  $2\frac{1}{2}$  to 6 feet thick and 1300 to 2200 feet below the surface. Another example also cited by Henry was a horizontal movement of over two feet due to mining a coal seam approximately 2000 feet below the surface.

Gibson (7) has reviewed some general data regarding subsidence over a coal mining area. He gives the following general observations; depth of working - 250 yards, seam thickness - 3'-5", total subsidence - 2'-9", maximum slope of the ground surface 1.61 inches in 10 feet and horizontal movements of the order of 4 inches in 100 feet.

An example of subsidence due to lowering the ground water table has occurred at Houston Texas (17) where a 30 mile diameter area has subsided a maximum of 3.5 feet. This has been accompanied by faulting and horizontal movements of from 6 to 16 inches.

Shoemaker and Thorley (23) have described a maximum subsidence of 20 feet over the Wilmington oil field of Long Beach, California. The affected area is approximately 5 x 10 miles and horizontal movements have been of the order of 2 to 4 feet. Speaking of the same general area Henry cited an example of 11 feet vertical subsidence accompanied by a 5' shortening of a 6000 foot base line.

The most serious effects of ground subsidence appeared to be a result of the horizontal movements of the earths surface (7, 10 and 23). Structures which have been adversely affected are buildings, sewers and





drains, pavements, bridges, rivers, canals and railroads.

Henry stated that for buildings at least, horizontal movements can be discerned before vertical movements yet they and their associated horizontal forces are more difficult to account for in the structural design than vertical movement. References 7, 10 and 11 describe various ways of designing structures to withstand subsidence. In general, all were agreed that the most stable structure for a subsiding area is one which is free to move with the ground. A large number of closely spaced expansion joints and flexible connections are recommended to allow for considerable horizontal and vertical movement. They also recommend that between the joints the structure be as rigid as possible.

#### Description of the Subsidence Curve

The available literature was agreed on the physical characteristics of ground subsidence caused by mining, and the characteristics of subsidence curves from other causes seemed to follow this same pattern. A good description of the subsidence curve is given by Rellensmann (22) and is summarized on Figure 61. He states that the horizontal shifting is always toward the region of greatest subsidence, and the maximum shift occurs at the point of greatest slope of the subsidence curve. There is no horizontal movement at the middle of the subsidence trough and outside the zone of vertical settlement. This results in tension or stretching of the soil near the outside edges of the curve and compression





or shortening toward the zone of maximum settlement. Since soil can take little tension the outside zone often contains cracks. Rellensmann points out however that the cracks may be too small to be seen and their presence is indicated only by measurements.

Theories have been developed to attempt to calculate in advance the magnitude of vertical and horizontal movement. Rellensmann states that most of this work has been done in Germany. King and Smith (13) performed model tests to estimate surface movements. This was done by removing small blocks from the bottom of a container of sand. Their results were only of a qualitative nature but agreed with actual observed cases. In a recent paper Perz (20) has summarized the attempts to solve the subsidence problems under the following headings.

1. Statistical evaluation of measurements -- good for only one district from which measurements came.
2. Mathematical treatment based on certain assumptions.
3. Precalculation based on properties of overlying rock -- limited because of inadequate knowledge of rock properties.
4. Model tests -- questionable if they can reproduce field conditions.

He suggests that although there has been numerous attempts to solve the problem none are adequate. He proposes a solution based on "general logic" along with the basic assumptions for horizontal movement as shown in Figure 62. He assumes the soil within the area of influence to be composed of a number of triangular wedges.



When ore is removed these wedges slide into the void. Because the area of influence is wider at the surface than at the ore seam the sliding wedges have a lateral component of motion as shown. By assuming that the soil can withstand some tension and compression thus giving zero motion at the edges and at the middle of the subsidence trough a horizontal displacement curve similar in shape to that of Figure 61 is obtained. The expression for vertical movement contains several physical constants to be evaluated from particular cases and is not of interest to the Kitimat problem.

The equation for horizontal movement is based on the geometric shape of the subsidence curve and the depth to the mine seam. This procedure of fitting certain calculated curves to observed data appeared to be the method of solution used by most investigators.

While the Perz solution was interesting it was not expected that the results from its use would give perfect agreement to the observed data at Kitimat. The main reason was because the solution is based on removal of material from a well defined rectangular volume and contains as a major factor the depth  $h$  from the surface to this volume.

The seat of settlement at the Kitimat Smeltersite was at some considerable distance below the surface but the boundary was not well defined, and the volume decrease within the soil was not a simple rectangular shape as it is with the Perz solution of the mining problem.



### Horizontal Displacement Caused by Soil Consolidation

Although the equations based on mining subsidence may not strictly apply to the problem at Kitimat, there are certain geometric similarities which suggest that the problems are related. The seat of settlement was at an appreciable depth below the surface, and the subsidence curves were similar. It has been shown that very little settlement has occurred within the gravel layer since the buildings were constructed. This layer including the fill is from 50 to 120 feet thick.

### Basic Assumptions

On the basis of the slope of the subsidence curve at Kitimat a possible method of explaining the associated horizontal movements is suggested. The basic assumptions are as follows and the physical conditions are shown on Figure 63.

1. No settlement occurs in the upper gravel layer.
2. The line between the firm gravel, and the consolidating soil beneath is well defined, and at depth  $h$  from the surface.
3. The vertical movement at the surface is equal to that at depth  $h$ , hence the subsidence curve at depth  $h$  is parallel to that at the surface.
4. The gravel can withstand sufficient tension and compression strains to give zero lateral motion at the point of zero, and maximum settlement.





5. Perfect friction exists at the gravel-silt interface, and no sliding can occur along this surface.
6. No cracks can form within the soil which do not originate at the surface.

These assumptions were of course not completely met in the field. A small amount of settlement will occur within the upper gravel layer. The boundary between the gravel, and the consolidating soil will not be well defined. As explained by Taylor (24) the soil near the drainage face consolidates at a faster rate than the soil in the middle of the layer. Thus as consolidation proceeds the depth  $h$  will increase. Assumptions 3 to 6 were probably in close agreement with field conditions.

#### Mechanism of Movements

Consider any element of soil ABCD within the gravel layer (Figure 63). As a soft soil beneath this element consolidates, C moves vertically down to C' and D moves to D'. Since point D settles more than C the new position of the base of the element, C'D', will be inclined at an angle  $\alpha$  to the original base CD. Since there can be no slipping or tearing at the base of this element the line C'D' must be vertically below CD. To keep the angle between the base and sides of the element constant the surface points A and B must move laterally as well as vertically. By simple geometry it follows that for this assumption to be fulfilled the horizontal movement  $v$  of any point can be expressed by

$$v = h \cdot \alpha \quad (7)$$



where  $\alpha$  is the angle between the initial and final position of the base of the element. Assuming the subsidence at the surface to be parallel to that at the base, then  $\alpha$  is the angle between the initial surface and the subsidence curve.

#### Application to the Kitimat Problem

The following assumptions were made when applying the above equation to the conditions at Kitimat

$h$  = total depth of fill and natural gravel as shown on Figure 2.

$\alpha$  = the slope of the curve of settlement of buildings since their construction.

Computations for the horizontal movement by this method are shown on Tables X and XI. The results are shown plotted on Figures 64 and 65. These plots also show a comparison to the actual measurements.

It was previously stated that the measurements between each column was made only at the elevation of the steel base plate. Figures 68 and 69 were used to determine the distance between the columns at the ground surface. Each concrete column was plotted in its relative position and at the measured lean. The departure from design distance between the columns at the ground surface was then measured directly from the plot. Some starting point, which could be assumed to have not moved laterally was required in order to compute the total horizontal movement of any particular column. According to all the available information on ground subsidence the three possible choices were at the



center of the subsidence trough or point of maximum settlement, and beyond either edge of the subsidence effect. Having no measurements beyond the zone of settlement, the approximate center and lowest spot of the subsidence trough was chosen as the point of zero lateral motion. In each direction from this point the deviations from design spacing were accumulated to give the total lateral movement of each column base. On the same plot, Figures 64 and 65, is shown the lateral movement as computed from the Perz equation for mining subsidence.

These results show several interesting and significant factors.

1. The point of zero lateral motion is common to both solutions and agrees with the actual measurements.
2. There is close agreement at the end columns.
3. The computed movement at the intermediate columns appears to fluctuate considerably.
4. The Perz equation gives results far too large.

The first observation was expected since it is a basic assumption of the Perz equation, and of the calculations from observed data. Since the subsidence curve was horizontal at this approximate location the horizontal movement was therefore zero.

The most significant factor is the close agreement of the end columns. Since the overall distance was more accurately known than the distances between individual columns the close agreement indicated the correct nature of the equation. Fluctuation of movement at intermediate columns is probably partly due to inaccuracies in determining the actual





subsidence curve. To smooth out these irregularities the results of a computation based on average major changes in slope is shown on Figures 66 and 67. These curves show fair agreement, especially in geometric shape, with observed values at intermediate as well as at the end columns. It should also be noted that both observed and computed curves show that most of the horizontal movement has taken place in the region of maximum slope of the subsidence curve.

### Discussion of Results

The deviation between the observed and calculated values may be due to several causes.

1. Inaccuracies in the initial column setting, both vertically and horizontally. Small deviations from the recommended setting position would go unnoticed in the field, but would induce an error into the calculated movement.
2. Inaccuracy in determining the actual movement at the ground surface. These values were computed on the basis of horizontal distances measured at the top of the concrete column and the slope of the column to the ground.
3. Incorrect choice of the depth of gravel  $h$ . This value was based on Figure 2 which was in turn based on a comparatively few widely spaced test holes. The value for  $h$  could probably be considered as somewhat greater than the depth of gravel





since the underlying silt layer would probably be nearly completely consolidated for some distance from this surface.

The equation does account for any tension or compression forces in the gravel due to rotation of these elements about a neutral axis at the base. It would seem that these forces would in effect tend to smooth out small irregularities. Compressive forces would probably tend to decrease the movement near the center of the subsidence trough. The soil probably cracks in the tension zone and these forces would have little effect.

The movement between the end columns, i.e. the lengthening or shortening of the overall column line is of more significance than the relative movement of individual columns. Based on measurements taken December 5, which are believed to be the most accurate due to the care in correcting for the temperature changes, the calculated shortening of both column lines G and H were within 25 percent of the measured value. Of the three separate measurements taken on each column line, the one taken December 5 gave the largest deviation from the calculated value. It was interesting to note that the shortening as computed from the



other two sets of measurements varies by 10 to 15 percent from the shortening calculated on the basis of those taken December 5th. More than average care and caution was used when taking all measurements yet the difference between actual and the theoretical shortening is not appreciably different from the difference between individual measurements. It should be said that the actual measured overall distances agreed within 0.05 feet in the 1097 feet or to an accuracy of 1 : 22,000.

There was no significant difference between the observed or computed movements of column lines G and H and they will not be discussed separately. Many unknowns existed in both measured and computed horizontal shortening of these column lines. In view of this fact it would be a useful contribution to find an explanation for the pattern of movement alone. The close agreement of the actual values not only supports the validity of the basic equation, but indicated that the results obtained from its use are of the correct order of magnitude.

#### Gravel as a Beam

The preceeding theoretical computation was based on the fact that there would be zero lateral movement at the gravel silt interface. Another similar approach was to consider the gravel layer as a beam in deflection. According to beam theory (29) a surface exists within a deflecting beam which suffers no lateral expansion or contraction. This is called the neutral surface and for homogeneous beams of



symmetrical cross section is at midheight. For small deflections the horizontal movement,  $v$ , of a point not on the neutral surface relative to another point the same distance from the neutral surface can be expressed by the equation:

$$v = y \alpha \quad (8)$$

where  $y$  is the distance from the neutral surface to the point and  $\alpha$  is the angle change at the neutral surface.

If the upper gravel layer is considered as a deflecting beam then by this theory  $y$  becomes equal to  $h/2$  and the horizontal displacement,  $v$ , of a point at the surface is expressed by:

$$v = \frac{h \alpha}{2} \quad (9)$$

This is exactly one half the value of the previous method, or equation 7.

Adopting this formula to the case of column lines G and H would in effect reduce the computed lateral movement at all points by one half. As shown on Figures 66 and 67 this results in close agreement with observed data in the central zone, but the disagreement at the ends of the building is greater than when computed by equation 7.

#### Comparison to Movement from Stress Computations

According to the beam theory, lateral movement would occur at both the upper and lower surfaces of the gravel layer. The direction of movement at the upper surface would be toward the zone of maximum settlement and the movement of the lower surface would be equal and in the opposite direction to that at the upper surface. Since no slipping





can occur at the gravel-silt interface the beam theory assumption requires lateral outward movement of the silt layer also. This movement at the lower gravel-silt interface would be a maximum in the zone of maximum differential settlement and decrease to zero at the outer edges and at the point of maximum settlement.

In one respect the beam theory agreed nicely with the horizontal movements computed from the three dimensional stress analysis in Chapter III. Both cases showed lateral outward movement at the gravel-silt interface. This outward movement was of approximately the same order of magnitude, 0.25 to 0.50 feet maximum for both cases. An important difference is the fact that movement based on beam theory was a maximum in the zone of maximum differential settlement which at Kitimat was near the middle of the area. The movement in this zone based on the stress analysis was a minimum. At the edges where the stress consideration gives maximum lateral movement, values from the beam theory are small.

Movement computed by the beam theory alone gave results which agreed well with the observed movement. However, if movement from the beam theory were modified to account for the effect of a non vertical major principal stress the result would be in even closer agreement to the observed condition. Outward movement at the edges based on the stress consideration would tend to increase the total outward movement at the gravel-silt interface. This outward movement at depth would be reflected as an increased inward movement at the surface due



to rotation of vertical elements about the neutral axis of the gravel "beam". An opposite effect would occur near the center of the loaded area where lateral movement from the non-vertical major principal stress is small. If the neutral axis were considered to be at midheight of the gravel layer the combined movement at the ends of the potroom would exceed the observed movement by 0.2 to 0.3 feet. This is in contrast to the fact that movement due to beam theory alone was approximately 0.2 to 0.3 feet less than observed. Although it was not shown, it is probable that some of the movement at the base of the gravel layer due to a non-vertical major principal stress would be damped out. This would mean that less movement would be reflected at the surface and the net result would be closer agreement with the observed condition.

It seemed a significant fact that according to the available literature, cases of horizontal movement associated with ground subsidence were only noticed in areas where the seat of settlement was at some considerable depth below the surface. On the other hand, settlement occurring in shallow deposits did not seem to be bothered with this problem. The classical example of ground subsidence is at Mexico City. Here the entire city has been settling as a result of lowering the ground water table. This settlement is deep seated in deposits of volcanic clay which extend from the surface to an unknown depth. Cummings (4) and Leonardo (16) have discussed the foundation problem in this city with respect to the more important shallow settlement which results from heavy building loads. Differential settlements from this cause have amounted to as much as 5 or 6 feet between adjacent buildings



yet no mention is made of any horizontal movement. The major principal stress within the soil due to the extreme variation in building loads would almost certainly not be vertical. The fact that there appears to be no horizontal displacements resulting from this shallow seated settlement helps to verify the statement that horizontal movements only occur where the seat of settlement is at some distance below the ground surface.

### General Summary

In preceeding sections it was shown that the distance between the ends of Potroom 2A have shortened approximately one half foot since the building was constructed, it was further shown that this shortening has occurred mainly in the region of maximum differential settlement. Theoretical time curve matching showed that no consolidation has taken place within the upper gravel layer after completion of building construction, hence all building movement has been a result of consolidation within the lower silts and clays.

Subsidence as a result of mining, or removal of oil or water from deep below the surface has resulted in horizontal movements of the ground surface over a wide area. No such horizontal movements have been recorded for settlement due to shallow seated consolidation. Research into the problem of mining subsidence has established the general trend of this lateral displacement to be toward the zone of maximum subsidence with the greatest movement occurring in the zone of maximum differential settlement. When plotted in the same manner, the





lateral movement along Potroom 2A agreed in general with that of mining subsidence.

Two equations were proposed to account for the observed horizontal movement. Both equations assumed rotation of a vertical element about a neutral axis in the upper gravel layer. They were in fact modifications of the beam theory applied to the upper ground crust. When the neutral axis was assumed to be at the base of the gravel stratum the computed horizontal movements were too large in the region of maximum settlement, and slightly too small toward the ends of the potroom. When the neutral axis was assumed at midheight of the gravel layer the computed horizontal movements agreed with the observations in the region of maximum differential settlement, but were too small at the ends of the potroom.

The results of a model test verified the findings, both computed and observed, that there was movement of the ends of the column lines toward the zone of maximum settlement.

An analysis was also made on the effect of consolidation proceeding in the direction of the major principal stress. When the computed movements based on beam analogy were modified to account for the effect of a non-vertical major principal stress the results showed even better agreement with the observed movement.

It should be noted that the results from beam analogy computations alone gave results which were in good agreement with actual conditions. The effect of modifying the computations by accounting for the non-





vertical major principal stress, while beneficial, was not of sufficient importance for it to be a routine procedure for future computations of this kind.

### Conclusions

In the foregoing discussion it was shown that horizontal movement along the column lines could be explained on the basis of the upper gravel layer acting as a deflecting beam resting on deep compressible material. It was further shown that the effect of the non-vertical major principal stress within the compressible material acted in such a way as to cause shortening of the column line. When the results of the beam analogy were modified to account for the effect of a non-vertical major principal stress the resulting computed movement was in closer agreement to the observed movement than that computed by the beam analogy alone.

### Future Movement

In Chapter III it was shown that the settlement within the silt and clay layers was at the time of writing approximately 60 percent completed. Since the column lines have shortened one half foot at the time of writing it is probable that the future shortening will amount to approximately 0.3 feet and the total ultimate shortening will be approximately 0.8 feet when the settlement is completed.



Damage to the Superstructure

A general observation of the distortion of the superstructure indicates the source of damage to be the lateral movement at the ground surface. A detailed analysis of these distortions is beyond the scope of this study. Should research along this line be attempted in the future the pertinent data can be found on Figures 68 and 69 enclosed herewith.



## BIBLIOGRAPHY

1. Biot, M. A. Effects of Certain Discontinuities on the Pressure Distribution in a Loaded Soil. Physics, Dec. 1935. Reprinted in Harvard University Publication No. 172, (1935-36).
2. Burmister, Donald M. The Theory of Stress Displacements in Layered Systems and Applications to the Design of Airport Runways. Proceedings of the Highway Research Board, Vol. 23, 1943, p. 126-154.
3. Casagrande, A. Discussion of Paper by A. E. Cummings, Distribution of Stress Under a Foundation. Transactions of the American Society of Civil Engineers, Vol. 101, 1936, p. 1122.
4. Cummings, A. E. The Foundation Problem in Mexico City. Proceedings of the Seventh Texas Conference on Soil Mechanics and Foundation Engineering, January 23, and 24, 1947. The University of Texas.
5. Cummings, A. E. Foundation Stresses in an Elastic Solid With Underlying Boundary. Civil Engineering, Vol. 11, 1941, p. 665.
6. Fadum, Ralph M. Influence Values for Estimating Stresses in Elastic Foundations. Second International Conference on Soil Mechanics, Vol. III, p. 77.
7. Gibson, Donald. Buildings without Foundations, A Lecture on the Problems of Building on Moving Ground. The Journal of the Royal Institute of British Architects, Vol. 65, No. 2, December 1957, p. 47 - 59.
8. Gould, J. P. Analysis of Pore Pressure and Settlement Observations at Logan International Airport. Harvard University, Department of Engineering Publication, No. 476, 1949.
9. Hardy, R. M. and Ripley, Charles F. Foundation Investigation for the Kitimat Smelter. The Engineering Journal, November 1954. Vol. 37, n. 11, p. 1460 - 1466.
10. Henry, F. D. C. The Design and Construction of Engineering Foundations. McGraw-Hill 1956.
11. Hurst, G. Avoiding Subsidence Effects in Surface Buildings. Colliery Engineering, Vol. 25, 1948, p. 158 - 163, 194 - 198, 230 - 234.





12. Jurgenson, Leo. The Application of the Theories of Elasticity and Plasticity to Foundation Problems. (1934) Boston Society of Civil Engineers Contributions to Soil Mechanics 1925-1940.
13. King, H. J., and Smith, H. G. Surface Movements due to Mining. Colliery Engineering, Vol. 31, 1954, p. 322 - 329.
14. Krynine, D. P. Shearing Stress Underneath a Spread Foundation. Proceedings Highway Research Board, Vol. 18, Part II (1938) p. 49 - 56.
15. Lambe, T. W. Soil Testing for Engineers. Wiley 1951.
16. Leonardo, Zeevaert Jr. The Outline of a Mat Foundation Design on Mexico City Clay. Proceedings of the Seventh Texas Conference on Soil Mechanics and Foundation Engineering, January 23, and 24, 1947. The University of Texas.
17. Lockwood, Mason G. Ground Subsides in the Houston Area. Civil Engineering, Volume 24, 1950, p. 370 - 372.
18. Love, A. E. H. The Stress Produced in a Semi-infinite Solid by Pressure on Part of the Boundary. Philosophical Transactions of the Royal Society of London. Series A, Vol. 228, (1929) p. 377.
19. Newmark, N. M. Influence Charts for Computation of Stresses in Elastic Foundations. University of Illinois Bulletin 338, Vol. 40, n. 12, 1942.
20. Perz, F. Mathematical Relationships and Subsidence Troughs. Mine and Quarry Engineering, Vol. 23, n. 6, 1957, p. 256 - 260.
21. Pickett, Gerald. Stress Distribution in a Loaded Soil With Some Rigid Boundaries. Proceedings Highway Research Board, Vol. 18, Part II, 1938, p. 35 - 48.
22. Rellensmann, Otto. Rock Mechanics in Regard to Static Loading caused by Mining Excavation. Quarterly of the Colorado School of Mines; Behaviour of Materials in the Earths Crust, Vol. 52, n. 3 1957.
23. Shoemaker, R. R., and Thorley, T. S. Problems in Ground Subsidence. Journal American Waterworks Association, Vol. 47, 1955, p. 412 - 418.
24. Taylor, Donald W. Fundamentals of Soil Mechanics, Wiley 1948.



25. Terzaghi, Karl. Theoretical Soil Mechanics. Wiley, 1943
26. Terzaghi, Karl. Undisturbed Clay Samples and Undisturbed Clays. Boston Society of Civil Engineers, Contributions to Soil Mechanics, 1941 to 1953.
27. Terzaghi, Karl, and Ralph B. Peck. Soil Mechanics in Engineering Practice. Wiley, 1948.
28. Timmoshenko, S., and Goodier, J. N. Theory of Elasticity. McGraw-Hill Book Co. Inc. (1951).
29. Timmoshenko, S., and MacCullough, Gleason H. Elements of Strength of Materials. D. Van Nostrand Company Ltd. New York, 1940.
30. Way, Stewart. Some Observations on the Theory of Contact Pressures. Transactions of the American Society of Mechanical Engineers. Vol. 62, 1940, p. A-147 - A.157.
31. Westergaard, H. M. A Problem in Elasticity Suggested by a Problem in Soil Mechanics: Soft Material Reinforced by Numerous Strong Horizontal Sheets. Contributions to Mechanics of Solids on the Occasion of the 60th Anniversary of S. Timmoshenko, 1938. TheMacmillan Company.



## APPENDIX A

## TIME FACTOR VALUES

The following are values for time factor (T) at different degrees of consolidation (U), which were used in this study to match a theoretical time curve to the observed settlement time plots for Settlement Gauges 1 to 15. These values were taken from Curve I of Reference 24, page 237 and represent the case of linear variation of initial excess hydrostatic pressure.

U%	T
10	.008
20	.031
30	.071
40	.126
50	.197
60	.287
70	.403
80	.567
90	.848

Where required, time factors for intermediate values of U were computed from the approximate expressions

$$U \text{ less than } 60\% \quad T = \frac{\pi}{4} U^2$$

$$U \text{ greater than } 60\% \quad T = -0.9332 \log_{10} (1-U) - 0.0851$$

# PROBLEM 1

Let  $X_1, X_2, \dots, X_n$  be independent random variables with probability density functions  $f_1, f_2, \dots, f_n$  respectively. Let  $Y = X_1 + X_2 + \dots + X_n$ . Find the probability density function of  $Y$ .

Solution:

$X_1$	$X_2$
1	1
1	2
1	3
1	4
1	5
1	6
1	7
1	8
1	9
1	10

Then, the probability of  $Y$  is the sum of the probabilities of all the outcomes of  $Y$ .

Let  $Y = X_1 + X_2$ . Then, the probability of  $Y$  is

$$P(Y = y) = \sum_{x_1+x_2=y} P(X_1 = x_1, X_2 = x_2)$$

$$= \sum_{x_1+x_2=y} P(X_1 = x_1) P(X_2 = x_2)$$

## APPENDIX B

## NOTATION

<u>Symbol</u>	<u>Name</u>	<u>Dimension</u>
$C_c$	Compressive Index	
$c_v$	Coefficient of consolidation	$\text{cm}^2/\text{sec}$ or $\text{ft}^2/\text{day}$
$e$	Void ratio	dimensionless
$e_o$	Initial void ratio	dimensionless
$\Delta e$	Change in void ratio	dimensionless
$G_s$	Specific gravity of soil particles	dimensionless
$h$	Depth	ft.
$H$	Thickness of a soil layer or depth to a particular point	ft.
$P$	Pressure	tons/sq.ft.
$P_o$	Initial pressure	tons/sq.ft.
$\Delta P$	Change in Pressure	tons/sq.ft.
$S$	Settlement	ft.
$t$	Time	days
$t_{90}$	Time for 90% consolidation	days
$T$	$\frac{c_v t}{H^2}$ Time factor in theory of consolidation	dimensionless
$T_{90}$	$\frac{c_v t_{90}}{H^2}$ Time factor at 90% consolidation	dimensionless
$U$	Degree of consolidation	%
$U'$	Intermediate degree of consolidation	%





<u>Symbol</u>	<u>Name</u>	<u>Dimension</u>
$z, x, y$	Rectangular or Cartesian coordinates z positive down x positive south y positive west	ft.
$\alpha$	Angle of inclination between the subsidence curve and original ground surface	
$\cos \alpha$ $\cos \phi$ $\cos \gamma$	Cosines of angles between the coordinate axes and principal stresses	dimensionless
$\gamma_b$	Buoyant unit weight of soil	#/ft <sup>3</sup>
$\gamma_w$	Unit weight of water	#/ft <sup>3</sup>
$\Delta_{100}$	Theoretical 100% settlement within a soil stratum	
$\mu$	Poisson's ratio	dimensionless
$\sigma_x, \sigma_y, \sigma_z$	Normal stress	tons/sq.ft.
$\sigma_1$	Major principal stress	tons/sq.ft.
$\tau_{xy}, \tau_{zx}, \tau_{zy}$	Shearing stress	tons/sq.ft.



## APPENDIX C

## T A B L E S









SG	H	t <sub>90</sub>	C <sub>v</sub>	H	t <sub>90</sub>	C <sub>v</sub>	H	t <sub>90</sub>	C <sub>v</sub>	H	t <sub>90</sub>	C <sub>v</sub>
	SILT - SERIES A			CLAY - SERIES A			SILT	SERIES B			CLAY	SERIES B
1	170	4400	<u>5.55</u>	65	4000	<u>.90</u>	170	4000	6.10	65	4400	<u>.82</u>
2	160	2500	8.68	50	5650	.38	160	5650	<u>3.84</u>	50	2500	<u>.85</u>
3	170	4000	<u>6.10</u>	65	2500	<u>1.43</u>	170	2500	9.78	65	4000	.90
4	150	1800	10.60	60	5000	.61	150	5000	<u>3.82</u>	60	1800	<u>1.70</u>
5	105	6000	<u>1.54</u>	70	5500	<u>.76</u>	105	5500	1.70	70	6000	.69
6	170	4000	<u>6.10</u>	65	2500	<u>1.43</u>	170	2500	9.78	65	4000	.90
7	140	1500	11.10	70	6300	.66	140	6300	<u>2.62</u>	70	1500	<u>2.75</u>
8	85	3500	<u>2.06</u>	80	5200	<u>1.04</u>	85	5200	1.39	80	3500	1.55
9	170	4000	<u>6.10</u>	65	2500	<u>1.43</u>	170	2500	9.78	65	4000	.90
10	140	1500	<u>11.10</u>	75	6200	<u>.91</u>	140	6200	2.68	75	1500	3.75
11	60	2000	<u>1.57</u>	90	3800	<u>1.81</u>	60	3800	.82	90	2000	3.43
12	170	3800	<u>6.44</u>	65	3000	<u>1.19</u>	170	3000	8.14	65	3800	.94
13	135	1300	<u>11.9</u>	80	6000	<u>.90</u>	135	6000	2.58	80	1300	4.17
14	42	1000	<u>1.50</u>	105	5390	<u>1.74</u>	42	5390	.28	105	2000	4.68
15	115	7000	<u>1.66</u>	60	5000	<u>.61</u>	115	5000	2.24	60	7000	.44

SG = SETTLEMENT GAUGE  
H = THICKNESS OF LAYER - FT.  
t<sub>90</sub> = TIME IN DAYS FOR LAYER  
OF SOIL TO REACH 90%  
CONSOLIDATION

T<sub>90</sub> = 0.848

$$C_v = \frac{T_{90} H^2}{t_{90}} \quad \text{FT}^2/\text{DAY}$$

MOST PROBABLE VALUE UNDERLINED

COMPUTATION OF C<sub>v</sub>  
COEFFICIENT OF CONSOLIDATION  
TABLE I





# GRAVEL - $\gamma_b = 62 \text{ #/ft}^3$

# SILT - $\gamma_b = 57 \text{ #/ft}^3$

# CLAY - $\gamma_b = 57 \text{ #/ft}^3$

SG	ELEVATION BOTTOM OF STRIPPING = BOTTOM OF FILL	ELEVATION BOTTOM OF GRAVEL LAYER	ELEVATION MID POINT GRAVEL BELOW FILL POINT X	ORIGINAL GROUND SURFACE ELEVATION	DEPTH: ORIGINAL GROUND TO POINT X "D" FT	INITIAL STRESS AT POINT X $\gamma_b D$ $P_0$ T/ft <sup>2</sup>	INITIAL THICKNESS GRAVEL LAYER H FT	INITIAL THICKNESS H FT	SILT $\frac{1}{2} \gamma H$ T/ft <sup>2</sup>	GRAVEL $\gamma H$ T/ft <sup>2</sup>	INITIAL STRESS AT MIDPOINT SILT LAYER $P_0$ T/ft <sup>2</sup>	INITIAL THICKNESS H FT	CLAY $\frac{1}{2} \gamma H$ T/ft <sup>2</sup>	SILT $\gamma H$ T/ft <sup>2</sup>	INITIAL STRESS AT MID POINT CLAY LAYER $P_0$ T/ft <sup>2</sup>
1	+19	-85	-33	+24	57	1.77	109	170	2.42	3.38	5.80	65	.93	4.85	9.63
2	+22	-70	-24	+32	56	1.74	102	160	2.28	3.16	5.44	50	.71	4.56	8.43
3	+17	-85	-34	+22	56	1.74	107	170	2.42	3.32	5.74	65	.93	4.85	9.10
4	+19	-70	-26	+28	54	1.67	98	150	2.14	3.04	5.18	60	.86	4.27	8.17
5	+32	-20	+6	+36	30	.93	56	105	1.50	1.74	3.24	70	1.00	3.00	5.74
6	+16	-85	-34	+21	55	1.70	106	170	2.42	3.30	5.72	65	.93	4.85	9.08
7	+18	-75	-28	+26	54	1.67	101	140	2.00	3.13	5.13	70	1.00	4.00	8.13
8	+28	-10	+9	+32	22	.68	42	85	1.21	1.30	2.51	80	1.14	2.42	4.86
9	+13	-85	-36	+21	57	1.77	106	170	2.42	3.30	5.72	65	.93	4.85	9.08
10	+16	-80	-32	+24	56	1.74	104	140	2.00	3.22	5.22	75	1.07	4.00	8.29
11	+22	0	+11	+28	17	.53	28	60	.86	.87	1.73	90	1.28	1.71	3.86
12	+13	-85	-36	+18	54	1.67	103	170	2.42	3.20	5.62	65	.93	4.85	8.98
13	+15	-85	-35	+21	56	1.74	106	135	1.92	3.30	5.22	80	1.14	3.85	8.29
14	+14	0	+7	+25	18	.56	25	42	.60	.78	1.38	105	1.50	1.20	3.48
15	+30	-30	0	+36	36	1.12	66	115	1.64	2.02	3.66	60	.86	3.28	6.16

SG = SETTLEMENT GAUGE  
 $\gamma_b$  = BUOYANT UNIT WEIGHT OF SOIL  
 GRAVEL =  $62 \text{ #/ft}^3 = .031 \text{ T/ft}^2$   
 SILT & CLAY =  $57 \text{ #/ft}^3 = .0285 \text{ T/ft}^2$

$P_0$  = INITIAL STRESS  
 # = POUNDS  
 T/ft<sup>2</sup> = TONS/SQ. FT.  
 ft<sup>3</sup> = CUBIC FOOT

ZERO ELEVATION  
 EQUALS LOW TIDE

COMPUTATION OF  
 INITIAL STRESS -  $P_0$   
 TABLE II





SILT - SERIES A										CLAY - SERIES A													
MIDDLE CURVE = SILT BOTTOM CURVE = CLAY										MIDDLE = CLAY BOTTOM = SILT													
SG	DEPTH TO MID POINT OF LAYER FT	$e_0 / P_0$ INITIAL VOID RATIO & PRESSURE T/P'	$\Delta P$ STRESS INCREASE AT MID PT. OF LAYER T/P'	$\frac{P_0 + \Delta P}{P_0}$	$\log_{10} \frac{P_0 + \Delta P}{P_0}$	THICKNESS OF LAYER H FT	$\frac{1+e_0}{H \log_{10} \frac{P_0 + \Delta P}{P_0}}$	MIDDLE CURVE = SILT		MIDDLE = CLAY		DEPTH TO MID POINT OF LAYER FT	$e_0 / P_0$ T/P'	$\Delta P$ T/P'	$\frac{P_0 + \Delta P}{P_0}$	$\log_{10} \frac{P_0 + \Delta P}{P_0}$	THICKNESS OF LAYER H FT	$\frac{1+e_0}{H \log_{10} \frac{P_0 + \Delta P}{P_0}}$	BOTTOM CURVE = CLAY		MIDDLE CURVE = CLAY		
								S	$C_c$	S	$C_c$								S	$C_c$	S	$C_c$	
1	189	0.87 5.80	1.18	1.20	.080	170	.138	1.60	.221	1.25	.172	307	0.83 9.63	1.04	1.11	.046	65	.612	1.25	.766	1.60	.980	
2	172	.88 5.44	1.18	1.22	.088	160	.134	1.60	.214	2.60	.338	277	.85 8.43	1.15	1.14	.056	50	.661	2.60	1.72	1.60	1.06	
3	187	.88 5.74	1.29	1.22	.088	170	.128	1.30	.163	1.00	.128	305	.83 9.10	1.19	1.13	.053	65	.532	1.00	.532	1.30	.690	
4	165	.88 5.18	1.45	1.28	.107	150	.170	1.90	.222	2.28	.388	270	.85 8.17	1.37	1.17	.067	60	.460	2.28	1.05	1.90	.875	
5	105	.91 3.24	.98	1.30	.114	105	.160	1.50	.240	2.05	.327	192	.88 5.74	.96	1.17	.068	70	.396	2.05	.810	1.50	.594	
6	186	.88 5.72	1.28	1.23	.088	170	.126	1.27	.160	1.00	.126	304	.83 9.08	1.18	1.13	.053	65	.532	1.00	.532	1.27	.675	
7	163	.89 5.13	1.64	1.32	.120	140	.113	1.85	.208	2.65	.299	268	.85 8.13	1.55	1.19	.076	70	.348	2.65	.924	1.85	.644	
8	81	.91 2.51	1.26	1.50	.176	85	.187	2.35	.433	2.35	.433	163	.89 4.86	1.25	1.26	.100	80	.236	2.35	.555	2.35	.555	
9	183	.88 5.72	1.45	1.25	.099	170	.112	1.33	.149	1.00	.112	301	.84 9.08	1.32	1.15	.059	65	.480	1.00	.480	1.33	.639	
10	166	.88 5.22	1.74	1.33	.125	140	.107	1.70	.182	2.50	.268	274	.85 8.29	1.66	1.20	.080	75	.308	2.50	.770	1.70	.525	
11	52	.92 1.73	1.51	1.87	.273	60	.119	1.50	.179	5.10	.606	127	.90 3.86	1.46	1.38	.140	90	.151	5.10	.770	1.50	.226	
12	183	.88 5.62	1.48	1.26	.112	170	.099	1.25	.123	1.20	.119	301	.84 8.98	1.16	1.13	.053	65	.534	1.20	.640	1.25	.666	
13	165	.88 5.22	1.67	1.32	.112	135	.114	1.50	.171	2.40	.272	273	.85 8.29	1.43	1.17	.069	80	.335	2.40	.805	1.50	.502	
14	35	.93 1.38	1.75	2.27	.356	42	.129	1.85	.249	5.30	.685	108	.90 3.48	1.61	1.46	.165	105	.110	5.30	.581	1.85	.203	
15	117	.90 3.66	.78	1.21	.084	115	.192	1.35	.266	2.75	.541	205	.87 6.16	.76	1.12	.051	60	.611	2.75	1.68	1.35	.825	
NOTE: FOR EXPLANATION OF COLUMNS SEE FIRST COLUMNS OF THE SERIES										SG = SETTLEMENT T/P' = TONS / SQ. FT.		GAUGE		$C_c = \frac{S}{H} \frac{1+e_0}{\log_{10} \frac{P_0 + \Delta P}{P_0}}$		MOST PROBABLE VALUE UNDERLINED		SERIES A COMPUTATION OF $C_c$ COMPRESSIVE INDEX TABLE III					

Date		Time		Location		Remarks	
1942	10/10	12:00	12:15	1000	1000	1000	1000
1942	10/11	12:00	12:15	1000	1000	1000	1000
1942	10/12	12:00	12:15	1000	1000	1000	1000
1942	10/13	12:00	12:15	1000	1000	1000	1000
1942	10/14	12:00	12:15	1000	1000	1000	1000
1942	10/15	12:00	12:15	1000	1000	1000	1000
1942	10/16	12:00	12:15	1000	1000	1000	1000
1942	10/17	12:00	12:15	1000	1000	1000	1000
1942	10/18	12:00	12:15	1000	1000	1000	1000
1942	10/19	12:00	12:15	1000	1000	1000	1000
1942	10/20	12:00	12:15	1000	1000	1000	1000
1942	10/21	12:00	12:15	1000	1000	1000	1000
1942	10/22	12:00	12:15	1000	1000	1000	1000
1942	10/23	12:00	12:15	1000	1000	1000	1000
1942	10/24	12:00	12:15	1000	1000	1000	1000
1942	10/25	12:00	12:15	1000	1000	1000	1000
1942	10/26	12:00	12:15	1000	1000	1000	1000
1942	10/27	12:00	12:15	1000	1000	1000	1000
1942	10/28	12:00	12:15	1000	1000	1000	1000
1942	10/29	12:00	12:15	1000	1000	1000	1000
1942	10/30	12:00	12:15	1000	1000	1000	1000
1942	10/31	12:00	12:15	1000	1000	1000	1000



SILT - SERIES B						CLAY - SERIES B					
MIDDLE CURVE = SILT				BOTTOM CURVE = SILT		BOTTOM CURVE = CLAY			MIDDLE CURVE = CLAY		
S G	$\log \frac{P_0 + \Delta P}{P_0}$	S	C <sub>c</sub>	S	C <sub>c</sub>	$\log \frac{P_0 + \Delta P}{P_0}$	S	C <sub>c</sub>	S	C <sub>c</sub>	
1	.138	1.60	.221	1.25	.172	.612	1.25	.766	1.60	.980	
2	.134	1.60	.214	2.40	<u>.322</u>	.661	2.40	1.59	1.60	<u>1.06</u>	
3	.128	1.20	.154	1.00	.128	.532	1.00	.532	1.20	.638	
4	.170	1.90	.222	2.28	<u>.388</u>	.460	2.28	1.05	1.90	<u>.875</u>	
5	.160	1.50	.240	2.05	.327	.396	2.05	.810	1.50	.594	
6	.126	1.27	.160	1.00	.126	.532	1.00	.532	1.27	.675	
7	.113	1.85	.208	2.20	.248	.348	2.20	.766	1.85	.644	
8	.187	2.35	.433	2.35	.433	.236	2.35	.555	2.35	.555	
9	.112	1.33	.149	1.00	.112	.480	1.00	.480	1.33	.639	
10	.107	1.60	.171	2.40	<u>.258</u>	.308	2.40	.74	1.60	<u>.493</u>	
11	.119	1.35	.161	4.60	.621	.151	4.60	.695	1.35	.204	
12	.099	1.25	.123	1.20	.119	.534	1.20	.640	1.25	.666	
13	.114	1.50	.111	1.90	<u>.216</u>	.335	1.90	.675	1.50	<u>.502</u>	
14	.129	1.85	.249	4.40	.567	.110	4.40	.484	1.850	.203	
15	.192	1.45	.278	2.75	.541	.611	2.75	1.68	1.45	.886	
FOR EXPLANATION OF TERMS SEE TABLE						SERIES B COMPUTATION OF C <sub>c</sub> COMPRESSIVE INDEX TABLE IV					
						MOST PROBABLE VALUE UNDERLINED					





# GRAVEL - MOST PROBABLE FIT

SG	DEPTH TO MID POINT OF LAYER	INITIAL STRESS AT MID PT. OF LAYER $P_0$ T/d'	INCREASE IN STRESS FROM FILL AT MID PT OF LAYER $\Delta P$ T/d'	$\frac{P_0 + \Delta P}{P_0}$	$\log \frac{P_0 + \Delta P}{P_0}$	THICKNESS OF LAYER BELOW FILL H FT	SETTLEMENT WITHIN LAYER S FT	$\frac{S(1+e_0)}{H \log \frac{P_0 + \Delta P}{P_0}}$ $C_c$ for $e_0 = 0.66$
1	52	1.77	1.29	1.73	.237	104	1.20	.08
2	46	1.74	1.20	1.69	.228	92	.20	.02
3	52	1.74	1.38	1.79	.253	104	1.40	.09
4	45	1.67	1.49	1.89	.277	90	1.00	.07
5	26	.93	1.00	2.08	.317	52	.10	.01
6	50	1.70	1.36	1.80	.255	100	1.28	.08
7	47	1.67	1.71	2.02	.306	94	.90	.05
8	19	.68	1.40	3.06	.485	38	.50	.05
9	49	1.77	1.58	1.89	.277	98	1.40	.09
10	48	1.74	1.80	2.04	.308	96	1.00	.06
11	11	.53	1.52	3.86	.586	22	.15	.02
12	52	1.67	1.76	2.05	.312	104	1.65	.09
13	50	1.74	1.93	2.10	.323	100	1.10	.06
14	7	.56	1.80	4.21	.624	14	.65	.12
15	30	1.12	0.80	1.71	.233	60	.45	.05

$$C_c = \frac{S}{H} \frac{1+e_0}{\log \frac{P_0 + \Delta P}{P_0}}$$

GRAVEL  
COMPUTATION OF  $C_c$   
COMPRESSIVE INDEX  
TABLE ✓

# TABLE 3. SUMMARY OF DATA - 1964

STATION	DATE	TIME	WIND DIRECTION	WIND SPEED	WAVE DIRECTION	WAVE PERIOD	WAVE HEIGHT	WAVE LENGTH
1	1/1	10:00	100	10	100	10	10	10
2	1/2	11:00	110	11	110	11	11	11
3	1/3	12:00	120	12	120	12	12	12
4	1/4	13:00	130	13	130	13	13	13
5	1/5	14:00	140	14	140	14	14	14
6	1/6	15:00	150	15	150	15	15	15
7	1/7	16:00	160	16	160	16	16	16
8	1/8	17:00	170	17	170	17	17	17
9	1/9	18:00	180	18	180	18	18	18
10	1/10	19:00	190	19	190	19	19	19
11	1/11	20:00	200	20	200	20	20	20
12	1/12	21:00	210	21	210	21	21	21
13	1/13	22:00	220	22	220	22	22	22
14	1/14	23:00	230	23	230	23	23	23
15	1/15	00:00	240	24	240	24	24	24
16	1/16	01:00	250	25	250	25	25	25
17	1/17	02:00	260	26	260	26	26	26
18	1/18	03:00	270	27	270	27	27	27
19	1/19	04:00	280	28	280	28	28	28
20	1/20	05:00	290	29	290	29	29	29
21	1/21	06:00	300	30	300	30	30	30
22	1/22	07:00	310	31	310	31	31	31
23	1/23	08:00	320	32	320	32	32	32
24	1/24	09:00	330	33	330	33	33	33
25	1/25	10:00	340	34	340	34	34	34
26	1/26	11:00	350	35	350	35	35	35
27	1/27	12:00	360	36	360	36	36	36
28	1/28	13:00	370	37	370	37	37	37
29	1/29	14:00	380	38	380	38	38	38
30	1/30	15:00	390	39	390	39	39	39
31	1/31	16:00	400	40	400	40	40	40
32	1/32	17:00	410	41	410	41	41	41
33	1/33	18:00	420	42	420	42	42	42
34	1/34	19:00	430	43	430	43	43	43
35	1/35	20:00	440	44	440	44	44	44
36	1/36	21:00	450	45	450	45	45	45
37	1/37	22:00	460	46	460	46	46	46
38	1/38	23:00	470	47	470	47	47	47
39	1/39	00:00	480	48	480	48	48	48
40	1/40	01:00	490	49	490	49	49	49
41	1/41	02:00	500	50	500	50	50	50
42	1/42	03:00	510	51	510	51	51	51
43	1/43	04:00	520	52	520	52	52	52
44	1/44	05:00	530	53	530	53	53	53
45	1/45	06:00	540	54	540	54	54	54
46	1/46	07:00	550	55	550	55	55	55
47	1/47	08:00	560	56	560	56	56	56
48	1/48	09:00	570	57	570	57	57	57
49	1/49	10:00	580	58	580	58	58	58
50	1/50	11:00	590	59	590	59	59	59
51	1/51	12:00	600	60	600	60	60	60
52	1/52	13:00	610	61	610	61	61	61
53	1/53	14:00	620	62	620	62	62	62
54	1/54	15:00	630	63	630	63	63	63
55	1/55	16:00	640	64	640	64	64	64
56	1/56	17:00	650	65	650	65	65	65
57	1/57	18:00	660	66	660	66	66	66
58	1/58	19:00	670	67	670	67	67	67
59	1/59	20:00	680	68	680	68	68	68
60	1/60	21:00	690	69	690	69	69	69
61	1/61	22:00	700	70	700	70	70	70
62	1/62	23:00	710	71	710	71	71	71
63	1/63	00:00	720	72	720	72	72	72
64	1/64	01:00	730	73	730	73	73	73
65	1/65	02:00	740	74	740	74	74	74
66	1/66	03:00	750	75	750	75	75	75
67	1/67	04:00	760	76	760	76	76	76
68	1/68	05:00	770	77	770	77	77	77
69	1/69	06:00	780	78	780	78	78	78
70	1/70	07:00	790	79	790	79	79	79
71	1/71	08:00	800	80	800	80	80	80
72	1/72	09:00	810	81	810	81	81	81
73	1/73	10:00	820	82	820	82	82	82
74	1/74	11:00	830	83	830	83	83	83
75	1/75	12:00	840	84	840	84	84	84
76	1/76	13:00	850	85	850	85	85	85
77	1/77	14:00	860	86	860	86	86	86
78	1/78	15:00	870	87	870	87	87	87
79	1/79	16:00	880	88	880	88	88	88
80	1/80	17:00	890	89	890	89	89	89
81	1/81	18:00	900	90	900	90	90	90
82	1/82	19:00	910	91	910	91	91	91
83	1/83	20:00	920	92	920	92	92	92
84	1/84	21:00	930	93	930	93	93	93
85	1/85	22:00	940	94	940	94	94	94
86	1/86	23:00	950	95	950	95	95	95
87	1/87	00:00	960	96	960	96	96	96
88	1/88	01:00	970	97	970	97	97	97
89	1/89	02:00	980	98	980	98	98	98
90	1/90	03:00	990	99	990	99	99	99
91	1/91	04:00	1000	100	1000	100	100	100
92	1/92	05:00	1010	101	1010	101	101	101
93	1/93	06:00	1020	102	1020	102	102	102
94	1/94	07:00	1030	103	1030	103	103	103
95	1/95	08:00	1040	104	1040	104	104	104
96	1/96	09:00	1050	105	1050	105	105	105
97	1/97	10:00	1060	106	1060	106	106	106
98	1/98	11:00	1070	107	1070	107	107	107
99	1/99	12:00	1080	108	1080	108	108	108
100	1/100	13:00	1090	109	1090	109	109	109

U.S. DEPARTMENT OF COMMERCE  
BUREAU OF MARINE RESEARCH  
WASHINGTON, D.C. 20540

U.S. DEPARTMENT OF COMMERCE  
BUREAU OF MARINE RESEARCH  
WASHINGTON, D.C. 20540



# TABLE VI

## SUMMARY OF THEORETICAL TIME CURVES MOST PROBABLE FIT

SETTLE- MENT GAUGE	THEORETICAL MAX. TOTAL SETLMT. FT.	TIME FOR 90% TOTAL SETLMT. DAYS	DATE FOR 90% TOTAL SETLMT.	% TOTAL SETLMT, COMPLETE SEPT. 1957	TOTAL SETLMT OF BLDG TO SEPT. '57 FT.	THEORETICAL TOTAL SETLMT OF BLDGS FT.	% BLDG SETLMT COMPLETE SEPT. 1957
1	4.05	3400	1962	77			
2	4.40	4300	1964	69			
3	3.70	2700	1960	84	1.4	2.0	70
4	5.18	3500	1962	81	2.3	3.3	70
5	3.65	6000	1969	61	1.4	2.9	48
6	3.55	2700	1960	82	1.3	1.9	68
7	5.40	4000	1963	76	2.1	3.4	62
8	5.18	4600	1965	70	2.1	3.7	57
9	3.75	2700	1960	84	1.1	1.8	62
10	5.00	3000	1961	81	2.0	3.1	64
11	6.75	3500	1962	74	3.0	4.8	63
12	4.10	2700	1960	83	1.2	1.9	63
13	4.50	2700	1960	85	1.7	2.4	71
14	7.80	4600	1965	72	3.2	5.5	58
15	4.65	6400	1970	61 JUNE 28			

NOTE: BUILDING SETTLEMENT REFERS ONLY  
TO POTLINES 1 & 2



# TABLE VII

## SUMMARY OF CONSOLIDATION FACTORS

	GRAVEL		SILT			CLAY	
	$C_c$		$C_v$ ft <sup>2</sup> /day	$C_c$		$C_v$ ft <sup>2</sup> /day	$C_c$
AVERAGE LAB. TESTS	No Tests		1.0 To 3.0	.14		0.4 To 0.8	.25
EXPECTED IN NATURE			3.0 To 9.0	.25 To .44		1.2 To 2.4	.34 To .60
SG 1	.08		5.6	.22		.9	.77
2	.02		3.8	.32		.9	1.06
3	.09		6.1	.16		1.4	.53
4	.07		3.8	.39		1.7	.88
5	.01		1.5	.33		.8	.59
6	.08		6.1	.16		1.4	.53
7	.05		2.6	.30		2.7	.64
8	.05		2.1	.43		1.0	.56
9	.09		6.1	.15		1.4	.48
10	.06		11.1	.26		.9	.49
11	.02		1.6	.18		1.8	.77
12	.09		6.4	.12		1.2	.64
13	.06		11.9	.22		.9	.50
14	.12		1.5	.25		1.7	.58
15	.05		1.7	.54		0.6	.83

NOTE:  $C_v$  IN NATURE EXPECTED TO BE APPROX. 3 TIMES LAB. TEST DUE TO LARGE HORIZONTAL PERMEABILITY (GOULD - Ref. 8)

$C_c$  IN NATURE ESTIMATED AS OUTLINED BY TERZAGHI & PECK (REF. 27)





LOCATION		POISSONS RATIO	COMPONENTS OF STRESS						MAJOR PRINCIPAL STRESS	HORIZONTAL COMPONENTS OF $\sigma_1$ IN PERCENT OF VERTICAL STRESS				SETTLEMENT OF POINT	THEORETICAL HORIZONTAL MOVEMENT			
Settlement Gauge No.	Depth Below Fill Ft.	$\mu$	$\sigma_x$ T/psf	$\sigma_y$ T/psf	$\sigma_z$ T/psf	$\tau_{xy}$ T/psf	$\tau_{zx}$ T/psf	$\tau_{zy}$ T/psf	$\sigma_1$ T/psf	X-direction + = South % - = North %		Y-direction + = East % - = West %		Depth of Pt. To JUNE 1957 Since Bldg Constructed Depth of silt & clay % Ft.	SOUTH Ft.	NORTH Ft.	EAST Ft.	WEST Ft.
6	50	0.5	1.24	1.14	1.37	-.04	-.03	+.17	1.50		- 19	+ 40		over 100	1.41		.27	.56
6	150	0.5	.98	.80	1.30	-.03	-.05	+.18	1.40		- 10	+ 30		85	1.24		.12	.33
6	250	0.5	.83	.65	1.20	-.02	-.07	+.18	1.29		- 15	+ 28		62	.71		.11	.20
6	150	0	.54	.36	1.30	-.01	-.05	+.18	1.32		- 6	+ 19		85	1.24		.07	.24
7	50	0.5	1.35	1.39	1.72	0	-.03	-.01	1.73		- 8		- 3	over 100	2.17		.15	.04
7	150	.5	1.08	1.17	1.65	-.03	-.03	-.04	1.66		- 5		- 8	72	1.56		.08	.12
7	250	.5	.92	.98	1.57	-.03	-.04	-.04	1.57		- 6		- 7	29	.63		.04	.04
7	150	0	.48	.49	1.65	+.04	-.03	-.04	1.65		- 3		- 3	72	1.56		.05	.05
8	50	.5	1.13	1.11	1.29	+.02	-.05	-.06	1.37		- 21		- 23	over 100	2.12		.44	.48
8	150	.5	.80	.82	1.26	0	-.05	-.16	1.35		- 9		- 30	40	.85		.08	.25
8	250	.5	.71	.69	1.20	0	-.14	-.21	1.29		- 24		- 35	-	-		0	0
8	150	0	.36	.28	1.26	-.01	-.05	-.16	1.28		- 6		- 16	40	.85		.05	.14

SG	Depth Ft.	X-Comp. $\mu=0.5$ %	X-Comp. $\mu=0$ %	RATIO $\frac{\tau_{\mu=0}}{\tau_{\mu=0.5}}$	Y-Comp. $\mu=0.5$ %	Y-Comp. $\mu=0$ %	RATIO $\frac{\tau_{\mu=0}}{\tau_{\mu=0.5}}$
6	150	-10	-6	.6	+30	+19	.6
7	150	-5	-3	.6	-8	-3	.4
8	150	-9	-6	.7	-30	-16	.5
9	150	+5	0		+28	+15	.5
10	150	+9	+6	.7	-8	-3	.4
11	150	0	0		-20	-10	.5

TABLE VIII

RESULTS OF STRESS  
COMPUTATION  
AND  
HORIZONTAL MOVEMENT

Table 1					Table 2		
Year	Month	Day	Time	Location	Year	Month	Day
1950	Jan	1	10:00	1000	1950	Jan	1
1950	Jan	2	10:00	1000	1950	Jan	2
1950	Jan	3	10:00	1000	1950	Jan	3
1950	Jan	4	10:00	1000	1950	Jan	4
1950	Jan	5	10:00	1000	1950	Jan	5
1950	Jan	6	10:00	1000	1950	Jan	6
1950	Jan	7	10:00	1000	1950	Jan	7
1950	Jan	8	10:00	1000	1950	Jan	8
1950	Jan	9	10:00	1000	1950	Jan	9
1950	Jan	10	10:00	1000	1950	Jan	10
1950	Jan	11	10:00	1000	1950	Jan	11
1950	Jan	12	10:00	1000	1950	Jan	12
1950	Jan	13	10:00	1000	1950	Jan	13
1950	Jan	14	10:00	1000	1950	Jan	14
1950	Jan	15	10:00	1000	1950	Jan	15
1950	Jan	16	10:00	1000	1950	Jan	16
1950	Jan	17	10:00	1000	1950	Jan	17
1950	Jan	18	10:00	1000	1950	Jan	18
1950	Jan	19	10:00	1000	1950	Jan	19
1950	Jan	20	10:00	1000	1950	Jan	20
1950	Jan	21	10:00	1000	1950	Jan	21
1950	Jan	22	10:00	1000	1950	Jan	22
1950	Jan	23	10:00	1000	1950	Jan	23
1950	Jan	24	10:00	1000	1950	Jan	24
1950	Jan	25	10:00	1000	1950	Jan	25
1950	Jan	26	10:00	1000	1950	Jan	26
1950	Jan	27	10:00	1000	1950	Jan	27
1950	Jan	28	10:00	1000	1950	Jan	28
1950	Jan	29	10:00	1000	1950	Jan	29
1950	Jan	30	10:00	1000	1950	Jan	30
1950	Jan	31	10:00	1000	1950	Jan	31

Table 3					Table 4		
Year	Month	Day	Time	Location	Year	Month	Day
1950	Jan	1	10:00	1000	1950	Jan	1
1950	Jan	2	10:00	1000	1950	Jan	2
1950	Jan	3	10:00	1000	1950	Jan	3
1950	Jan	4	10:00	1000	1950	Jan	4
1950	Jan	5	10:00	1000	1950	Jan	5
1950	Jan	6	10:00	1000	1950	Jan	6
1950	Jan	7	10:00	1000	1950	Jan	7
1950	Jan	8	10:00	1000	1950	Jan	8
1950	Jan	9	10:00	1000	1950	Jan	9
1950	Jan	10	10:00	1000	1950	Jan	10
1950	Jan	11	10:00	1000	1950	Jan	11
1950	Jan	12	10:00	1000	1950	Jan	12
1950	Jan	13	10:00	1000	1950	Jan	13
1950	Jan	14	10:00	1000	1950	Jan	14
1950	Jan	15	10:00	1000	1950	Jan	15
1950	Jan	16	10:00	1000	1950	Jan	16
1950	Jan	17	10:00	1000	1950	Jan	17
1950	Jan	18	10:00	1000	1950	Jan	18
1950	Jan	19	10:00	1000	1950	Jan	19
1950	Jan	20	10:00	1000	1950	Jan	20
1950	Jan	21	10:00	1000	1950	Jan	21
1950	Jan	22	10:00	1000	1950	Jan	22
1950	Jan	23	10:00	1000	1950	Jan	23
1950	Jan	24	10:00	1000	1950	Jan	24
1950	Jan	25	10:00	1000	1950	Jan	25
1950	Jan	26	10:00	1000	1950	Jan	26
1950	Jan	27	10:00	1000	1950	Jan	27
1950	Jan	28	10:00	1000	1950	Jan	28
1950	Jan	29	10:00	1000	1950	Jan	29
1950	Jan	30	10:00	1000	1950	Jan	30
1950	Jan	31	10:00	1000	1950	Jan	31



# PRECISE MEASUREMENT BETWEEN CENTER

## LINES OF STEEL COLUMNS G & H 1 to 48

### AT THE ELEVATION OF THE STEEL BASEPLATE

#### NOVEMBER & DECEMBER 1957

DATE OF MEASUREMENT AND REMARKS	COLUMN LINE G			COLUMN LINE H	
	MEASURE- MENT	DEVIATION FROM DESIGN		MEASURE- MENT	DEVIATION FROM DESIGN
DESIGN DISTANCE	1096.667	0		1096.667	0
NOV. 25, 1957 — at steel base plates. Chain supported at each column. Temperature read at 23 & 73 Ft. Mk.	1096.185	-.482		1096.292	-.375
NOV. 26, 1957 — along working floor. Chain fully supported. Temp. at 25 & 75 Ft. Mk.	1096.212	-.455		1096.252	-.415
DEC. 5, 1957 — at steel base plate. Chain supported at each column. Temp at each column.	1096.159	-.508		1096.220	-.447
Difference in length - H longer than G as aligned by transit.			.047		
Effect of concrete column lean on measured shortening at ground	Shortening decreased	+ 0.10		Shortening increased	-.031
Deviation from design at ground calculated from measured distance and column lean	<div> Nov. 25 Nov. 26 Dec. 5. </div>	<div> -.472 -.445 -.498 </div>			<div> -.406 -.446 -.478 </div>

### COMPARISON OF DIFFERENT CALCULATIONS

	% DIFF.	VALUE	% DIFF.	VALUE
DEC. 5 measurement assumed correct	0	.498	0	.478
Difference between end columns from accumulative measurement	10	.45	4	.46
Difference between end columns calculated by $v = h\alpha$	23	.380	25	.356
Difference between end columns calculated by $v = \frac{h\alpha^2}{2}$	62	.19	62	.18

TABLE IX

MEASURED & COMPUTED HORIZONTAL DISTANCES



TABLE X

## COLUMN LINE G - HORIZONTAL DISPLACEMENT

COMPUTED FROM $V = h \times \alpha$				FIELD CONDITION	
COLUMNS	SLOPE	h	HORIZ. MOVEMENT	DEPARTURE FROM DESIGN SPACING	ACCUMULATIVE HORIZONTAL MOVEMENT
	$\alpha$ %	FT.	$h \cdot \alpha$ FT	FT	FT
1 - 2	0.344 E	50	.172 E	+ .02	-.16
2 - 3	.386	55	.216	-.02	-.18
3 - 4	.214	55	.118	-.04	-.16
4 - 5	.172	60	.103	+ .01	-.12
5 - 6	.214	60	.128	-.02	-.13
6 - 7	.214	65	.138	-.02	-.11
7 - 8	.300	70	.210	0	-.09
8 - 9	.258	75	.194	+ .02	-.09
9 - 10	.300	75	.225	-.08	-.11
10 - 11	.343	80	.274	+ .01	-.03
11 - 12	.129	85	.110	- .04	-.04
12 - 13	.300 E	85	.256 E	0	0
13 - 14	0	90	0	0	0
14 - 15	.172 E	90	.155 E	-.09	-.09
15 - 16	.129 W	95	.123 W	+ .01	-.08
16 - 17	.172	100	.172	+ .01	-.07
17 - 18	.086	105	.096	+ .06	-.13
18 - 19	.258	105	.271	+ .01	-.12
19 - 20	.129	110	.142	+ .04	-.11
20 - 21	.300	115	.333	-.04	-.15
21 - 22	.300	115	.345	-.02	-.17
22 - 23	.300	115	.345	-.09	-.26
23 - 24	.343	120	.412	-.03	-.29
24 - 25	.558	120	.665	+ .03	-.26
25 - 26	.412	120	.566	+ .09	-.17
26 - 27	.258	120	.310	-.14	-.31
27 - 28	.386	120	.475	0	-.31
28 - 29	.600	120	.720	+ .01	-.30
29 - 30	.086	120	.098	-.03	-.33
30 - 31	.257	120	.308	+ .04	-.29
31 - 32	.386	120	.424	-.02	-.31
32 - 33	.129	120	.155	+ .01	-.30
33 - 34	.172	120	.206	0	-.30
34 - 35	.043	120	.052	+ .03	-.27
35 - 36	.343	120	.412	-.02	-.29
36 - 37	.086	120	.103	+ .01	-.28
37 - 38	0	120	0	0	-.28
38 - 39	.172	120	.206	-.03	-.31
39 - 40	.172	120	.206	+ .02	-.29
40 - 41	.129	120	.155	-.01	-.30
41 - 42	.129	120	.155	+ .02	-.28
42 - 43	0	120	0	-.04	-.32
43 - 44	.300	120	.360	-.03	-.35
44 - 45	0	120	0	+ .02	-.33
45 - 46	.214	120	.257	-.03	-.36
46 - 47	.214	120	.257	+ .07	-.29
47 - 48	.172	120	.208	0	-.29

(13)

ASSUME ZERO MOVEMENT OF COLUMN



COAST GUARD LINE C - HORIZONTAL

COAST GUARD LINE C - HORIZONTAL

COAST GUARD LINE C - HORIZONTAL

STATION	COORDINATE	COORDINATE	COORDINATE	COORDINATE
1	1000	1000	1000	1000
2	1000	1000	1000	1000
3	1000	1000	1000	1000
4	1000	1000	1000	1000
5	1000	1000	1000	1000
6	1000	1000	1000	1000
7	1000	1000	1000	1000
8	1000	1000	1000	1000
9	1000	1000	1000	1000
10	1000	1000	1000	1000
11	1000	1000	1000	1000
12	1000	1000	1000	1000
13	1000	1000	1000	1000
14	1000	1000	1000	1000
15	1000	1000	1000	1000
16	1000	1000	1000	1000
17	1000	1000	1000	1000
18	1000	1000	1000	1000
19	1000	1000	1000	1000
20	1000	1000	1000	1000
21	1000	1000	1000	1000
22	1000	1000	1000	1000
23	1000	1000	1000	1000
24	1000	1000	1000	1000
25	1000	1000	1000	1000
26	1000	1000	1000	1000
27	1000	1000	1000	1000
28	1000	1000	1000	1000
29	1000	1000	1000	1000
30	1000	1000	1000	1000
31	1000	1000	1000	1000
32	1000	1000	1000	1000
33	1000	1000	1000	1000
34	1000	1000	1000	1000
35	1000	1000	1000	1000
36	1000	1000	1000	1000
37	1000	1000	1000	1000
38	1000	1000	1000	1000
39	1000	1000	1000	1000
40	1000	1000	1000	1000
41	1000	1000	1000	1000
42	1000	1000	1000	1000
43	1000	1000	1000	1000
44	1000	1000	1000	1000
45	1000	1000	1000	1000
46	1000	1000	1000	1000
47	1000	1000	1000	1000
48	1000	1000	1000	1000
49	1000	1000	1000	1000
50	1000	1000	1000	1000
51	1000	1000	1000	1000
52	1000	1000	1000	1000
53	1000	1000	1000	1000
54	1000	1000	1000	1000
55	1000	1000	1000	1000
56	1000	1000	1000	1000
57	1000	1000	1000	1000
58	1000	1000	1000	1000
59	1000	1000	1000	1000
60	1000	1000	1000	1000
61	1000	1000	1000	1000
62	1000	1000	1000	1000
63	1000	1000	1000	1000
64	1000	1000	1000	1000
65	1000	1000	1000	1000
66	1000	1000	1000	1000
67	1000	1000	1000	1000
68	1000	1000	1000	1000
69	1000	1000	1000	1000
70	1000	1000	1000	1000
71	1000	1000	1000	1000
72	1000	1000	1000	1000
73	1000	1000	1000	1000
74	1000	1000	1000	1000
75	1000	1000	1000	1000
76	1000	1000	1000	1000
77	1000	1000	1000	1000
78	1000	1000	1000	1000
79	1000	1000	1000	1000
80	1000	1000	1000	1000
81	1000	1000	1000	1000
82	1000	1000	1000	1000
83	1000	1000	1000	1000
84	1000	1000	1000	1000
85	1000	1000	1000	1000
86	1000	1000	1000	1000
87	1000	1000	1000	1000
88	1000	1000	1000	1000
89	1000	1000	1000	1000
90	1000	1000	1000	1000
91	1000	1000	1000	1000
92	1000	1000	1000	1000
93	1000	1000	1000	1000
94	1000	1000	1000	1000
95	1000	1000	1000	1000
96	1000	1000	1000	1000
97	1000	1000	1000	1000
98	1000	1000	1000	1000
99	1000	1000	1000	1000
100	1000	1000	1000	1000

TABLE XI

COLUMN LINE H - HORIZONTAL DISPLACEMENT						
COMPUTED FROM $v = h \cdot \alpha$				FIELD CONDITION		
COLUMNS	SLOPE	h	HORIZ. MOVEMENT		DEPARTURE FROM DESIGN SPACING	ACCUMULATIVE HORIZONTAL MOVEMENT
	$\alpha$ %	FT	$h \cdot \alpha$ FT		FT	FT
1 to 2	0.300 E	50	0.150 E	-	- .03	- .17
2 - 3	.172	55	.094		+ .05	+ .14
3 - 4	.214	55	.118		- .02	- .19
4 - 5	.300	60	.180		- .01	- .17
5 - 6	.129	60	.077		+ .02	- .16
6 - 7	.343	65	.223		- .01	- .18
7 - 8	.386	70	.270		- .01	- .17
8 - 9	.214	75	.161		- .04	- .16
9 - 10	.300	75	.225		- .04	- .12
10 - 11	.471	80	.377		+ .05	- .08
11 - 12	.214	85	.207		+ .04	- .13
12 - 13	.129	85	.110		0	- .09
13 - 14	.172	90	.155		0	- .09
14 - 15	.257	90	.231		- .09	0
15 - 16	.086	95	.082		- .02	0
16 - 17	.129 E	100	.129 E		+ .02	+ .02
17 - 18	0	105	0		- .04	- .04
18 - 19	.043 W	105	.045 W		- .03	- .07
19 - 20	.043	110	.047		- .03	- .10
20 - 21	.300	110	.330		+ .01	- .09
21 - 22	.214	115	.246		- .03	- .12
22 - 23	.214	115	.246		- .02	- .14
23 - 24	.471	120	.565		- .09	- .23
24 - 25	.471	120	.565		+ .05	- .18
25 - 26	.086	120	.103		- .07	- .25
26 - 27	.428	120	.514		+ .05	- .20
27 - 28	.343	120	.411		- .08	- .28
28 - 29	.556	120	.666		+ .04	- .24
29 - 30	.428	120	.514		+ .04	- .20
30 - 31	.300	120	.360		- .05	- .25
31 - 32	.172	120	.206		0	- .25
32 - 33	.129	120	.155		0	- .25
33 - 34	.129	120	.155		+ .05	- .20
34 - 35	.257	120	.321		+ .01	- .19
35 - 36	.214	120	.256		- .02	- .21
36 - 37	.214	120	.256		0	- .21
37 - 38	.172	120	.206		+ .01	- .20
38 - 39	.300	120	.360		- .02	- .22
39 - 40	.257	120	.308		0	- .22
40 - 41	.471	120	.565		0	- .22
41 - 42	.257	120	.308		- .02	- .24
42 - 43	.129	120	.155		0	- .24
43 - 44	.086	120	.103		- .01	- .25
44 - 45	.172	120	.206		+ .01	- .24
45 - 46	.129	120	.155		- .02	- .26
46 - 47	.172	120	.206		0	- .26
47 - 48	.172	120	.206		- .03	- .29

ASSUME ZERO MOVEMENT OF COLUMN ⑩

## 18 31807



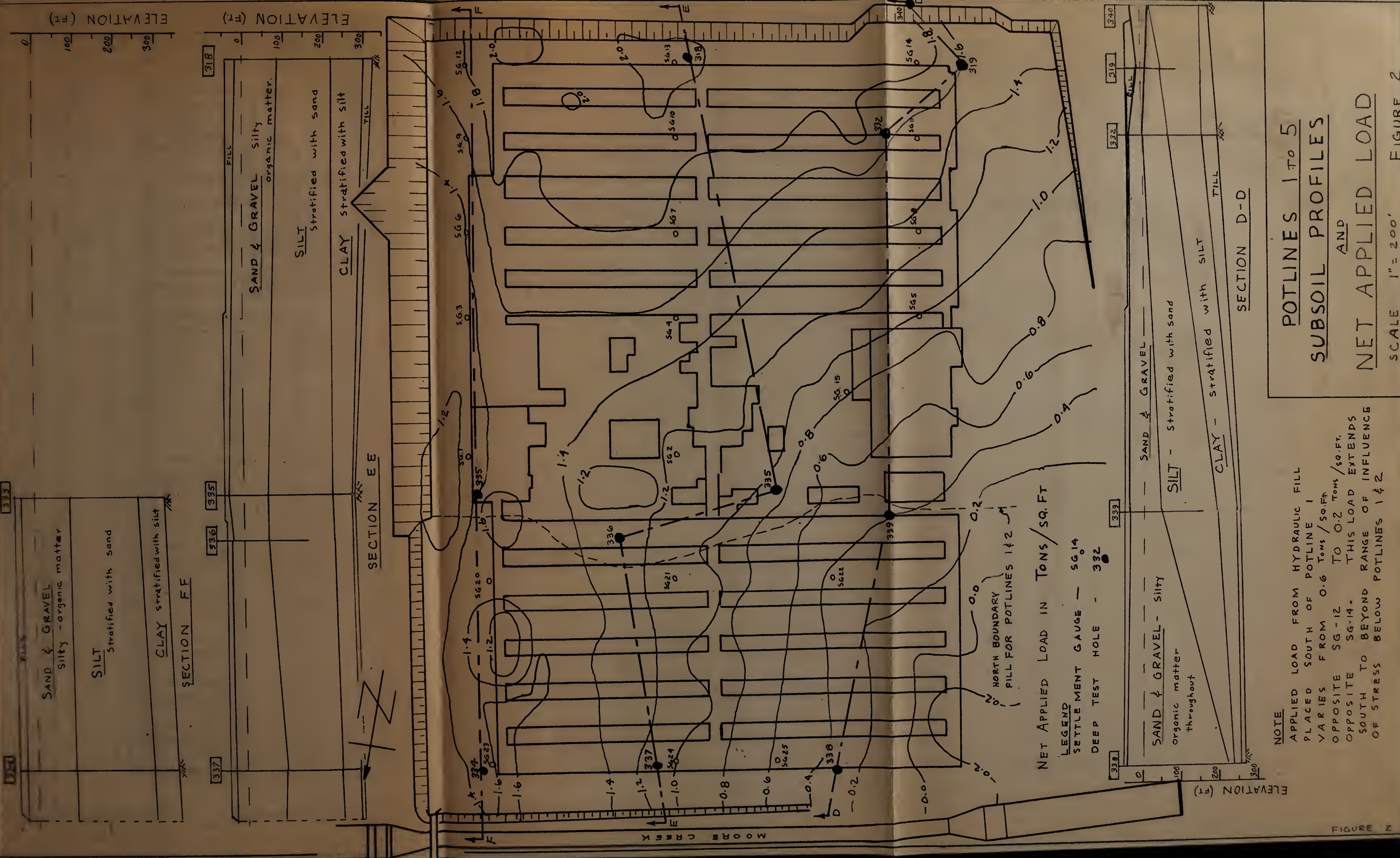


APPENDIX D

FIGURES

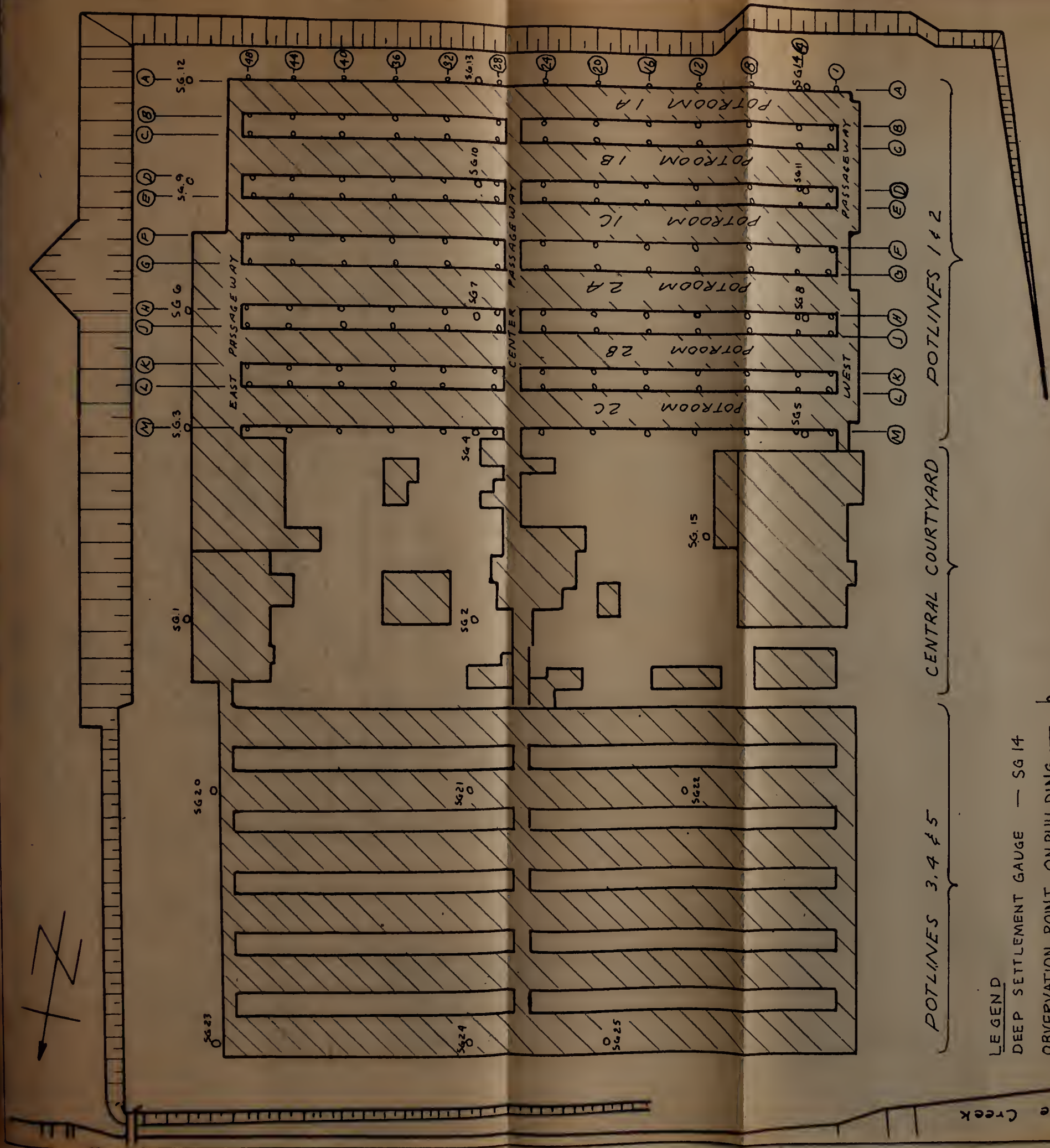












**LEGEND**

DEEP SETTLEMENT GAUGE — SG 14

OBSERVATION POINT ON BUILDING — AI

THESE POINTS ARE CALLED BY

COLUMN NUMBER eg. — AI

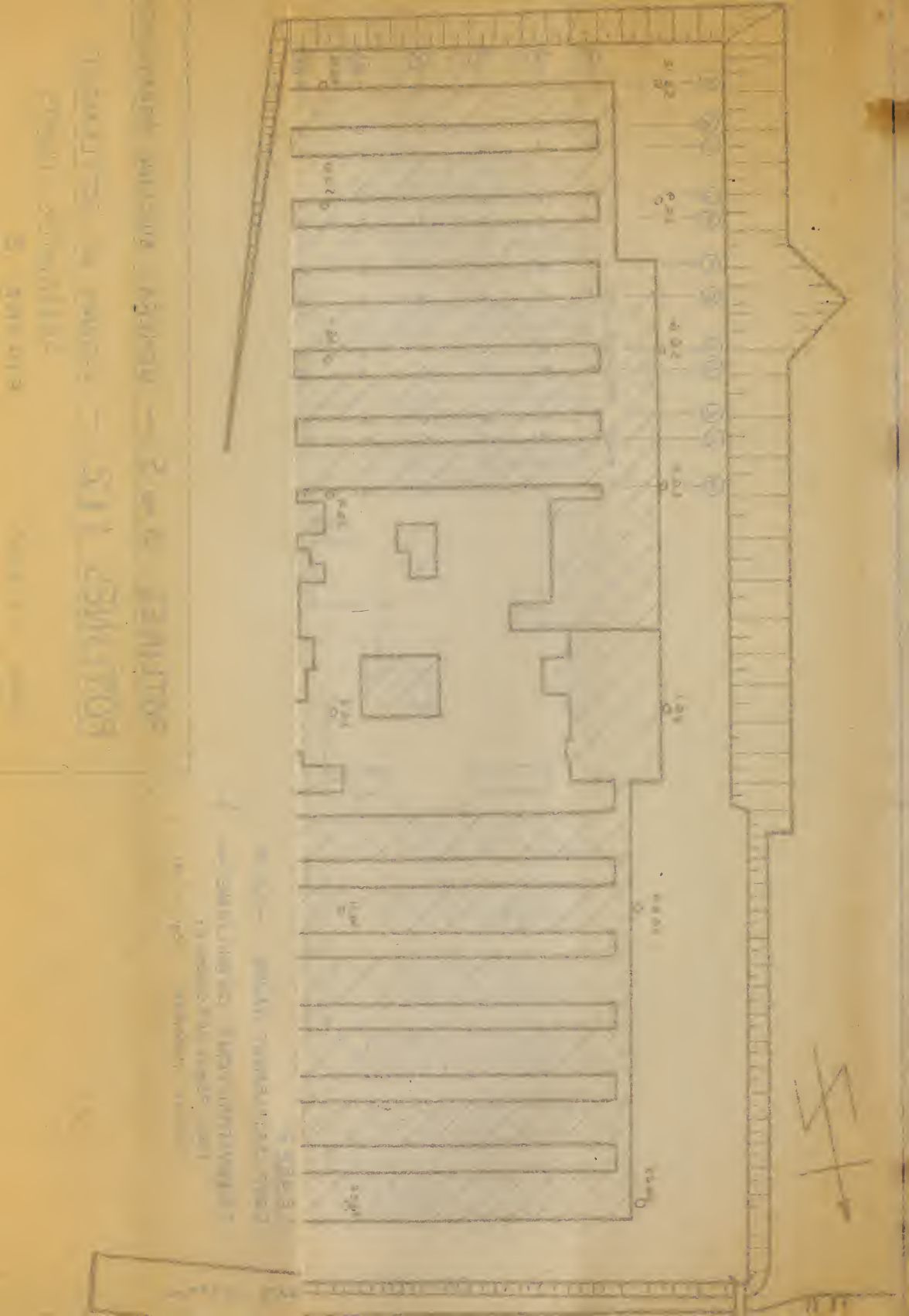
POTLINES 3 to 5 — GENERAL BUILDING ARRANGEMENT

POTLINES 1 & 2 — LOCATION OF SETTLEMENT

OBSERVATION POINTS

FIGURE 3

SCALE 1" = 200'

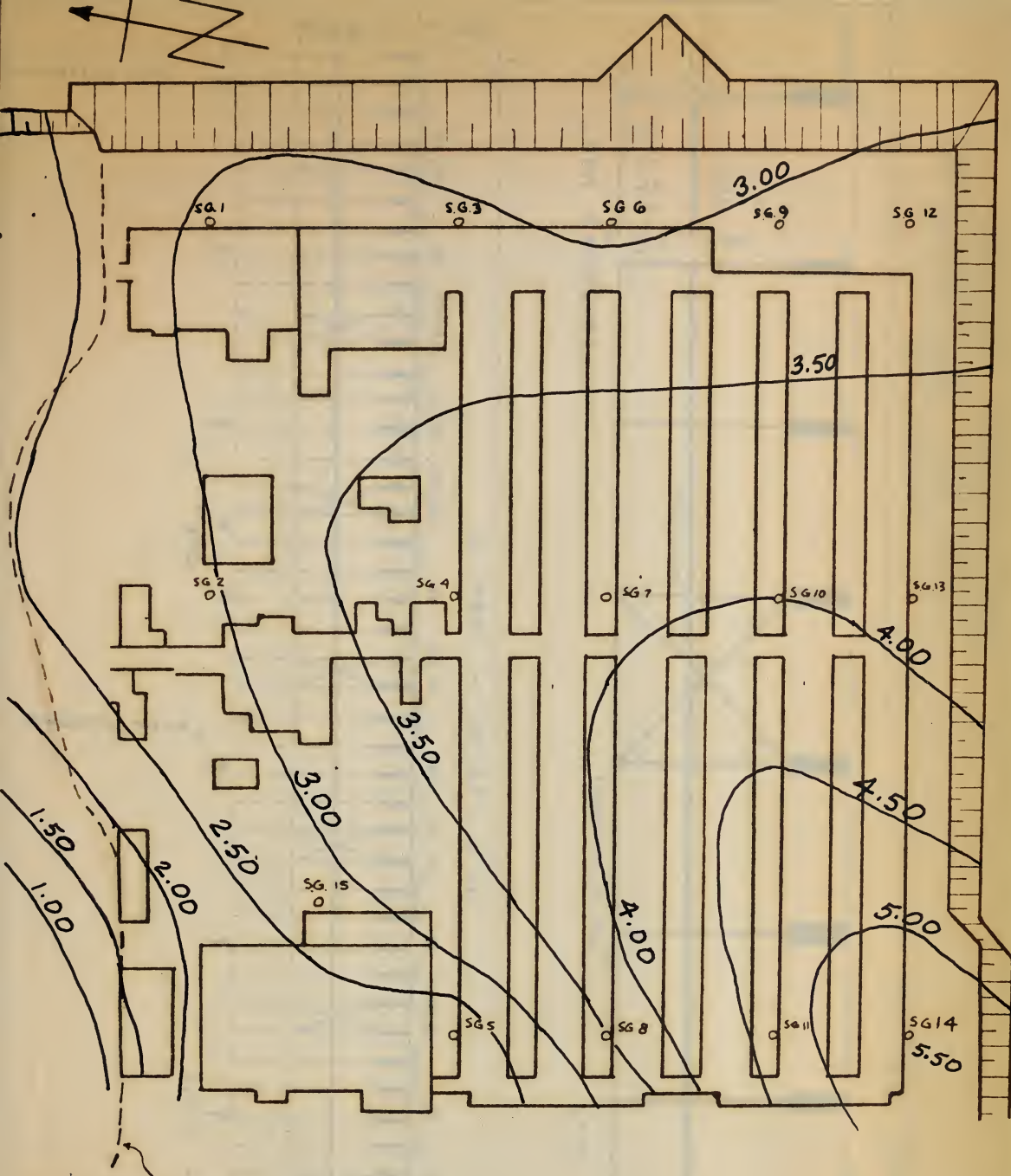


आवक ११५ - ११५००० - ११५०००  
आवक ११५ - ११५००० - ११५०००

आवक ११५ - ११५००० - ११५०००  
आवक ११५ - ११५००० - ११५०००

115





NORTH BOUNDARY OF  
FILL FOR POTLINES 1 & 2

SETTLEMENT IN FEET  
CONTOUR INTERVAL 0.50 Ft.

## POTLINES 1 & 2

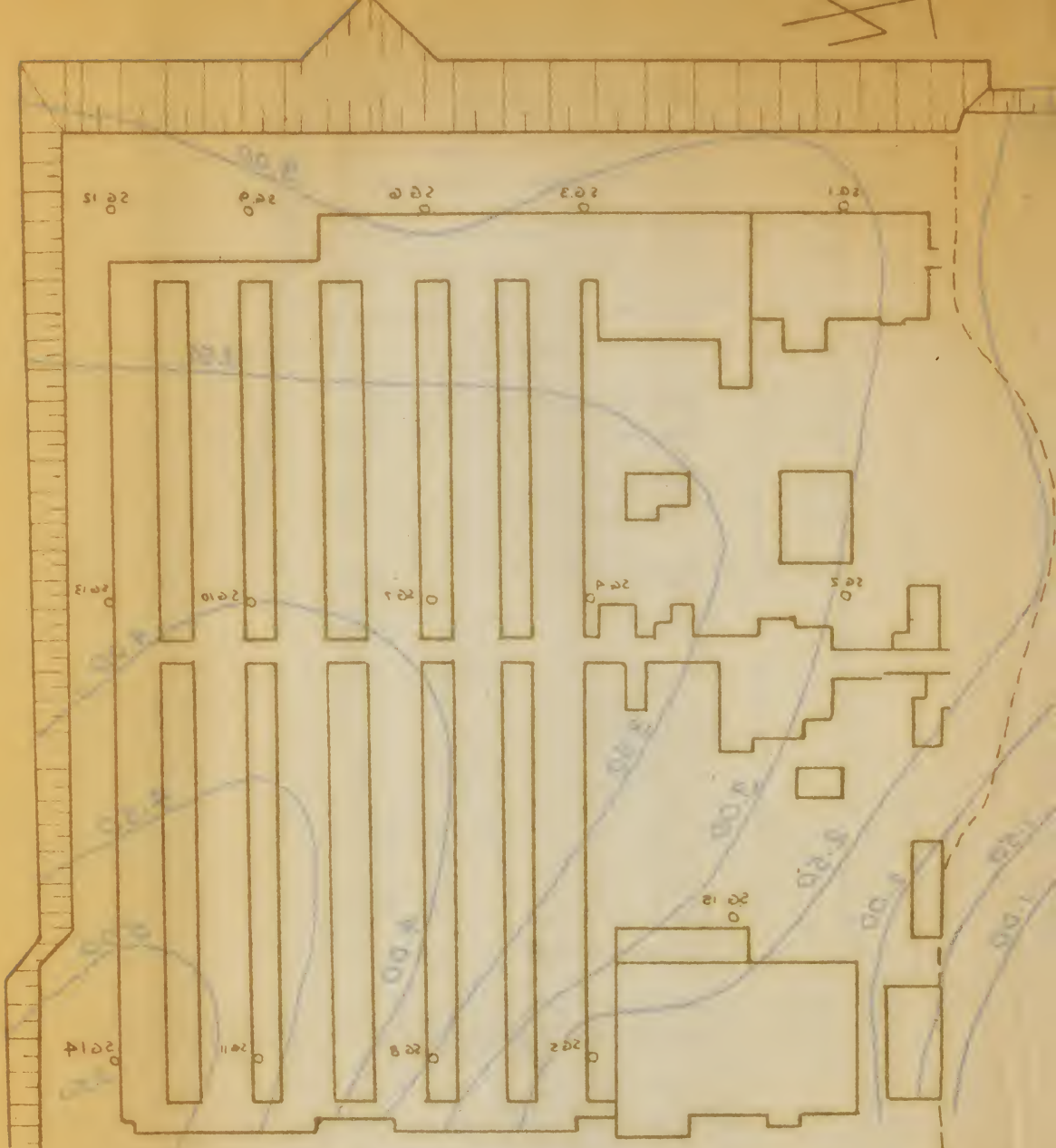
CONTOURS OF TOTAL  
FOUNDATION SETTLEMENT  
TO JUNE 28, 1957

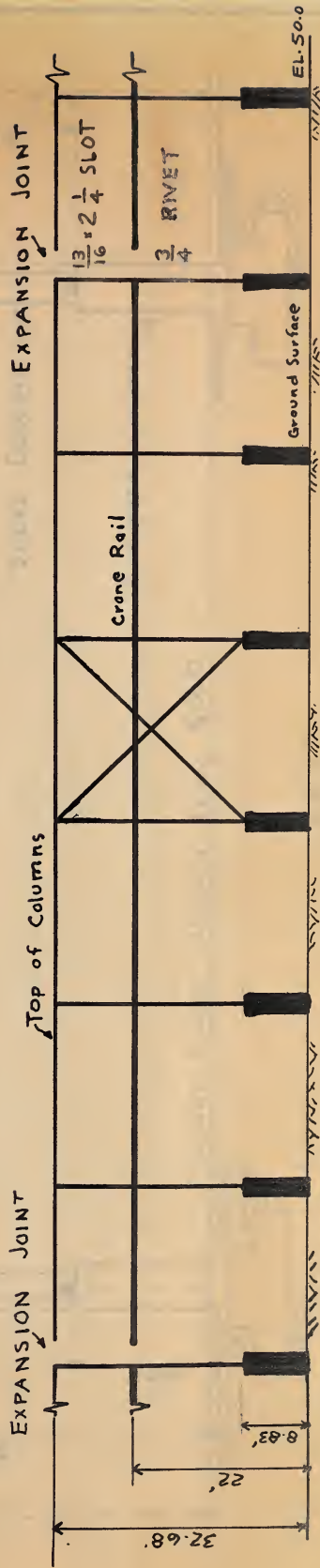
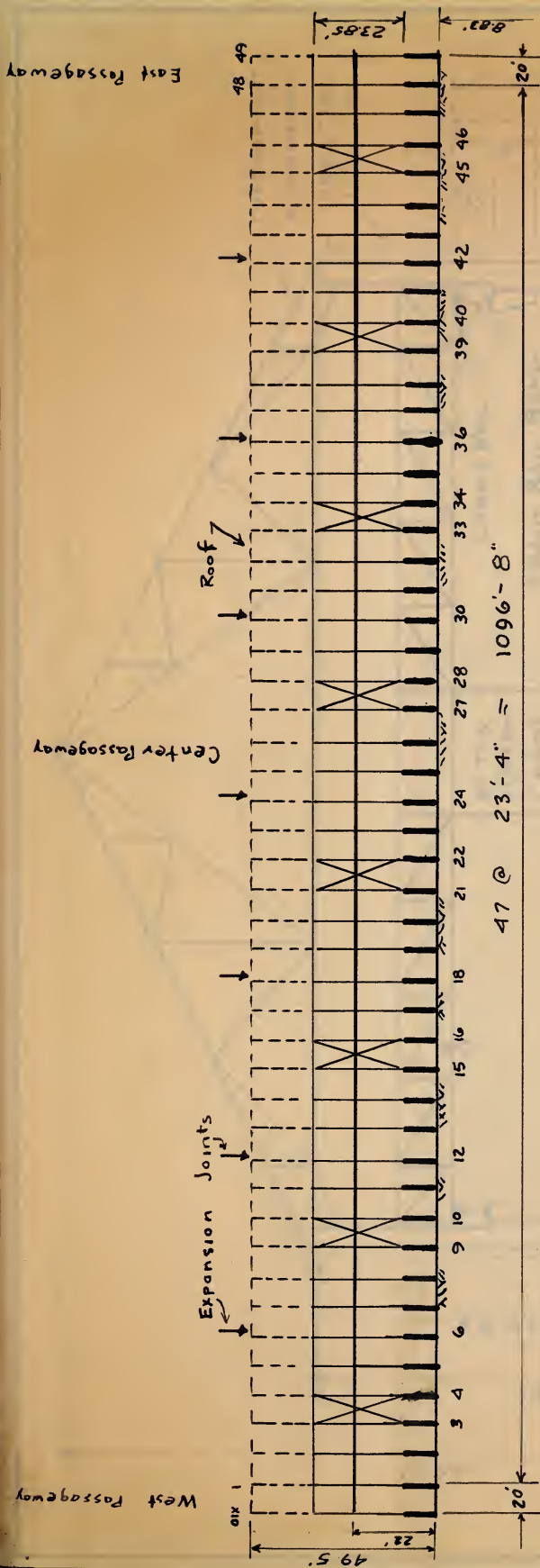
SCALE 1" = 200'

FIGURE 4



NORTH BOUNDARY OF





ENLARGED PARTIAL SECTION

FIGURE 5

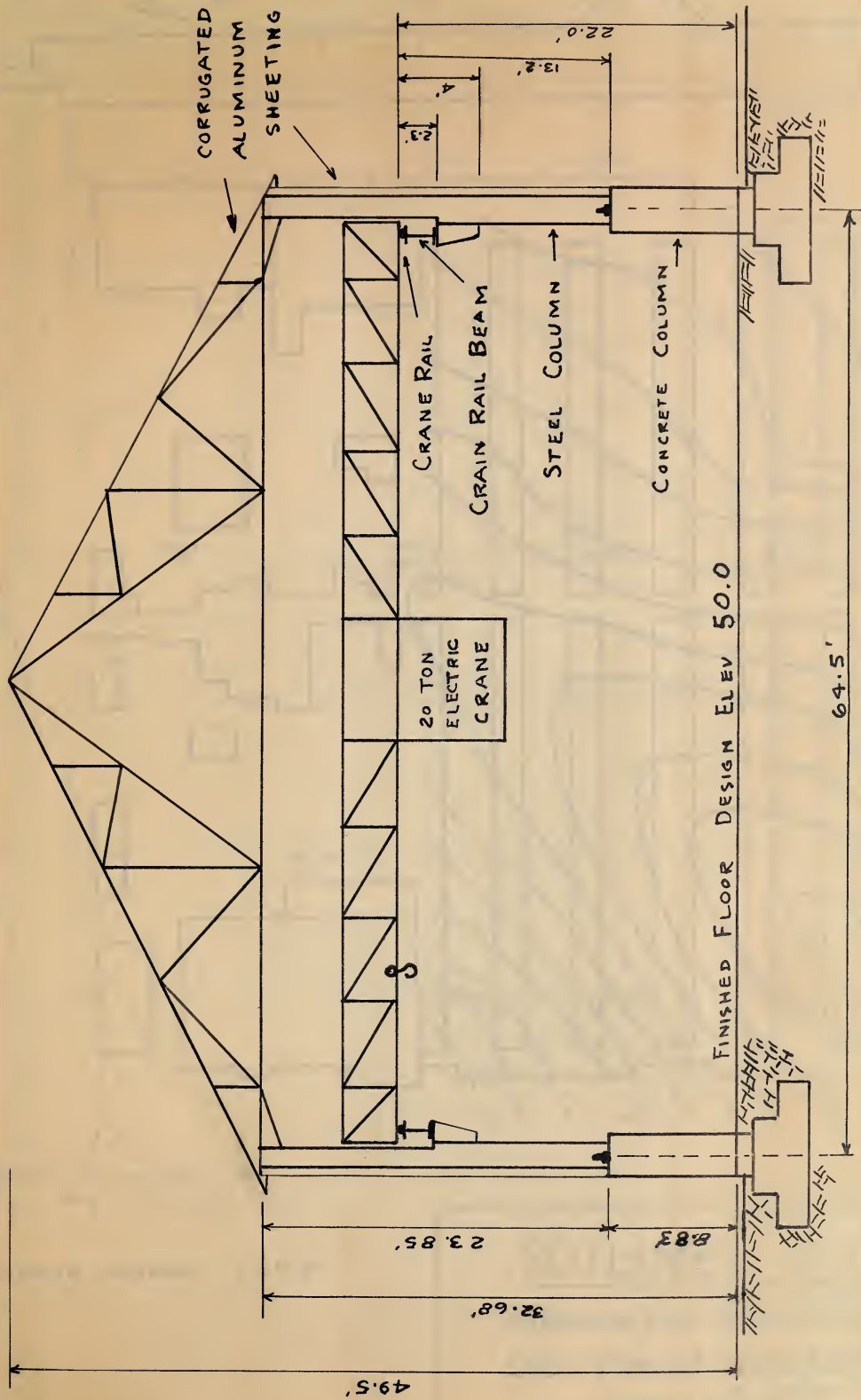
TYPICAL POTROOM  
LONGITUDINAL SECTION

FIGURE 5

2 EQUINE  
MOOSTON JACINTA  
MOITCE JACINTA



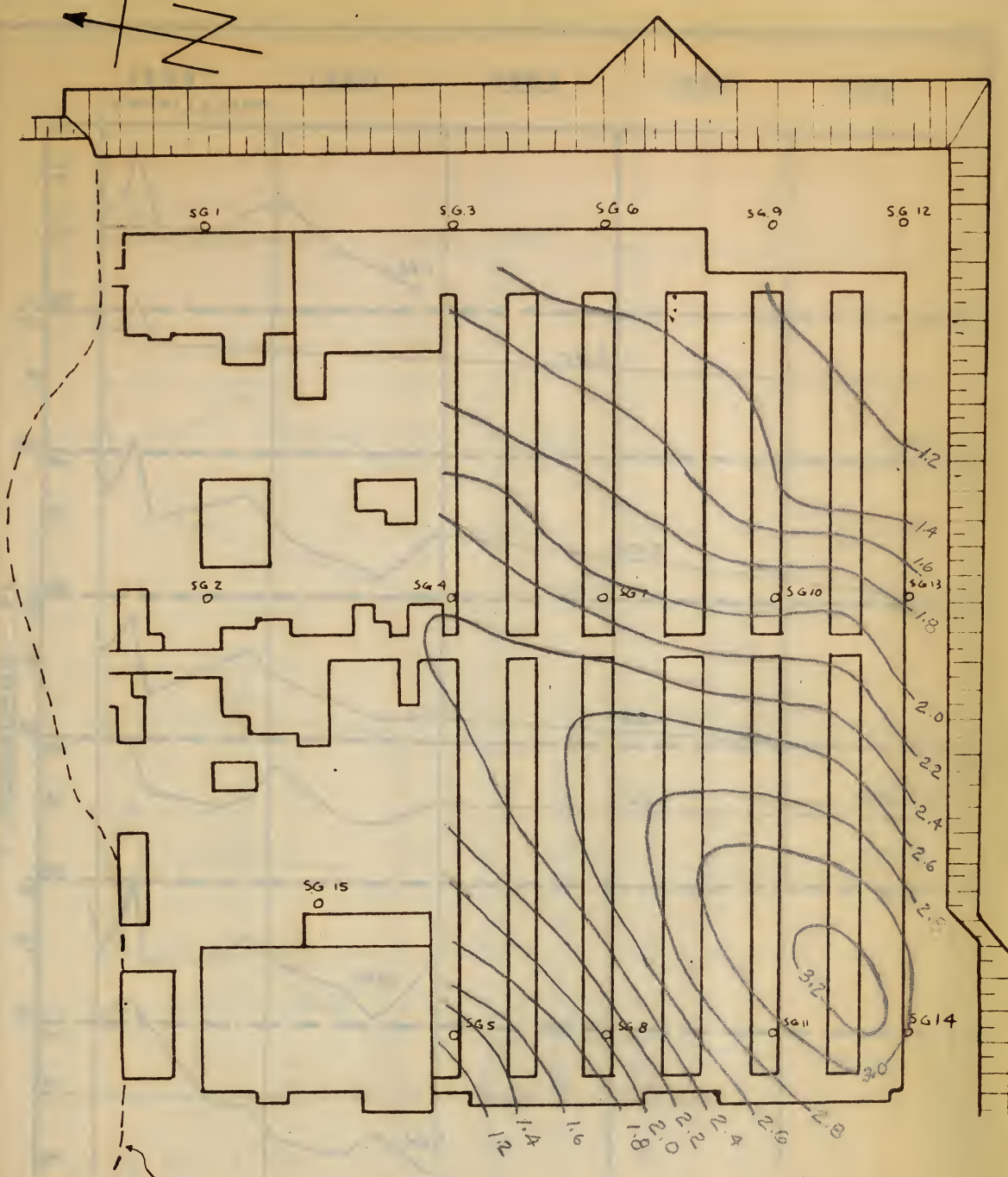




NOTE: NOT TO SCALE

TYPICAL POTROOM  
SECTIONAL VIEW  
FIGURE 6

SECTIONAL VIEW



NORTH BOUNDARY OF  
FILL FOR POTLINES 1 & 2

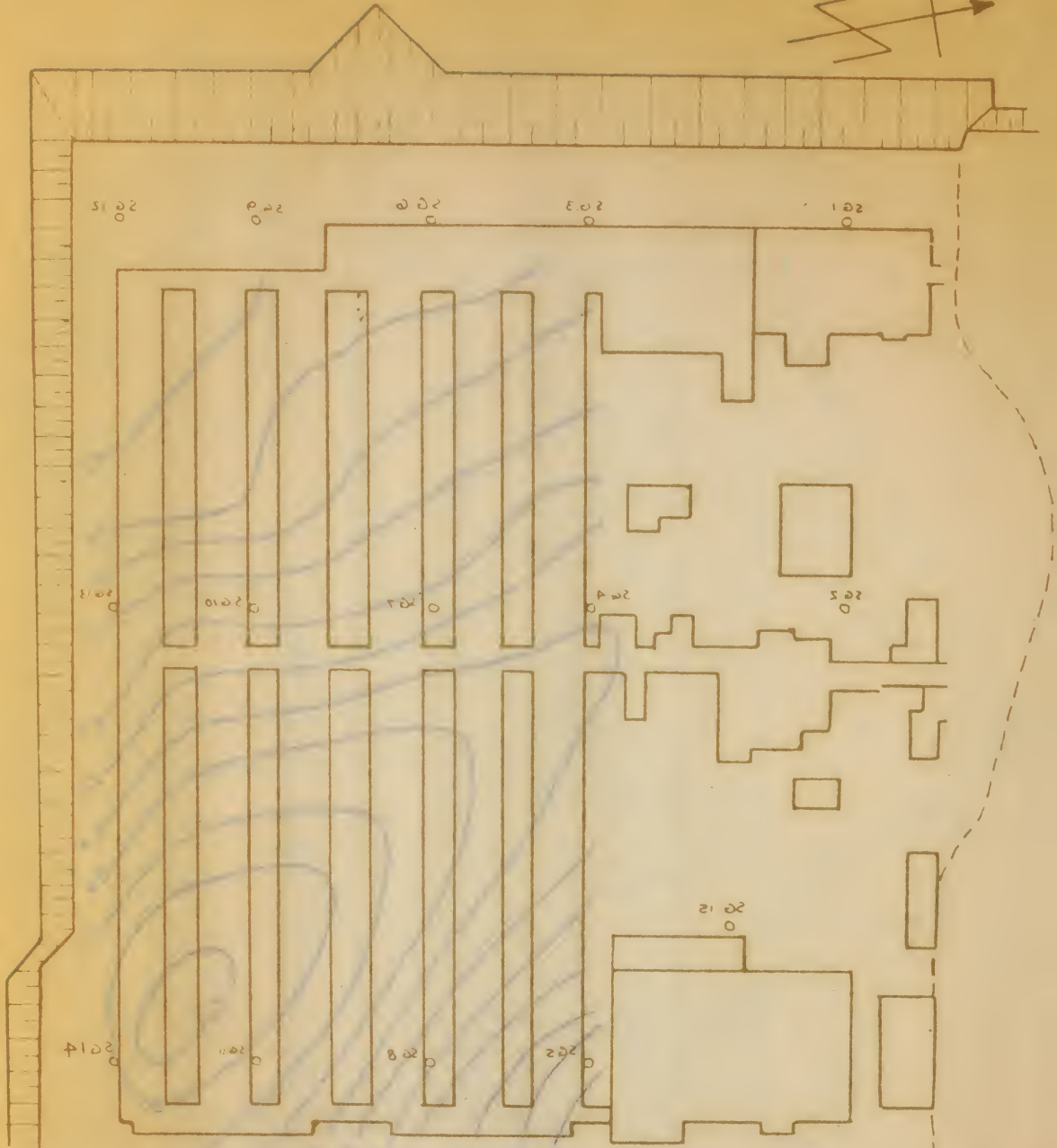
CONTOUR INTERVAL 0.20 ft.

## POTLINES 1 & 2

CONTOURS OF TOTAL EQUAL SETTLEMENT  
FROM START OF CONSTRUCTION TO  
JUNE 28, 1957

FIGURE 7





NORTH BOUNDARY OF  
THE SITE FOR POTLINES 1 & 2

POTLINES 1 & 2

CO. ROAD OF THE TOWN OF POTLINES

FROM STATE OF CALIFORNIA

DATE 5-1-21

1-2000

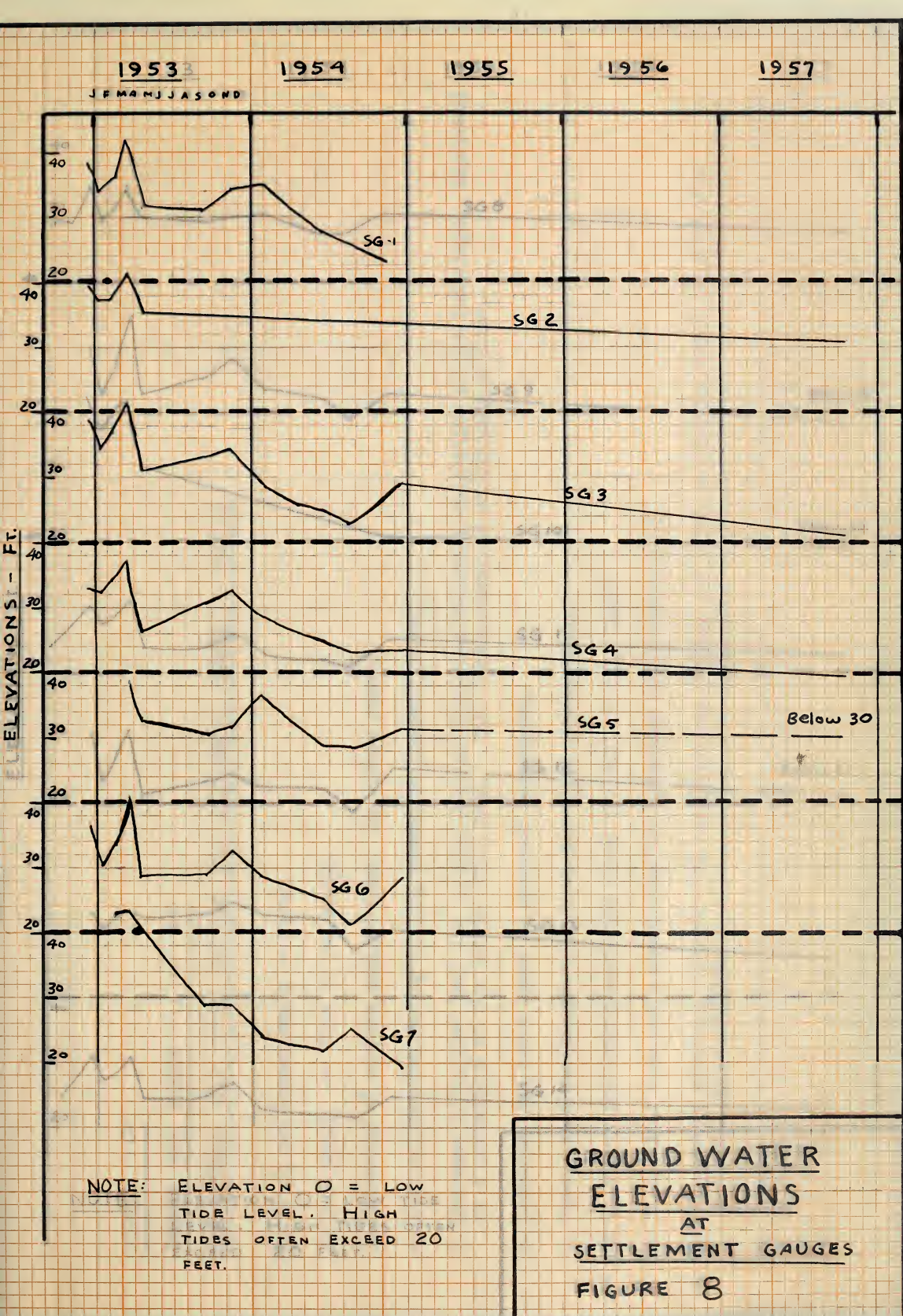
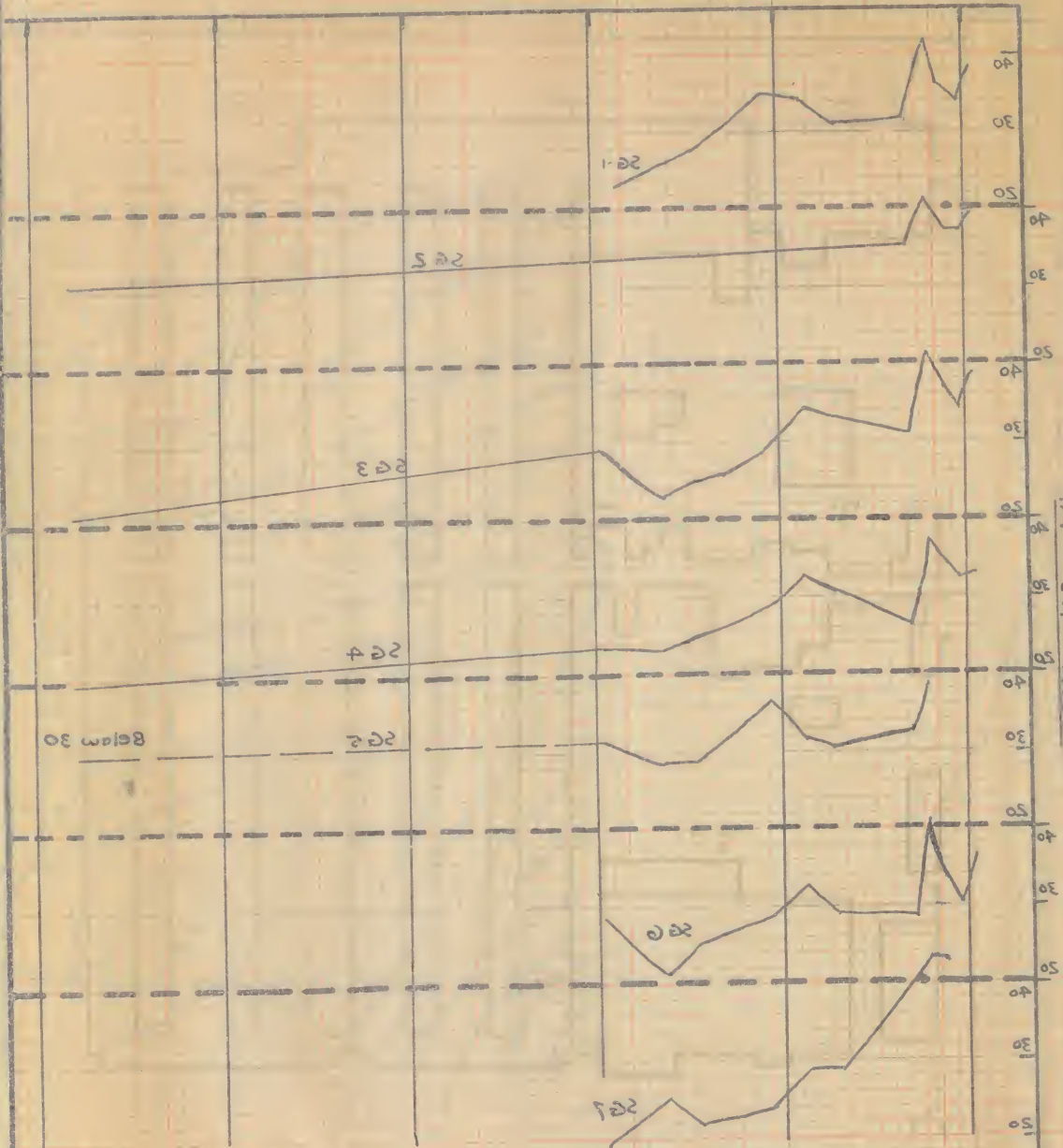




FIGURE 8  
SETTLEMENT GAUGES  
AT  
ELEVATIONS  
GROUND WATER

NOTE: ELEVATION 0 = LOW  
TIDE LEVEL. HIGH  
TIDES OFTEN EXCEED 50  
FEET.



1953  
JFMAMJJASOND

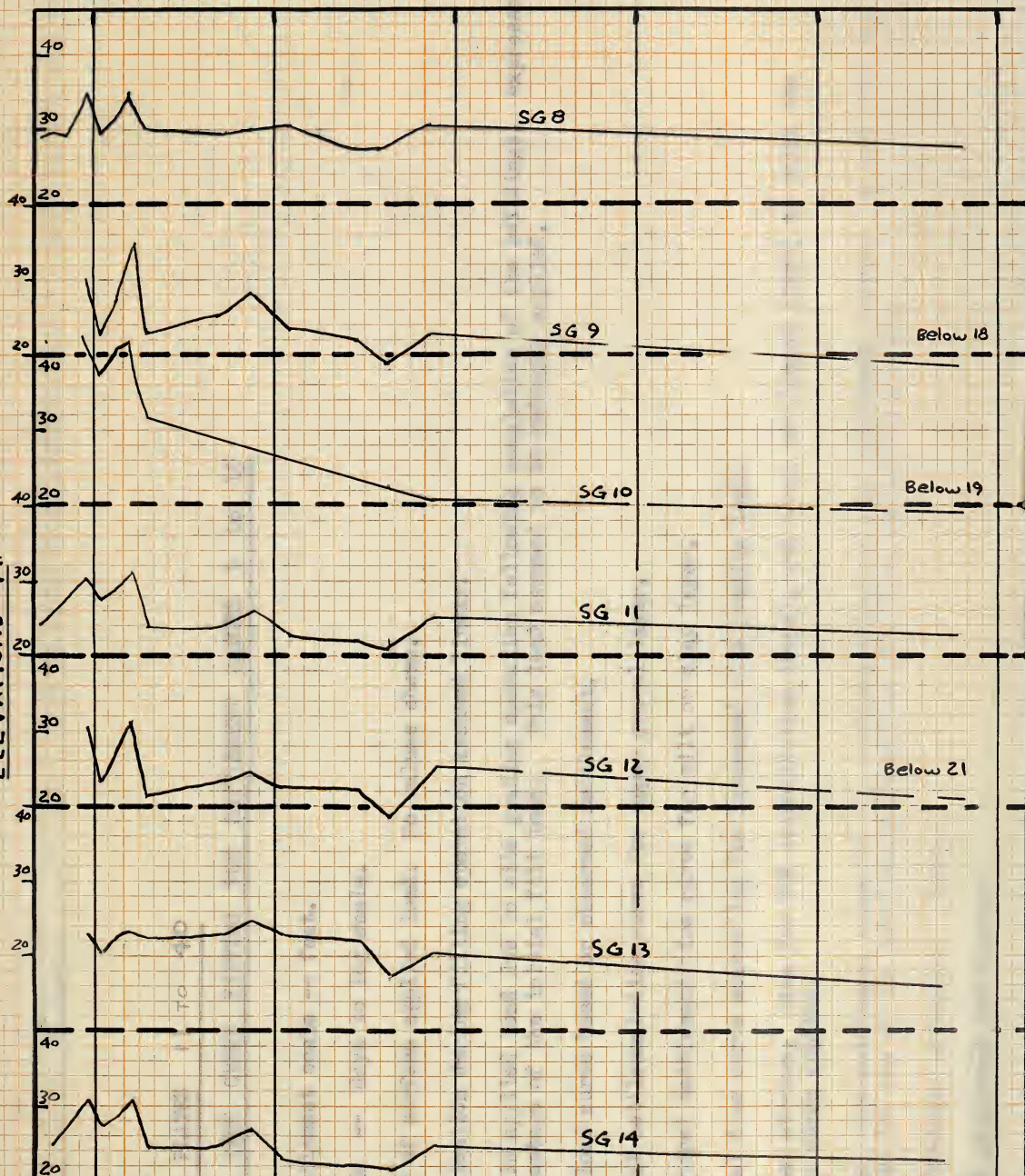
1954

1955

1956

1957

ELEVATIONS - FT.



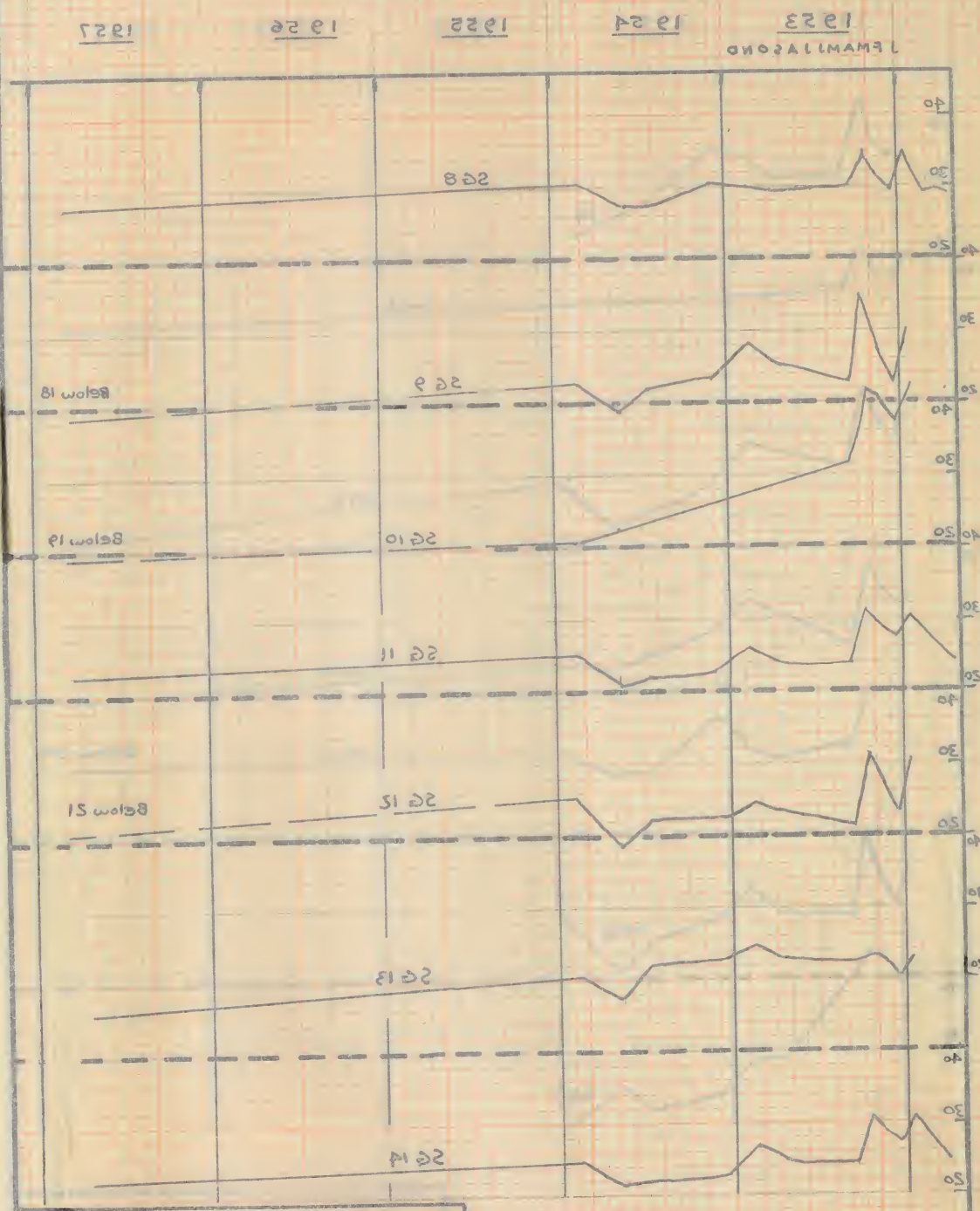
NOTE: ELEVATION 0 = LOW TIDE  
LEVEL. HIGH TIDES OFTEN  
EXCEED 20 FEET.

GROUND WATER  
ELEVATIONS  
AT  
SETTLEMENT GAUGES  
FIGURE 9



FIGURE 2  
SETTLEMENT GAUGES  
AT  
ELEVATIONS  
GROUND WATER

NOTE: ELEVATION 0 = LOW TIDE  
LEVEL. HIGH TIDES OFTEN  
EXCEED 50 FEET.



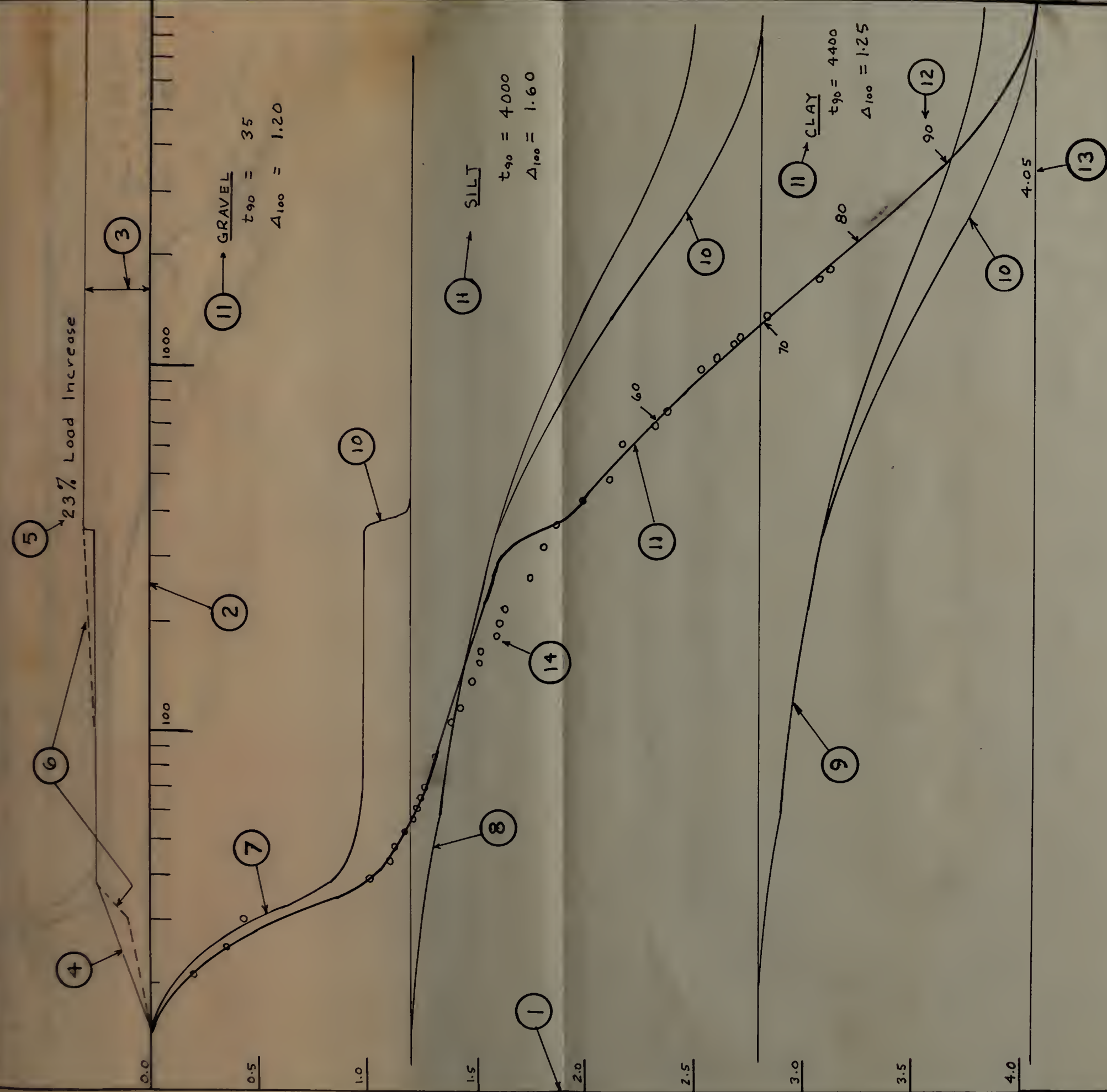


FIGURE 10

LEGEND FOR PLATES 11 TO 40

THEORETICAL TIME CURVE FITTING FOR SETTLEMENT GAUGES 1 to 15

1. Total settlement scale -- feet.
2. Time scale -- days to log scale.
3. Intensity of surface applied load. No values shown.
4. Load application during filling operation assumed linear.
5. Increase in applied load due to site grading operation following completion of the buildings, expressed as a percentage of the initial fill load. This load assumed to be suddenly applied.
6. Probable load curve based on observed settlement.
7. Theoretical settlement-time curve for upper gravel layer.
- 8 and 9. Theoretical settlement-time curve for silt or clay layer.
10. Theoretical time curve accounting for increased site grading load.
11. The assumed stratum, time for 90% consolidation (days), and total settlement (feet) to which the particular curve applies.
12. Theoretical time-settlement curve for the combined effect of each individual stratum. At any time this curve shows the sum of the settlements of each of the three individual strata.
13. Total theoretical settlement (feet).
14. Plot of observed settlement.



44. Plot of observed settlement.

31. Total Isotopes themselves. (see)

• 24. The following are the names of the persons who have been appointed to the various committees of the Board of Directors:

ist mit uns zu

CS  
 INSTALLED  
 Sept 28  
 1952

GRAVEL  
 $t_{90} = 25$   
 $\Delta_{100} = 1.20 \text{ FT}$   
 $C_c = .08$

SILT  
 $t_{90} = 4400 \text{ DAYS}$   
 $\Delta_{100} = 1.60 \text{ FT}$   
 $C_v = 5.6 \text{ FT}^2/\text{DAY}$   
 $C_c = .22$

CLAY  
 $t_{90} = 4000 \text{ DAYS}$   
 $\Delta_{100} = 1.25 \text{ FT}$   
 $C_v = 0.9 \text{ FT}^2/\text{DAY}$   
 $C_c = .77$

FIGURE =

SETTLEMENT GAUGE  
SERIES A  
MOST PROBABLE FIT

FIGURE 11

10

100

1000

5.0

4.5

4.0

3.5

3.0

2.5

2.0

1.0

4.05

90

80

70

60



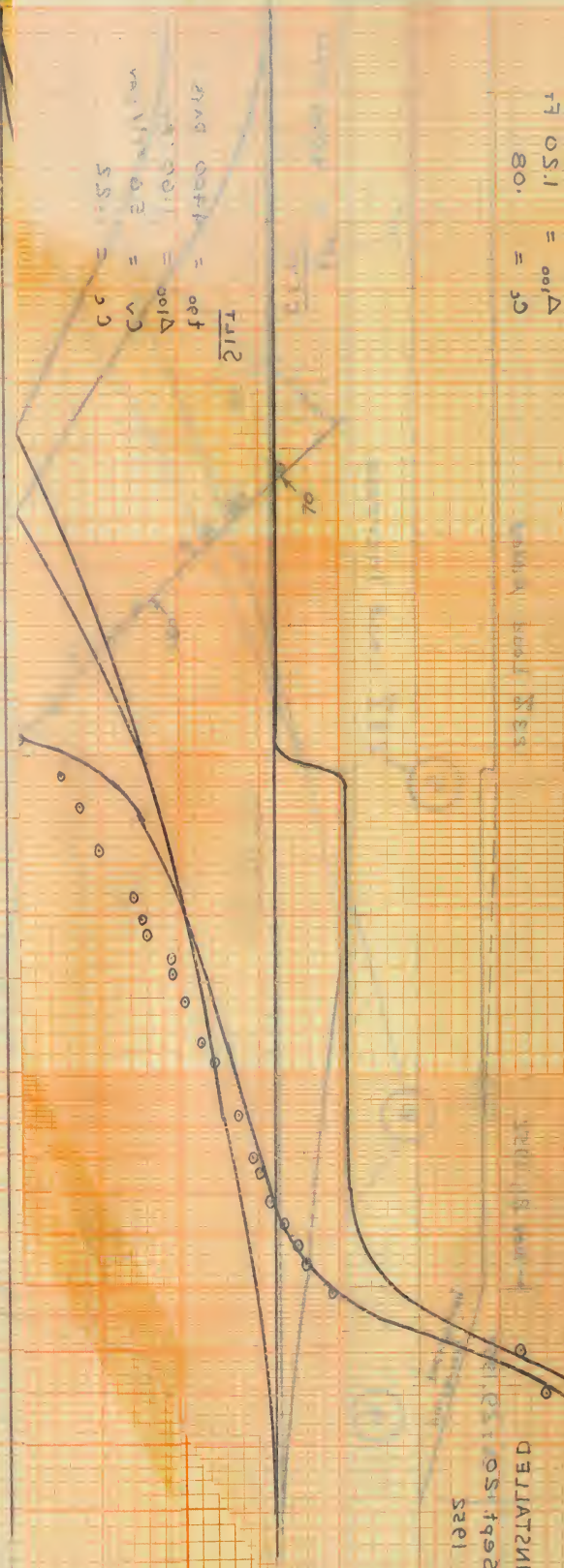
17	05.1	"	00.1	Δ
00.		"	00.	Δ

10  
 11  
 12  
 13  
 14  
 15  
 16  
 17  
 18  
 19  
 20  
 21  
 22  
 23  
 24  
 25  
 26  
 27  
 28  
 29  
 30  
 31  
 32  
 33  
 34  
 35  
 36  
 37  
 38  
 39  
 40  
 41  
 42  
 43  
 44  
 45  
 46  
 47  
 48  
 49  
 50  
 51  
 52  
 53  
 54  
 55  
 56  
 57  
 58  
 59  
 60  
 61  
 62  
 63  
 64  
 65  
 66  
 67  
 68  
 69  
 70  
 71  
 72  
 73  
 74  
 75  
 76  
 77  
 78  
 79  
 80  
 81  
 82  
 83  
 84  
 85  
 86  
 87  
 88  
 89  
 90  
 91  
 92  
 93  
 94  
 95  
 96  
 97  
 98  
 99  
 100  
 101  
 102  
 103  
 104  
 105  
 106  
 107  
 108  
 109  
 110  
 111  
 112  
 113  
 114  
 115  
 116  
 117  
 118  
 119  
 120  
 121  
 122  
 123  
 124  
 125  
 126  
 127  
 128  
 129  
 130  
 131  
 132  
 133  
 134  
 135  
 136  
 137  
 138  
 139  
 140  
 141  
 142  
 143  
 144  
 145  
 146  
 147  
 148  
 149  
 150  
 151  
 152  
 153  
 154  
 155  
 156  
 157  
 158  
 159  
 160  
 161  
 162  
 163  
 164  
 165  
 166  
 167  
 168  
 169  
 170  
 171  
 172  
 173  
 174  
 175  
 176  
 177  
 178  
 179  
 180  
 181  
 182  
 183  
 184  
 185  
 186  
 187  
 188  
 189  
 190  
 191  
 192  
 193  
 194  
 195  
 196  
 197  
 198  
 199  
 200  
 201  
 202  
 203  
 204  
 205  
 206  
 207  
 208  
 209  
 210  
 211  
 212  
 213  
 214  
 215  
 216  
 217  
 218  
 219  
 220  
 221  
 222  
 223  
 224  
 225  
 226  
 227  
 228  
 229  
 230  
 231  
 232  
 233  
 234  
 235  
 236  
 237  
 238  
 239  
 240  
 241  
 242  
 243  
 244  
 245  
 246  
 247  
 248  
 249  
 250  
 251  
 252  
 253  
 254  
 255  
 256  
 257  
 258  
 259  
 260  
 261  
 262  
 263  
 264  
 265  
 266  
 267  
 268  
 269  
 270  
 271  
 272  
 273  
 274  
 275  
 276  
 277  
 278  
 279  
 280  
 281  
 282  
 283  
 284  
 285  
 286  
 287  
 288  
 289  
 290  
 291  
 292  
 293  
 294  
 295  
 296  
 297  
 298  
 299  
 300  
 301  
 302  
 303  
 304  
 305  
 306  
 307  
 308  
 309  
 310  
 311  
 312  
 313  
 314  
 315  
 316  
 317  
 318  
 319  
 320  
 321  
 322  
 323  
 324  
 325  
 326  
 327  
 328  
 329  
 330  
 331  
 332  
 333  
 334  
 335  
 336  
 337  
 338  
 339  
 340  
 341  
 342  
 343  
 344  
 345  
 346  
 347  
 348  
 349  
 350  
 351  
 352  
 353  
 354  
 355  
 356  
 357  
 358  
 359  
 360  
 361  
 362  
 363  
 364  
 365  
 366  
 367  
 368  
 369  
 370  
 371  
 372  
 373  
 374  
 375  
 376  
 377  
 378  
 379  
 380  
 381  
 382  
 383  
 384  
 385  
 386  
 387  
 388  
 389  
 390  
 391  
 392  
 393  
 394  
 395  
 396  
 397  
 398  
 399  
 400  
 401  
 402  
 403  
 404  
 405  
 406  
 407  
 408  
 409  
 410  
 411  
 412  
 413  
 414  
 415  
 416  
 417  
 418  
 419  
 420  
 421  
 422  
 423  
 424  
 425  
 426  
 427  
 428  
 429  
 430  
 431  
 432  
 433  
 434  
 435  
 436  
 437  
 438  
 439  
 440  
 441  
 442  
 443  
 444  
 445  
 446  
 447  
 448  
 449  
 450  
 451  
 452  
 453  
 454  
 455  
 456  
 457  
 458  
 459  
 460  
 461  
 462  
 463  
 464  
 465  
 466  
 467  
 468  
 469  
 470  
 471  
 472  
 473  
 474  
 475  
 476  
 477  
 478  
 479  
 480  
 481  
 482  
 483  
 484  
 485  
 486  
 487  
 488  
 489  
 490  
 491  
 492  
 493  
 494  
 495  
 496  
 497  
 498  
 499  
 500  
 501  
 502  
 503  
 504  
 505  
 506  
 507  
 508  
 509  
 510  
 511  
 512  
 513  
 514  
 515  
 516  
 517  
 518  
 519  
 520  
 521  
 522  
 523  
 524  
 525  
 526  
 527  
 528  
 529  
 530  
 531  
 532

REGISTERED

05192

5261



2112

Oct 21 1895

$$\Delta_{100} = 1.22$$

5  
D  
.  
-  
v  
C.  
fl  
H  
C  
C

11

EDUAD TNEWTTES

A 231932

WOST 6609 BT EIT

113417

10001

1001

9

11. 220017

and emit gas. It is important that these individuals do not serve themselves and do not eat to the point of discomfort and do not eat to the point of discomfort and do not eat to the point of discomfort.

31. Total Interest Paid. (See)

It is observed that the settlement.



26% Load Increase

P. Oct 31, 1952

Sept 23 1952  
Uniformly  
Increase

GRAVEL  $t_{90} = 35$   $\Delta_{100} = 0.20$   
 $C_c = 1.02$

0.5-  
Aug 10, 1952

CLAY  
 $t_{90} = 2500$   
 $\Delta_{100} = 1.60$   
 $C_v = .9$   
 $C_c = 1.06$

SILT  
 $t_{90} = 5650$   
 $\Delta_{100} = 2.60$   
 $C_v = 3.8$   
 $C_c = .32$

1000

100

10

SETTLEMENT GAUGE 2

SERIES A

MOST PROBABLE FIT

FIGURE 12

FIGURE 12

5.0



Special bond % 25

SEP 15 1950

SEP 25 1952

time of  
penetration

05.0 = 001 Δ 25 = 003

50.1 = 22

LEVA 20

YAL 2

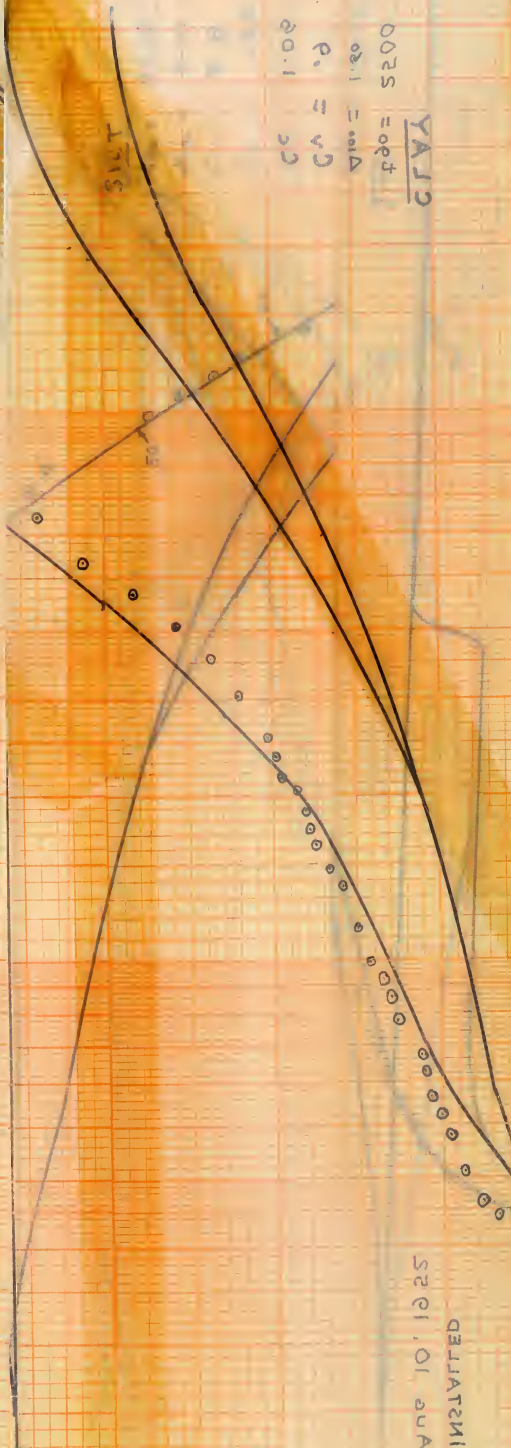
0025 = 003 f

02.1 = 001 Δ

P. = V 2

20.1 22

SEALING  
SEP 10 1951



SETTLEMENT GAUGE

SERIES A

THE BROADBENT

FIGURE 15



23% Load Increase

Nov. 21, 1952

Oct 27, 1952

Uniformly Increasing

# GRAVEL

$t_{90} = 32$   
 $\Delta_{100} = 1.40$   
 $C_c = .09$

0.5  
 1.0  
 1.5  
 2.0  
 2.5  
 3.0  
 3.5  
 4.0

INSTALLED  
 SEPT. 24  
 1952

# SILT

$t_{90} = 4000$   
 $\Delta_{100} = 1.30$   
 $C_v = 6.1$   
 $C_c = .16$

# CLAY

$t_{90} = 2500$   
 $\Delta_{100} = 1.00$   
 $C_v = 1.43$   
 $C_c = .53$

3.70

FIGURE 13

SETTLEMENT GAUGE 3  
 SERIES A  
 MOST PROBABLE FIT

FIGURE 13

1000

100

10



FIGURE 15

MOST PROBABLE FIT

SERIES A

SETTLEMENT GAUGE 5

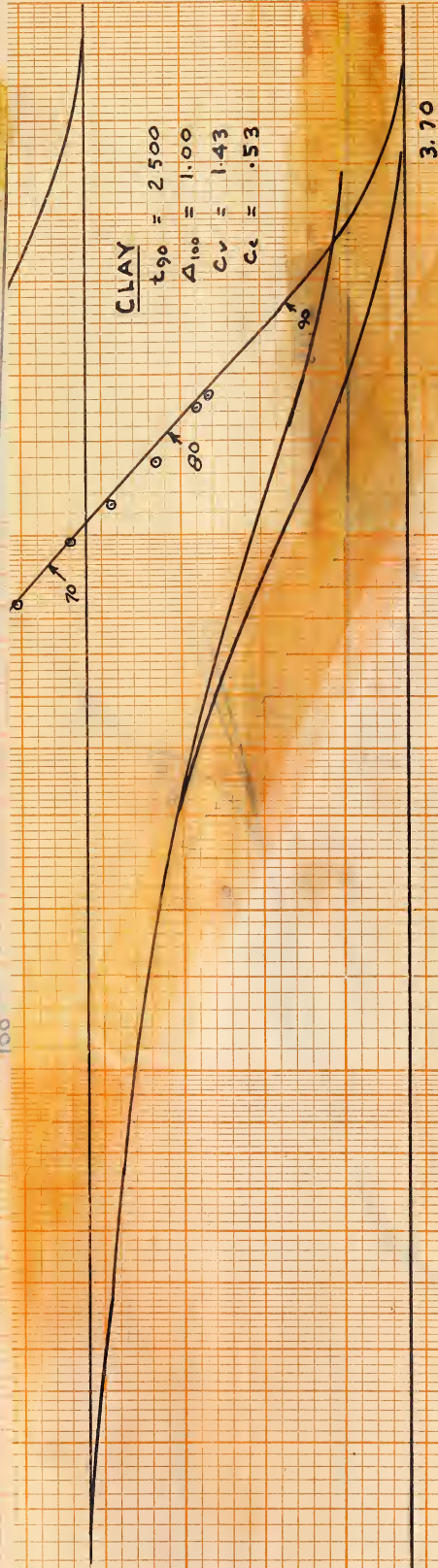


FIGURE 13

SETTLEMENT GAUGE 3

SERIES A

MOST PROBABLE FIT

FIGURE 13

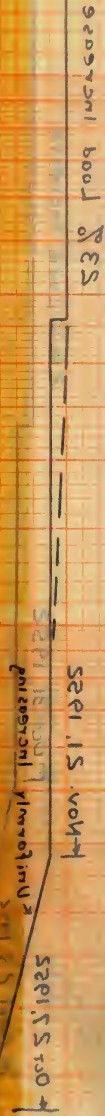
1000

100

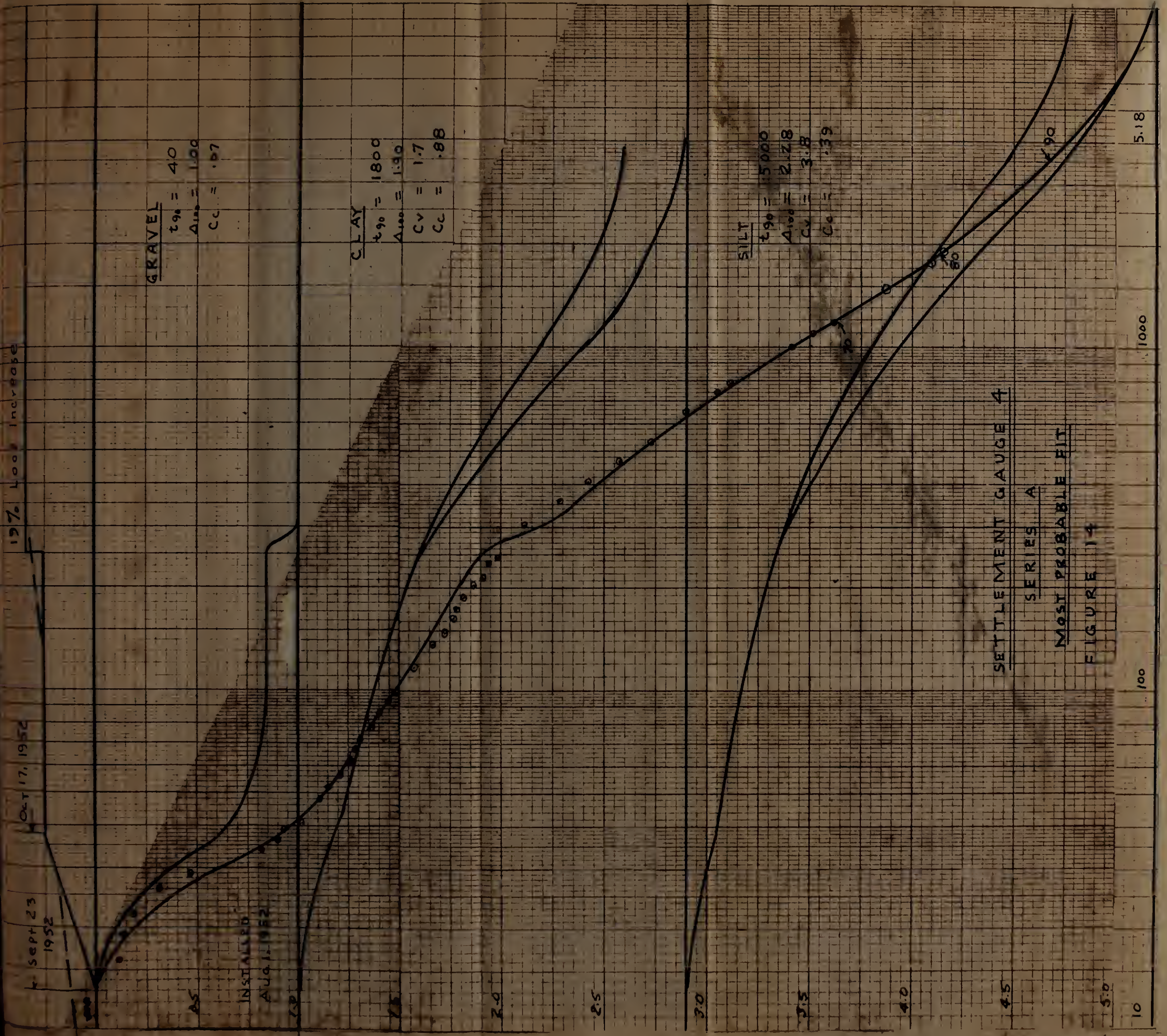
10

38 = 0.3

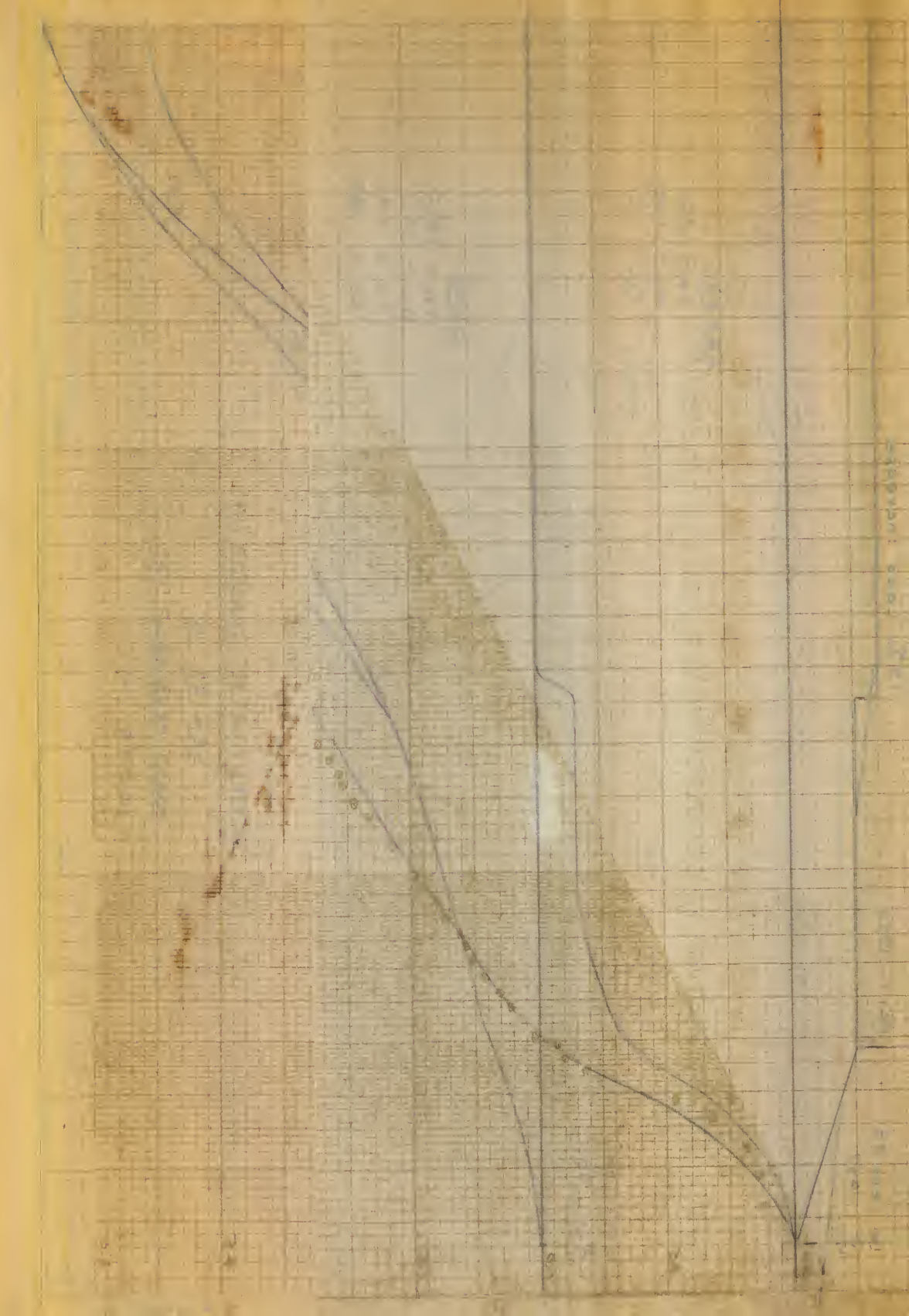
GRAVEL









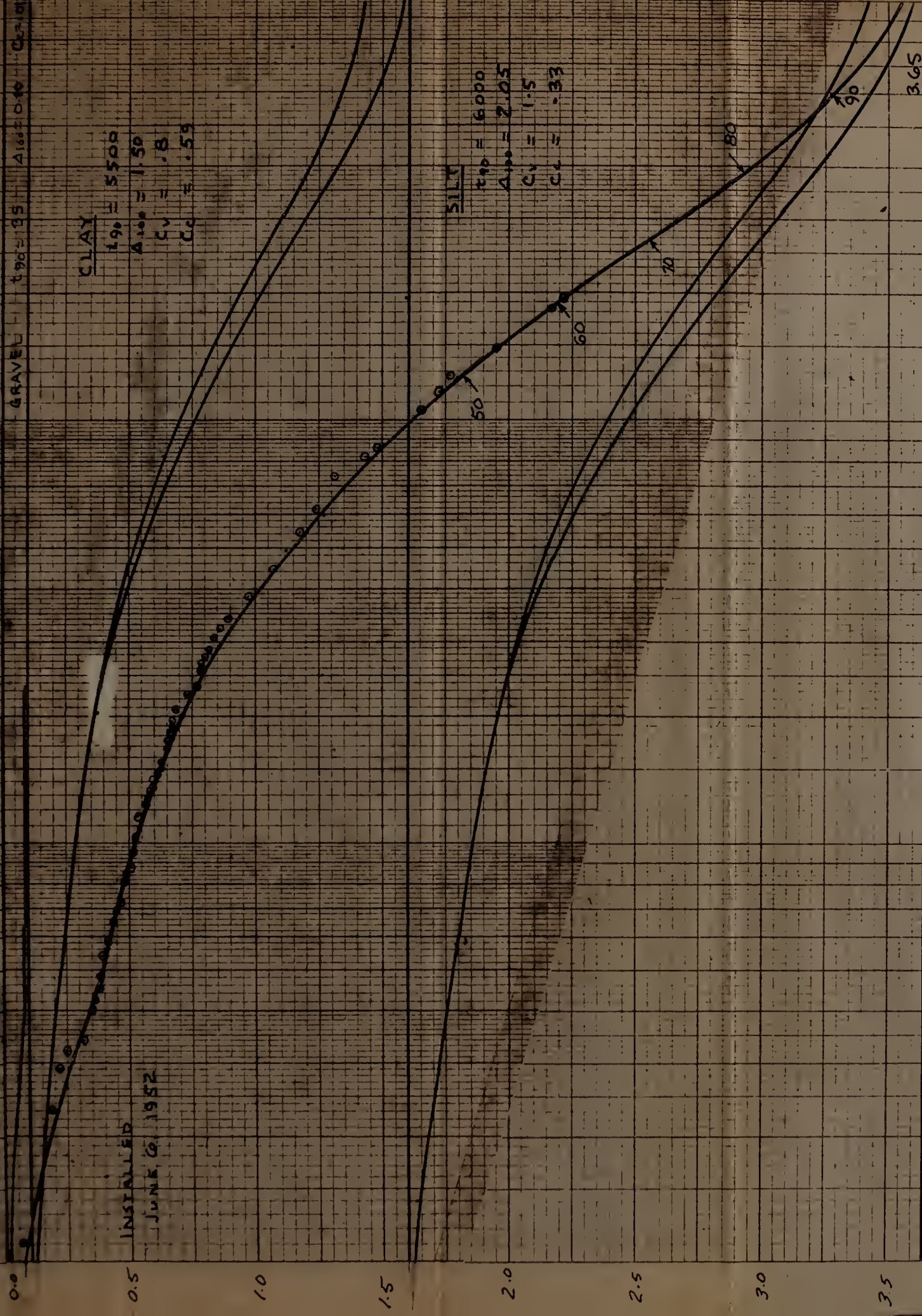




$t_{10}$  @ Load = 0  
June 6, 1952

July 18, 1952

11% Load Increase



INCHES

10

100

1000







Insert  
Foldout  
Here



UNITED STATES ARMY

ENGINEER REGIMENT

5281 NS 120

PLM  
UNION

GRAVEL

100  
100  
100

SECTION TWENTY

A 251273

THE TUGBOAT TON

21 30012

5281

201

201

201



23% Load Applied

Nov. 21, 1952

Oct. 27, 1952

Settlement

GRAVEL

GRAVEL

$t_{90} = 32$   
 $\Delta_{100} = 1.28$   
 $C_c = .08$

SILT

$t_{90} = 4000$   
 $\Delta_{100} = 1.27$   
 $C_v = 6.1$   
 $C_c = .16$

CLAY

$t_{90} = 2500$   
 $\Delta_{100} = 1.00$   
 $C_v = 1.4$   
 $C_c = .53$

SETTLEMENT GAUGE 6

SERIES A

MOST PROBABLE FIT

FIGURE 16

1000

100

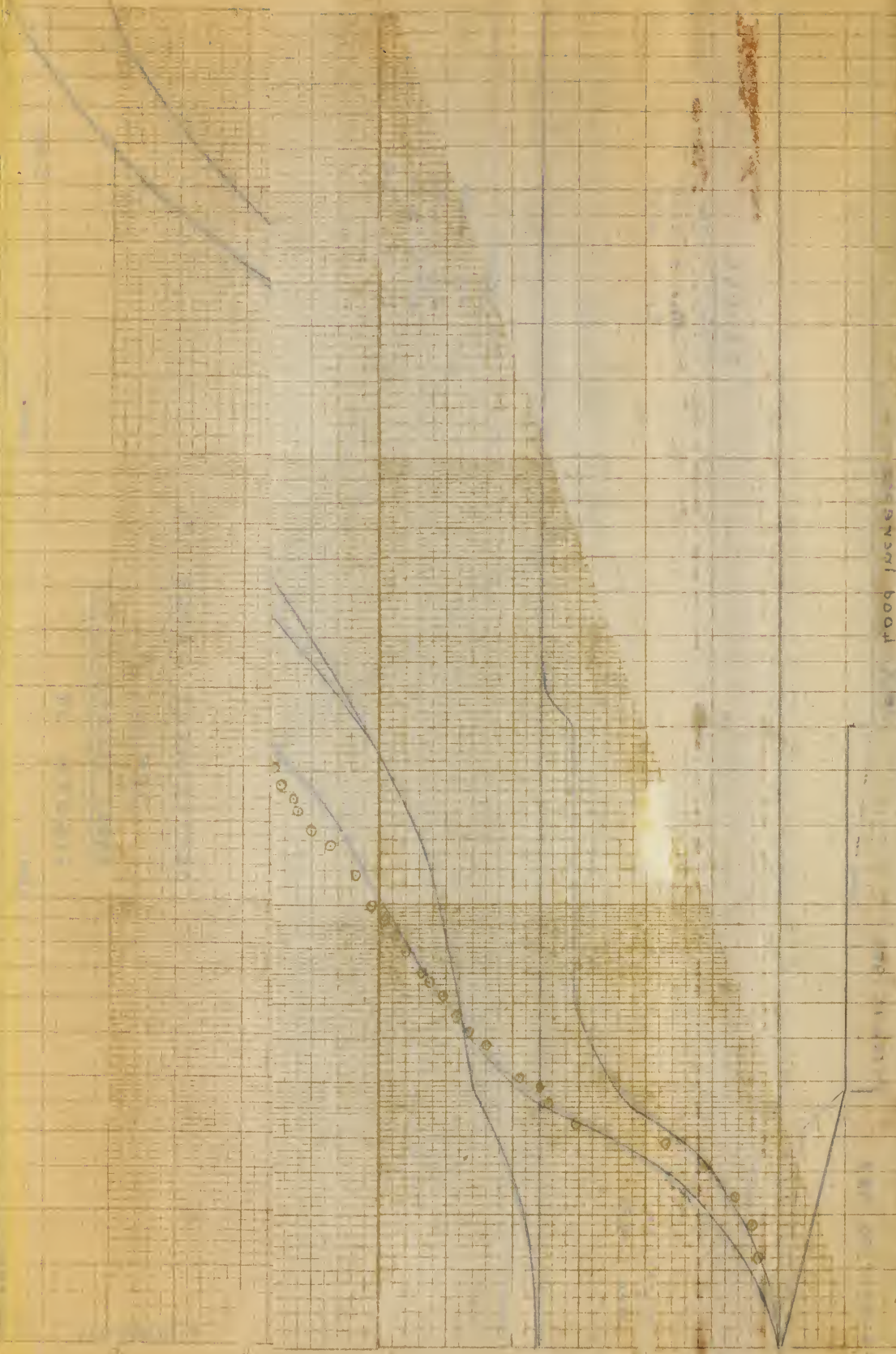
10

5.0

FIGURE 16



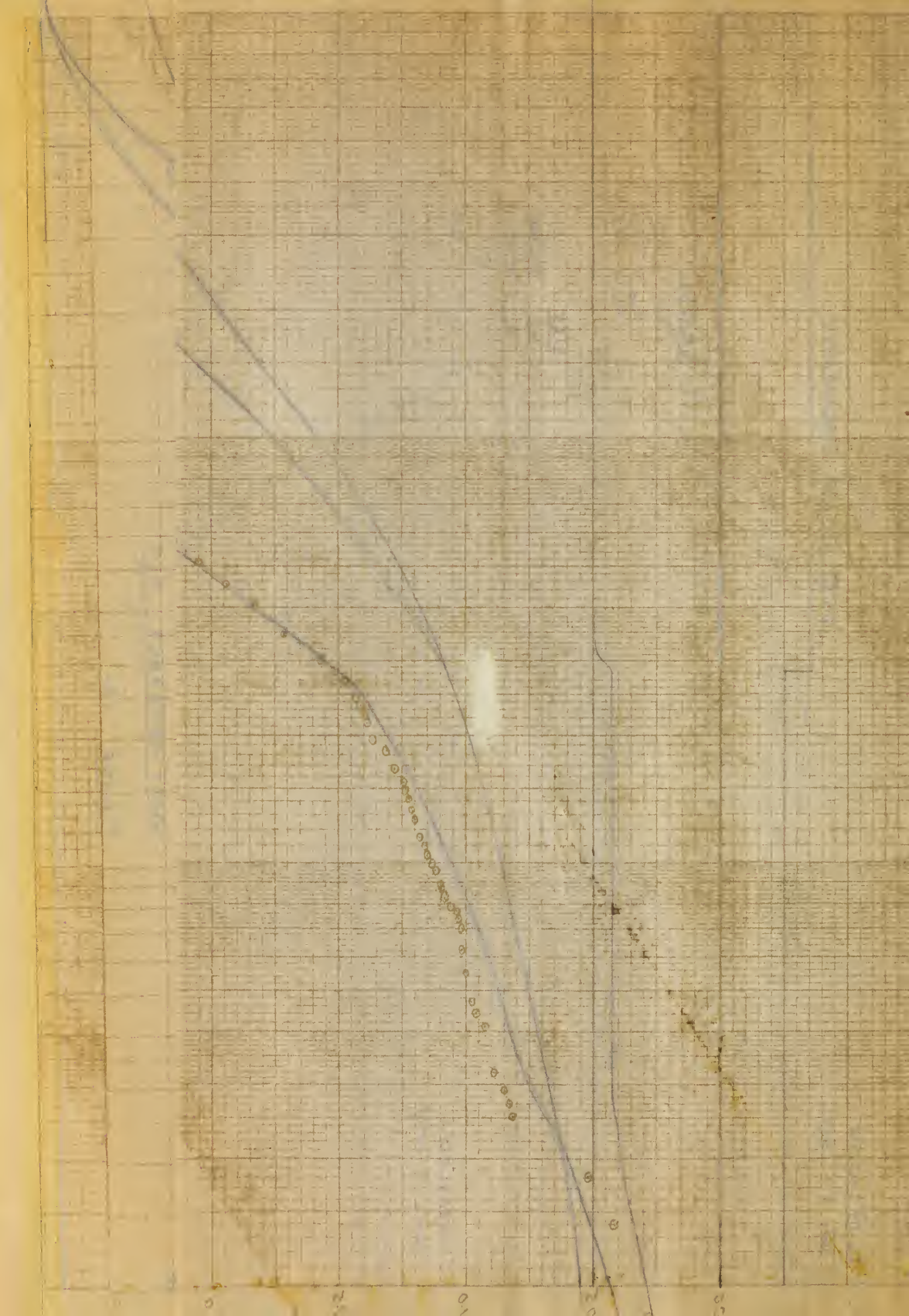
1009 1264



Insert  
Foldout  
Here









16% Load Increase

Oct. 17, 1952

Sept. 30, 1952

GRAVEL

$t_{90} = 38$   
 $\Delta_{100} = 0.90$   
 $C_c = 0.95$

CLAY

$t_{90} = 11500$   
 $\Delta_{100} = 1.85$   
 $C_v = 2.75$   
 $C_c = 0.64$

SILT

$t_{90} = 6300$   
 $\Delta_{100} = 2.65$   
 $C_v = 2.62$   
 $C_c = 0.30$

SETTLEMENT GAUGE 7

SERIES A

MOST PROBABLE FIT

FIGURE 17

FIGURE 17

10

100

1000

5.40

90

80

70

60

45

40

35

30

25

20

15

10

05

00



Oct 20 1921

20

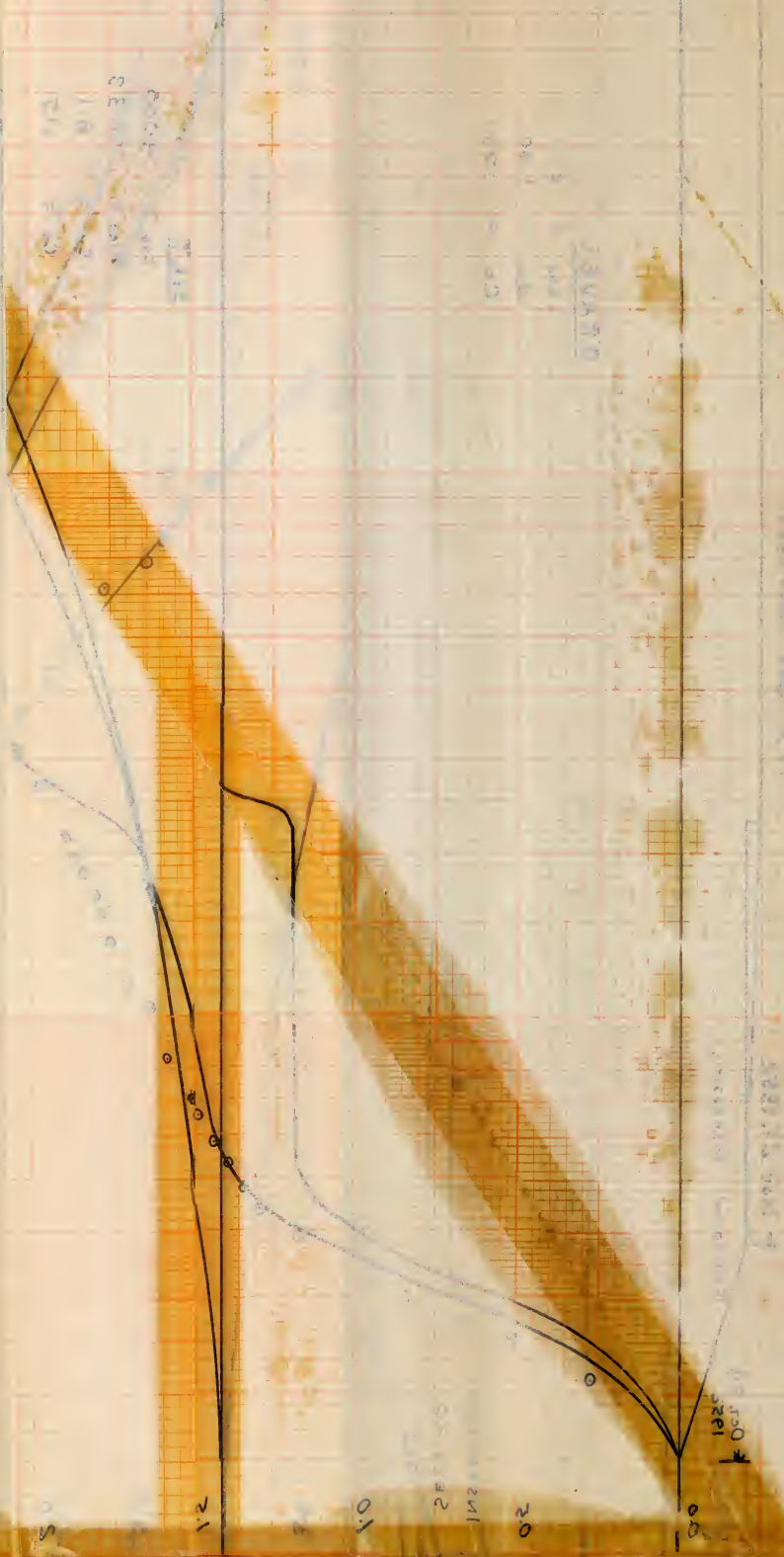
2

02

21

2

୧୨ ଅକ୍ଟୋବର





CG 10420  
July 23 1952

21% LOAD INCREASE

GRAVEL

$t_{90} = 20$   
 $\Delta t_{100} = 0.50$   
 $C_c = 1.05$

SILT

$t_{90} = 3500$   
 $\Delta t_{100} = 2.35$   
 $C_v = 2.11$   
 $C_c = 1.43$

INSTALLED  
JUNE 13, 1952

CLAY

$t_{90} = 5200$   
 $\Delta t_{100} = 2.35$   
 $C_v = 1.04$   
 $C_c = 1.56$

SETTLEMENT GAUGE 8

SERIES A

MOST PROBABLE FIT

FIGURE 18

5.18

FIGURE 18



SEP 10 1961

SEP 10 1961

SEP 10 1961

Handwritten  
Pencil

1000

1000

1000

1000

1000

1000

1000

1000

1000

1000

1000

1000

1000

1000

1000

1000



19% Load Increase

Nov. 21, 1952

Oct. 29  
1952

Uniformly Increasing

# GRAVEL

$t_{90} = 27$   
 $\Delta_{100} = 1.40$   
 $C_c = 1.09$

# SILT

$t_{90} = 4000$   
 $\Delta_{100} = 1.33$   
 $C_v = 6.1$   
 $C_c = .15$

# CLAY

$t_{90} = 2500$   
 $\Delta_{100} = 1.02$   
 $C_v = 1.4$   
 $C_c = .48$

SETTLEMENT GAUGE 9

SERIES A

MOST PROBABLE FIT

FIGURE 19

1000

100

10

5.0







15% Load Increase

Oct 31, 1952

Sept 25, 1952

Uniformly Increasing

INSTALLED  
AUG 1, 1952

### GRAVEL

$t_{90} = 60$   
 $\Delta_{100} = 1.00$   
 $C_c = .06$

### CLAY

$t_{90} = 6200$   
 $\Delta_{100} = 1.60$   
 $C_v = 0.9$   
 $C_c = .49$

### SILT

$t_{90} = 1500$   
 $\Delta_{100} = 2.40$   
 $C_v = 11.1$   
 $C_c = .26$

SETTLEMENT GAUGE 10

SERIES B

MOST PROBABLE FIT

FIGURE 20

FIGURE 20

10

100

1000

5.00



SECTION 40

100 L 5000 100 100

RELATIVE HUMIDITY

100

100

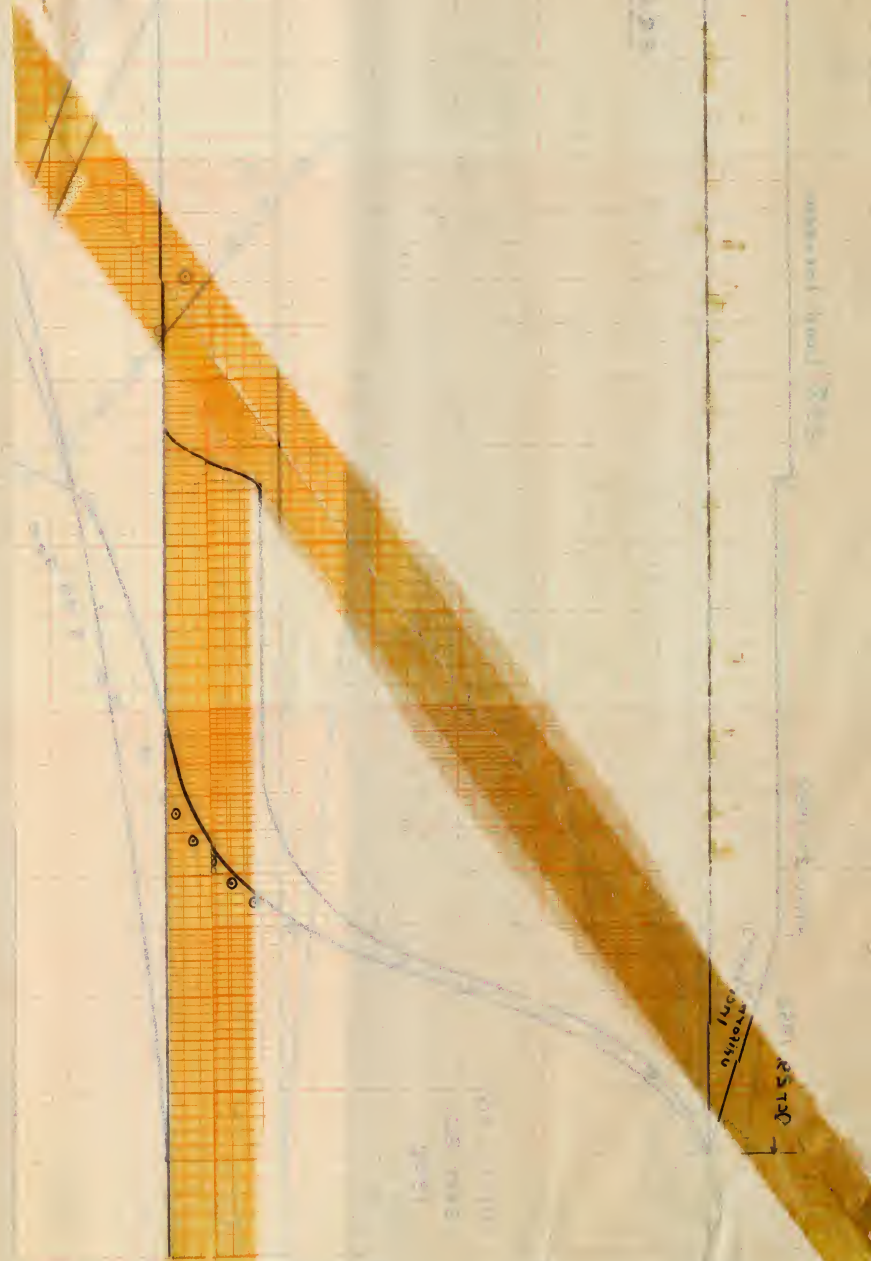
100

100 100

100 100

100 100

100 100



100 100 100

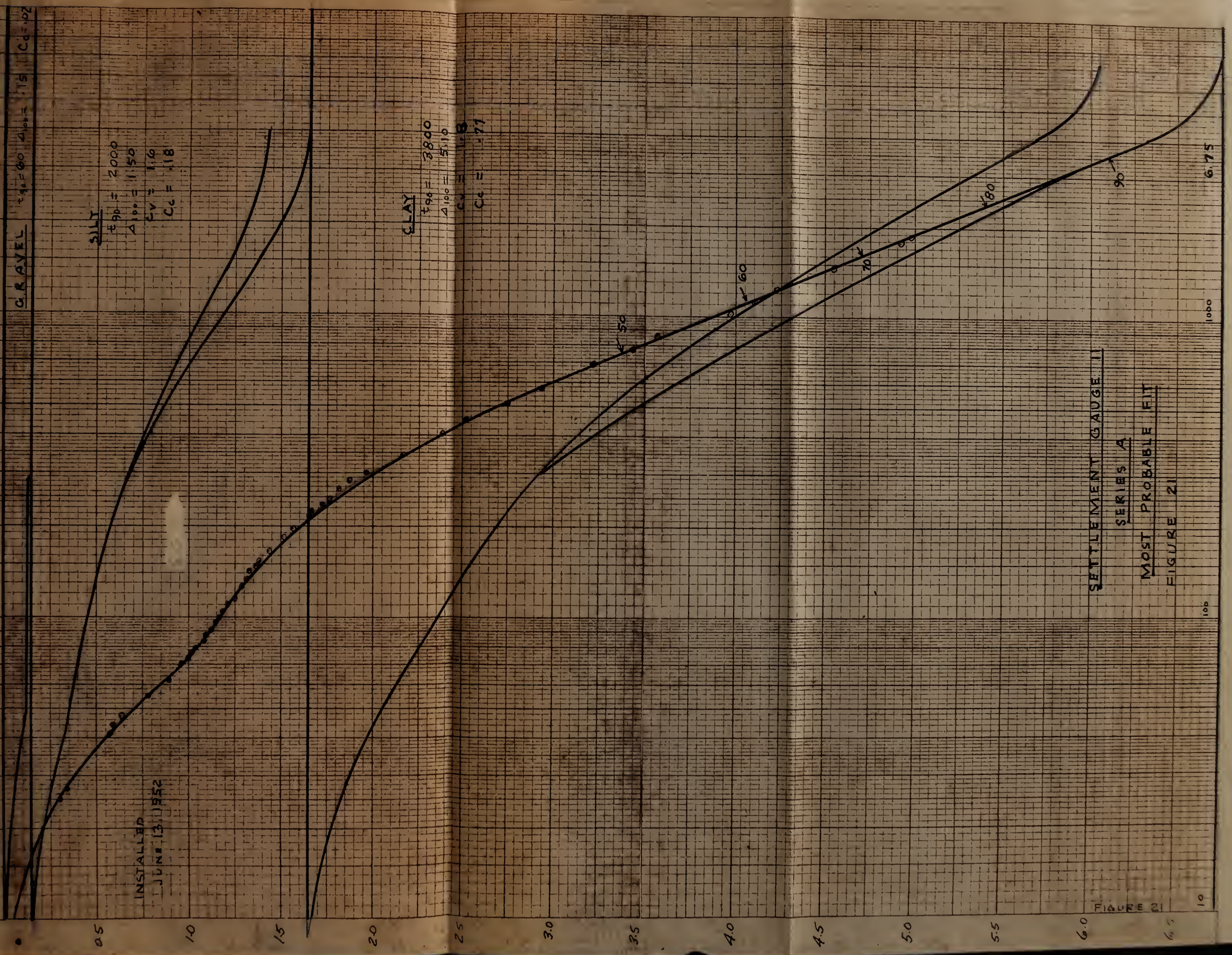
100 100



July 23, 1952

← Sept. 19, 1952

16% Load increase



SETTLEMENT GAUGE II  
SERIES A  
MOST PROBABLE FIT  
FIGURE 21



SECTION 16, T12N, R10E

SECTION 16, T12N, R10E

SECTION 16, T12N, R10E

SECTION 16, T12N, R10E

SECTION 16, T12N, R10E

SECTION 16, T12N, R10E

SECTION 16, T12N, R10E

SECTION 16, T12N, R10E

SECTION 16, T12N, R10E

SECTION 16, T12N, R10E

SECTION 16, T12N, R10E

SECTION 16, T12N, R10E

SECTION 16, T12N, R10E

SECTION 16, T12N, R10E

SECTION 16, T12N, R10E

SECTION 16, T12N, R10E



23% Load Increase

Nov. 21, 1952

Sept. 19, 1952

Increasing

# GRAVEL

$t_{90} = 35$   
 $\Delta t_{100} = 1.65$   
 $C_c = .09$

# SILT

$t_{90} = 3800$   
 $\Delta t_{100} = 1.25$   
 $C_v = 6.4$   
 $C_c = .12$

# CLAY

$t_{90} = 3000$   
 $\Delta t_{100} = 1.20$   
 $C_v = 1.2$   
 $C_c = .64$

SETTLEMENT GAUGE 12

SERIES A

MOST PROBABLE FIT

FIGURE 22

1000

100

10

5.0

FIGURE 22

4.5

4.0

3.0

2.5

2.0

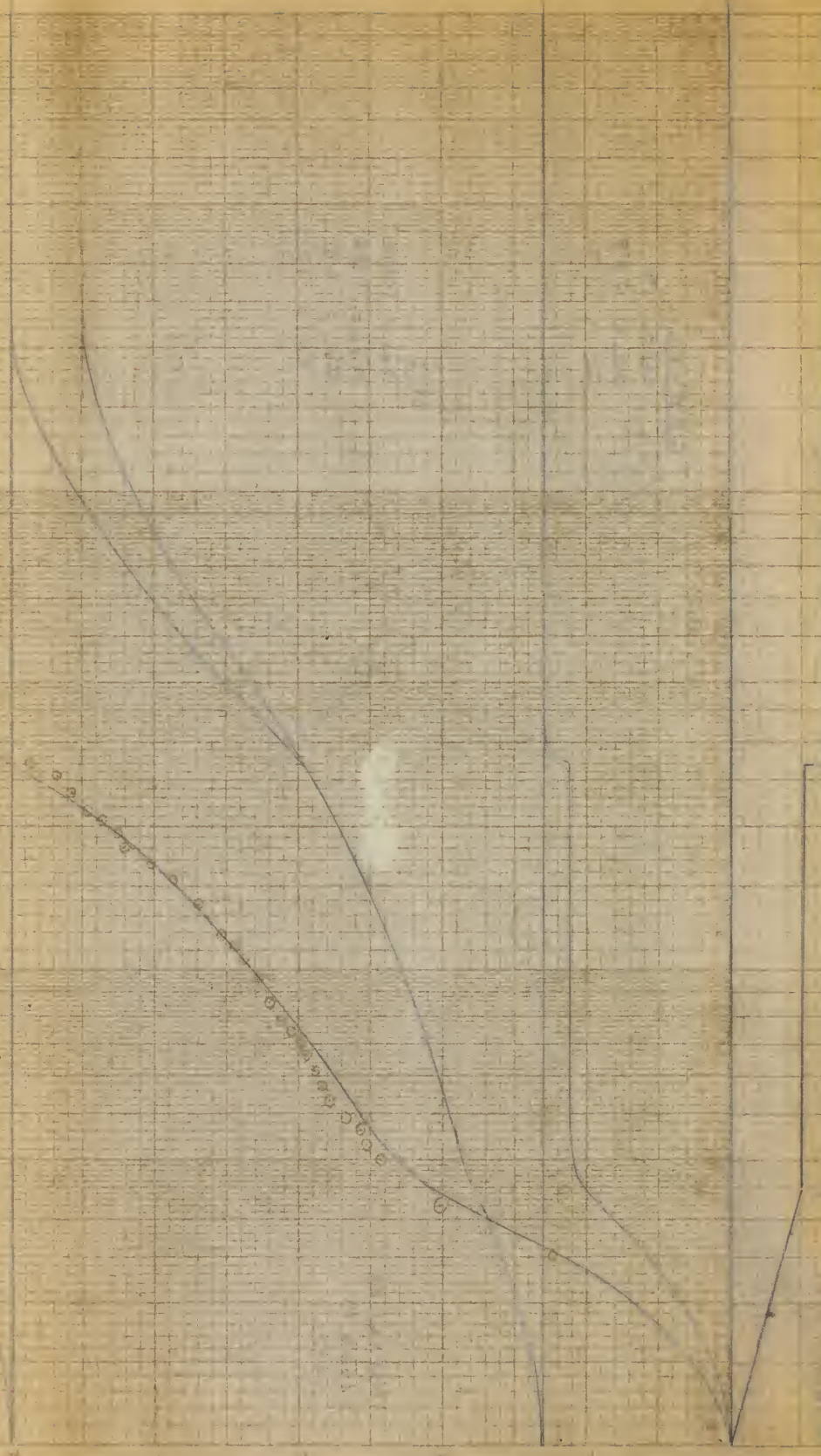
1.0

0.5

0.0

INSTALLED  
 SEPT. 20,  
 1952







14% Load Increase

4-Oct 31, 1952

Mr Aug 25, 1952

Settlement increasing

GRAVEL  
 $t_{90} = 80$   
 $\Delta_{100} = 1.10$   
 $C_c = .06$

INSTALLED  
AUG. 1, 1952

CLAY  
 $t_{90} = 6000$   
 $\Delta = 1.50$   
 $C_v = 0.9$   
 $C_c = 0.50$

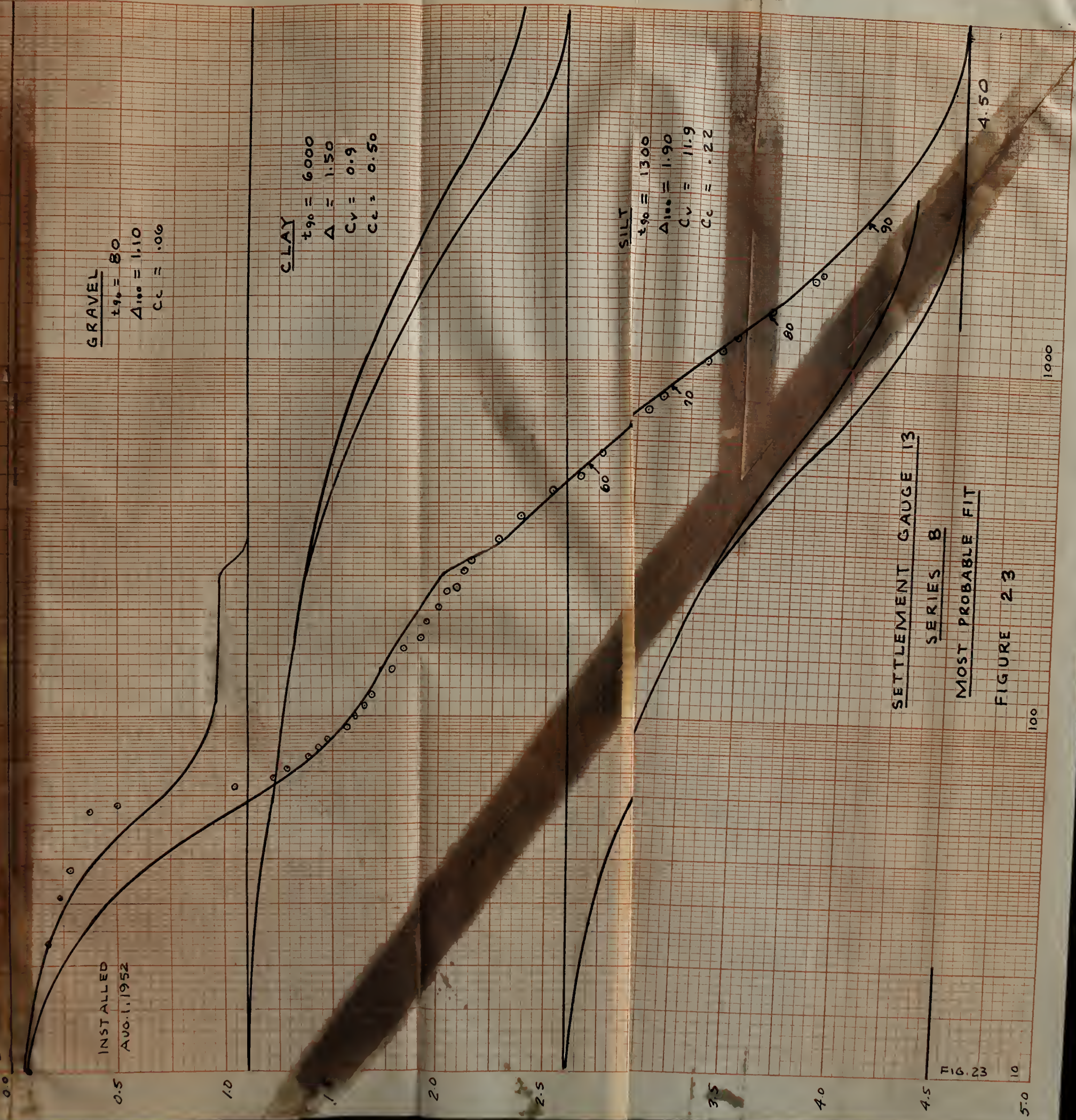
SILT  
 $t_{90} = 1300$   
 $\Delta_{100} = 1.90$   
 $C_v = 11.9$   
 $C_c = .22$

SETTLEMENT GAUGE 13

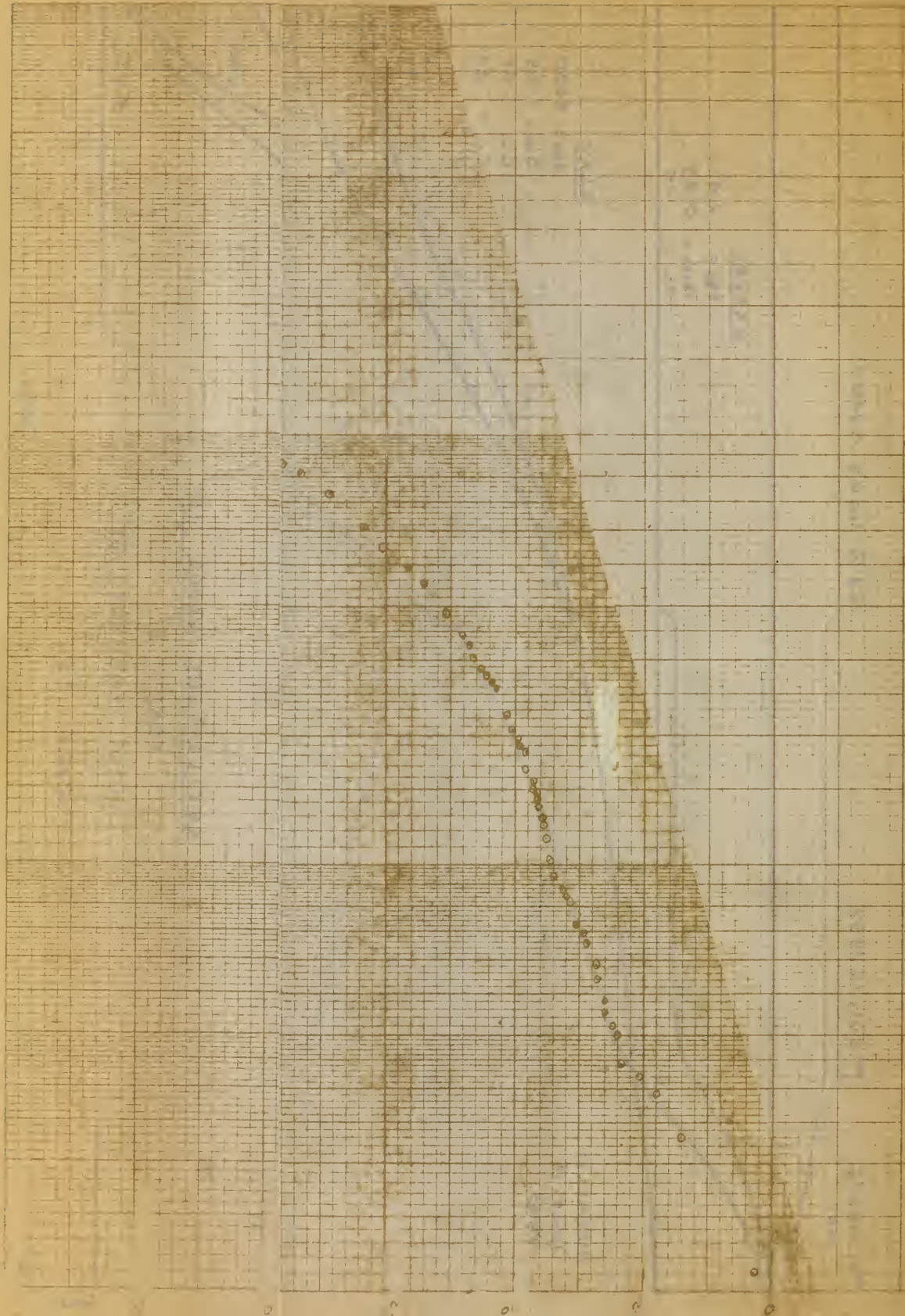
SERIES B

MOST PROBABLE FIT

FIGURE 23









10% Load Increase

Sept 1, 1952

Sept 26, 1952

GRAVEL

$t_{90} = 19$   
 $\Delta t_{100} = 0.65$   
 $C_c = 1.12$

SILT

$t_{90} = 1000$   
 $\Delta t_{100} = 1.85$   
 $C_v = 1.5$   
 $C_c = 1.25$

INSTALLED  
JUNE 13  
1952

CLAY

$t_{90} = 5390$   
 $\Delta t_{100} = 5.30$   
 $C_v = 1.74$   
 $C_c = 1.58$

SETTLEMENT GAUGE 14

SERIES A

MOST PROBABLE FIT

FIGURE 24

FIGURE 24

10

100

1000

7.80





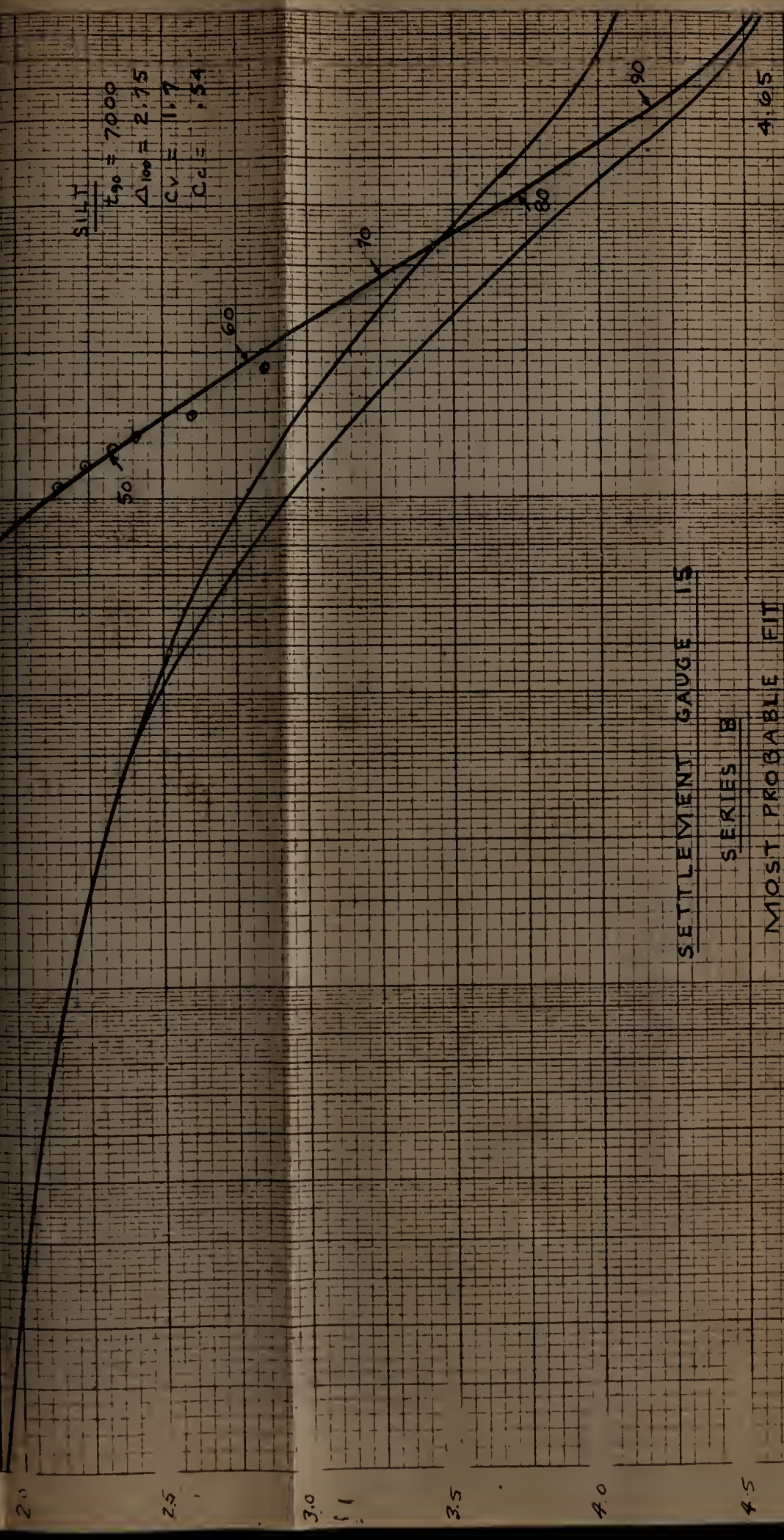


JUNE 22 1952

23% Load Added



INSTALLED  
JUNE 13  
1952



SETTLEMENT GAUGE IS

SERIES B

MOST PROBABLE FIT

FIGURE 25

Fig 25







23% Load Added

Nov 21, 1952

Nov 21, 1952

GRAVEL

$t_{90} = 25$

$\Delta t_{90} = 1.20$

$t_{90} = 4000$

$\Delta t_{90} = 1.60$

$t_{90} = 4400$

$\Delta t_{90} = 1.25$

4.05

SETTLEMENT GAUGE 1

ALTERNATE FIT

SERIES B

FIGURE 26

1000

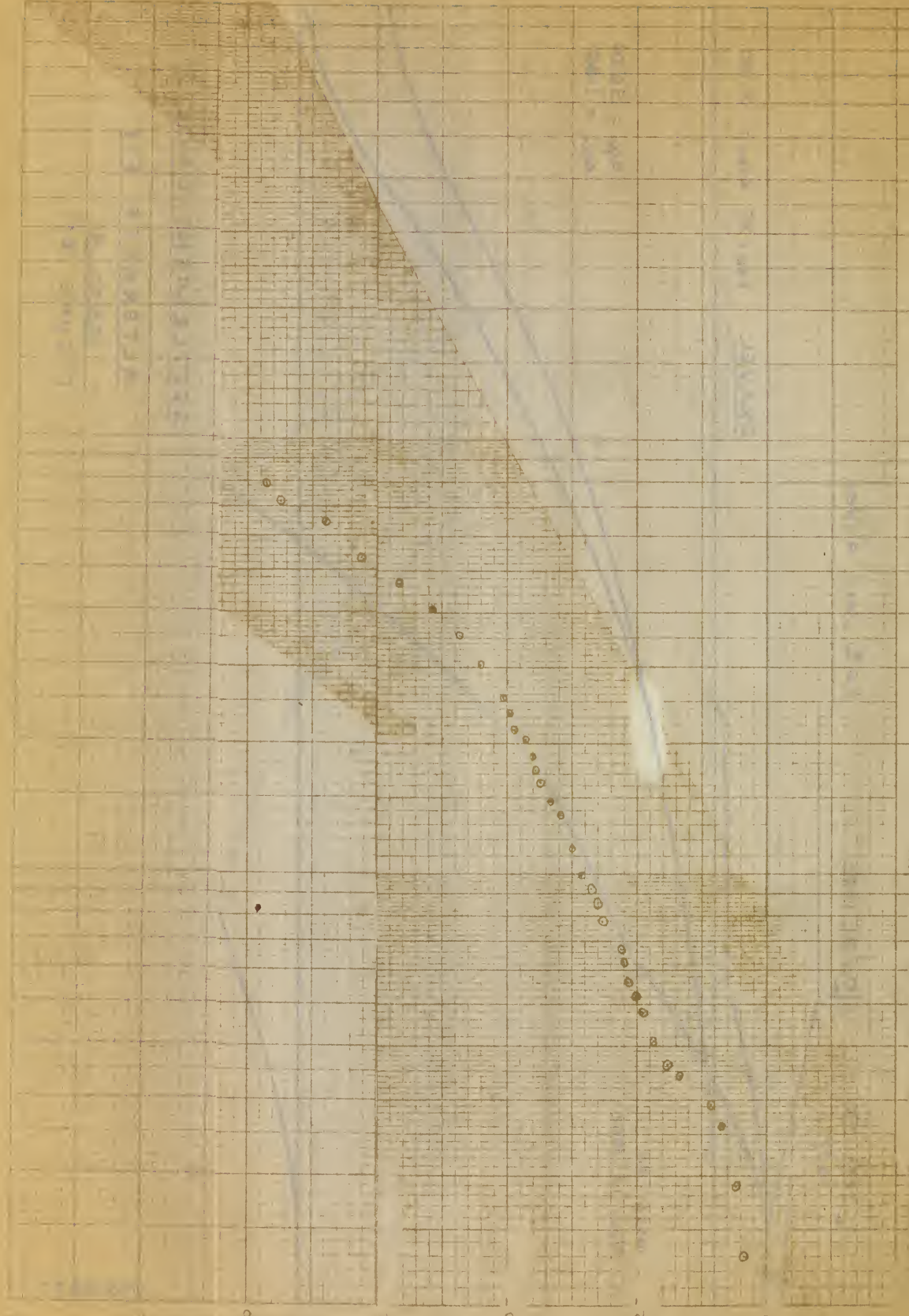
100

FIGURE 26

10

5.0







26% Load Added

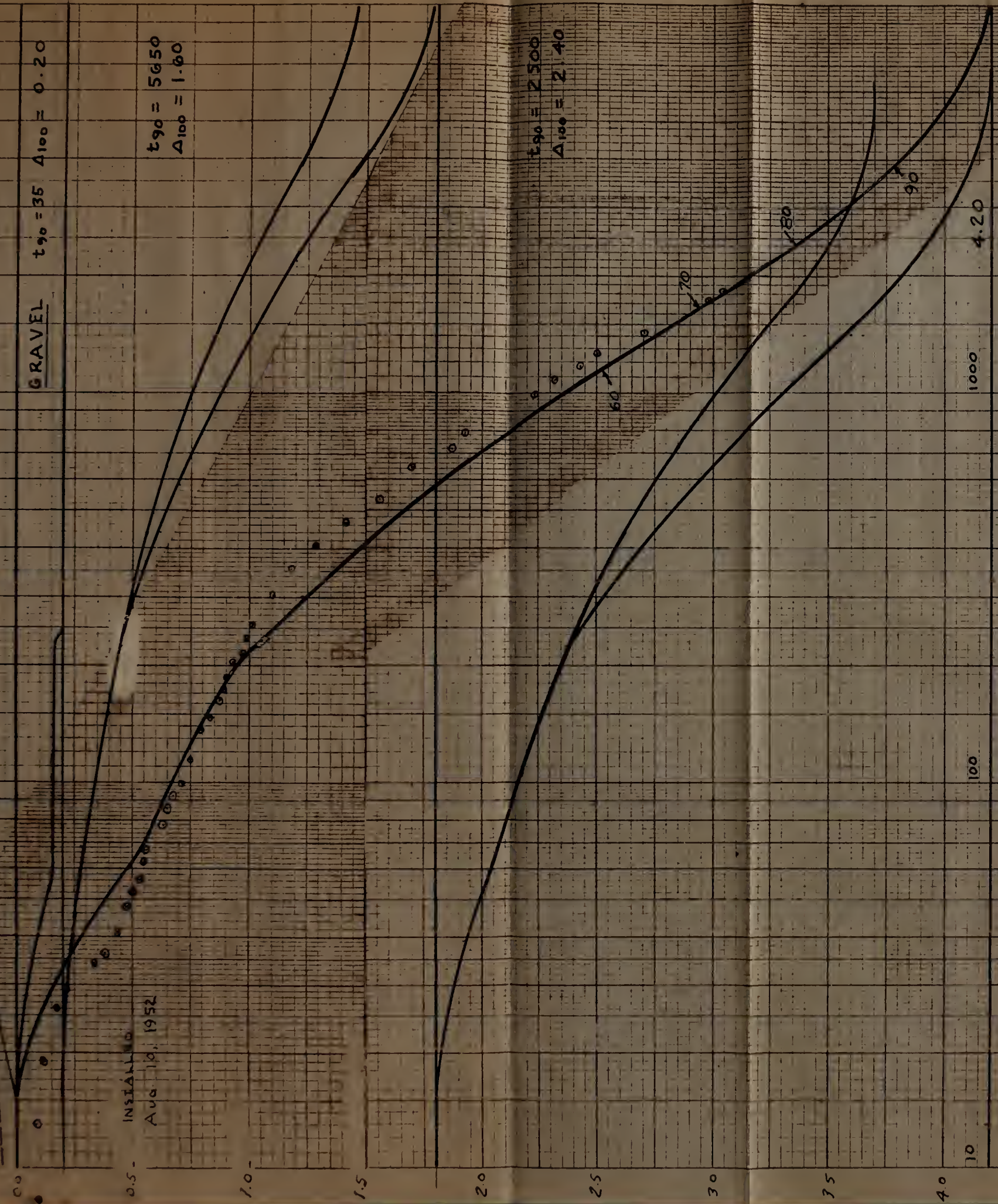
Oct 31, 1952

SEPT 25, 1952

GRAVEL  $t_{90} = 35$   $\Delta_{100} = 0.20$

$t_{90} = 5650$   
 $\Delta_{100} = 1.60$

$t_{90} = 2500$   
 $\Delta_{100} = 2.40$



SETTLEMENT GAUGE 2

ALTERNATE FIT

SERIES B

FIGURE 27

FIGURE 27



15. 30. 1917

0000 = 0.17  
0000 = 0.17

0000 = 0.17

0000 = 0.17

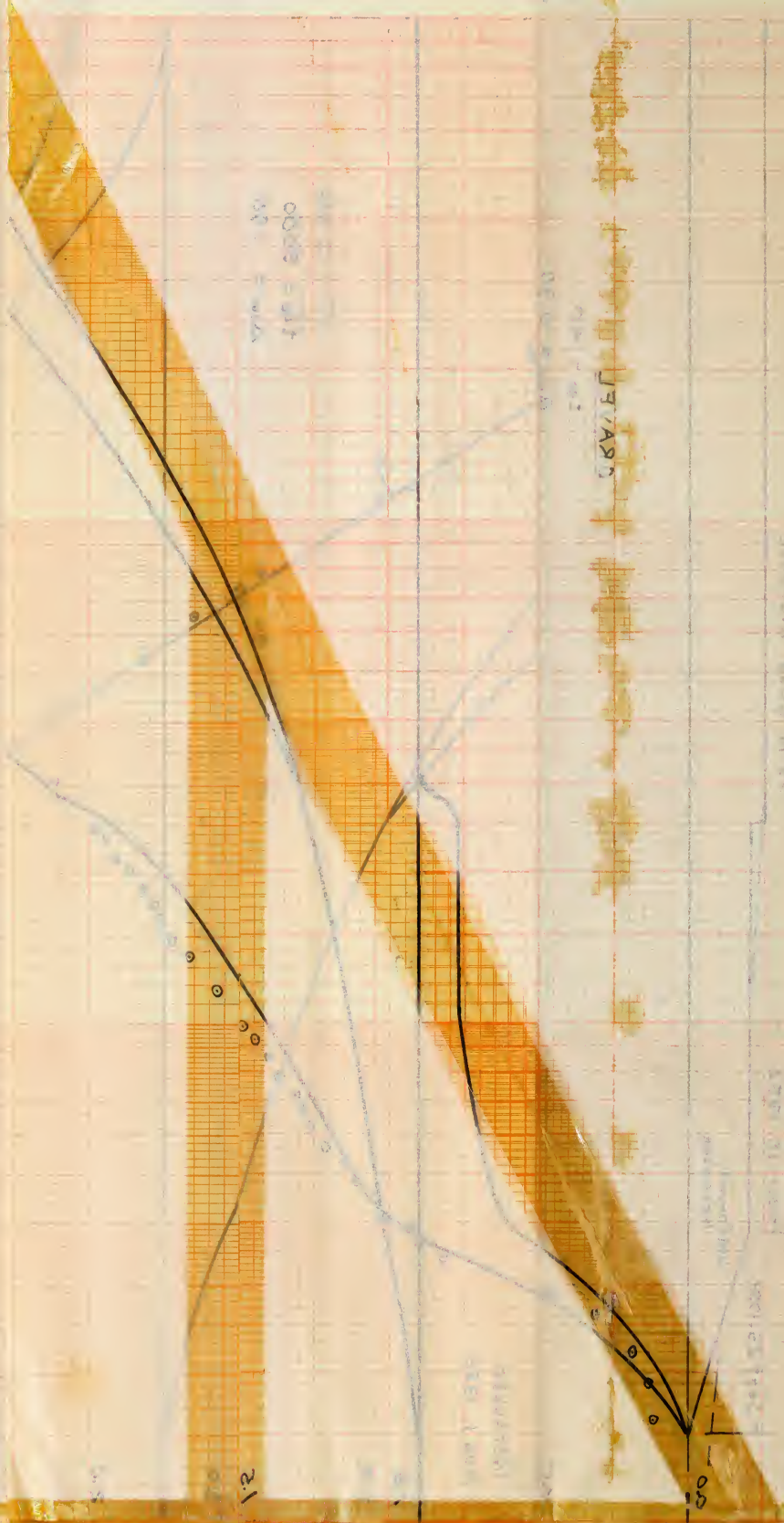
0000 = 0.17

0000 = 0.17

0000 = 0.17

0000 = 0.17

12





23% Load Added

Nov 21, 1952

Oct 27, 1952

INSTALLED  
SEPT 24  
1952

GRAVEL

$t_{90} = 32$

$\Delta_{100} = 1.40$

$t_{90} = 2500$

$\Delta_{100} = 1.20$

$t_{90} = 4000$

$\Delta_{100} = 1.00$

FIGURE 28

SETTLEMENT GAUGE 3

SERIES B

ALTERNATE FIT

10

100

1000

FIGURE 28

10,000



1000

100

Figure 30

THE STATION

Figure 30

$\Delta H = 1.20$   
 $\Delta P = 0.000$

Figure 30  $\Delta H = 1.20$   $\Delta P = 0.000$

Figure 30

Figure 30

Figure 30



19% Load Increase

Oct 17, 1952

Sept 23, 1952

Uniformly Increasing

GRAVEL

$t_{90} = 40$   
 $\Delta_{100} = 0.90$

INSTALLED  
Aug 1, 1952

$t_{90} = 5000$   
 $\Delta_{100} = 1.90$

$t_{90} = 1800$   
 $\Delta_{100} = 2.88$

SETTLEMENT GAUGE 4

SERIES B

ALTERNATE FIT

FIGURE 29

FIGURE 29

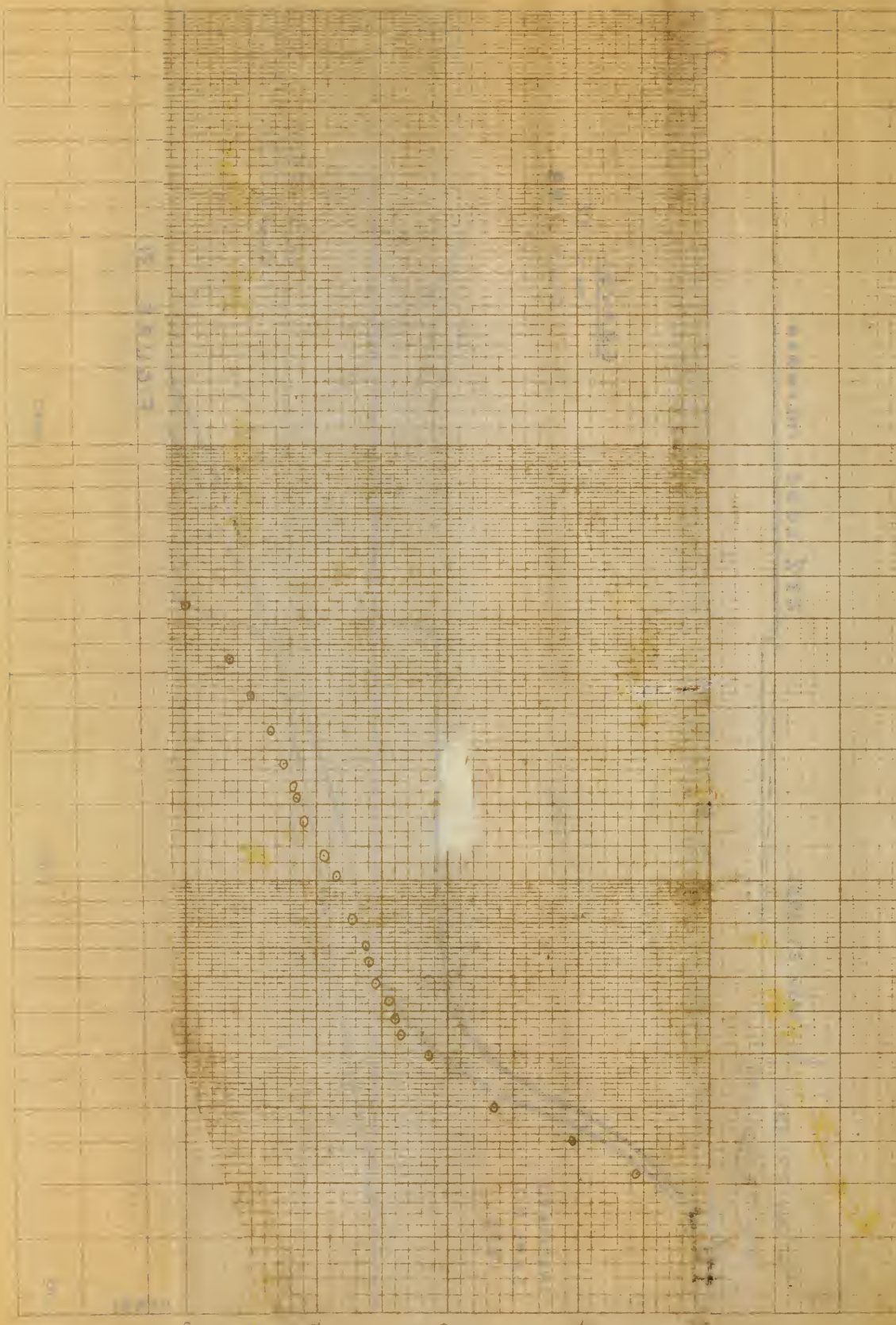
10

100

1000

5.08







11% Load Increase

$t = 0$  @ load = 0  
June 6, 1952

July 18, 1952

GRAVEL  $t_{90} \approx 35$   $\Delta_{100} \approx 0.10$

$t_{90} = 6000$   
 $\Delta_{100} = 1.50$

INSTALLED  
JUNE 6, 1952

$t_{90} \approx 5500$   
 $\Delta_{100} \approx 2.05$

SETTLEMENT GAUGE 5

SERIES A

ALTERNATE FIT

FIGURE 30

1000

100

10

50



25 25 25

25 25 25

25 25 25

$\Delta_{100} = 1.22$   
25 25 25

25 25 25

25 25 25

25 25 25

SEP 10 1963  
ENTREPRENEUR



23% Load Increase

Nov 21, 1952

OCT 27, 1952

0.0

0.5

1.0

1.5

2.0

2.5

3.0

3.5

4.0

4.5

10

100

1000

GRAVEL

$t_{90} = 32$

$\Delta_{100} = 1.28$

$t_{90} = 2500$

$\Delta_{100} = 1.27$

$t_{90} = 4000$

$\Delta_{100} = 1.00$

355

SETTLEMENT GAUGE 6

SERIES B

ALTERNATE FIT

FIGURE 31

FIGURE 31



2200000 67.1 7.0

12 VASD

gms = 0.20  
lbs = 0.04

gms = 0.20  
lbs = 0.04

0.20 gm  
0.04 lb

0.20 gm  
0.04 lb



16% Load Increase

Oct 17, 1952

Sept 30, 1952

Uniformly Increasing

GRAVEL

$t_{90} = 38'$   
 $\Delta_{100} = 0.90$

$t_{90} = 6300$   
 $\Delta_{100} = 1.85$

$t_{90} = 1500$   
 $\Delta_{100} = 2.30$

5.05

SETTLEMENT GAUGE 7

SERIES B

ALTERNATE FIT

FIGURE 32

1000

100

10

FIGURE 32

5.5

0.0

0.5

1.0

1.5

2.0

2.5

3.0

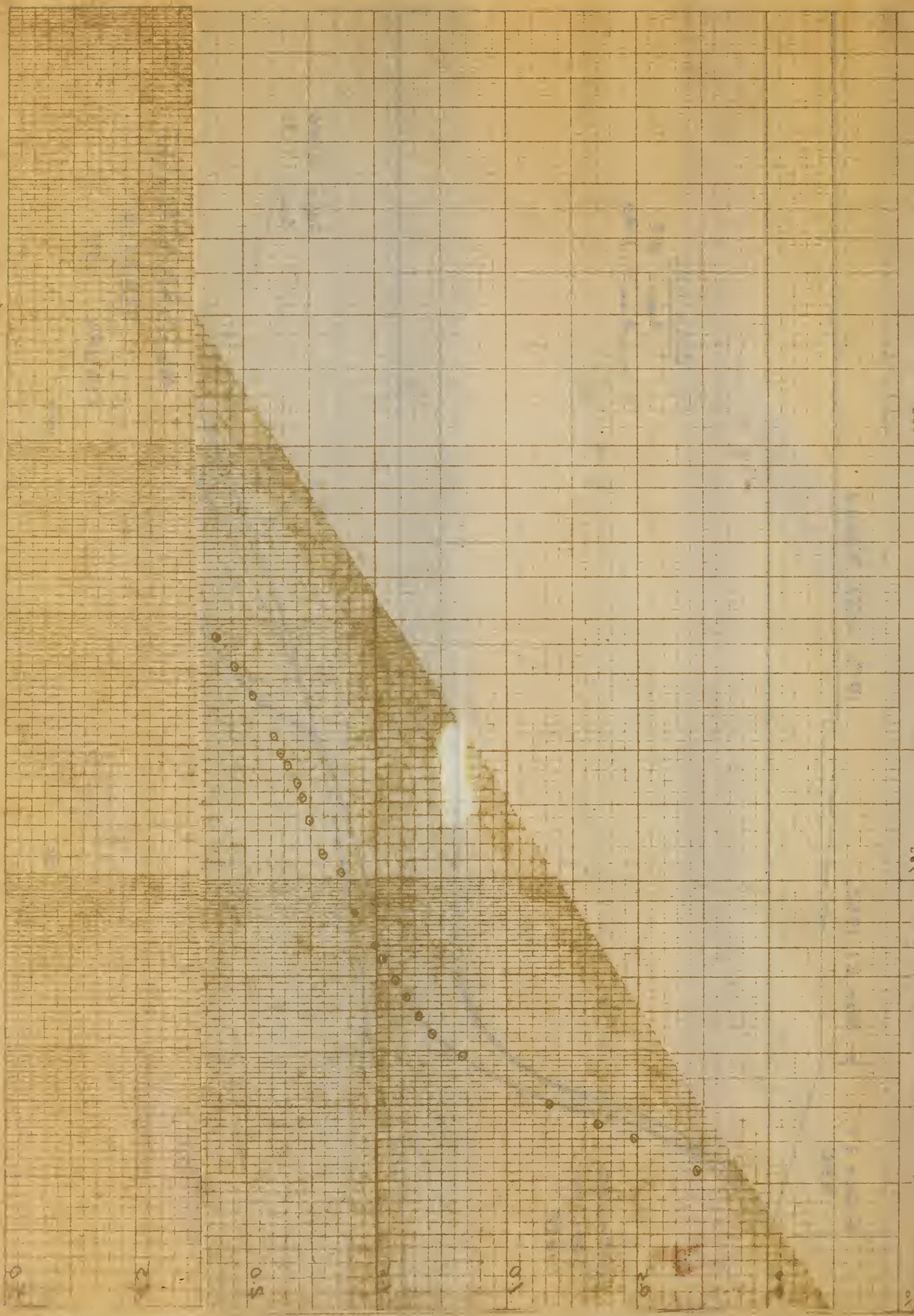
3.5

4.0

4.5

5.0







Day 0 = July 23, 1952

21% Load Increase

GRAVEL

$t_{90} = 2.0$   
 $\Delta_{100} = 0.50$

$t_{90} = 5200$   
 $\Delta_{100} = 2.35$

INSTALLED  
JUNE 13, 1952

$t_{90} = 3500$   
 $\Delta_{100} = 2.35$

SETTLEMENT GAUGE 8

SERIES B  
ALTERNATE FIT

FIGURE 33

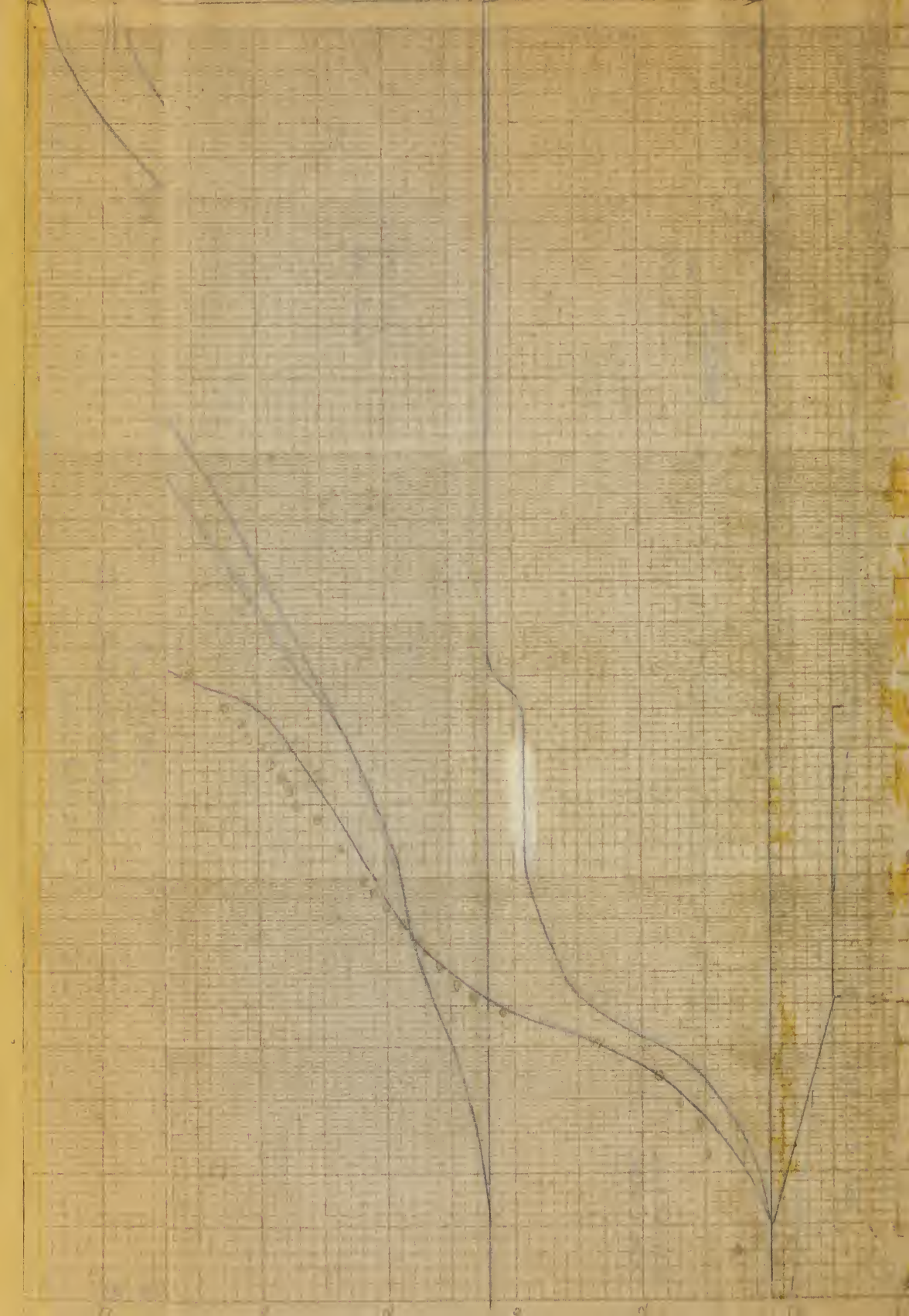
1000

100

10

FIGURE 33







19% Load Added

Nov. 21, 1952

Oct 29  
1952

GRAVEL

$$t_{90} = 27$$

$$\Delta_{100} = 1.40$$

$$t_{90} = 2500$$

$$\Delta_{100} = 1.33$$

$$t_{90} = 4000$$

$$\Delta_{100} = 1.00$$

3.73

SETTLEMENT GAUGE 9

ALTERNATE FIT

SERIES B

FIGURE 34

1000

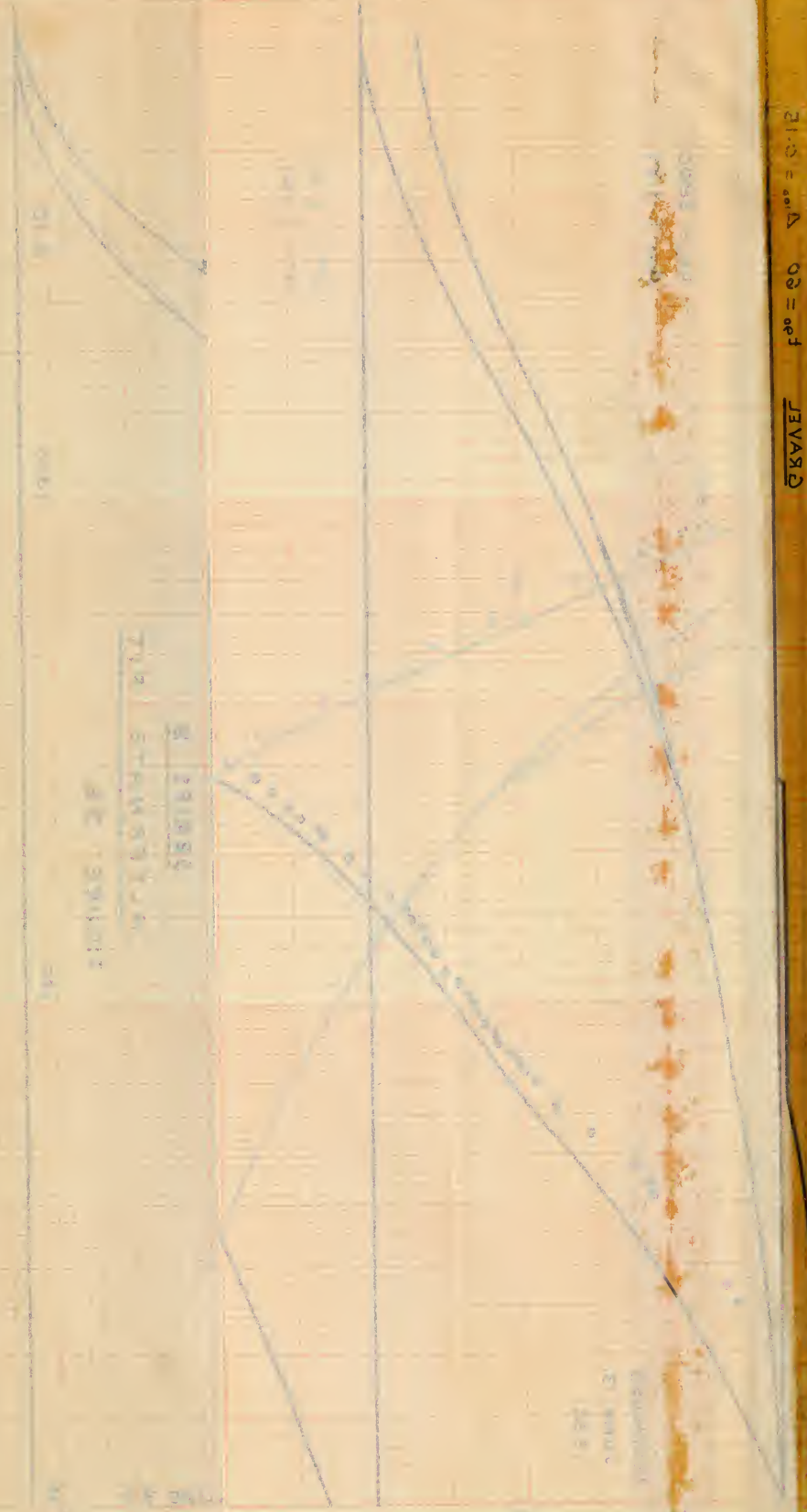
100

10

50

FIGURE 34





1900  
 1910  
 1920  
 1930

$f^0 = 0.0$   $\Delta^0 = 0.12$

1900  
 1910  
 1920  
 1930



SEP 25, 1952

OCT 31, 1952

1.5% Load Added

INSTALLED  
AUG 1, 1952

GRAVEL

$t_{90} = 60$   
 $\Delta H_{90} = 1.10$

$t_{90} = 1500$   
 $\Delta H_{90} = 1.70$

$t_{90} = 6200$   
 $\Delta H_{90} = 2.50$

FIGURE 35

SETTLEMENT GAUGE 10  
SERIES A  
ALTERNATE FIT

FIGURE 35

10

100

1000

5.30







2.0 @ load = 0  
July 23 1952

Sept 19, 1952

16% Load Increase

Uniformly increasing

GRAVEL  $t_{90} = 60$   $\Delta_{100} = 0.15$

$t_{90} = 3800$   
 $\Delta_{100} = 1.35$

INSTALLED  
JUNE 13,  
1952

$t_{90} = 2000$   
 $\Delta_{100} = 4.60$

FIGURE 36

SETTLEMENT GAUGE II

SERIES B

ALTERNATE FIT

FIGURE 36

6.0 10

100

1000

6.10

90

80

70

60

50







23% Load Added

Nov 21, 1952

Oct 29, 1952

0.0

0.5

1.0

1.5

2.0

2.5

3.0

3.5

4.0

4.5

5.0

100

1000

GRAVEL

$t_{90} = 35$   
 $\Delta_{100} = 1.65$

INSTALLED  
SEPT 20  
1952

$t_{90} = 3000$   
 $\Delta_{100} = 1.25$

$t_{90} = 3800$   
 $\Delta_{100} = 1.20$

FIGURE 37

SETTLEMENT GAUGE 12

SERIES B

ALTERNATE FIT

FIGURE 37



1000

1000

1000

1000

1000

1000

1000

1000





14.7% Load Increase

Oct 31, 1952

AUG 25  
1952

GRAVEL

$$t_{90} = 80$$

$$\Delta_{100} = 1.10$$

INSTALLED  
AUG 11  
1952

$$t_{90} = 1300$$

$$\Delta_{100} = 1.50$$

$$t_{90} = 6000$$

$$\Delta_{100} = 2.40$$

SETTLEMENT GAUGE 13

SERIES A  
ALTERNATE FIT

FIGURE 38

FIGURE 38

10

100

1000

5.00



16% Load Increase

Sept 26 1952

Sept 1, 1952

Uniformly Increasing

GRAVEL  
GRAVEL

$$t_{90} = 19$$
$$\Delta_{100} = 0.65$$

$$t_{90} = 5390$$
$$\Delta_{100} = 1.85$$

$$t_{90} = 2000$$
$$\Delta_{100} = 4.40$$

INSTALLED  
JUNE 13  
1952

SETTLEMENT GAUGE 14

SERIES B  
ALTERNATE FIT

FIGURE 39

FIGURE 39

10

100

1000

6.90



June 22 1952

23% Load Increase

Uniformly Increasing

GRAVEL

$$t_{90} = 24$$
$$\Delta_{100} = .45$$

INSTALLED

JUNE 13  
1952

$$t_{90} = 7000$$
$$\Delta_{100} = 1.35$$

$$t_{90} = 5000$$
$$\Delta_{100} = 2.75$$

FIG. 40

SETTLEMENT GAUGE 15

SERIES A  
ALTERNATE FIT  
FIGURE 40

10

100



STATION 10000  
STATION 10000  
STATION 10000

STATION 10000  
STATION 10000  
STATION 10000

STATION 10000  
STATION 10000  
STATION 10000

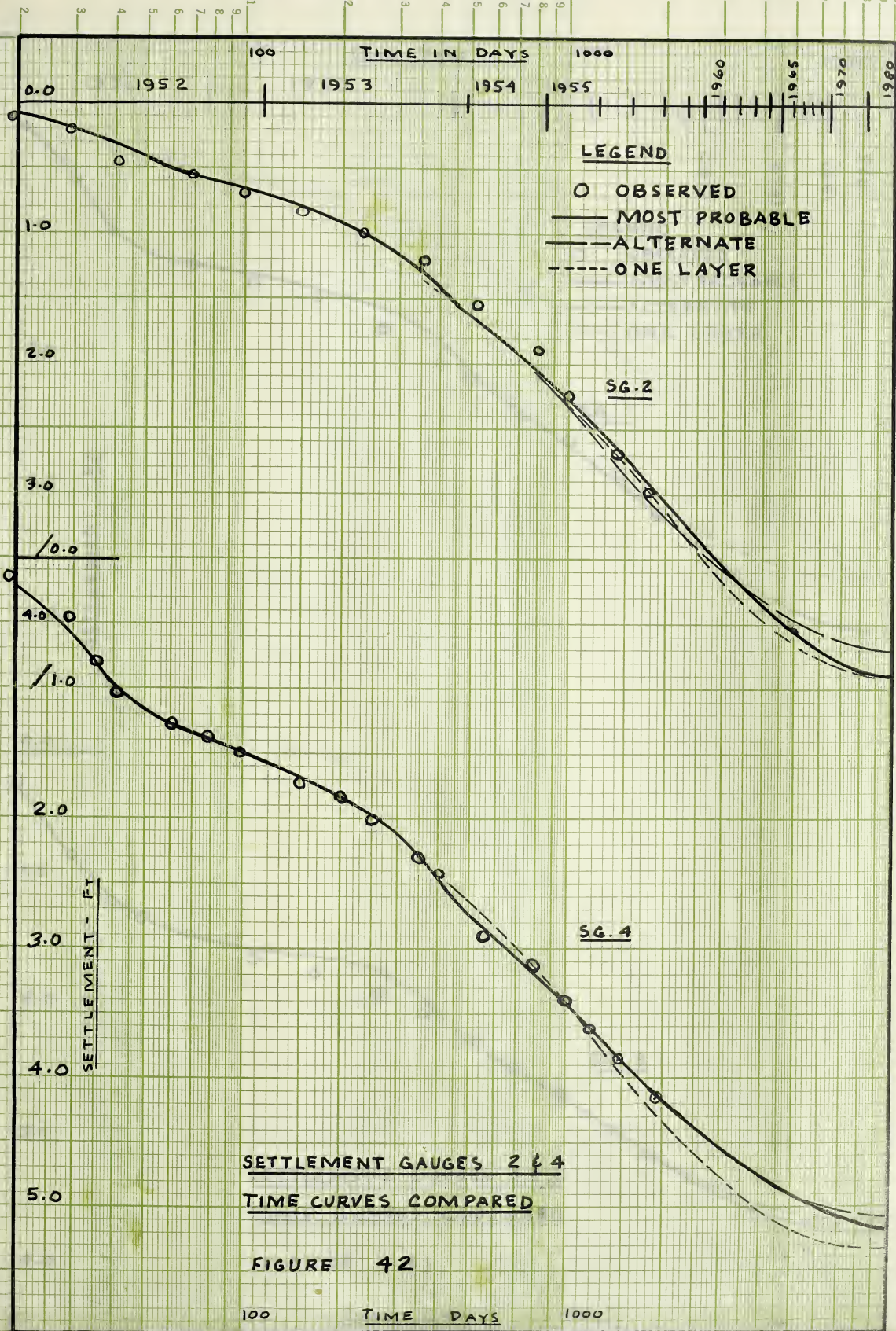
STATION 10000  
STATION 10000  
STATION 10000

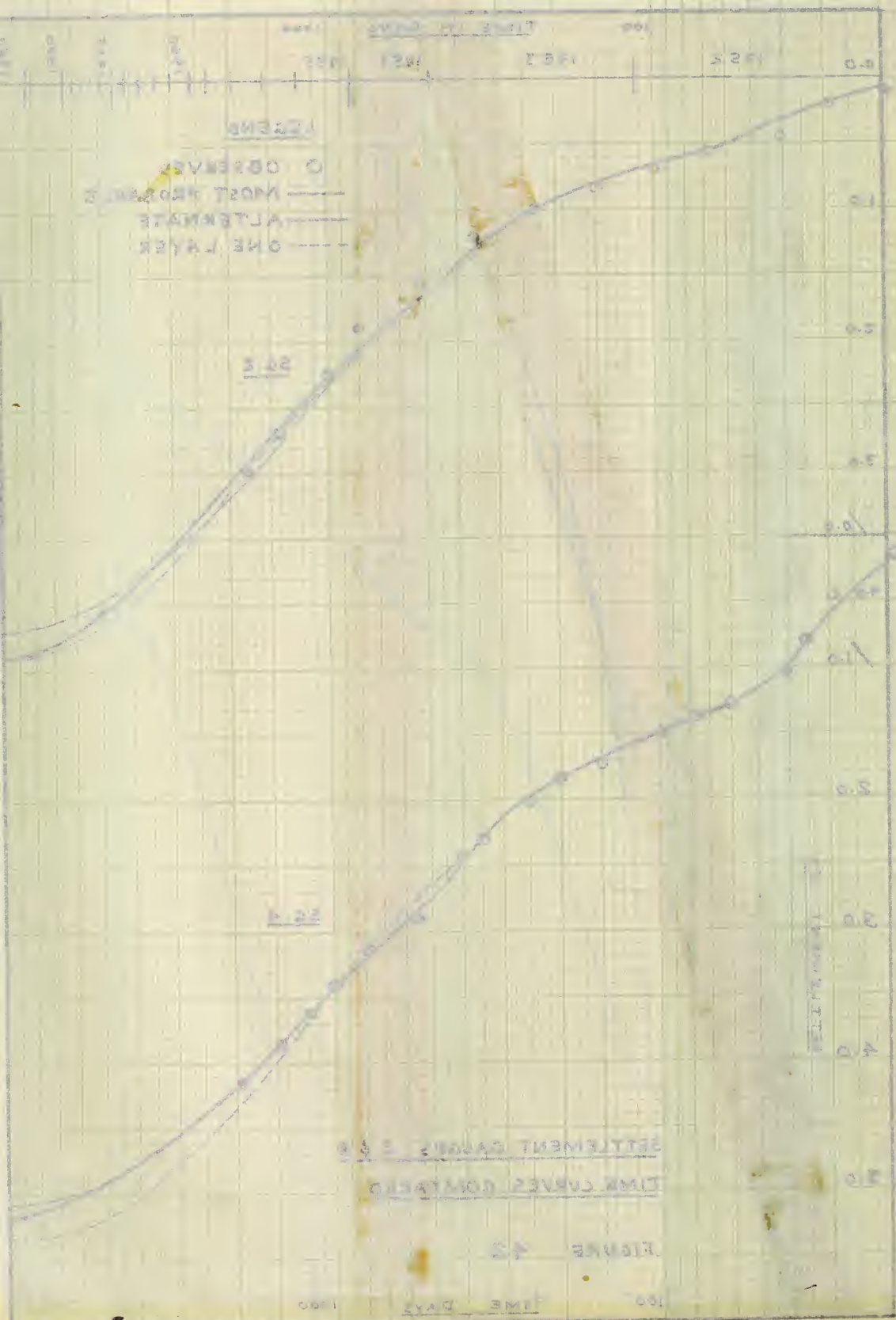
STATION 10000  
STATION 10000  
STATION 10000

STATION 10000  
STATION 10000  
STATION 10000

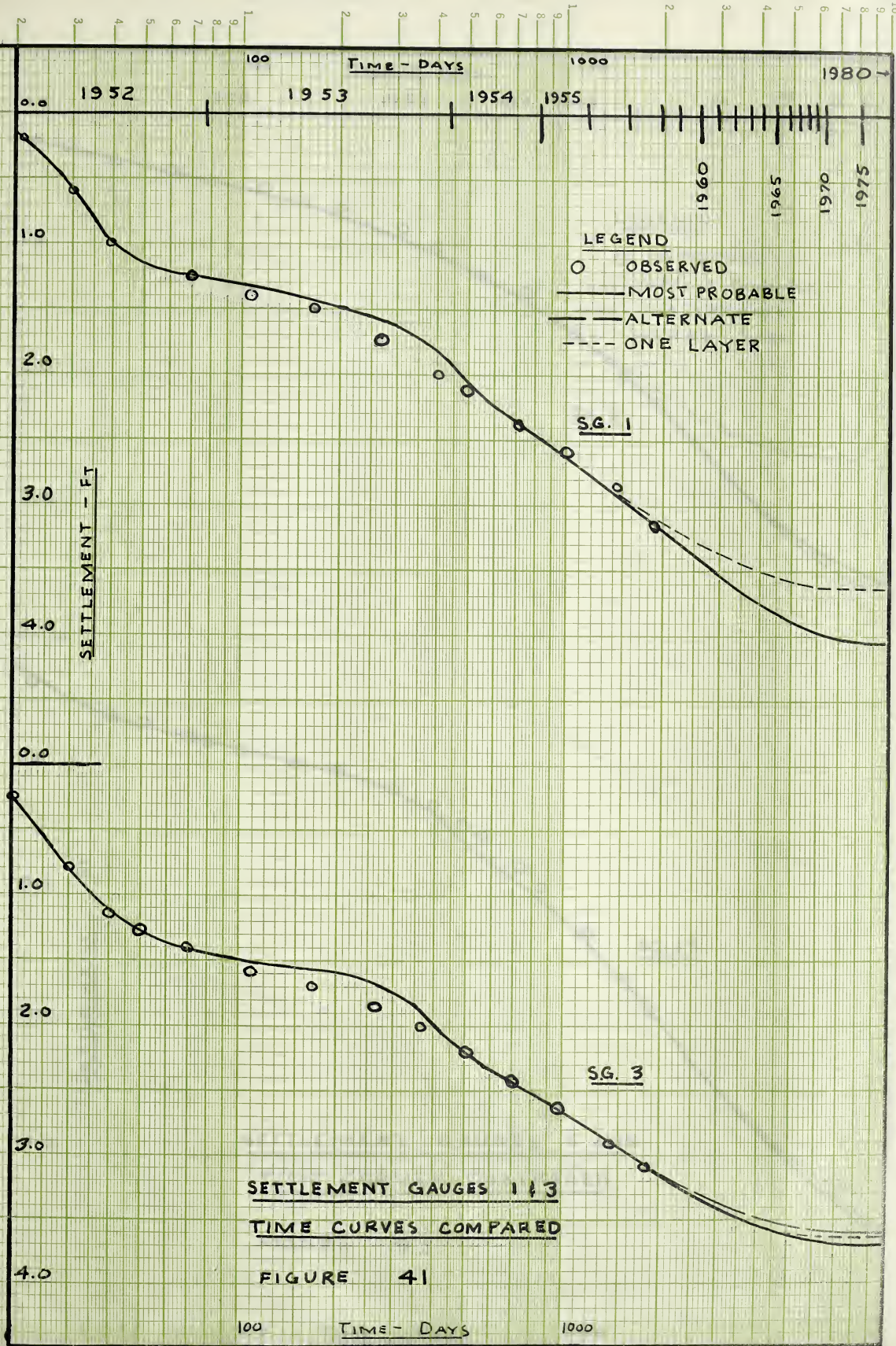
STATION 10000  
STATION 10000  
STATION 10000



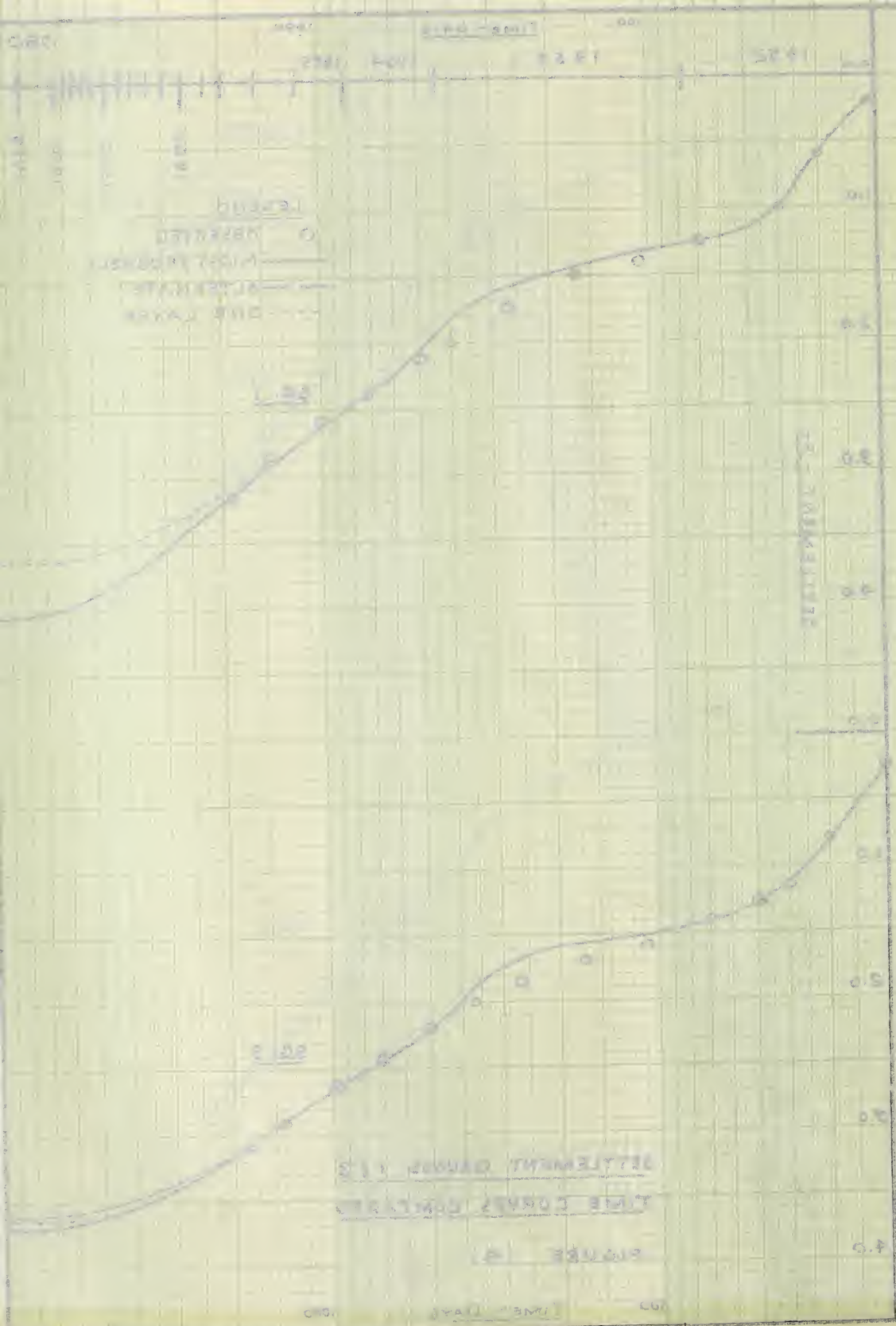


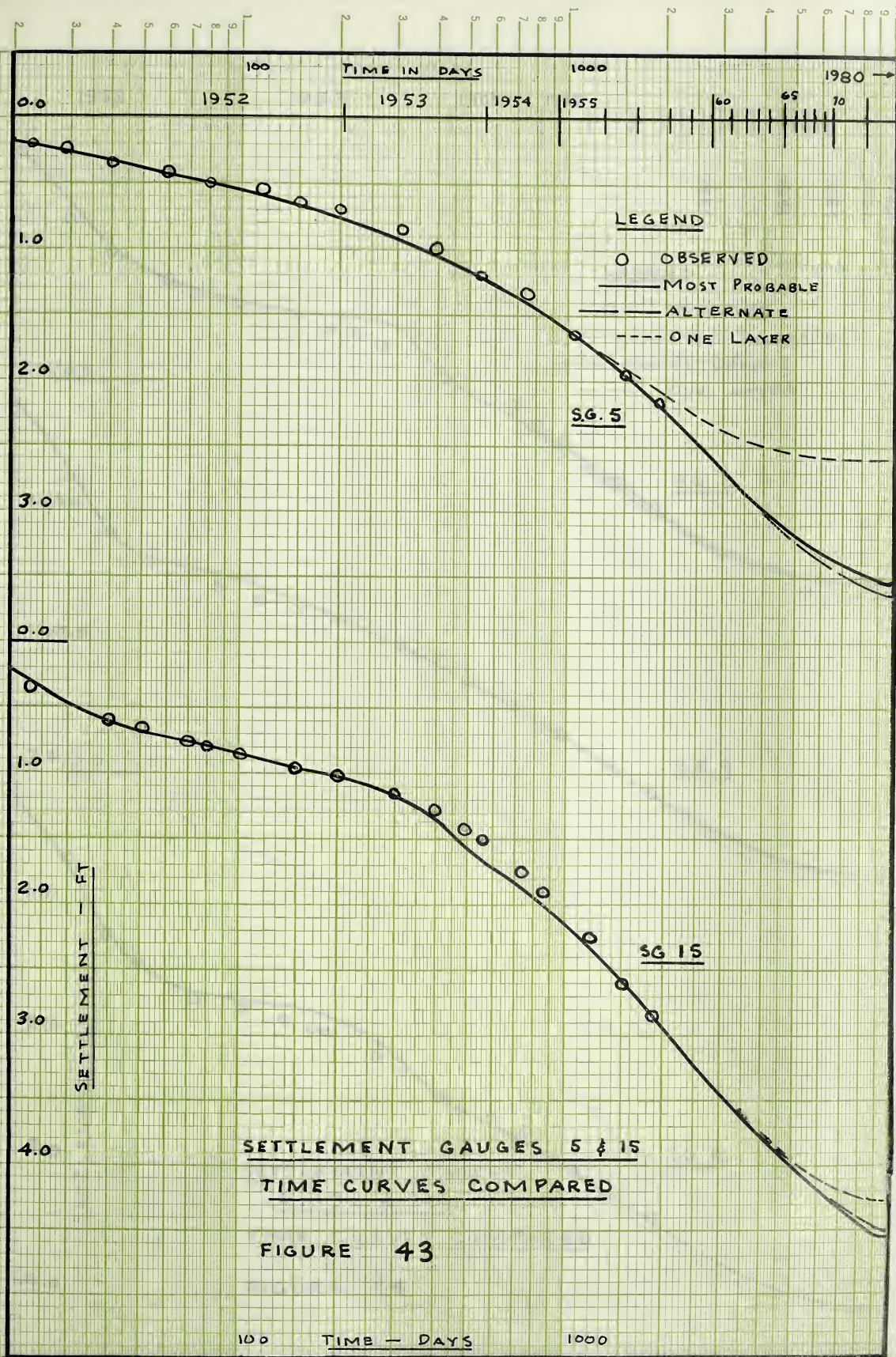




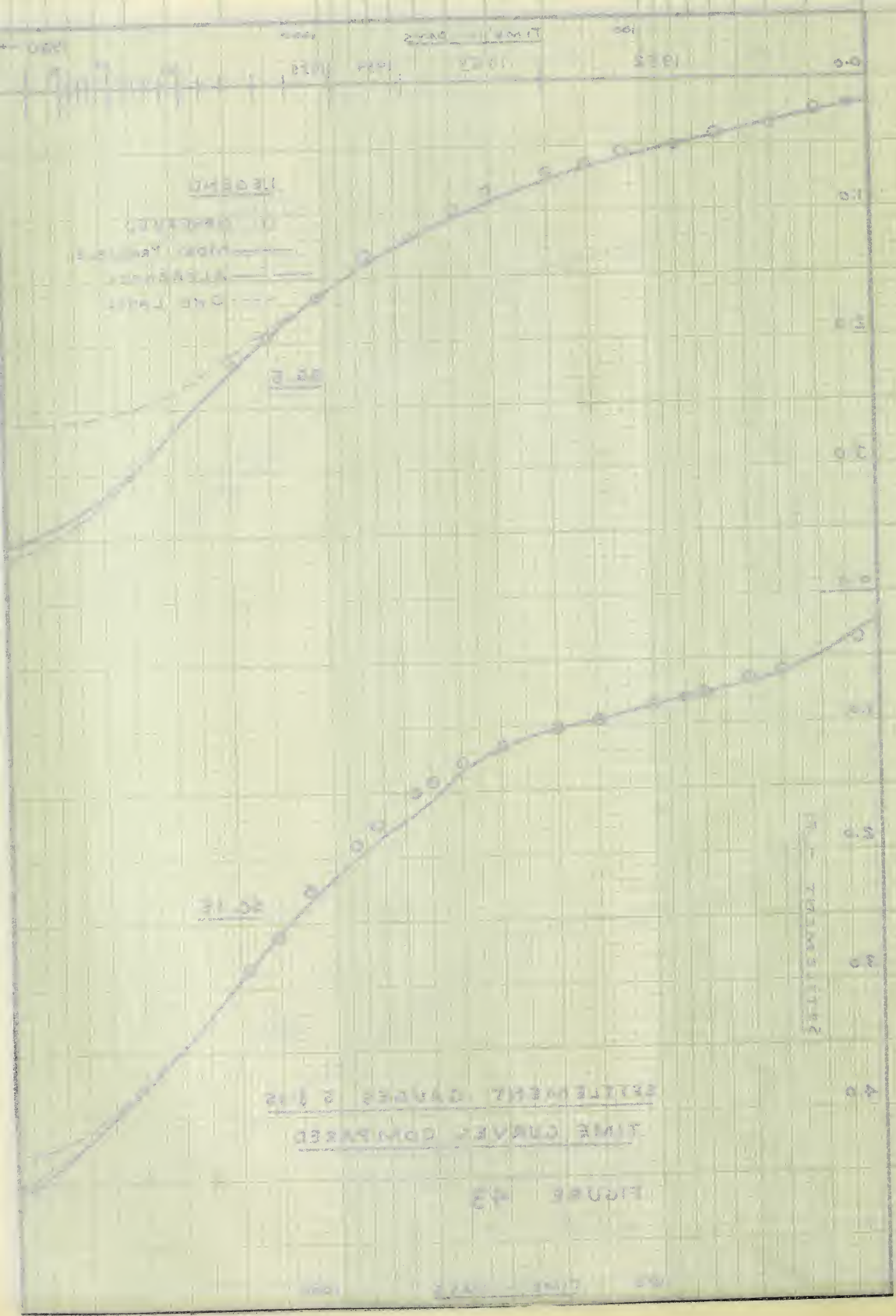




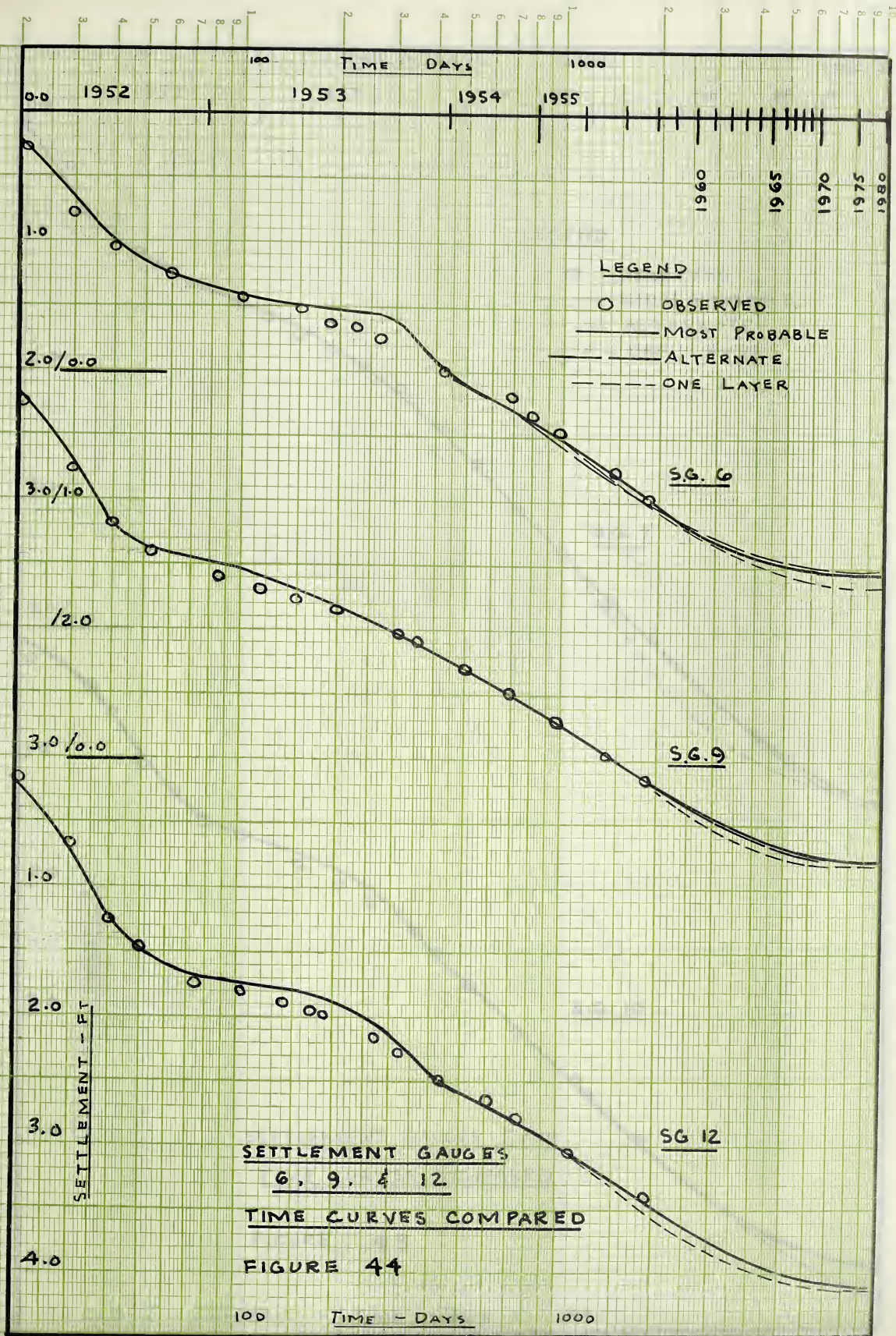




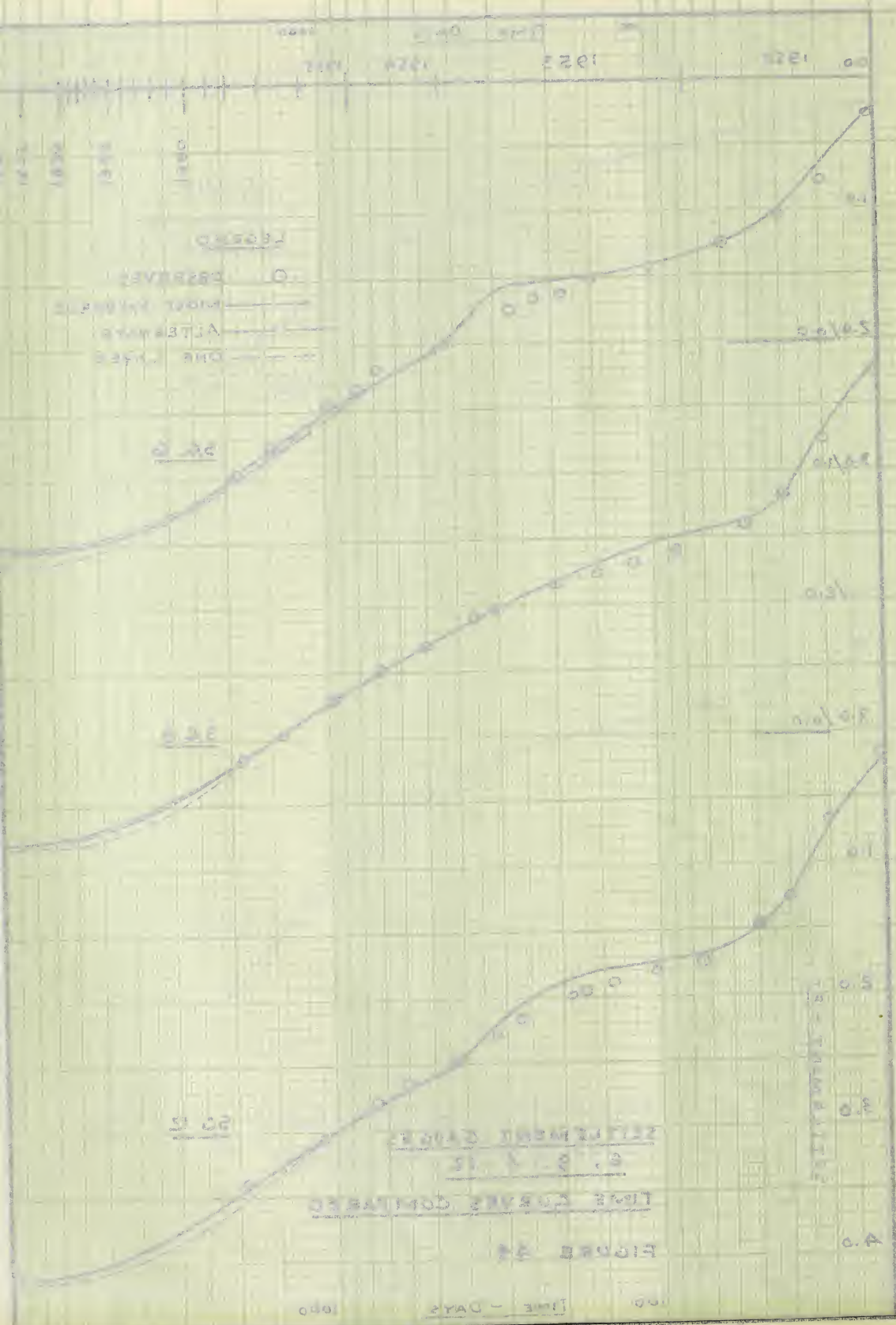


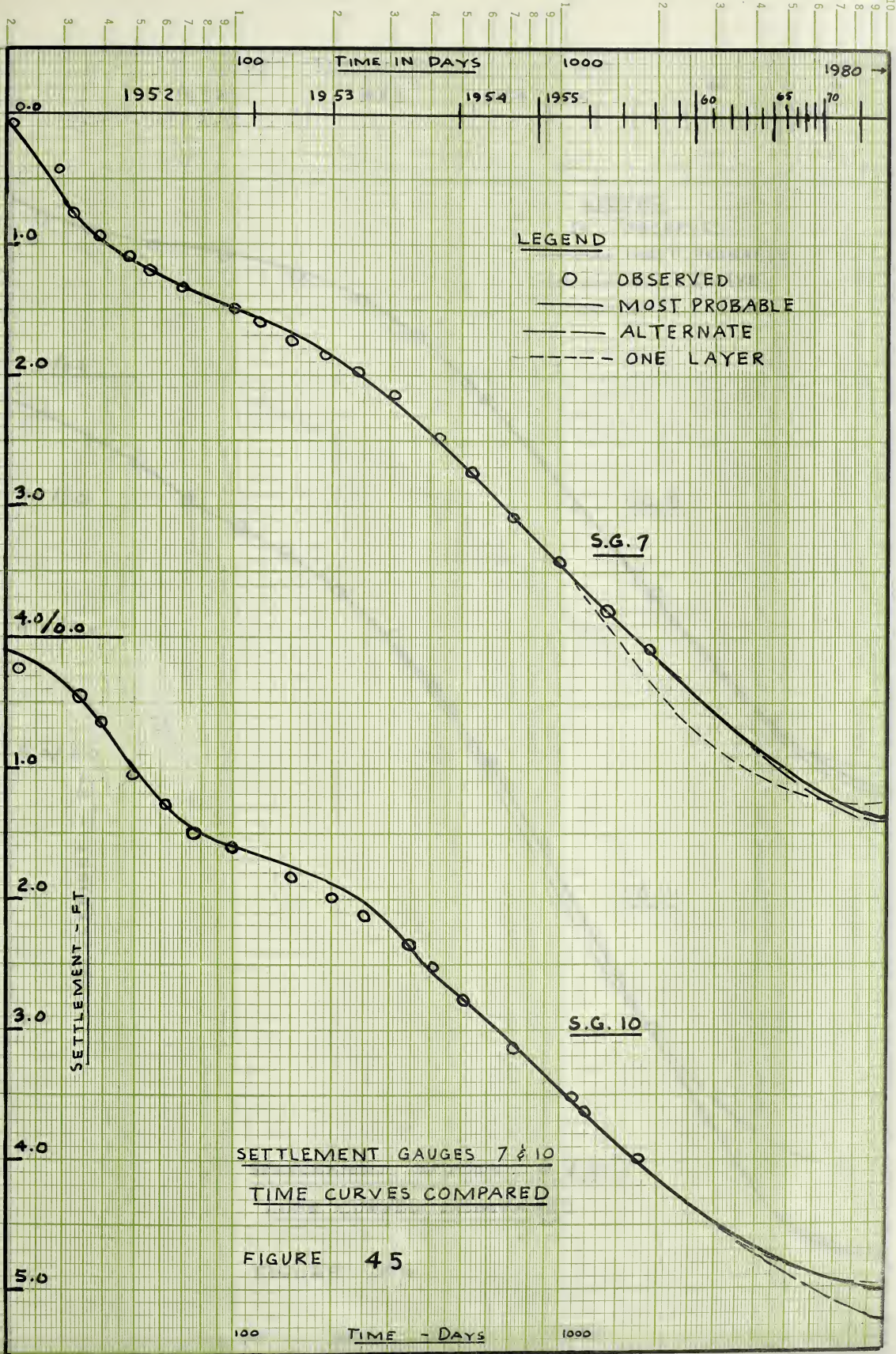




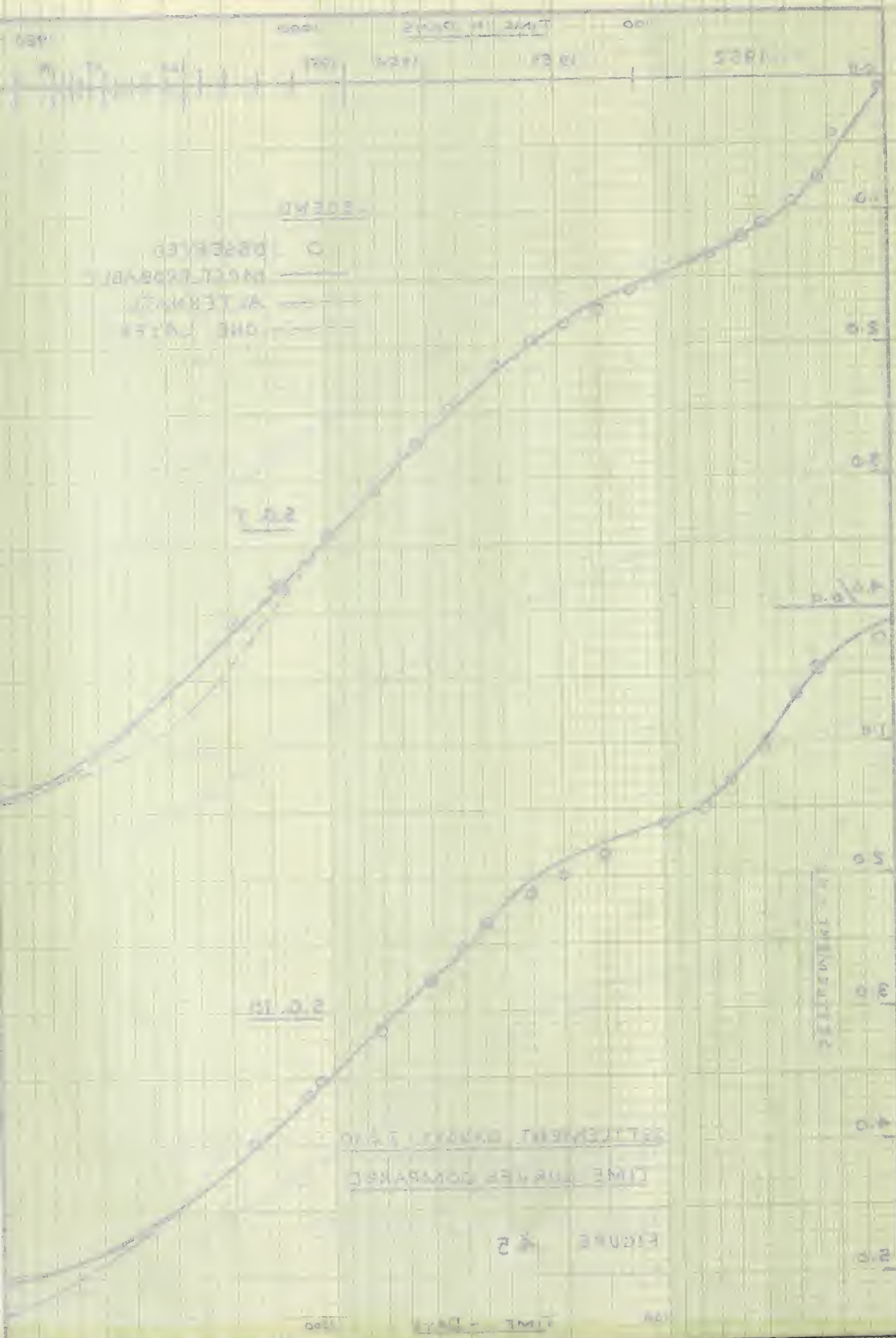




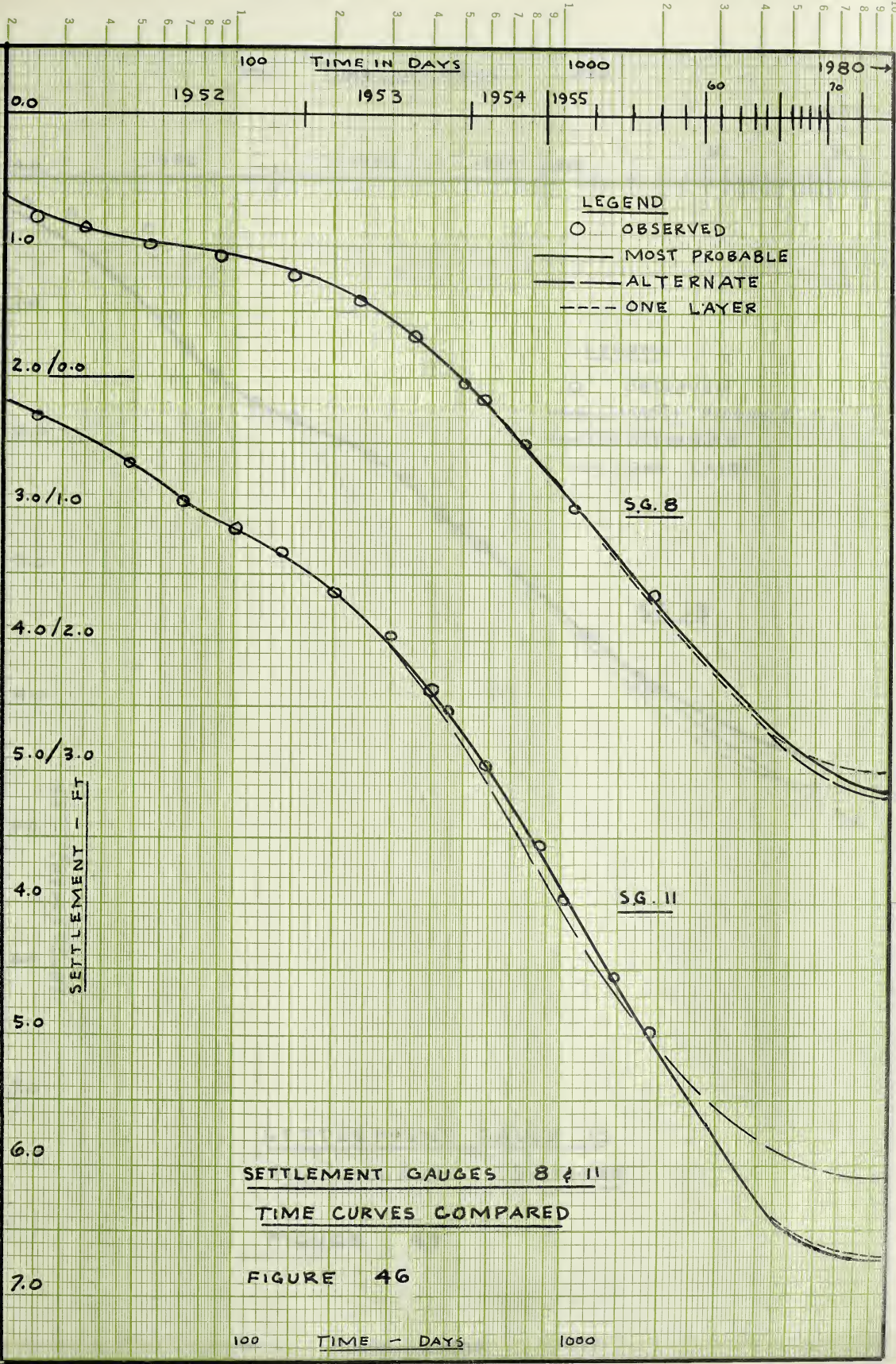




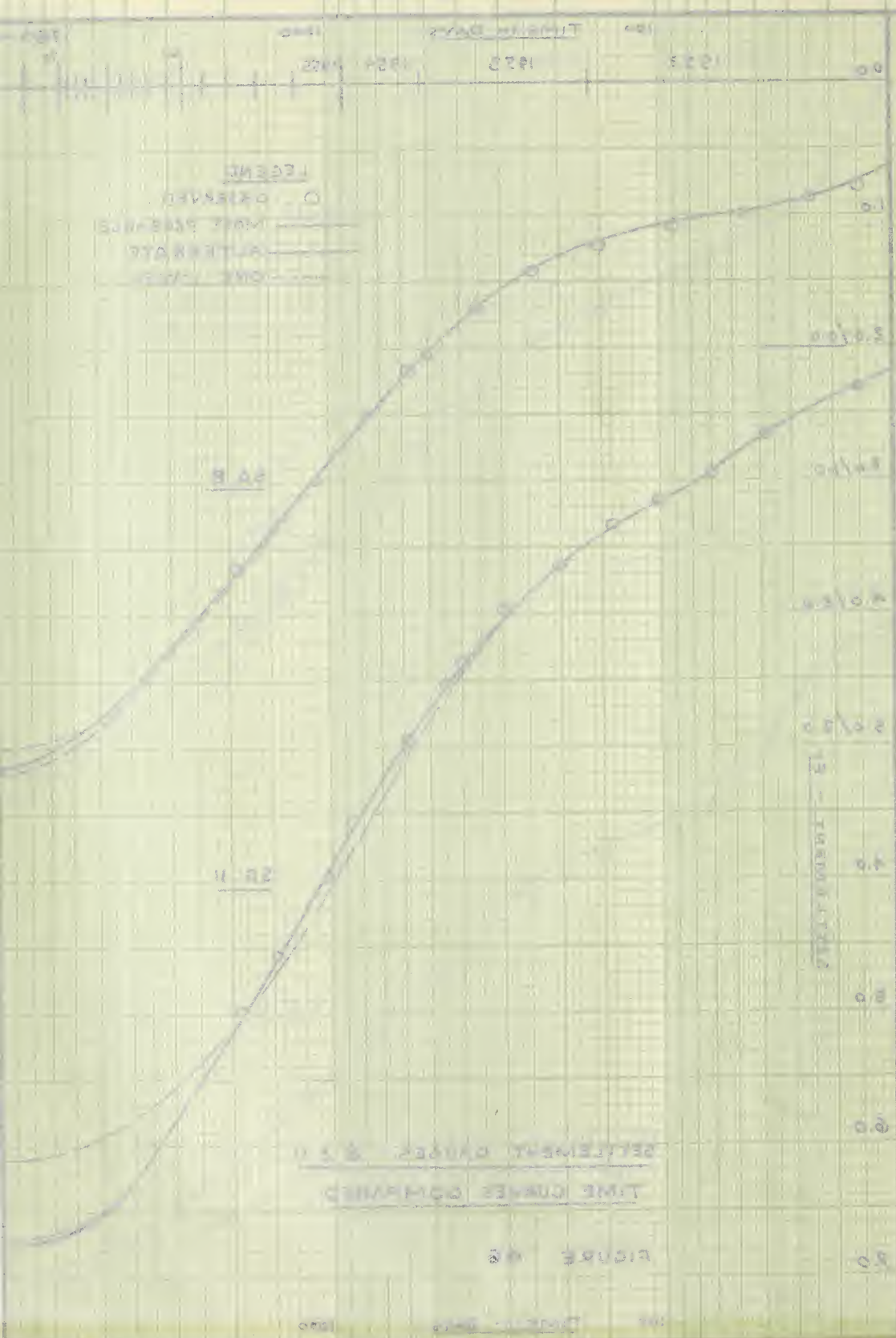




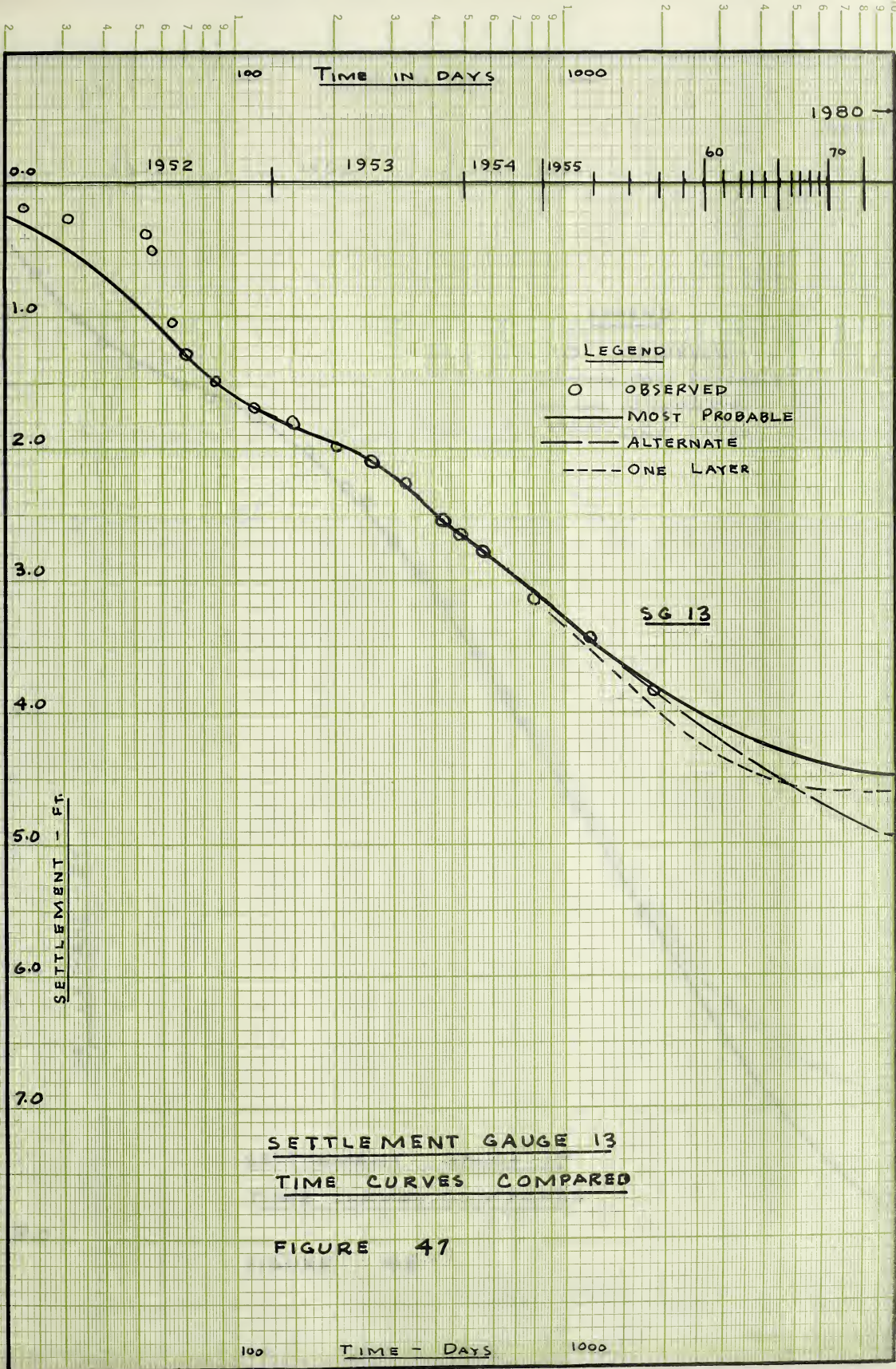






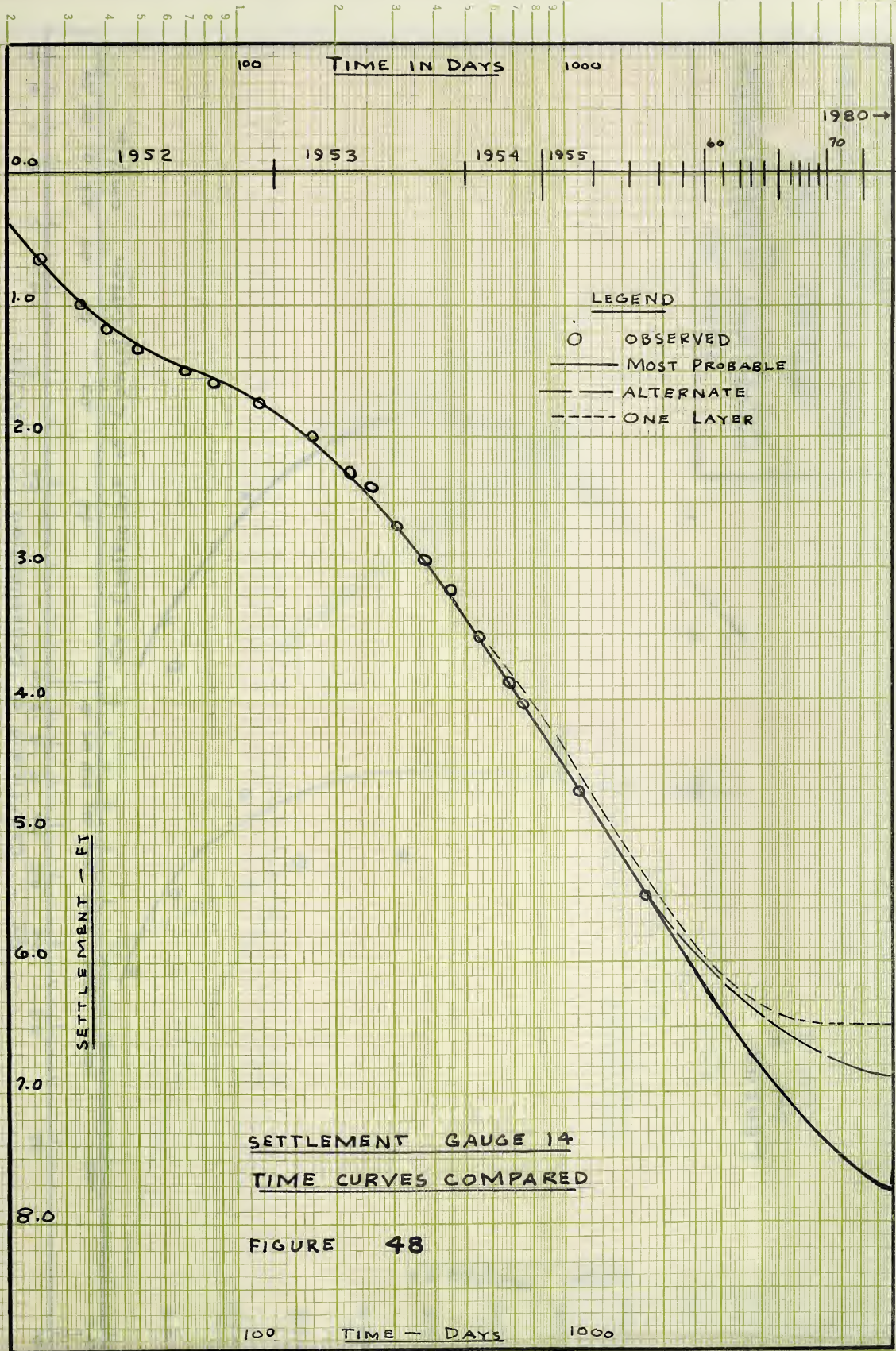




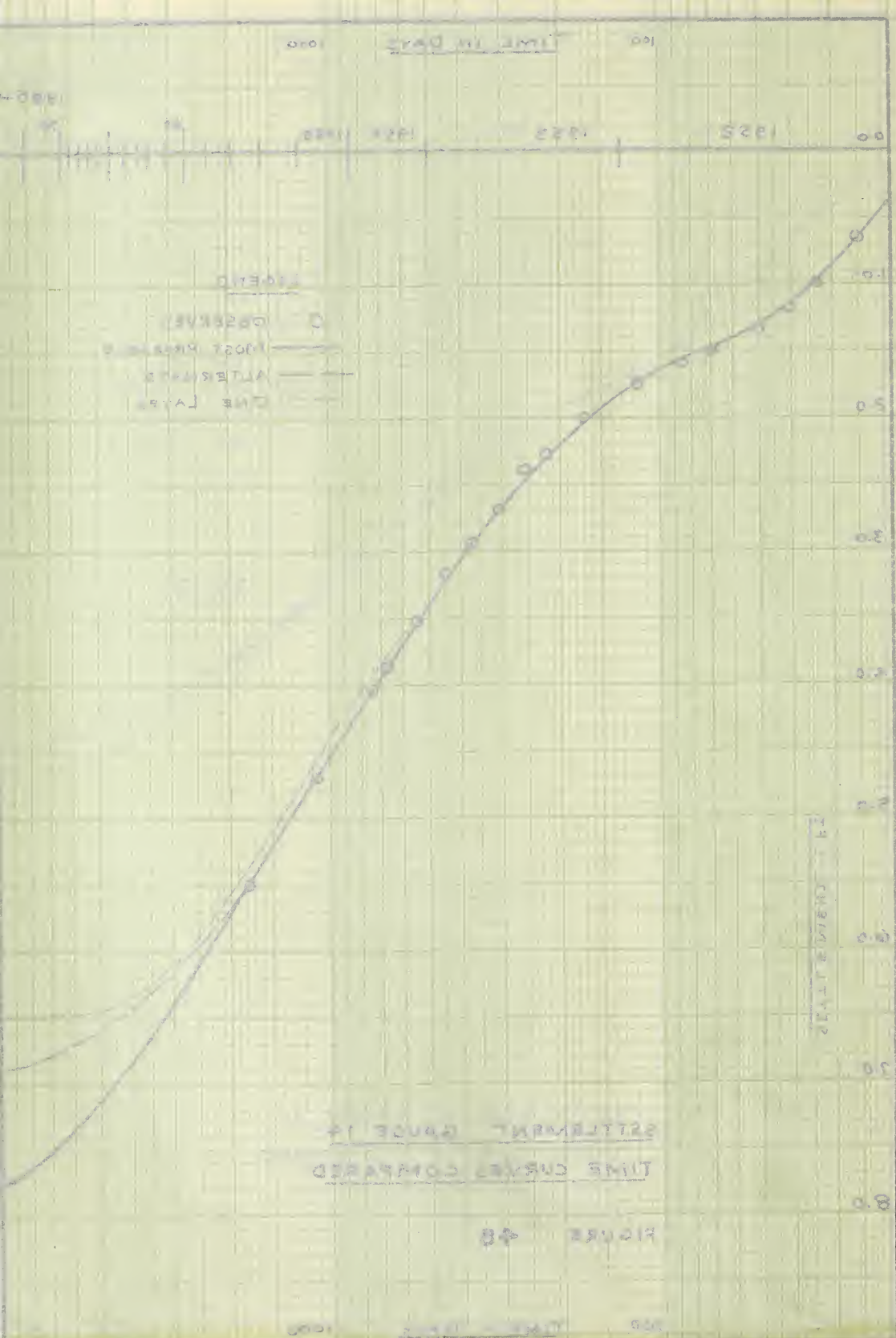












**SETTLEMENT CURVE OF  
TIME CURVES COMPARED**

**FIGURE 48**

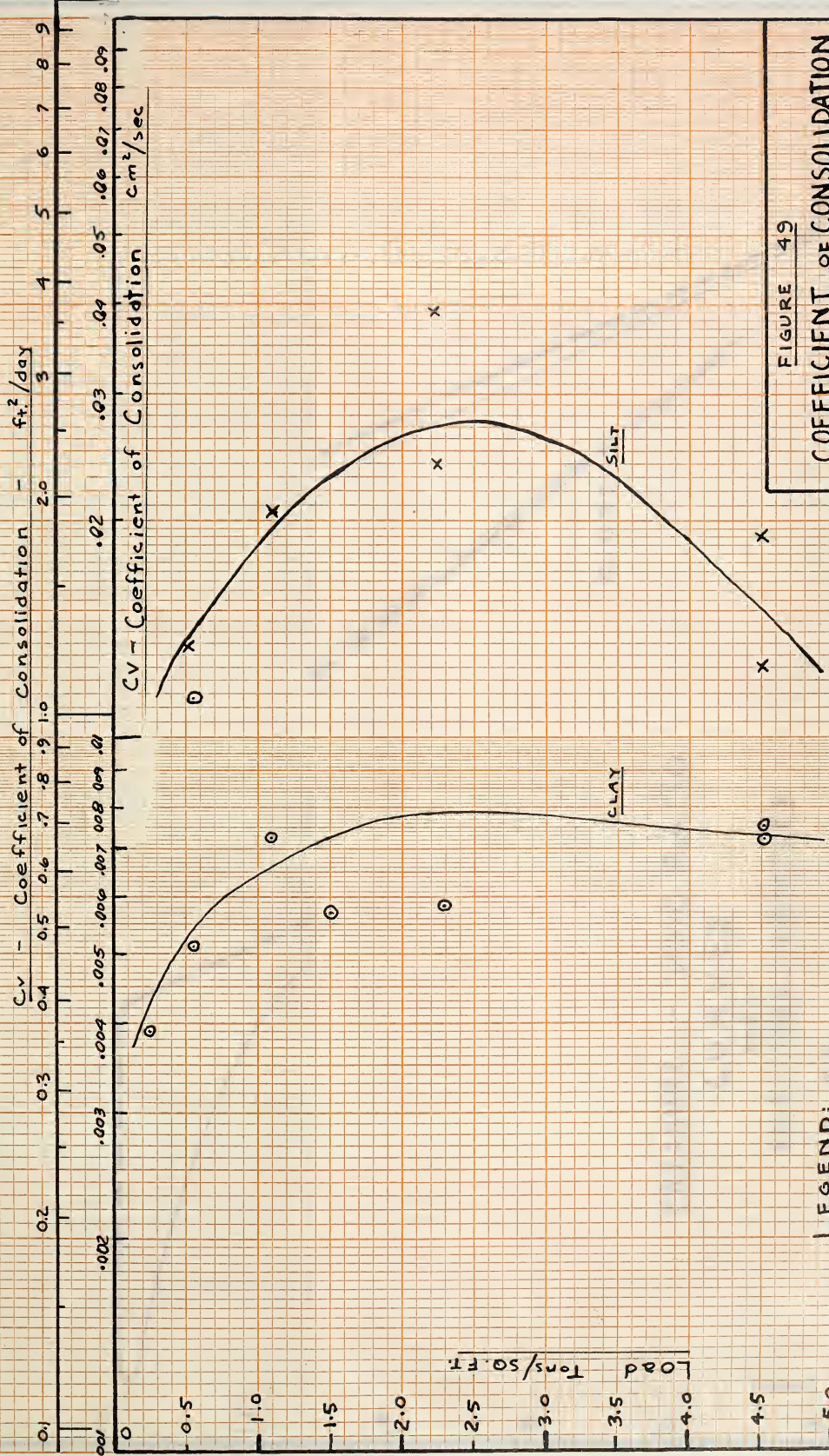


FIGURE 49

**COEFFICIENT OF CONSOLIDATION**

VS

**APPLIED LOAD**

FROM LABORATORY CONSOLIDATION TESTS



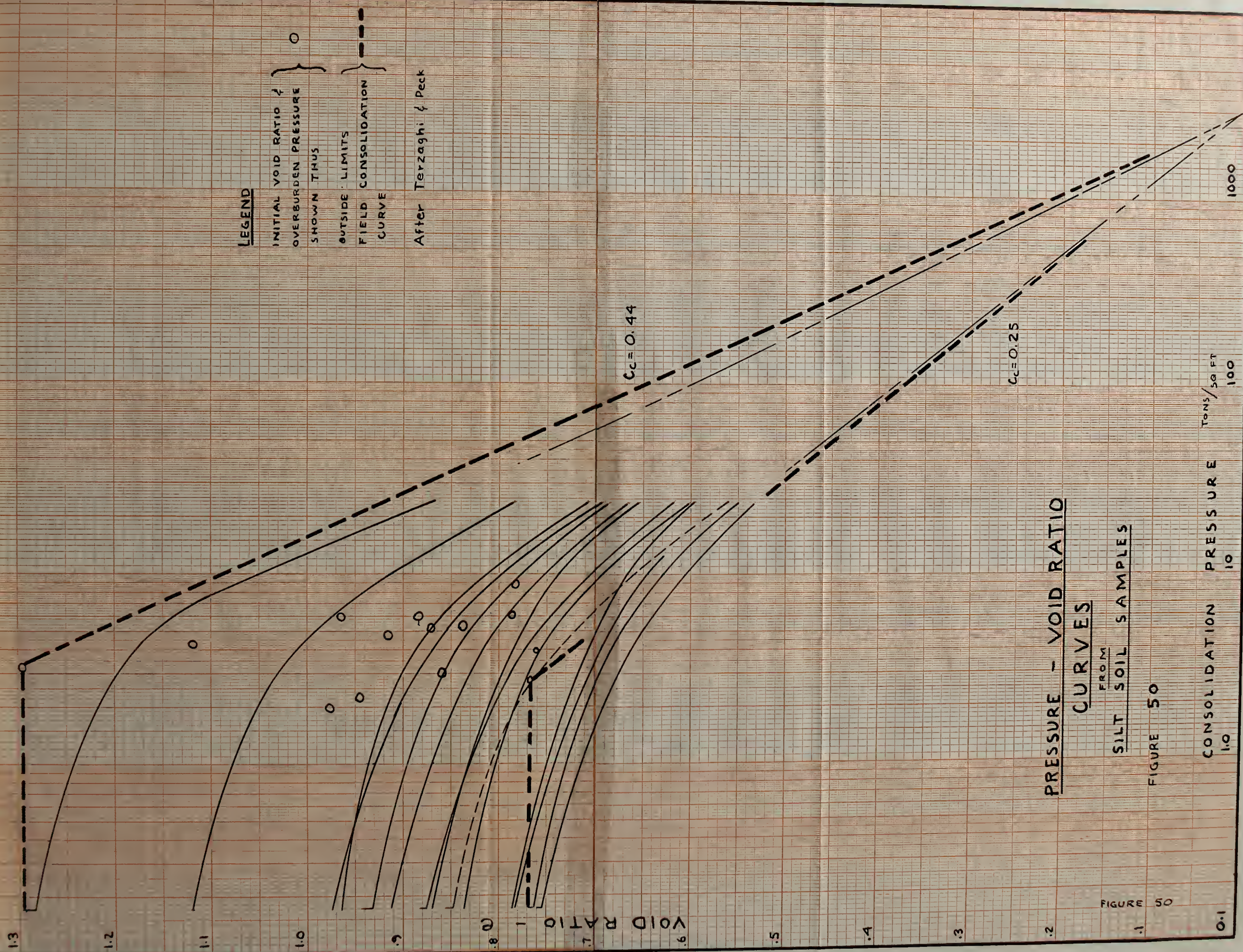
1. 2. 3. 4. 5. 6. 7. 8. 9. 10. 11. 12. 13. 14. 15. 16. 17. 18. 19. 20. 21. 22. 23. 24. 25. 26. 27. 28. 29. 30. 31. 32. 33. 34. 35. 36. 37. 38. 39. 40. 41. 42. 43. 44. 45. 46. 47. 48. 49. 50. 51. 52. 53. 54. 55. 56. 57. 58. 59. 60. 61. 62. 63. 64. 65. 66. 67. 68. 69. 70. 71. 72. 73. 74. 75. 76. 77. 78. 79. 80. 81. 82. 83. 84. 85. 86. 87. 88. 89. 90. 91. 92. 93. 94. 95. 96. 97. 98. 99. 100.



1. 2. 3. 4. 5. 6. 7. 8. 9. 10. 11. 12. 13. 14. 15. 16. 17. 18. 19. 20. 21. 22. 23. 24. 25. 26. 27. 28. 29. 30. 31. 32. 33. 34. 35. 36. 37. 38. 39. 40. 41. 42. 43. 44. 45. 46. 47. 48. 49. 50. 51. 52. 53. 54. 55. 56. 57. 58. 59. 60. 61. 62. 63. 64. 65. 66. 67. 68. 69. 70. 71. 72. 73. 74. 75. 76. 77. 78. 79. 80. 81. 82. 83. 84. 85. 86. 87. 88. 89. 90. 91. 92. 93. 94. 95. 96. 97. 98. 99. 100.

1. 2. 3. 4. 5. 6. 7. 8. 9. 10. 11. 12. 13. 14. 15. 16. 17. 18. 19. 20. 21. 22. 23. 24. 25. 26. 27. 28. 29. 30. 31. 32. 33. 34. 35. 36. 37. 38. 39. 40. 41. 42. 43. 44. 45. 46. 47. 48. 49. 50. 51. 52. 53. 54. 55. 56. 57. 58. 59. 60. 61. 62. 63. 64. 65. 66. 67. 68. 69. 70. 71. 72. 73. 74. 75. 76. 77. 78. 79. 80. 81. 82. 83. 84. 85. 86. 87. 88. 89. 90. 91. 92. 93. 94. 95. 96. 97. 98. 99. 100.







10

1897  
10  
10  
10  
10  
10

42574.03 026700 01211

STERN DIENST  
MONTAG 10. NOVEMBER  
2011 14.000

017930

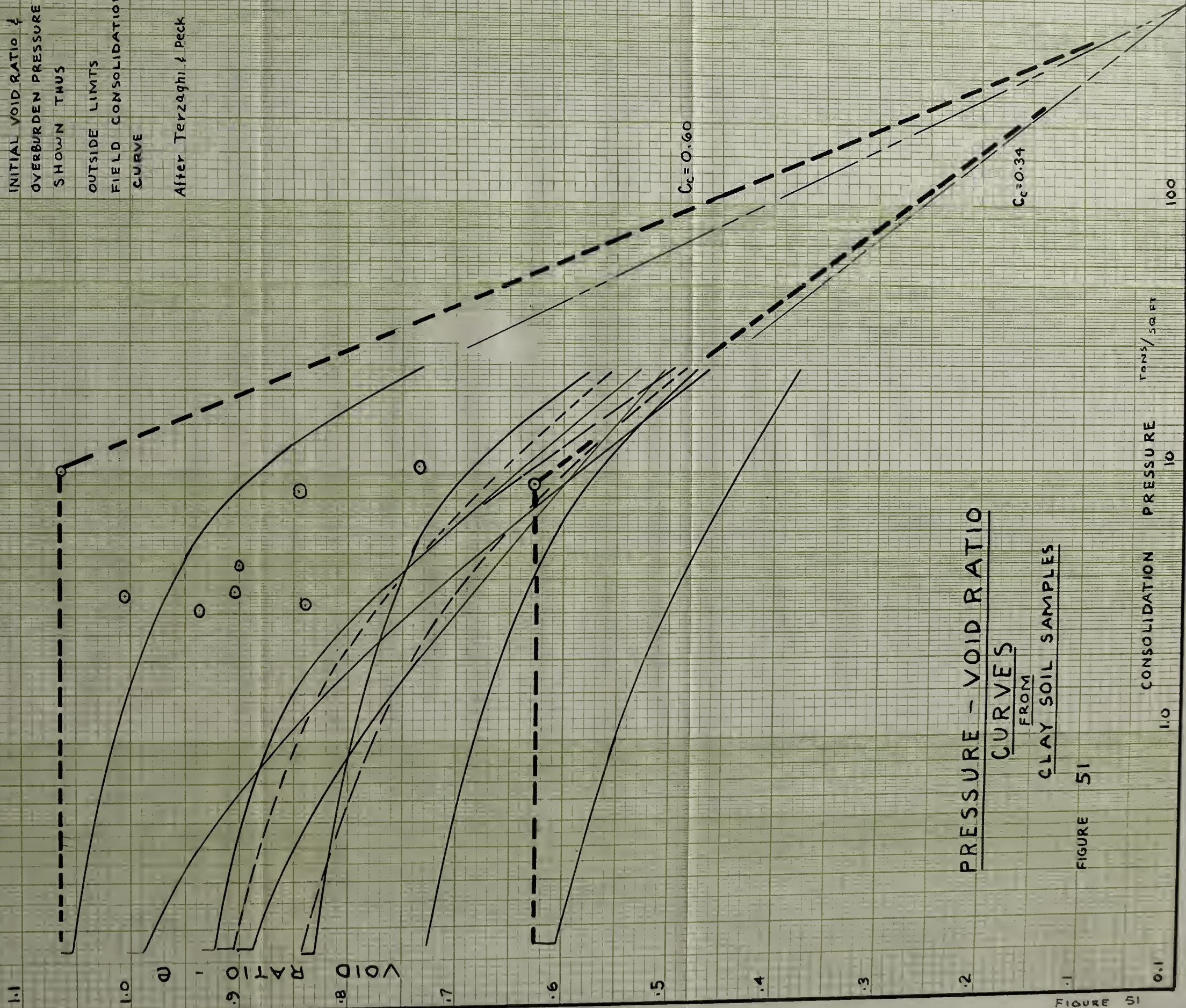


LEGEND

INITIAL VOID RATIO &  
OVERBURDEN PRESSURE  
SHOWN THUS ○

OUTSIDE LIMITS  
FIELD CONSOLIDATION  
CURVE

After Terzaghi & Peck



PRESSURE - VOID RATIO  
CURVES

FROM  
CLAY SOIL SAMPLES

FIGURE 51

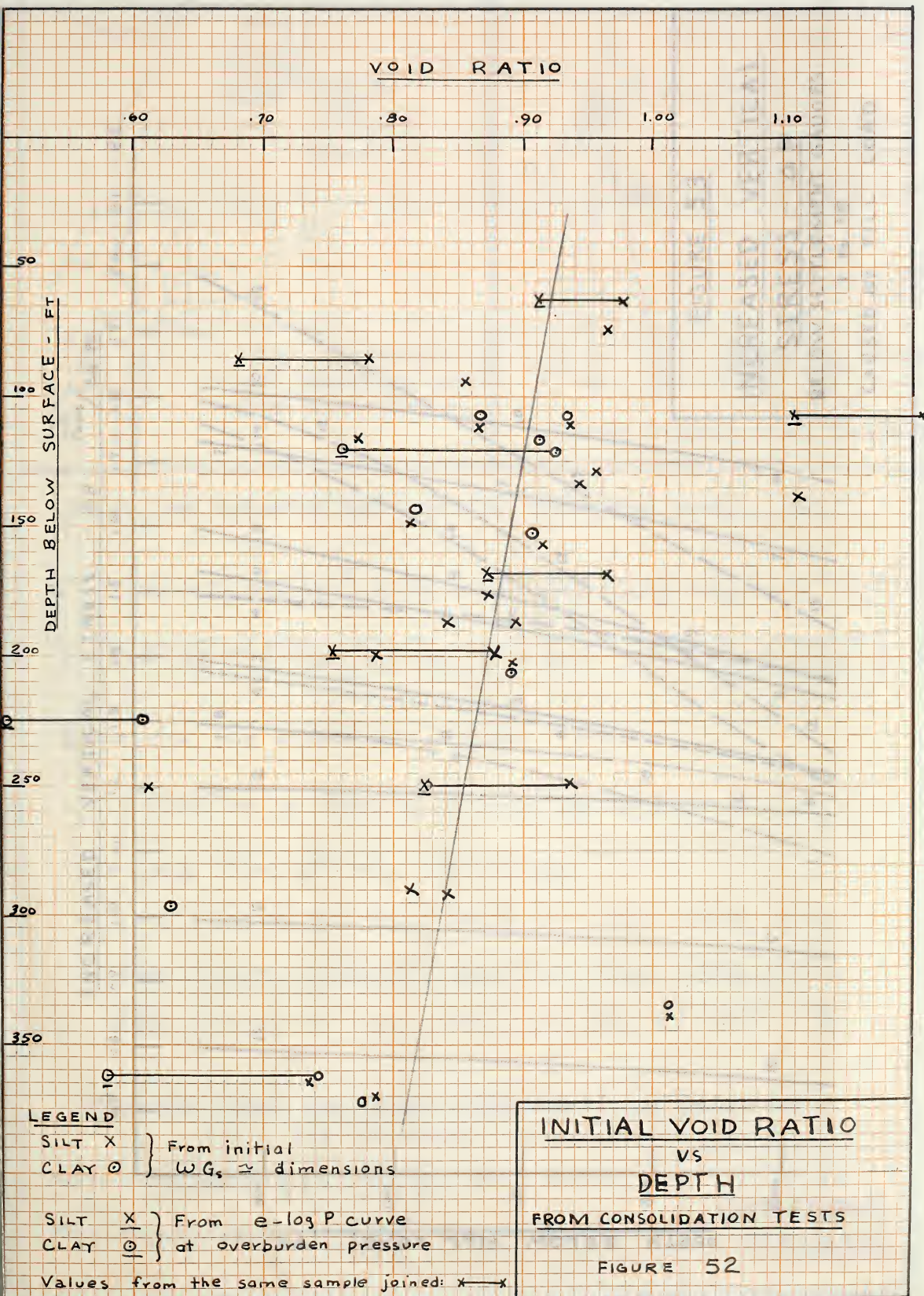
FIGURE 51



CONTOUR LINES



CHART  
HIGH CONCENTRATION  
OUTSIDE RANGE  
SHOWING DATA  
OXYGENATED BENZENE  
WATER (1000000)





INITIAL VOID RATIO  
VS  
DEPTH

FROM CONSOLIDATION TESTS

FIGURE 25

Values from the same sample joined by X  
CLAY @ of overconsolidated pressure  
SLIT X } From e-log p curve

CLAY @ } W.G. & dimensions  
SLIT X } From initial

LEGEND

DEPTH BELOW SURFACE - FT

VOID RATIO

1.00 0.90 0.80 0.70 0.60 0.50

120 100 80 60 40 20 0





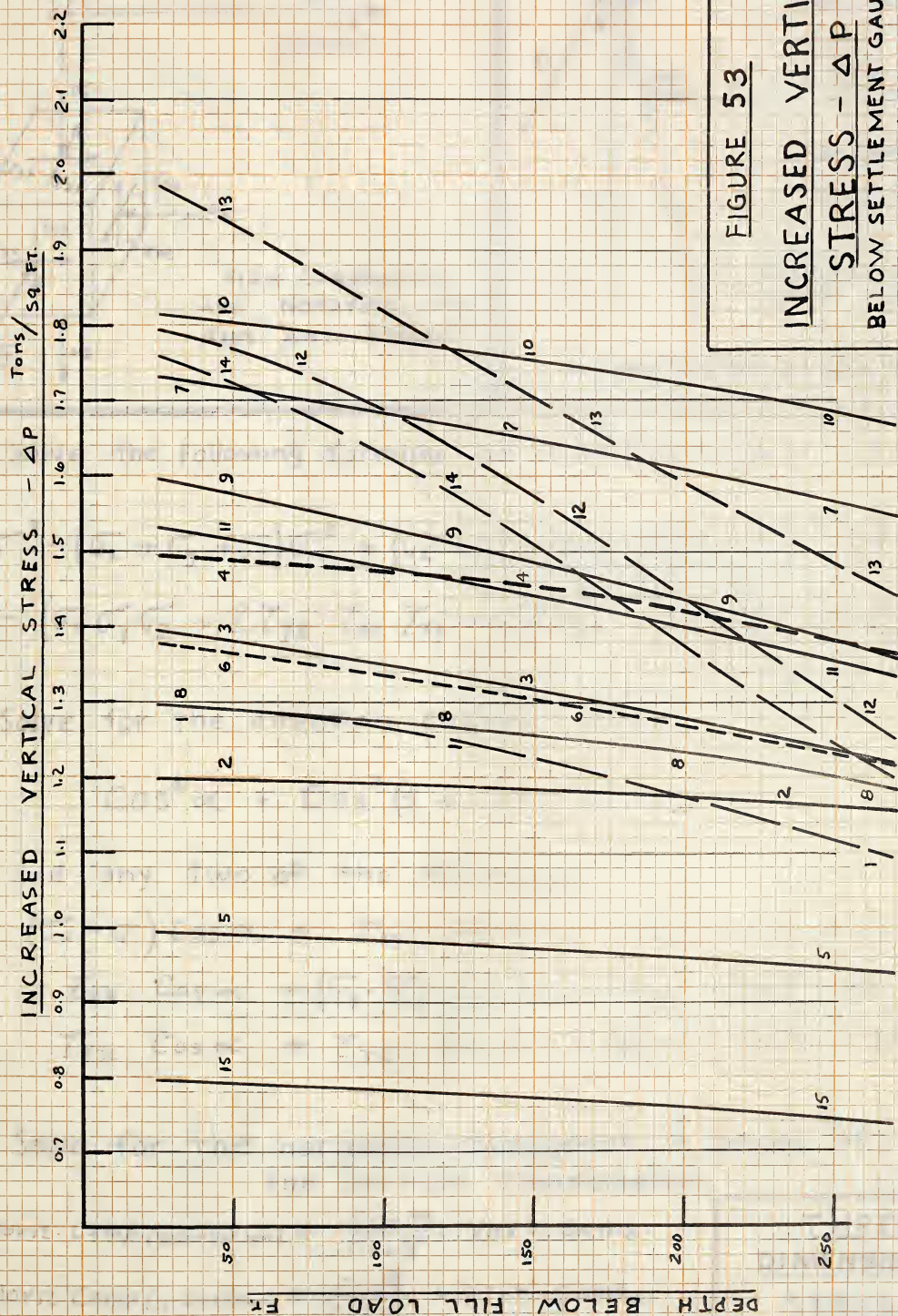


FIGURE 53

INCREASED VERTICAL

STRESS -  $\Delta P$

BELOW SETTLEMENT GAUGES

1 TO 15

CAUSED BY FILL LOAD

CAUSED BY EIGHT LOAD

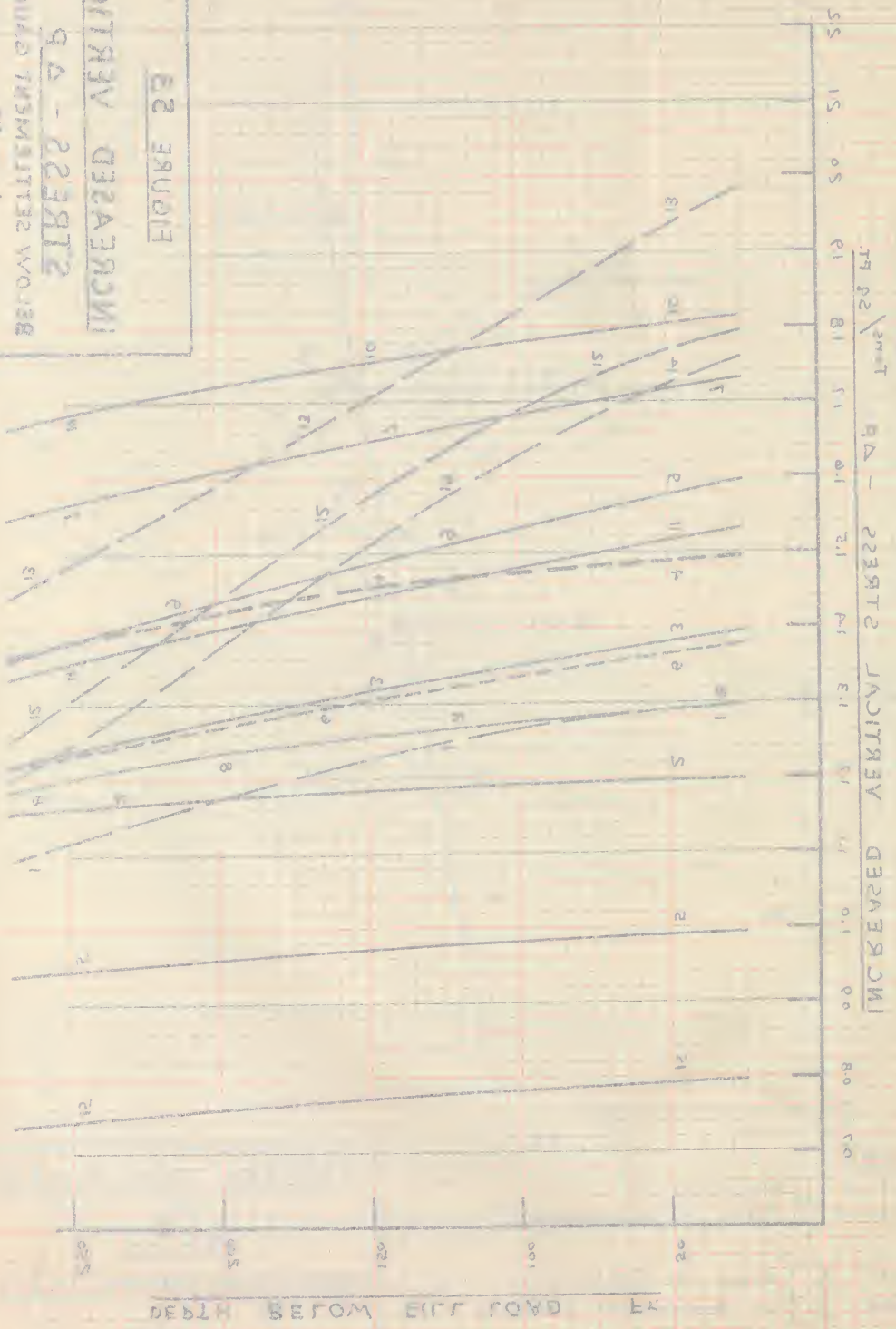
1 TO 12

BEFORE SETTLEMENT OCCURRED

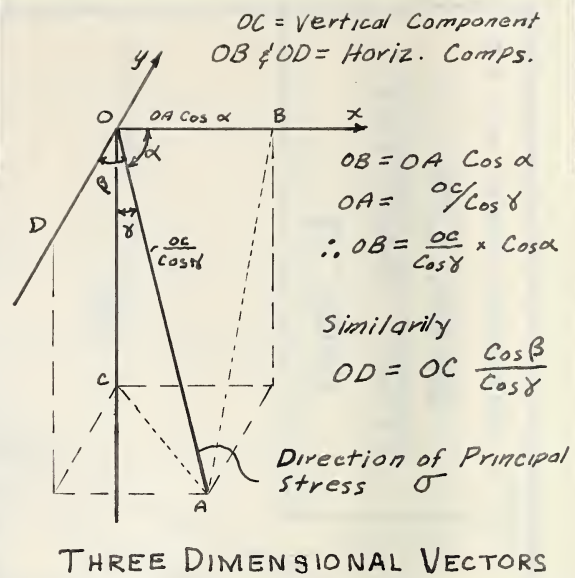
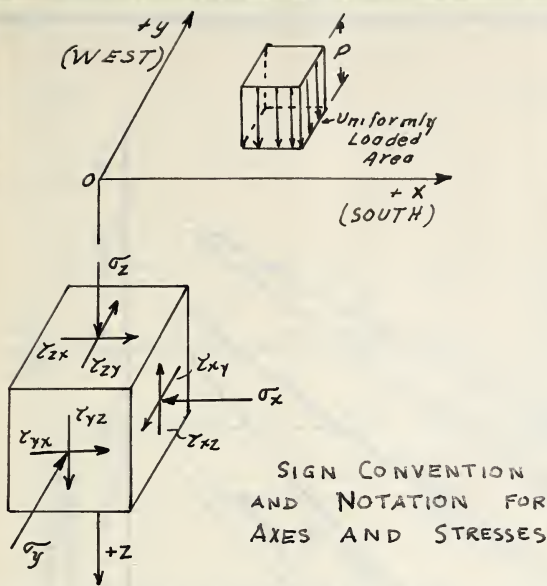
218522 - 75

INCREASED VERTICAL

FIGURE 23







Solve the following formula for principal stress -  $\sigma$

$$\sigma^3 - (\sigma_x + \sigma_y + \sigma_z)\sigma^2 + (\sigma_x\sigma_y + \sigma_y\sigma_z + \sigma_x\sigma_z - \tau_{yz}^2 - \tau_{xz}^2 - \tau_{xy}^2)\sigma - (\sigma_x\sigma_y\sigma_z + 2\tau_{yz}\tau_{xz}\tau_{xy} - \sigma_x\tau_{yz}^2 - \sigma_y\tau_{xz}^2 - \sigma_z\tau_{xy}^2) = 0$$

Solve for the direction cosines from:

$$\cos^2 \alpha + \cos^2 \beta + \cos^2 \gamma = 1$$

and any two of the following:

$$(\sigma_x - \sigma)\cos \alpha + \tau_{xy}\cos \beta + \tau_{xz}\cos \gamma = 0$$

$$\tau_{yx}\cos \alpha + (\sigma_y - \sigma)\cos \beta + \tau_{yz}\cos \gamma = 0$$

$$\tau_{zx}\cos \alpha + \tau_{yz}\cos \beta + (\sigma_z - \sigma)\cos \gamma = 0$$

Solve for the horizontal component in terms of the vertical component:

$$\text{Horiz. Comp (x-direction)} = \frac{\cos \alpha}{\cos \gamma} \times \text{Vert. Comp.}$$

$$\text{Horiz. Comp (y-direction)} = \frac{\cos \beta}{\cos \gamma} \times \text{Vert. Comp.}$$

**THREE  
DIMENSIONAL  
STRESSES**



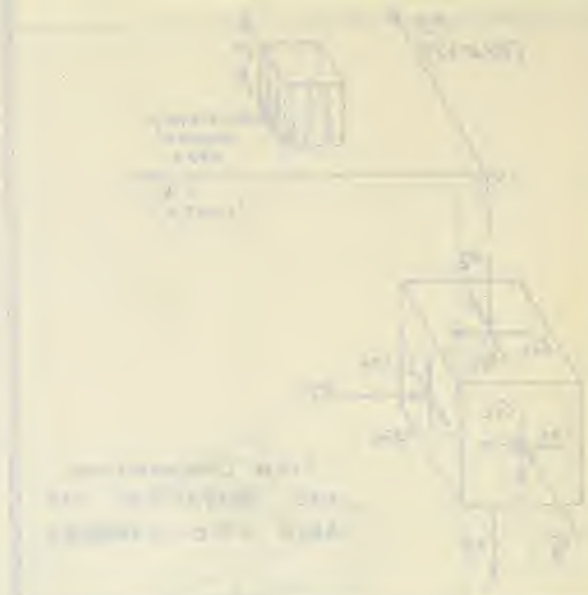


Figure 1: A rectangular prism with dimensions  $l$ ,  $b$ , and  $h$ .

Figure 2: A rectangular prism with dimensions  $l$ ,  $b$ , and  $h$ .

Figure 3: A rectangular prism with dimensions  $l$ ,  $b$ , and  $h$ .

Figure 4: A rectangular prism with dimensions  $l$ ,  $b$ , and  $h$ .

Figure 5: A rectangular prism with dimensions  $l$ ,  $b$ , and  $h$ .

Figure 6: A rectangular prism with dimensions  $l$ ,  $b$ , and  $h$ .

STRESS CAUSED BY FILL - TONS/SQFT

1.5  
1.4  
1.3  
1.2  
1.1  
1.0  
0.9  
0.8  
0.7  
0.6  
0.5  
0.4  
0.3  
0.2  
0.1  
0  
-0.1  
-0.2

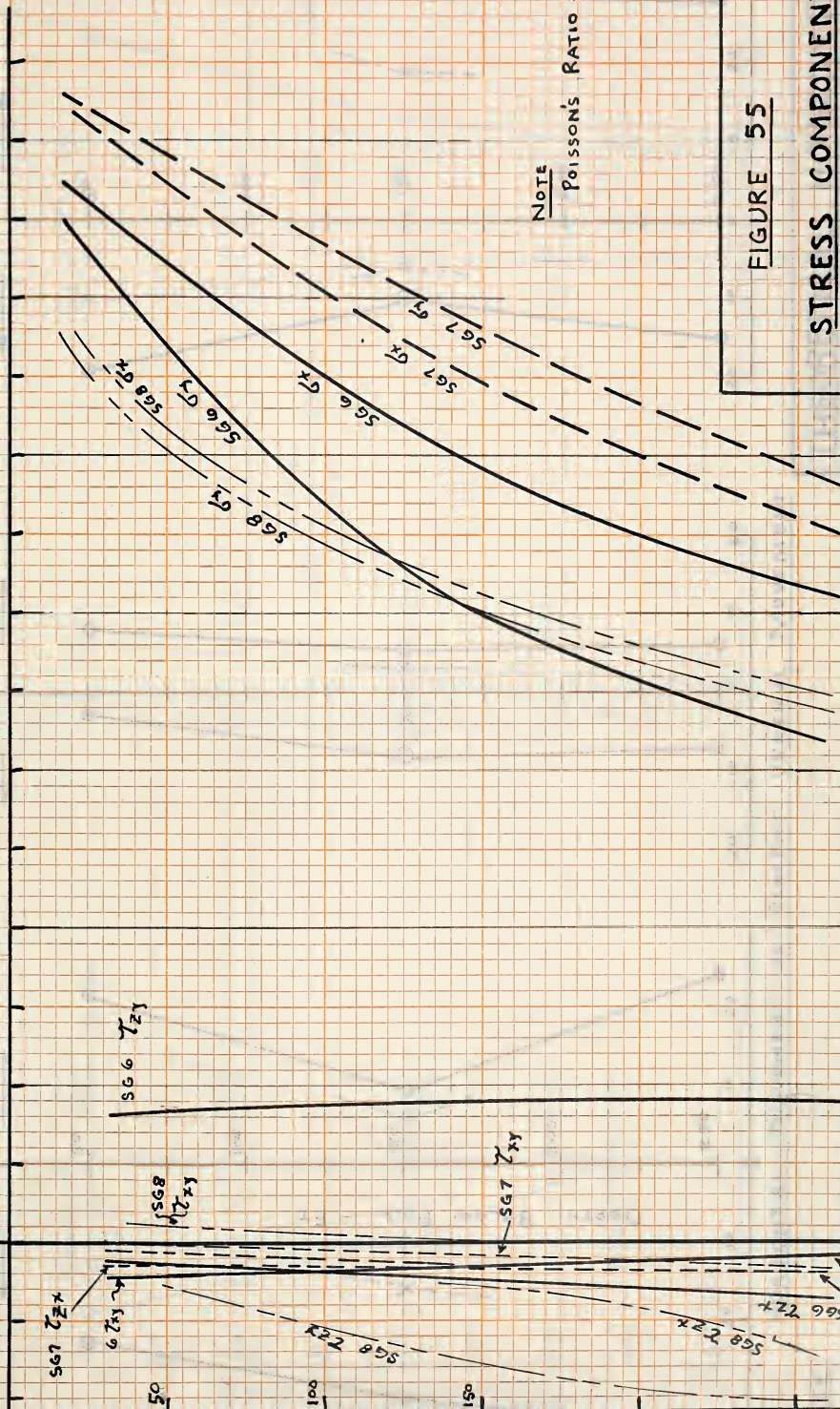


FIGURE 55

# STRESS COMPONENTS BELOW FILL

AT SETTLEMENT GAUGES 6, 7, & 8

DEPTH BELOW FILL - FT

FIGURE 55



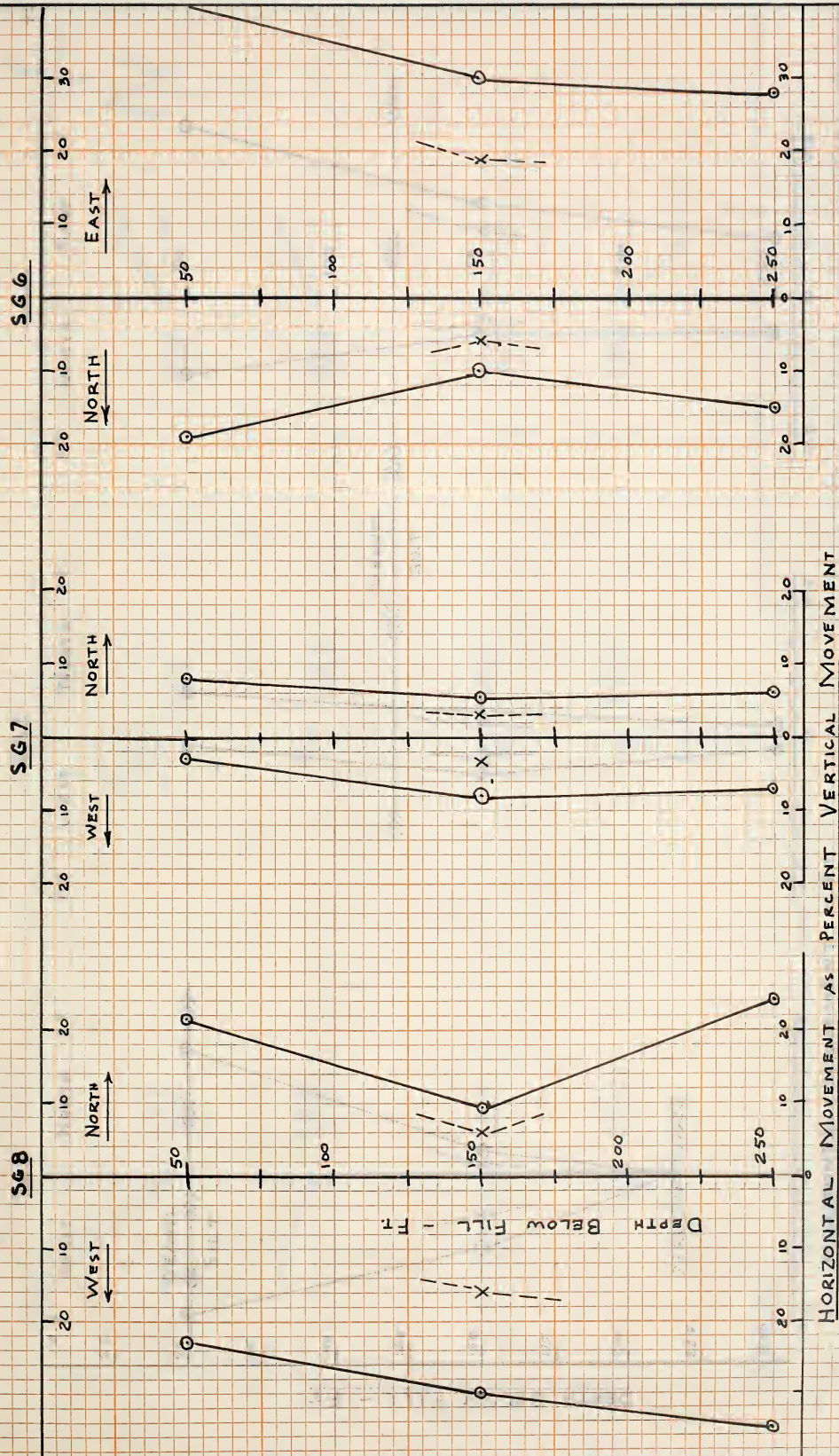
ДЕБЛН ВЕГОМ ЕЛГ - ЕЛ

STANFORD 223716

Page 22

2019  
2019-2020





# THEORETICAL HORIZONTAL MOVEMENT VS DEPTH

FIGURE 56

NOTE

BOUSSINESQ EQUATIONS

$$u = 0.5$$

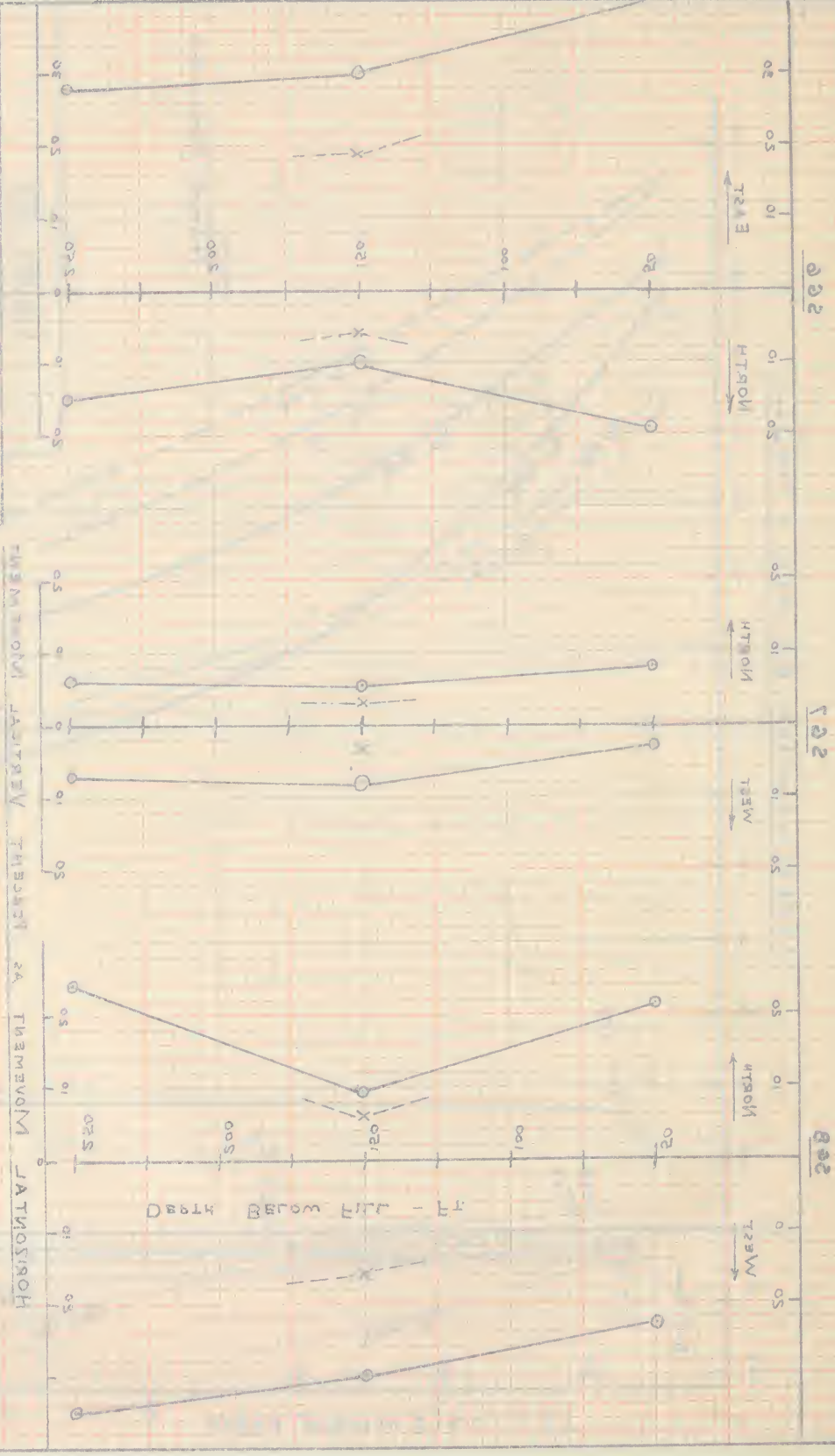
$$u = 0$$

FIGURE 56

NOTE  
 BOULDER CONCENTRATION  
 $\eta = 0$   
 $\eta = 0.0$   
 ---X---

FIGURE 20

THEORETICAL HORIZONTAL  
 MOVEMENT AS DEPTH









NOTE

$\mu = 0$   
 $\mu = 0.2$   
 $\mu = 0.5$

POSSIBLE EQUATIONS

JUNE 1921  
 START OF BUILDING TO  
 MOVEMENT FOR PERIOD

HORIZONTAL MOVEMENT - FT.

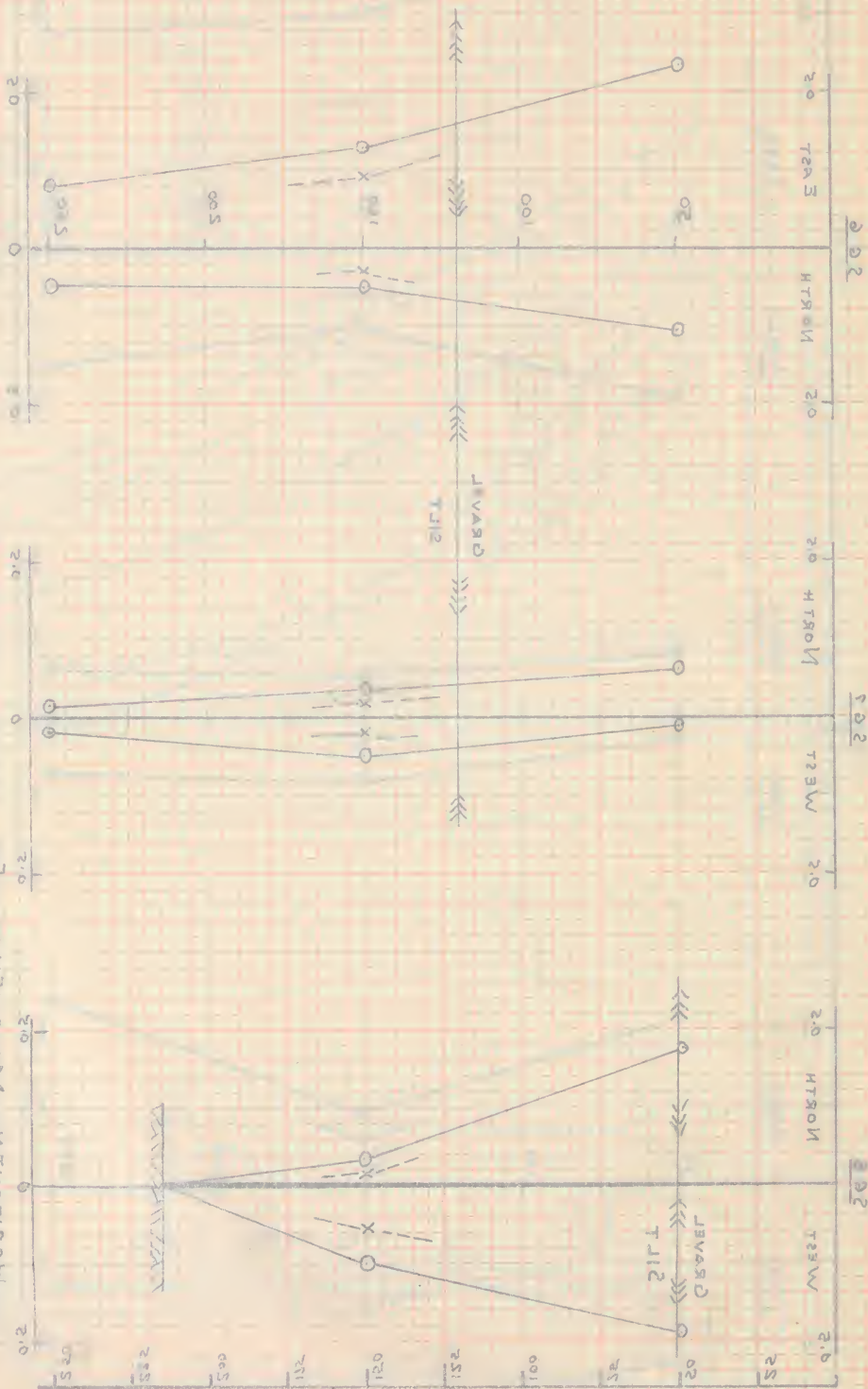
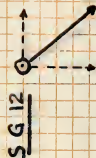
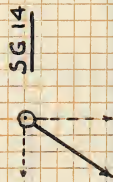
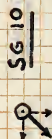
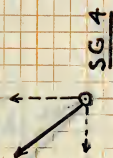
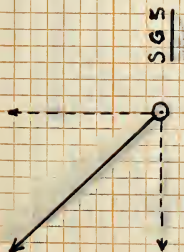
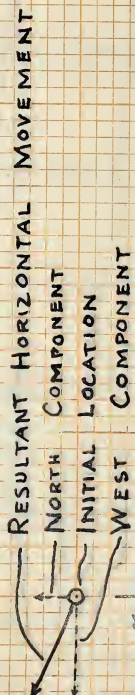


FIGURE 23

MOVEMENT AS DEPTH  
 THEORETICAL HORIZONTAL



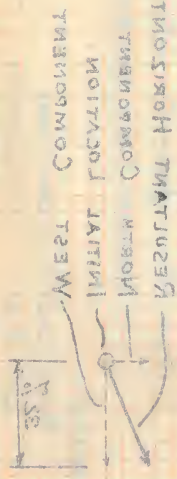
LEGEND



POISSON'S RATIO = 0.5

VECTOR DIAGRAM  
HORIZONTAL MOVEMENT AS  
PERCENT VERTICAL MOVEMENT  
FOR DEPTH 150 FEET  
Scale 1" = 50% FIGURE 58



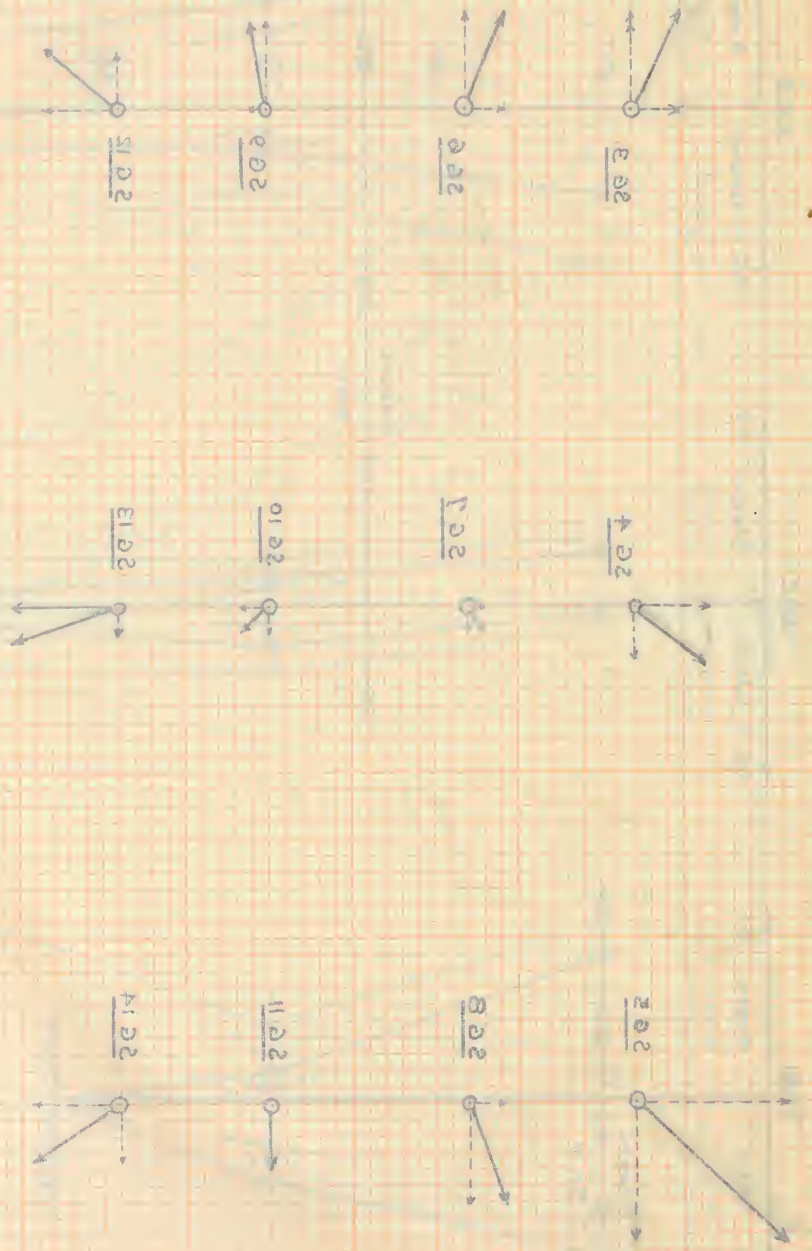


LEGEND

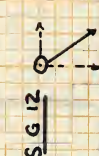
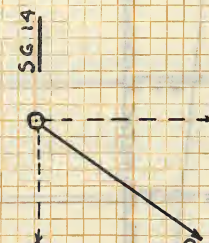
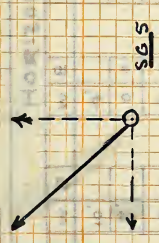
20 = 0.174 210 = 0.2

Scale 1" = 20%

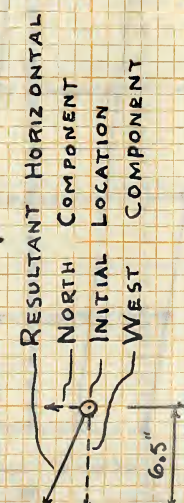
FOR DEPTH 120 FEET  
PERCENT VERTICAL MOVEMENT  
HORIZONTAL MOVEMENT AS  
VECTOR DIAGRAM







LEGEND

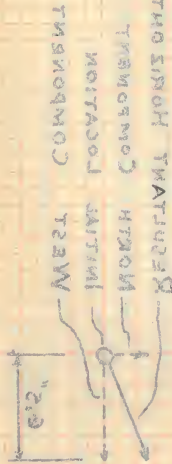


VECTOR DIAGRAM  
THEORETICAL HORIZONTAL MOVEMENT  
AT DEPTH 150 FEET  
SINCE BUILDINGS COMPLETED

POISSON'S RATIO = 0.5

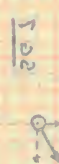
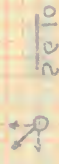
Scale 1" = 10" FIGURE 59





2.0 = 0.175 10.0

SINCE BUILDING COMPLETED  
AT DEPTH 120 FEET  
THEORETICAL HORIZONTAL MOVEMENT  
VECTOR DIAGRAM



# RESULTS Distances Measured to Horizontal Scale 1" = 50'

| X     | HORIZONTAL MOVEMENT OF GROUND SURFACE AT COLUMN LINES (FT) |   |     |   |    |   |    |   |    |   |    |   | Y  |       |
|-------|--|---|-----|---|----|---|----|---|----|---|----|---|----|-------|
|       | W  | E | W   | E | W  | E | W  | E | W  | E | W  | E | W  | E     |
| 250'  | 10'  |   | 10' |   | 4' |   | 2' |   | 1' |   | 0  |   | 3' | 125'  |
| 500'  | 4'   |   | 0   |   | 0  |   | 0  |   | 1' |   | 2' |   | 0  | 250'  |
| 2500' | 0  |   | 0   |   | 0  |   | 0  |   | 0  |   | 0  |   | 0  | 2000' |

Column Nos  
 (48) ←  
 (44)  
 (40)  
 (36)  
 (32)  
 (28)  
 (24)  
 (20)  
 (16)  
 (12)  
 (8)  
 (4)  
 (0)

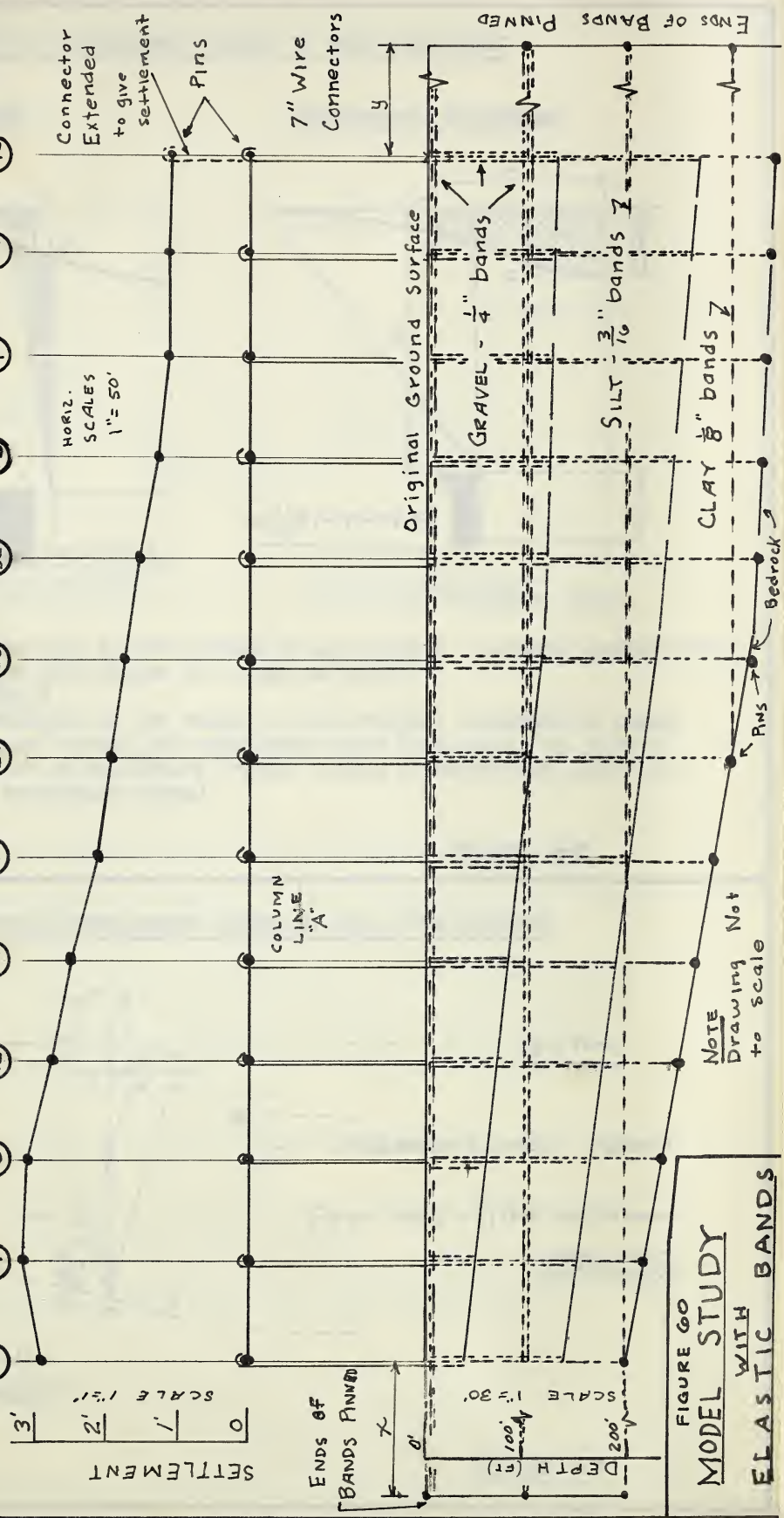


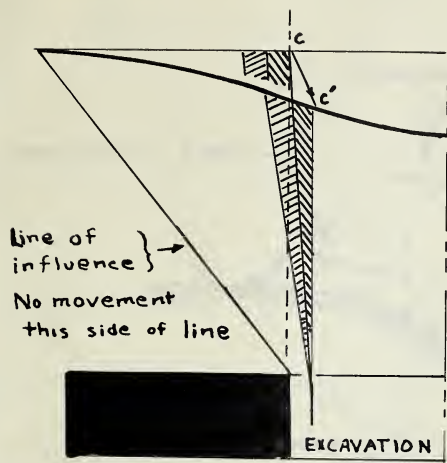
FIGURE 60  
 MODEL STUDY  
 WITH  
 ELASTIC BANDS



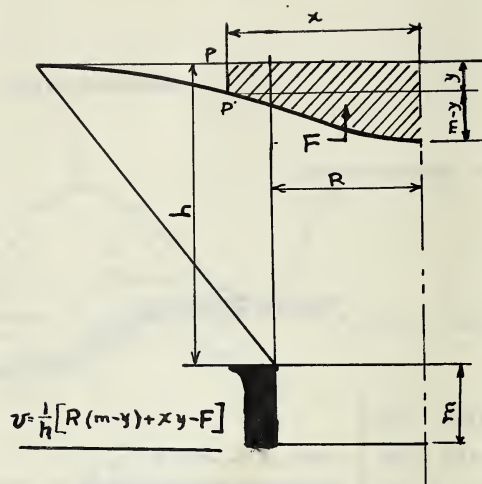


## HORIZONTAL DISPLACEMENT CAUSED BY MINE SUBSIDENCE

### Basic Assumptions



### Displacement Equations



(After Perz)

### Symbols

- v = horizontal displacement at the surface of any point P (always toward center)
- x = horizontal distance from center of trough to point P
- y = subsidence of point P
- m = total maximum subsidence at the center of the trough = thickness of seam
- F = area between original ground and subsidence curve from center to point P
- R = distance from center of subsidence trough to edge of excavation (point of maximum slope of subsidence curve)

FIGURE 62

## HORIZONTAL DISPLACEMENT CAUSED BY SOIL CONSOLIDATION

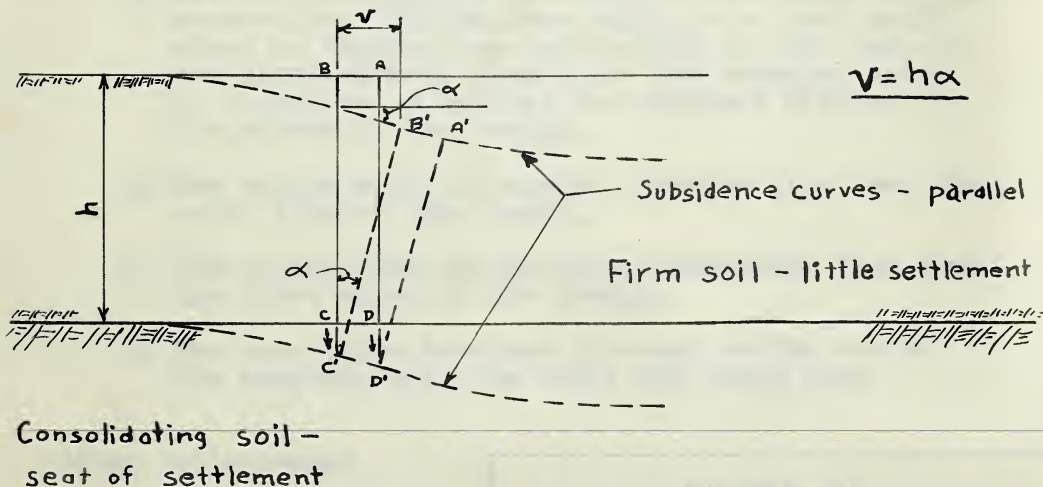
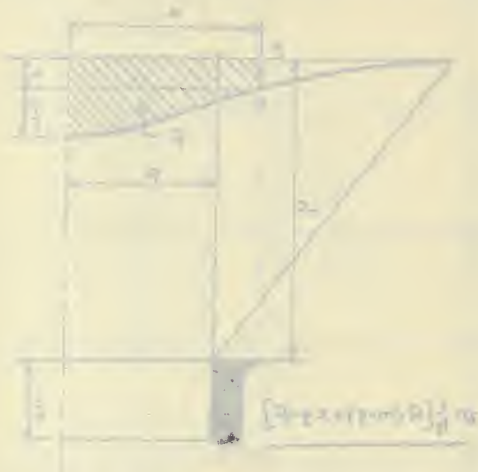


FIGURE 63

# HORIZONTAL DISPLACEMENT CAUSED BY MINE SUBSIDENCE

## Basic Assumptions

## Displacement Equations



## Symbols

- $v$  = horizontal displacement at the surface of any point P ( always toward center
- $x$  = horizontal distance from center of trough to point P
- $y$  = subsidence of point P
- $m$  = total maximum subsidence at the center of the trough = thickness of seam
- $T$  = area between original ground and subsidence curve from center to point P
- $R$  = distance from center of subsidence trough to edge of excavation (point of maximum slope of subsidence curve)

FIGURE 02

# HORIZONTAL DISPLACEMENT CAUSED BY SOIL CONSOLIDATION

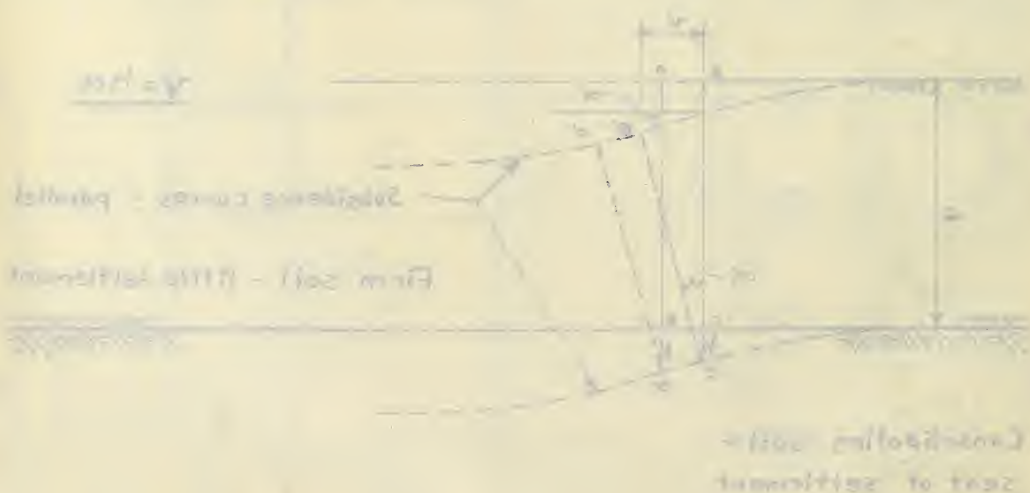
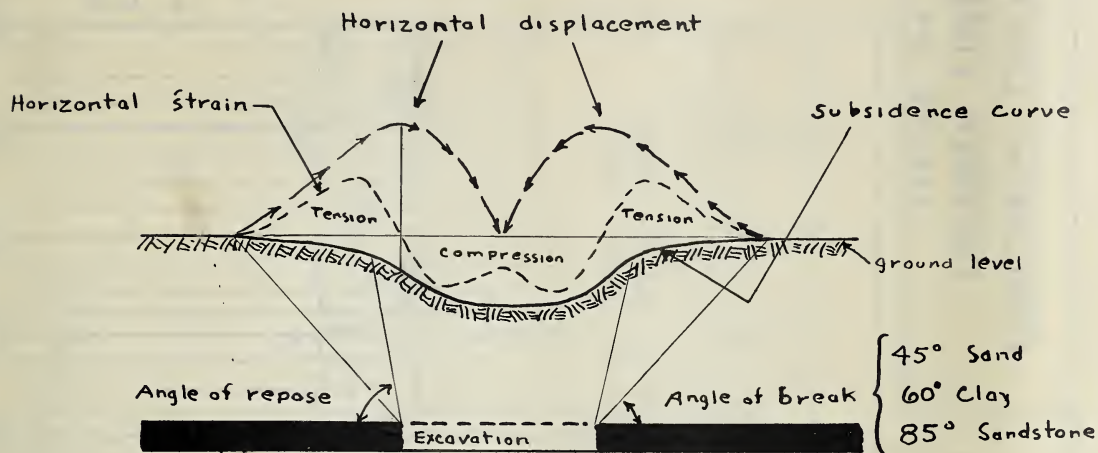


FIGURE 03



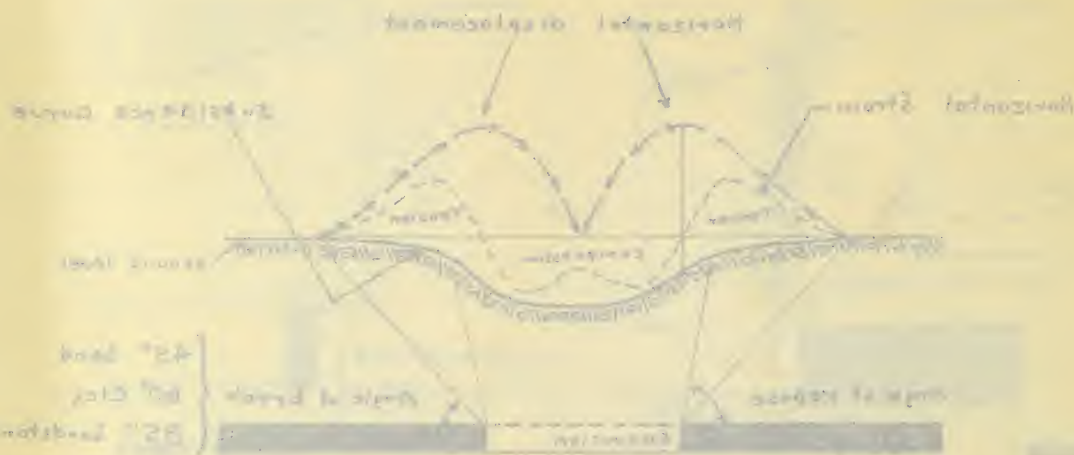


#### SUMMARY OF OBSERVATIONS OF MINE SUBSIDENCE CURVES

1. The maximum sinking is in the middle of the trough. Here there is no shifting.
2. All the shifting is directed to the center of the excavation. The maximum shift is at that point where no tension and compression occurs; here is the point without stress and the changing point of curvature as well as the steepest dipping in the course of the trough.
3. The region with the maximum tension lies near the outer edge of the trough.
4. The region with the maximum compression lies near the inner edges of the trough.
5. The sum of the tensions is equal to the sum of the compressions, the total sum being zero.

(After Rellensmann)

**FIGURE 61**  
**MINE SUBSIDENCE CURVE**



# SUMMARY OF OBSERVATIONS OF MINE SUBSIDENCE CURVES

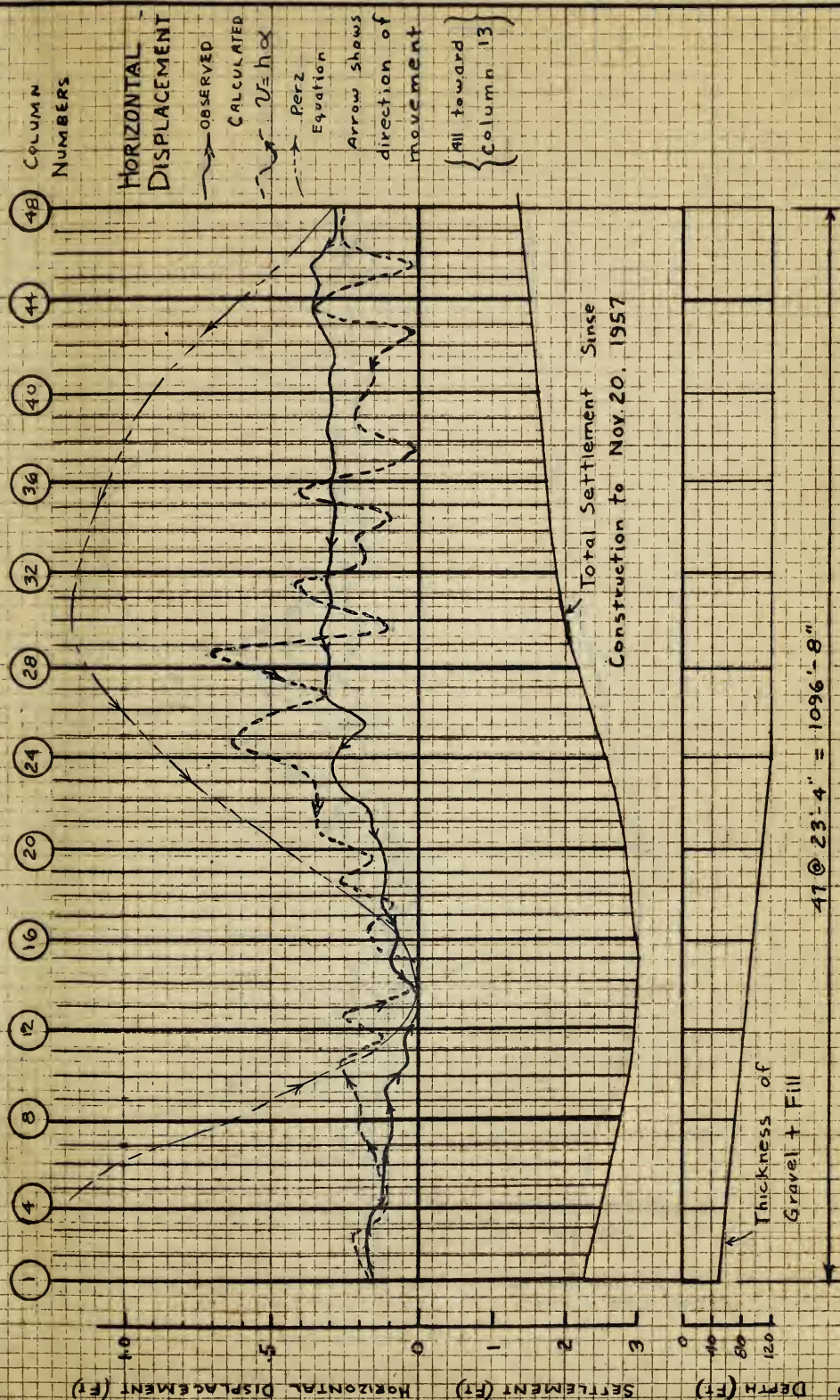
1. The maximum sinking is in the middle of the trough. Here there is no shifting.
2. All the shifting is directed to the center of the excavation. The maximum shift is at that point where no tension and compression occurs; here is the point without stress and the changing point of curvature as well as the steepest dipping in the course of the trough.
3. The region with the maximum tension lies near the outer edge of the trough.
4. The region with the maximum compression lies near the inner edges of the trough.
5. The sum of the tensions is equal to the sum of the compressions, the total sum being zero.

(After Reilemann)

FIGURE 21

MINE SUBSIDENCE CURVE





**NOTE:**  
 Curves give horizontal movement of point at ground surface.  
 Observed curve based on measurements at top of concrete column and slope of concrete column to ground.  
 Movement of column 13 assumed = zero.

**FIGURE G4**  
**COLUMN LINE G**  
**HORIZONTAL DISPLACEMENT**

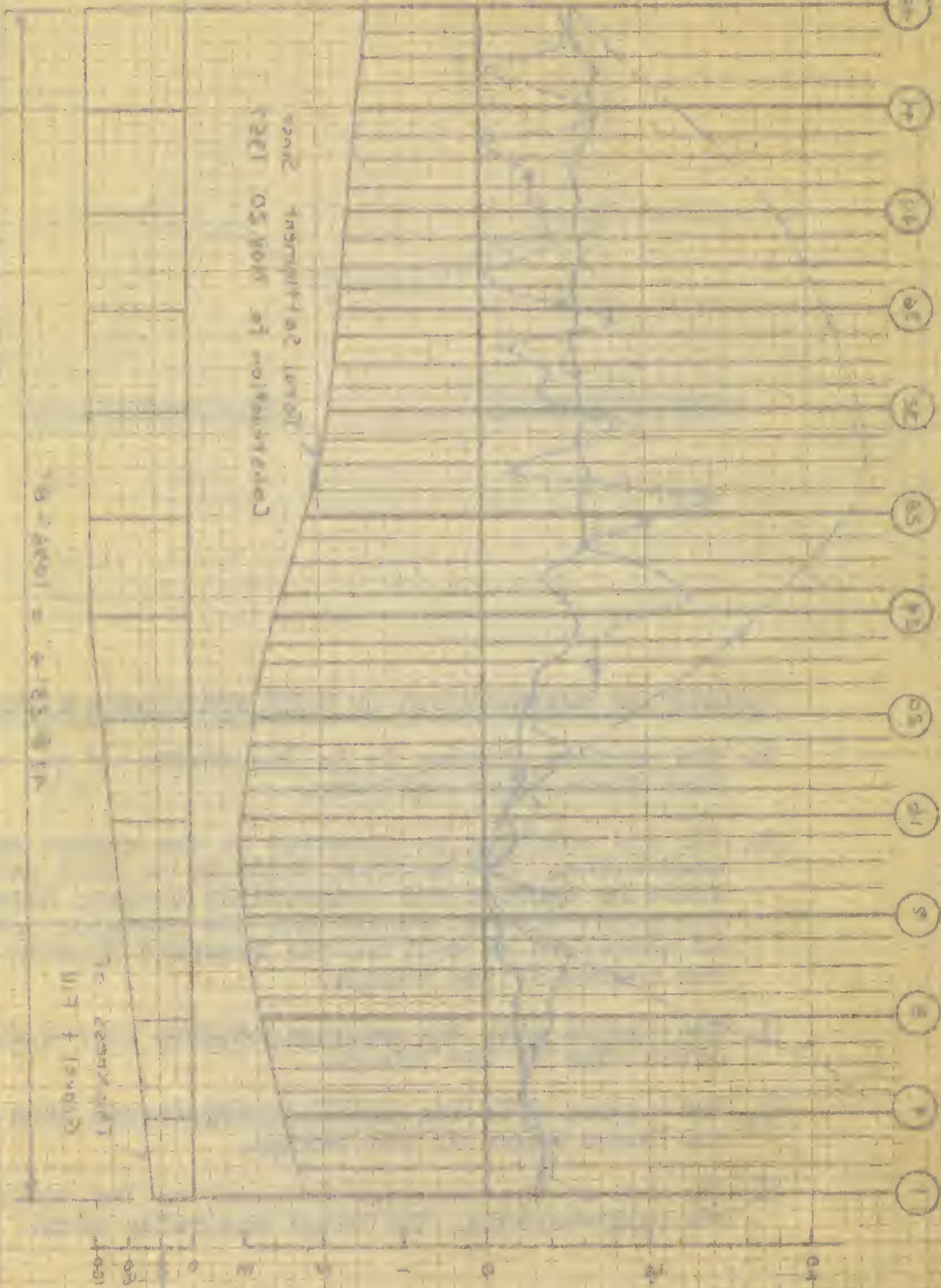


# ГОРИЗОНТАЛЬНЫЙ ПРОФИЛЬ

ГОРИЗОНТАЛЬНЫЙ  
ПРОФИЛЬ

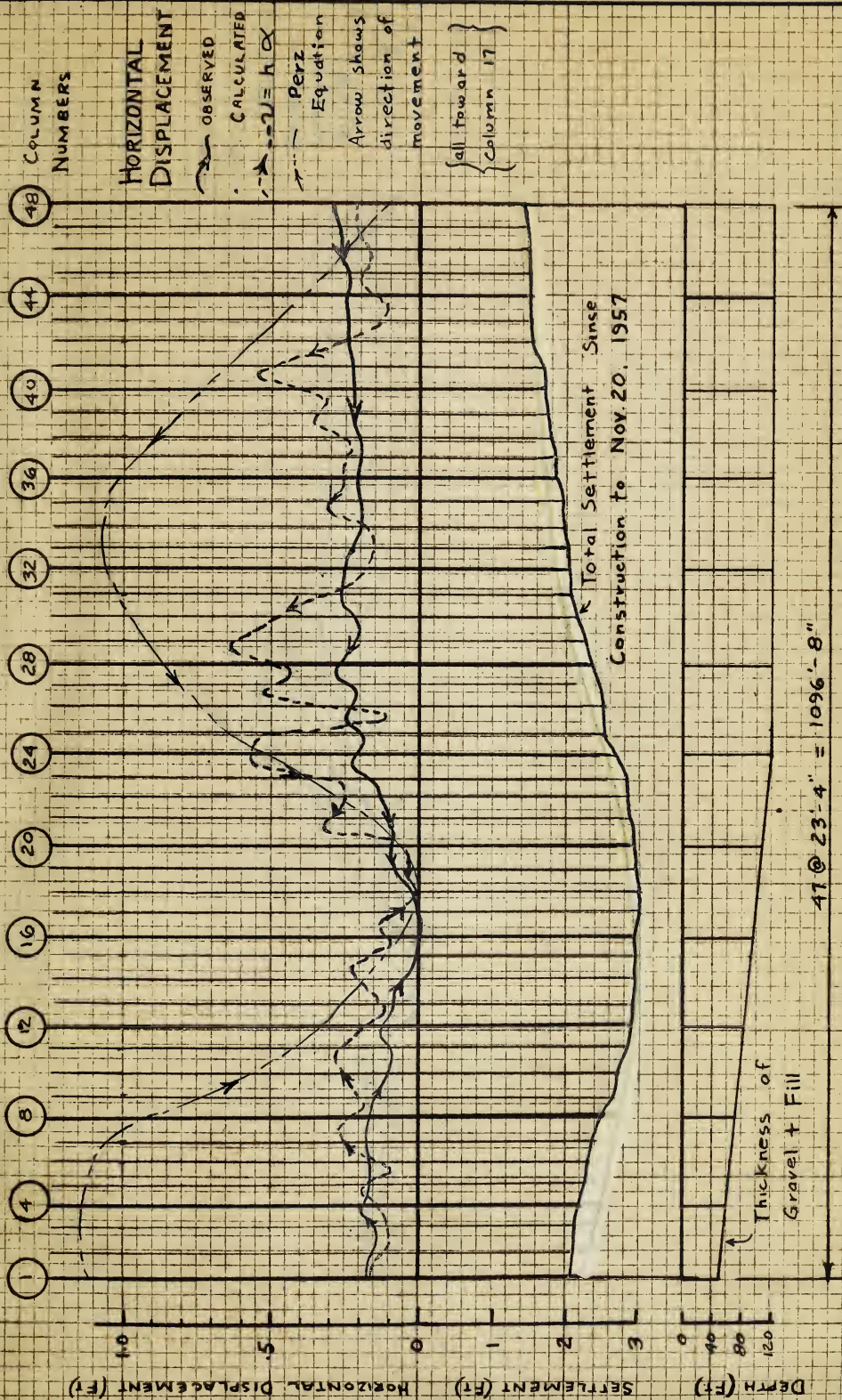
ПРОФИЛЬ

Указание: Водяная линия (голубая) показывает положение воды в скважине. Глубина воды в скважине 10 м. Водяная линия (голубая) показывает положение воды в скважине. Глубина воды в скважине 10 м.



ГЛУБИНА (М)      ПРОФИЛЬ      ГОЛУБАЯ ЛИНИЯ





**NOTE**

Curves give horizontal movement of point at ground surface.

Observed curve based on measurements at top of concrete column and slope of concrete column to ground.

Movement of column 17 assumed = Zero

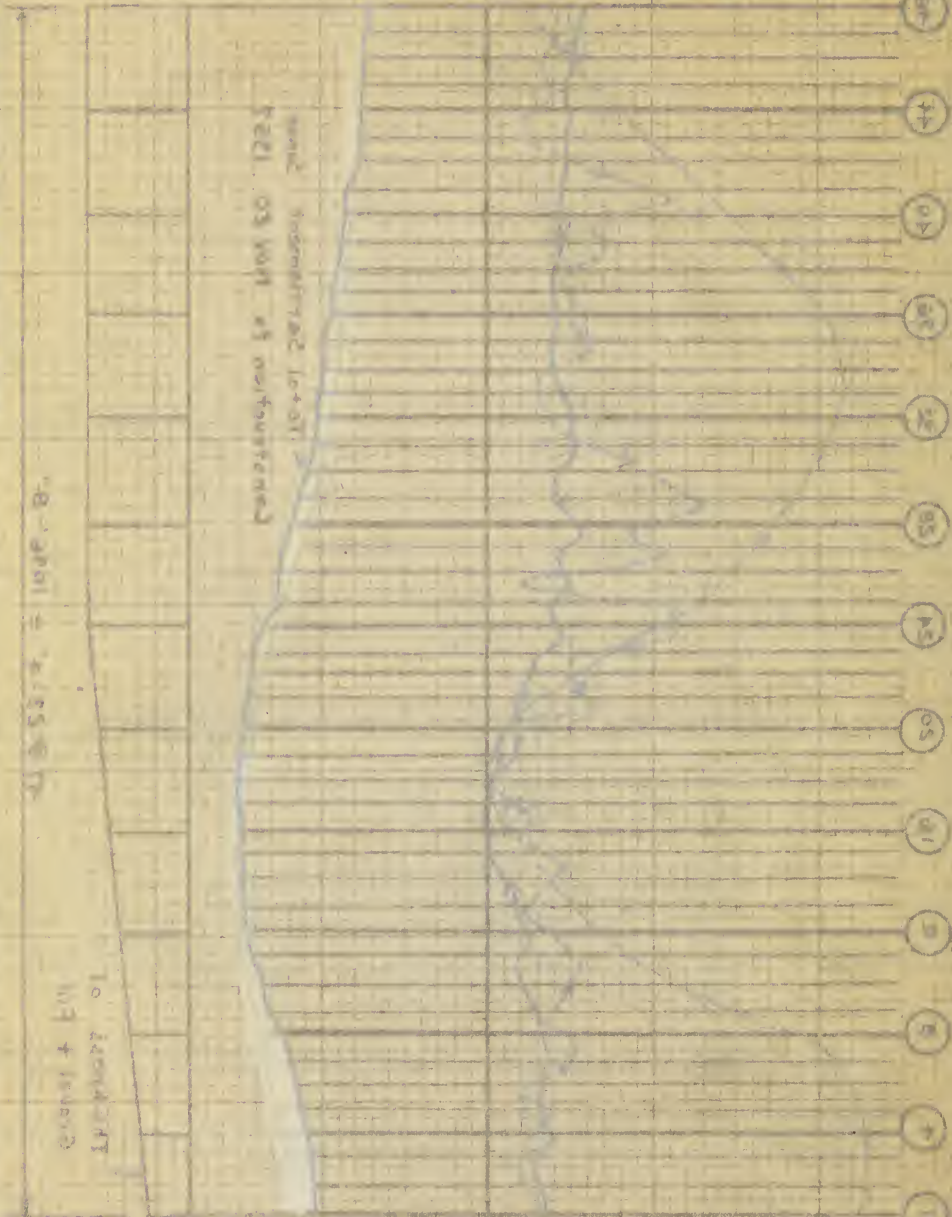
**FIGURE 65**

# **COLUMN LINE H** **HORIZONTAL DISPLACEMENT**



# TEMPERATURE DISPLACEMENT CORRELATION TIME

STATION 100



TEMPERATURE DISPLACEMENT CORRELATION TIME (HOURS)

DISTANCE (MILES)

STATION 100

- 1
- 2
- 3
- 4
- 5
- 6
- 7
- 8
- 9
- 10
- 11
- 12
- 13
- 14
- 15
- 16
- 17
- 18
- 19
- 20
- 21
- 22
- 23
- 24
- 25
- 26
- 27
- 28
- 29
- 30
- 31
- 32
- 33
- 34
- 35
- 36
- 37
- 38
- 39
- 40
- 41
- 42
- 43
- 44
- 45
- 46
- 47
- 48
- 49
- 50
- 51
- 52
- 53
- 54
- 55
- 56
- 57
- 58
- 59
- 60
- 61
- 62
- 63
- 64
- 65
- 66
- 67
- 68
- 69
- 70
- 71
- 72
- 73
- 74
- 75
- 76
- 77
- 78
- 79
- 80
- 81
- 82
- 83
- 84
- 85
- 86
- 87
- 88
- 89
- 90
- 91
- 92
- 93
- 94
- 95
- 96
- 97
- 98
- 99
- 100



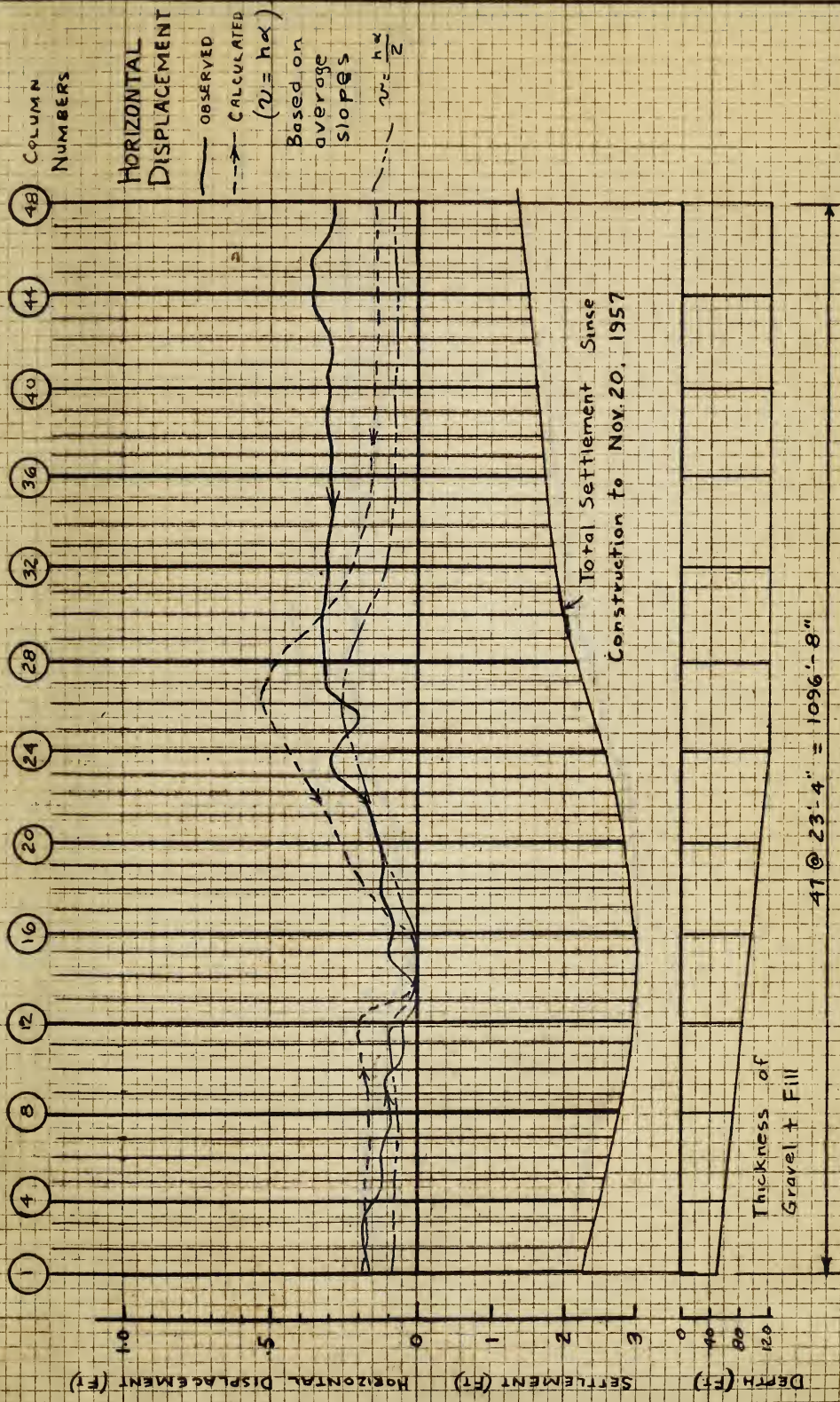


FIGURE 66

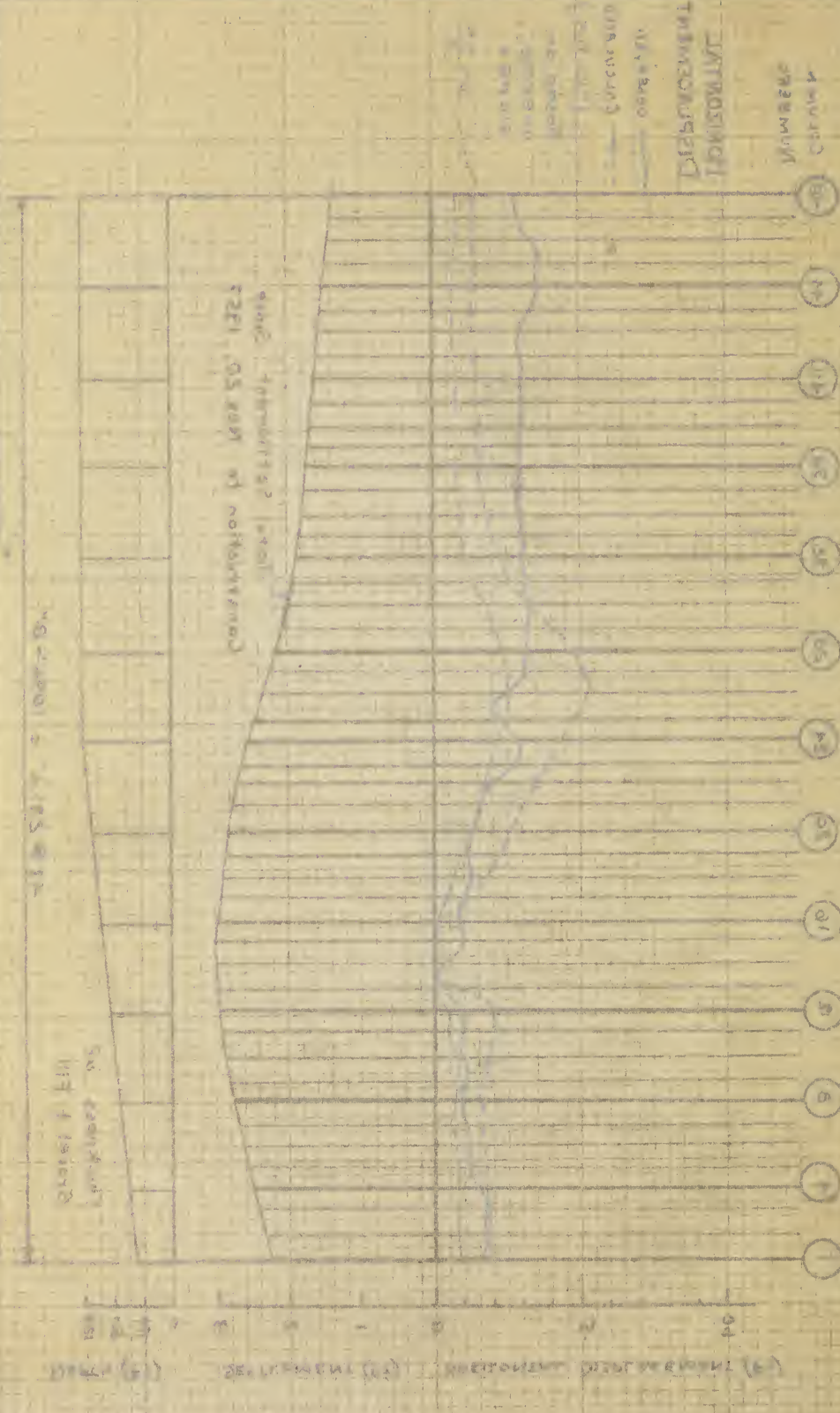
COLUMN LINE G

HORIZONTAL DISPLACEMENT

AVERAGE VALUES



# HORIZONTAL DISTANCE COLUMN TIME



HORIZONTAL DISTANCE (ft)      COLUMN TIME (min)



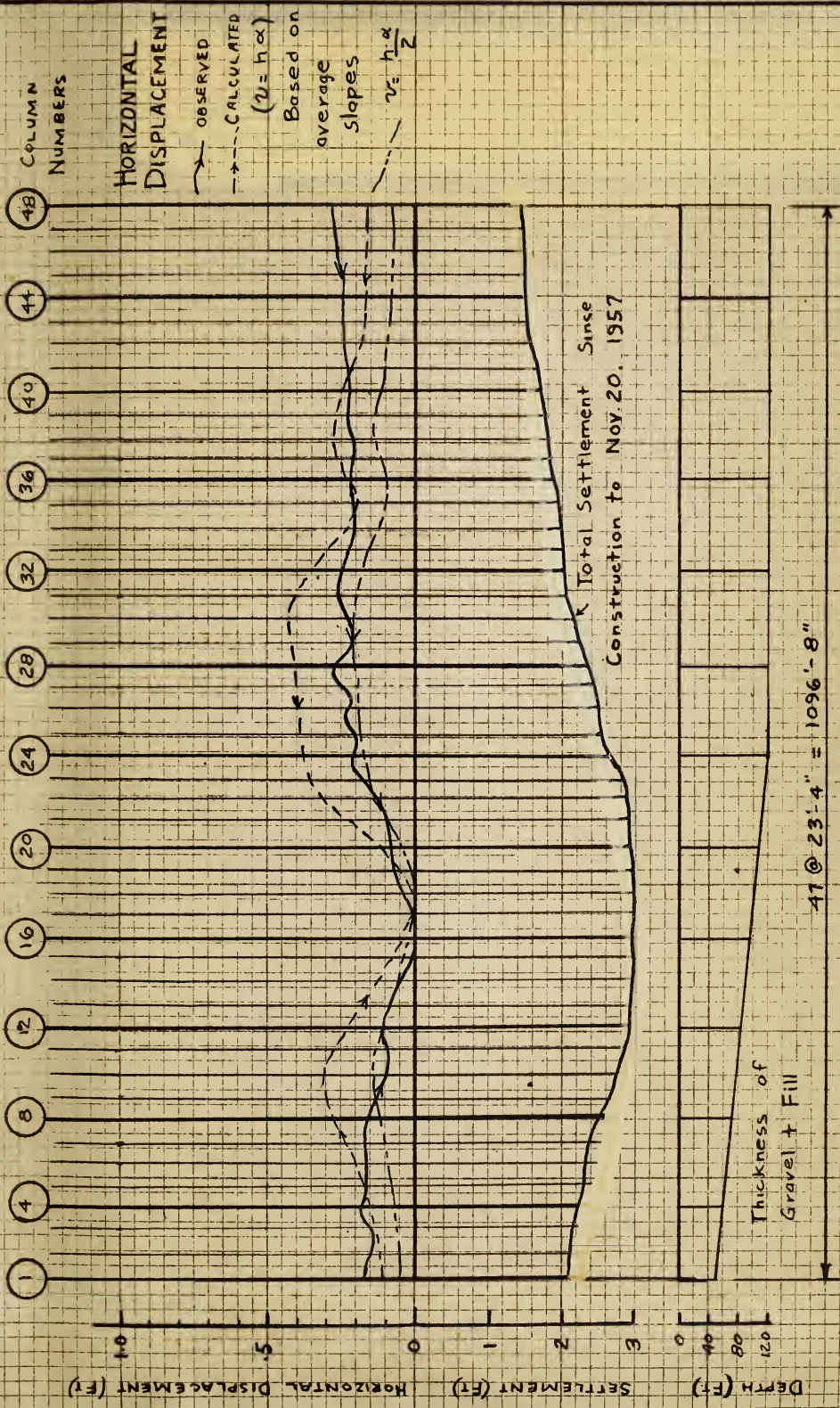


FIGURE 67

COLUMN LINE H

HORIZONTAL DISPLACEMENT

AVERAGE VALUES



# HORIZONTAL DISTANCE CORRECTION

1000000



1000000

1000000

1000000

1000000

1000000

1000000

1000000

1000000

1000000

1000000

1000000

1000000

1000000

1000000

1000000

1000000

1000000

1000000

1000000





06'

05'

04'

03'

02'

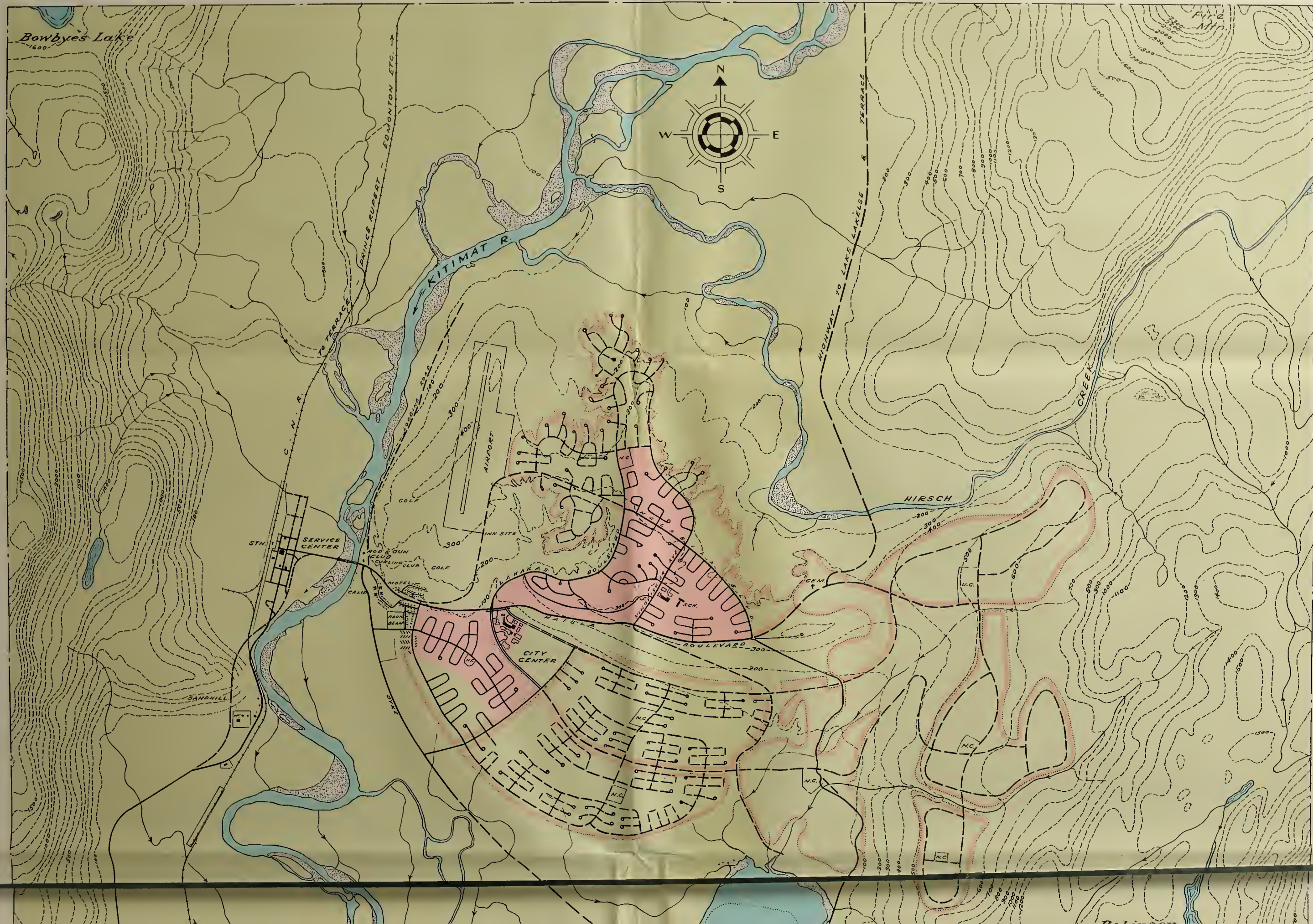
06'

05'

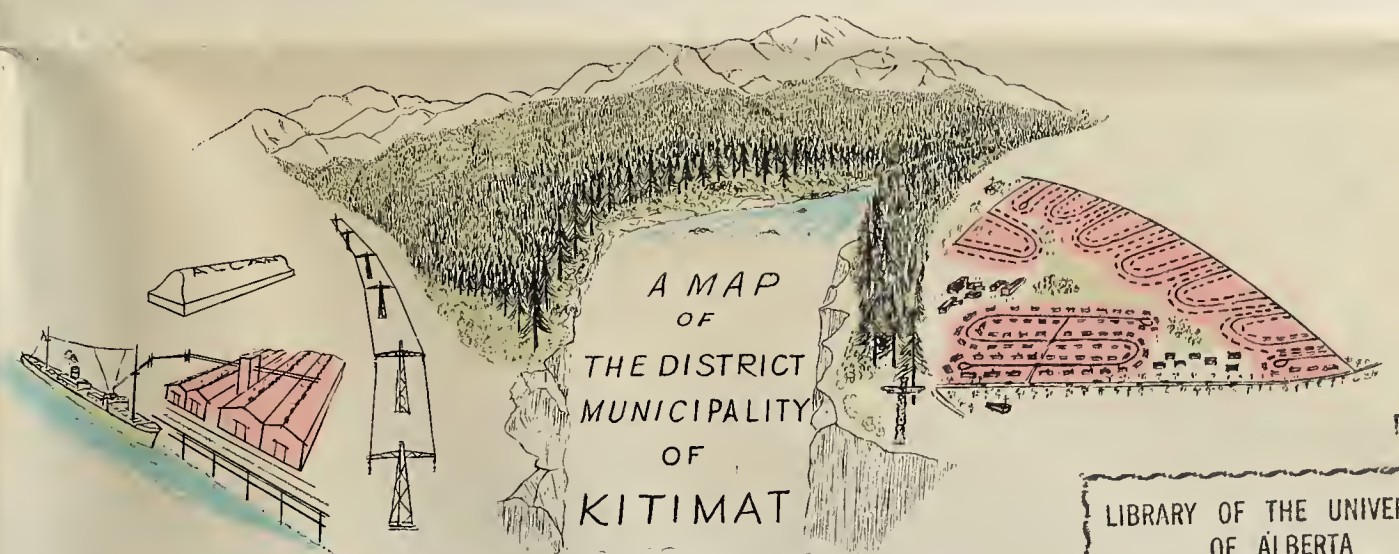
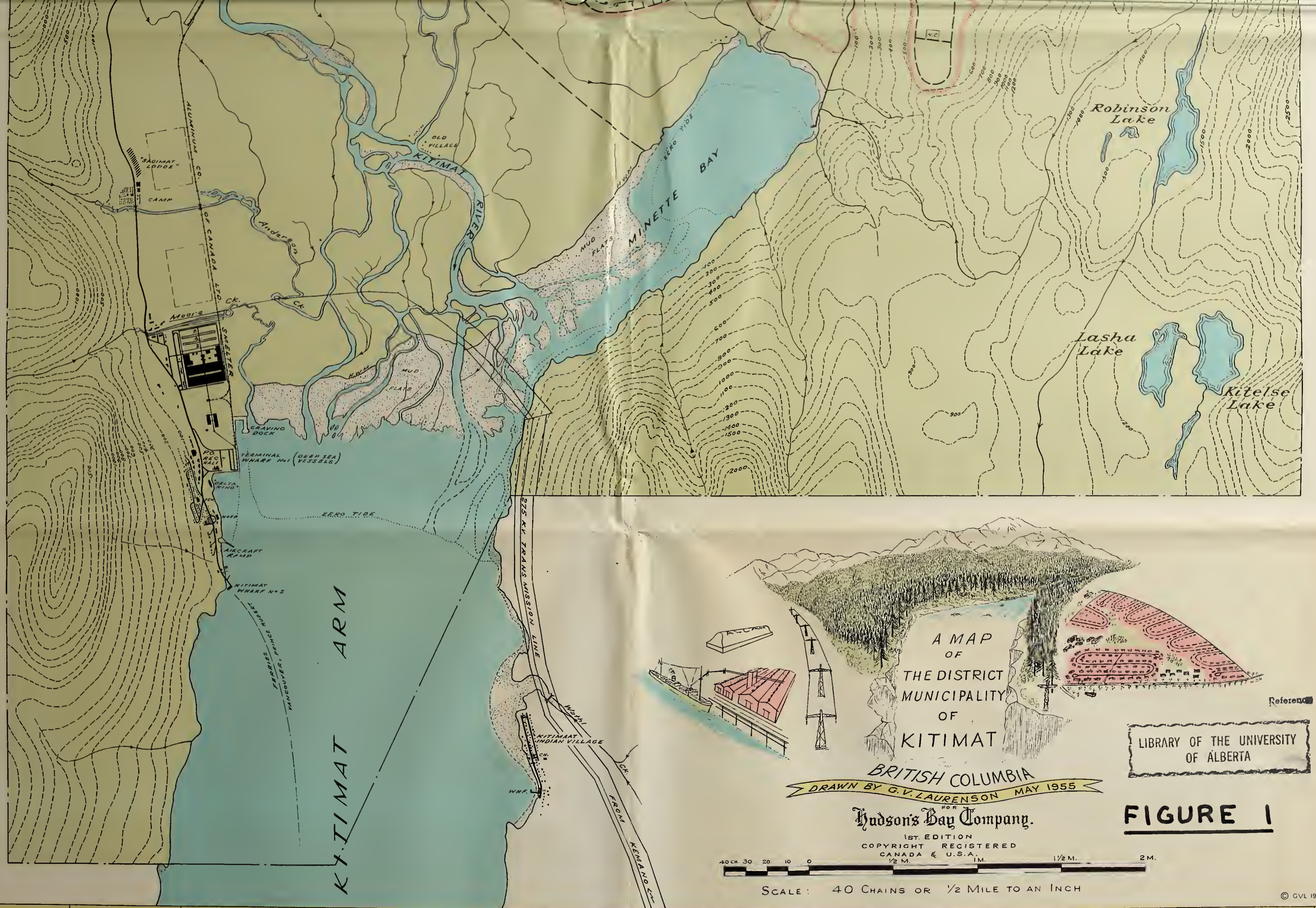
04'

03'

02'







BRITISH COLUMBIA  
DRAWN BY G.V. LAURENSEN MAY 1955

Hudson's Bay Company.

1ST. EDITION  
COPYRIGHT REGISTERED  
CANADA & U.S.A.

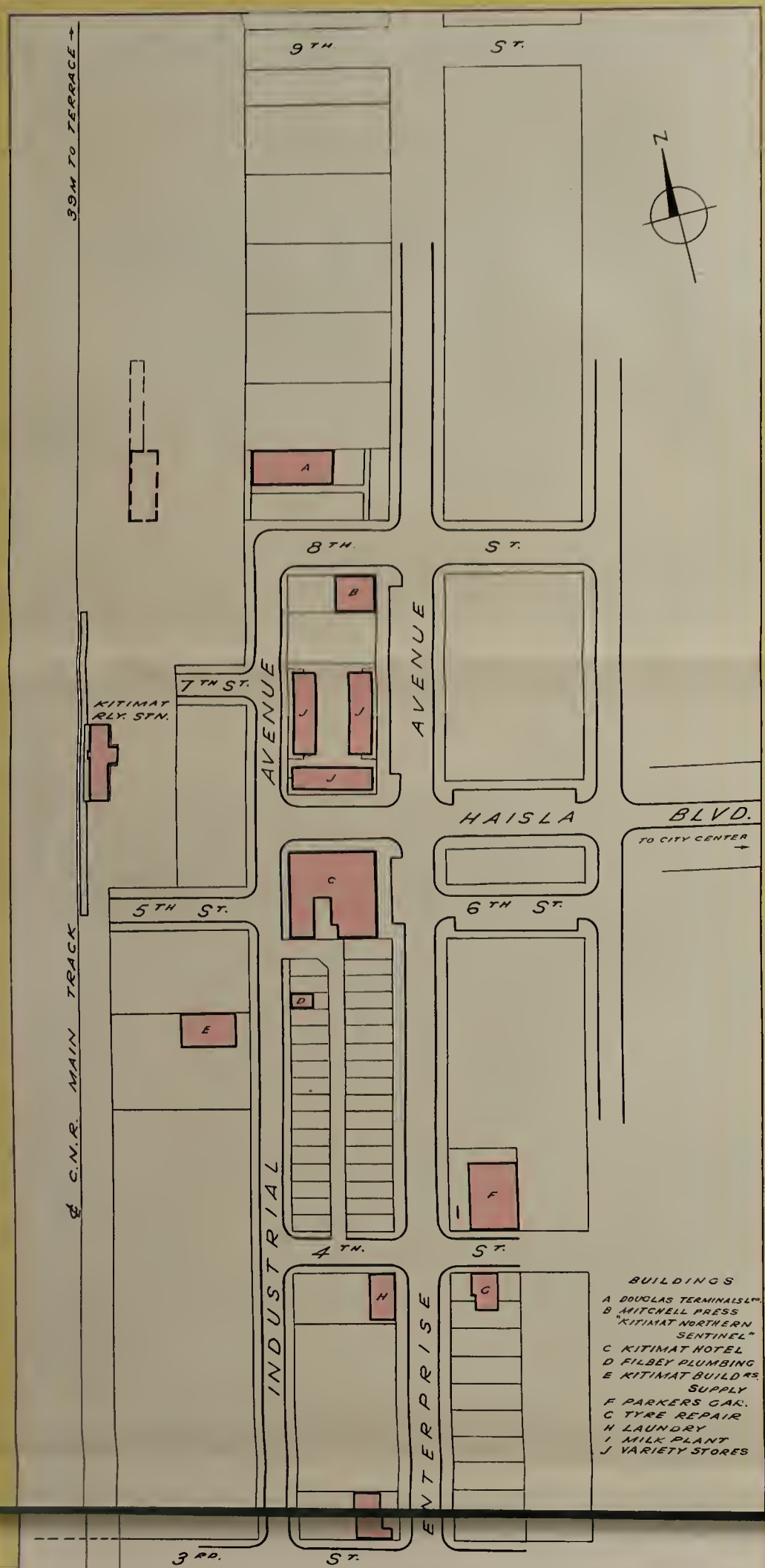


SCALE: 40 CHAINS OR 1/2 MILE TO AN INCH

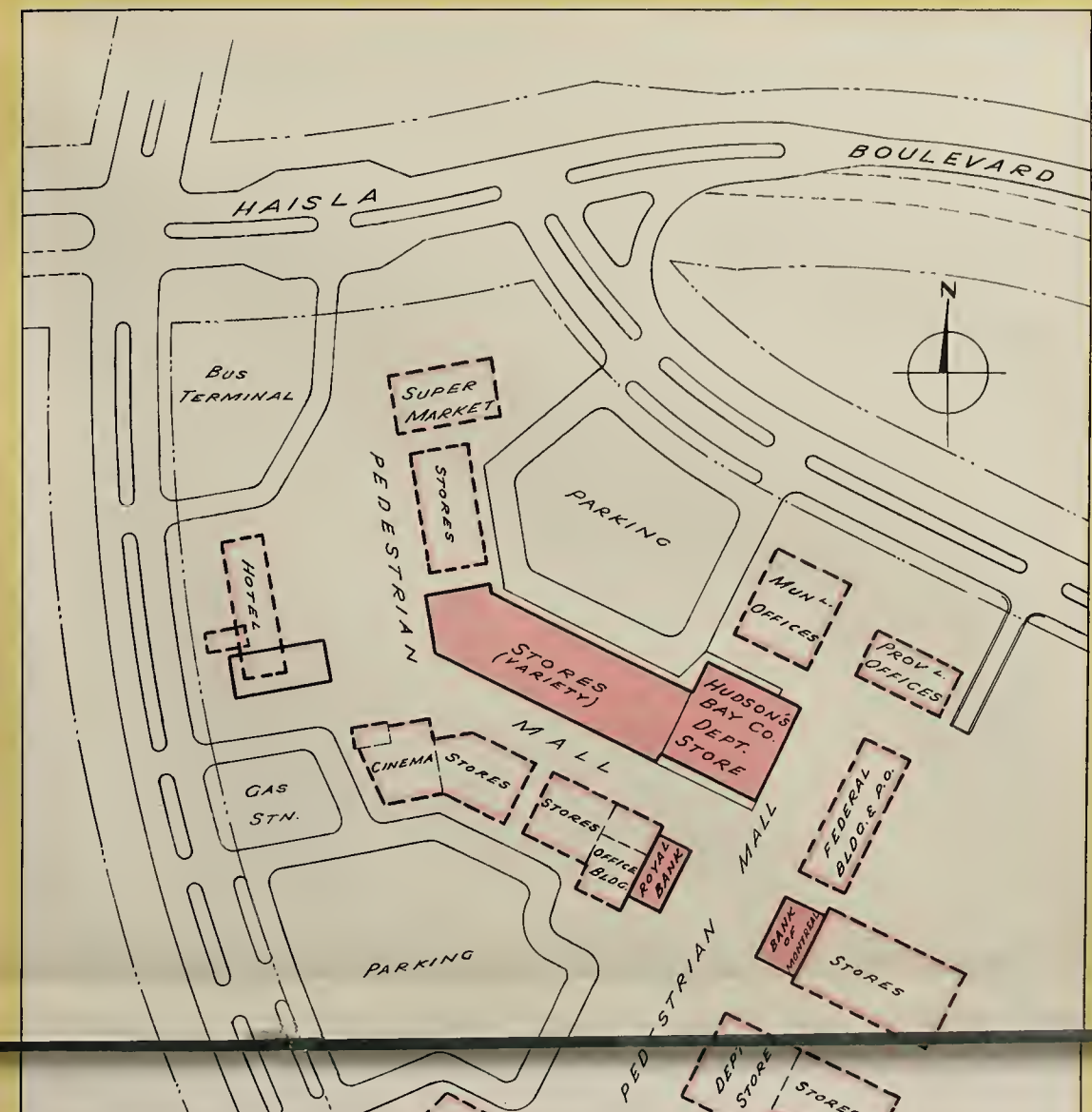
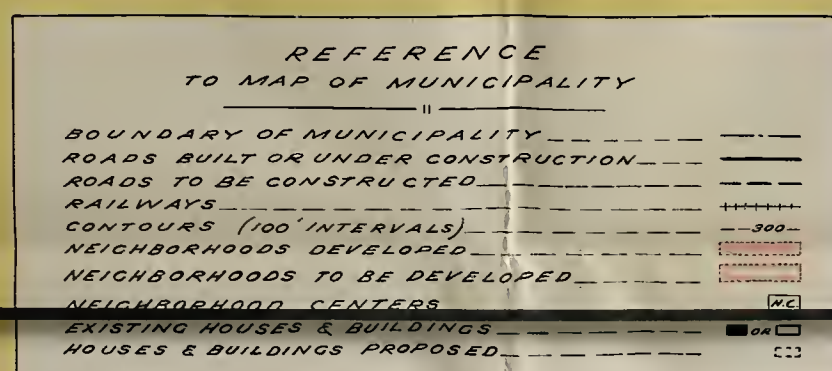
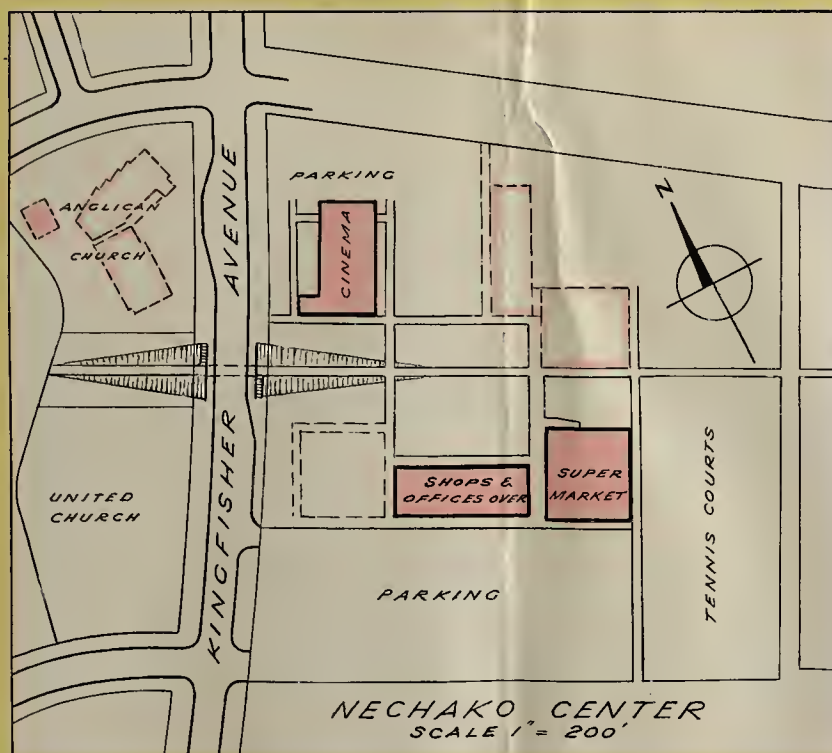
LIBRARY OF THE UNIVERSITY  
OF ALBERTA

FIGURE 1

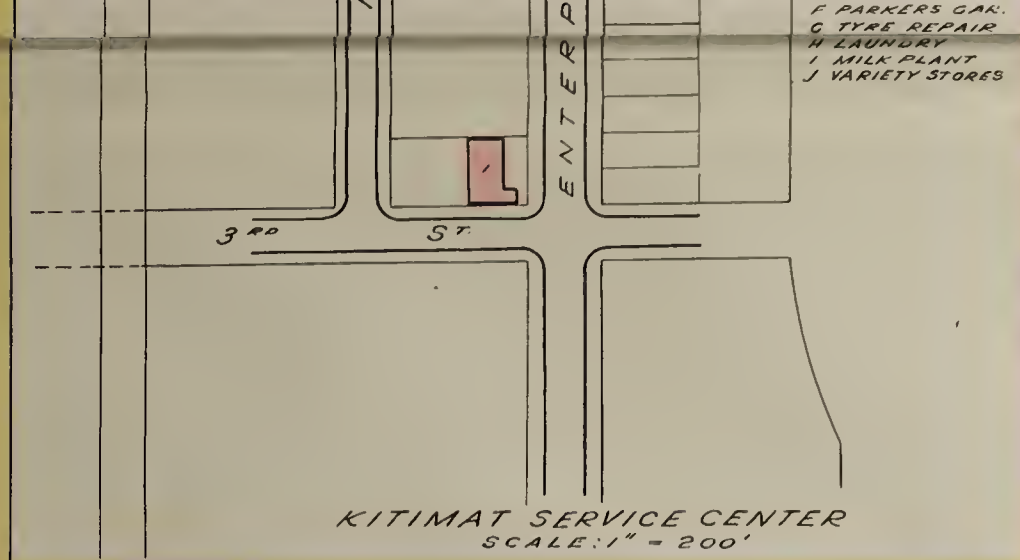




- BUILDINGS**
- A DOUGLAS TERMINALS
  - B MITCHELL PRESS
  - C KITIMAT HOTEL
  - D FILBEY PLUMBING
  - E KITIMAT BUILDINGS
  - F PARKERS GAR.
  - G TYRE REPAIR
  - H LAUNDRY
  - I MILK PLANT
  - J VARIETY STORES







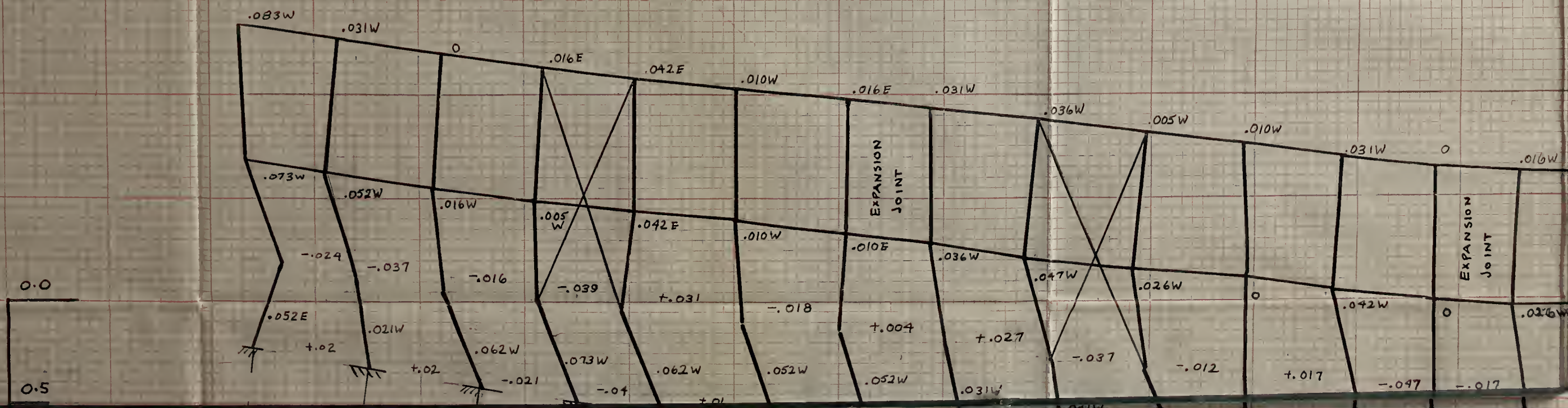
ROADS BUILT OR UNDER CONSTRUCTION  
 ROADS TO BE CONSTRUCTED  
 RAILWAYS  
 CONTOURS (100' INTERVALS)  
 NEIGHBORHOODS DEVELOPED  
 NEIGHBORHOODS TO BE DEVELOPED  
 NEIGHBORHOOD CENTERS  
 EXISTING HOUSES & BUILDINGS  
 HOUSES & BUILDINGS PROPOSED

POPULATION  
 MARCH 1953 - 2040      MARCH 1955 - 4190

NEIGHBORHOOD 'A' or "NECHAKO"  
 SCALE: 1" = 600'









| DISTANCE &<br>MEASURE |
|-----------------------|
| DATE                  |
| COLUMN                |
| G 6                   |
| G 12                  |
| G 18                  |
| G 24                  |
| G 30                  |
| G 36                  |
| G 42                  |







# LEGEND

23'-4"

DESIGN DISTANCE BETWEEN

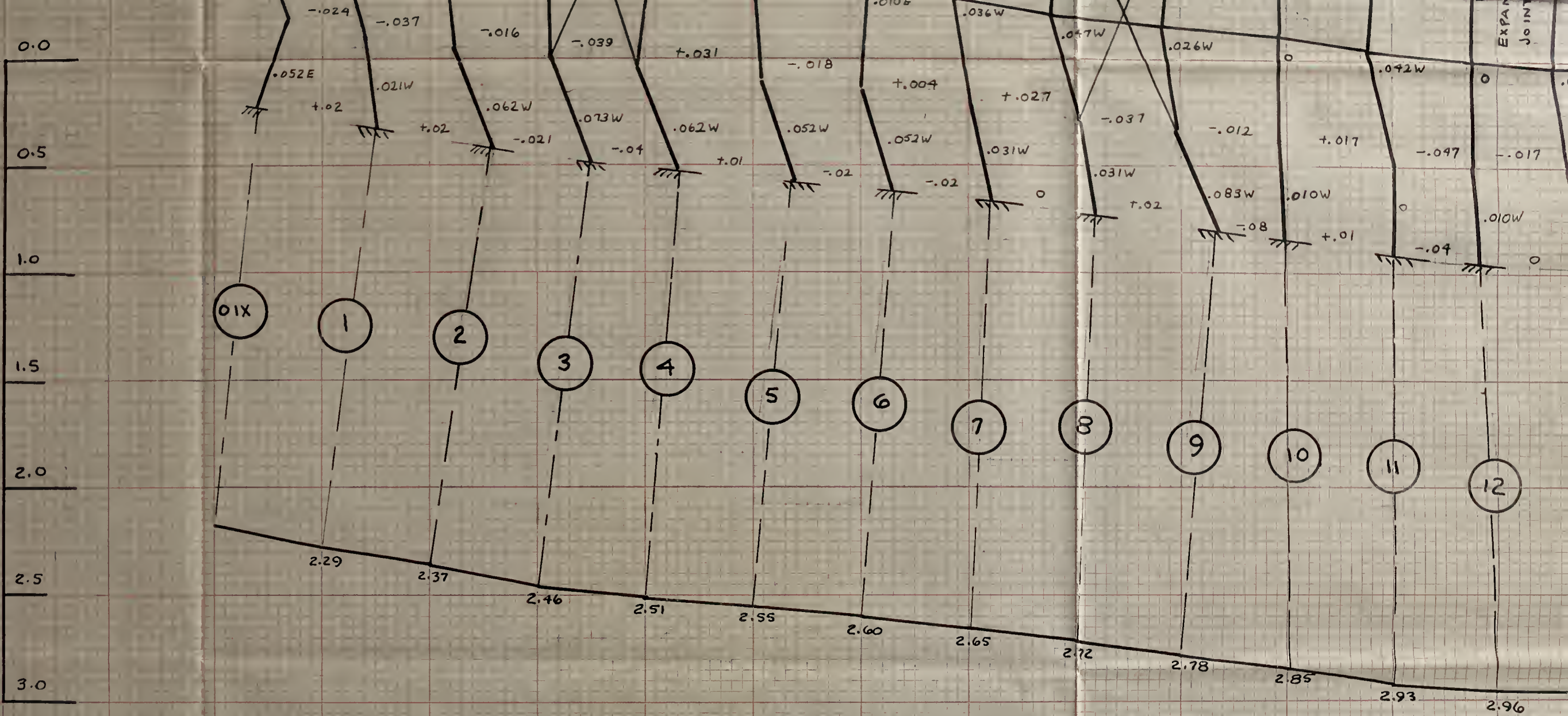
{ DEVIATION FROM DESIGN DISTANCE  
AT STEEL BASE PLATE -

{ DEVIATION FROM DESIGN DISTANCE  
AT GROUND SURFACE -

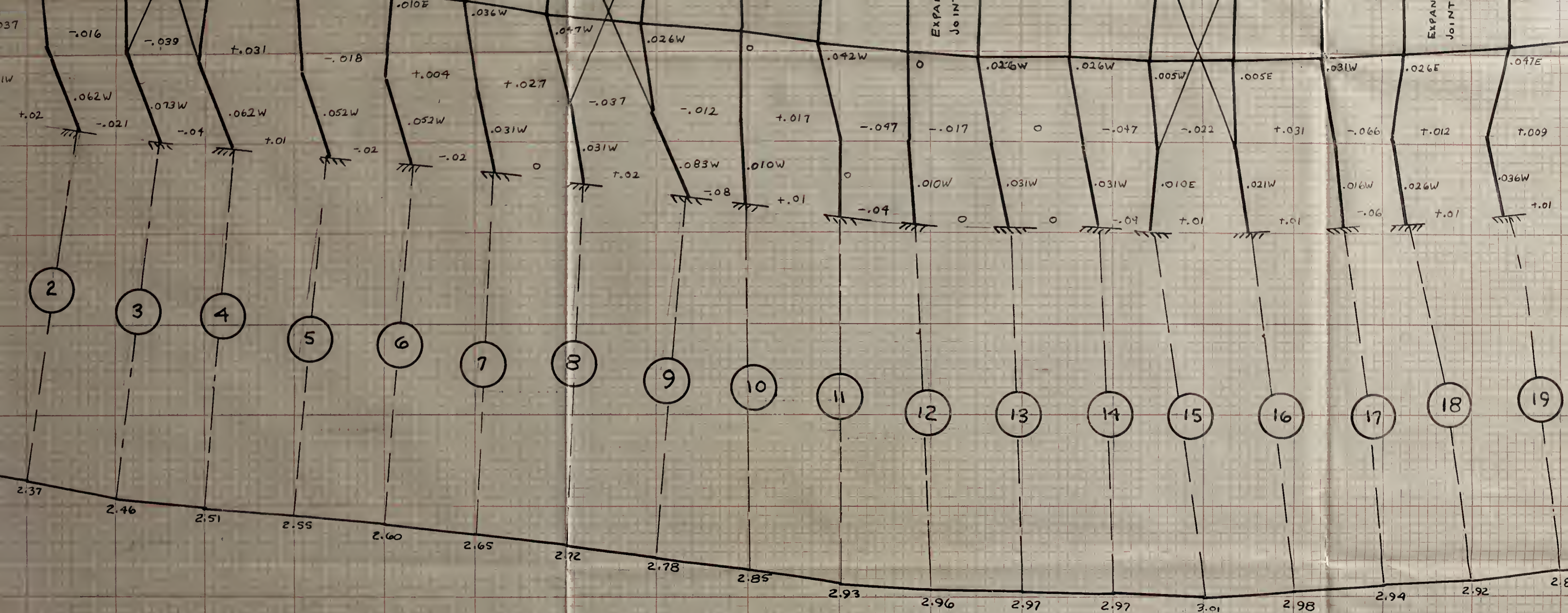




SETTLEMENT - FT



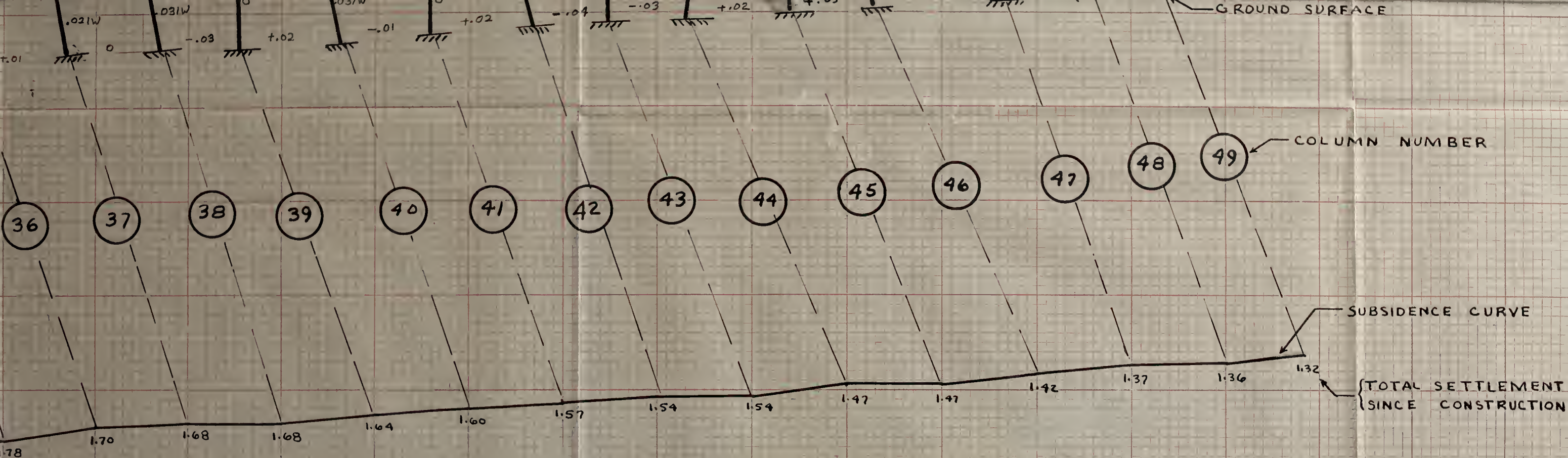












MAY 1, 1953  
MAY 15, 1953

FIGURE 68

LIBRARY OF THE UNIVERSITY OF ALBERTA

COLUMN LINE G

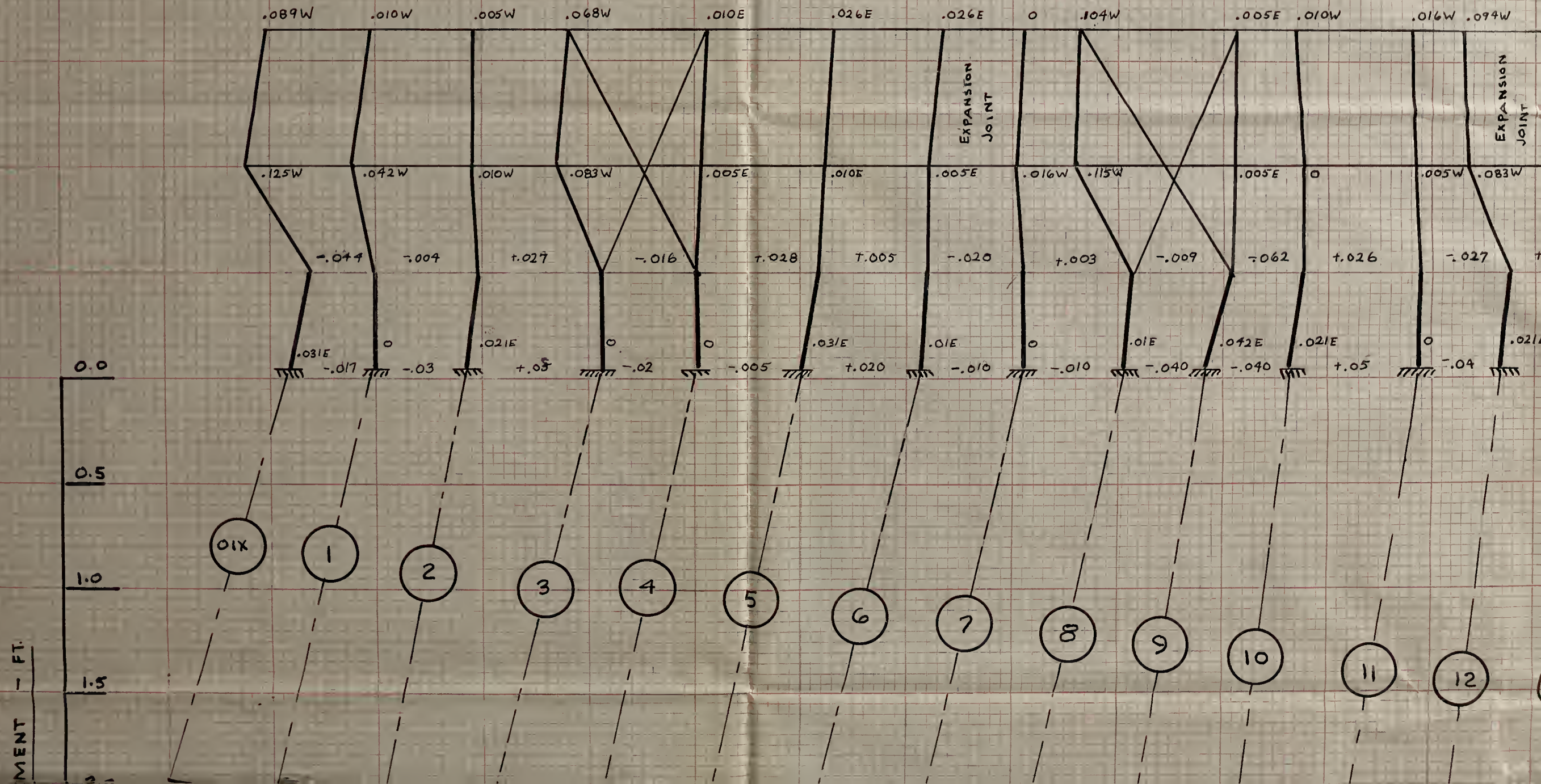
HORIZONTAL AND VERTICAL

MOVEMENT

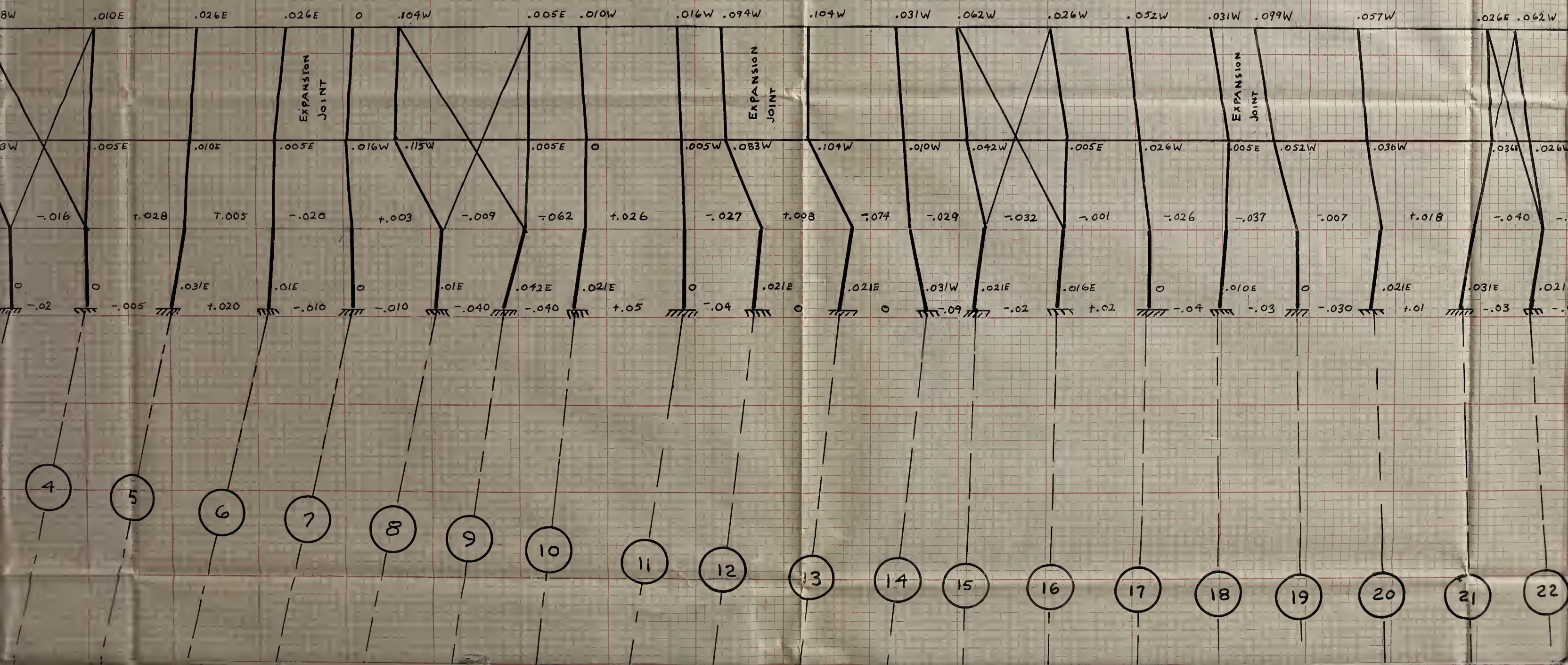
FROM

MAY 1953 TO DECEMBER 1957

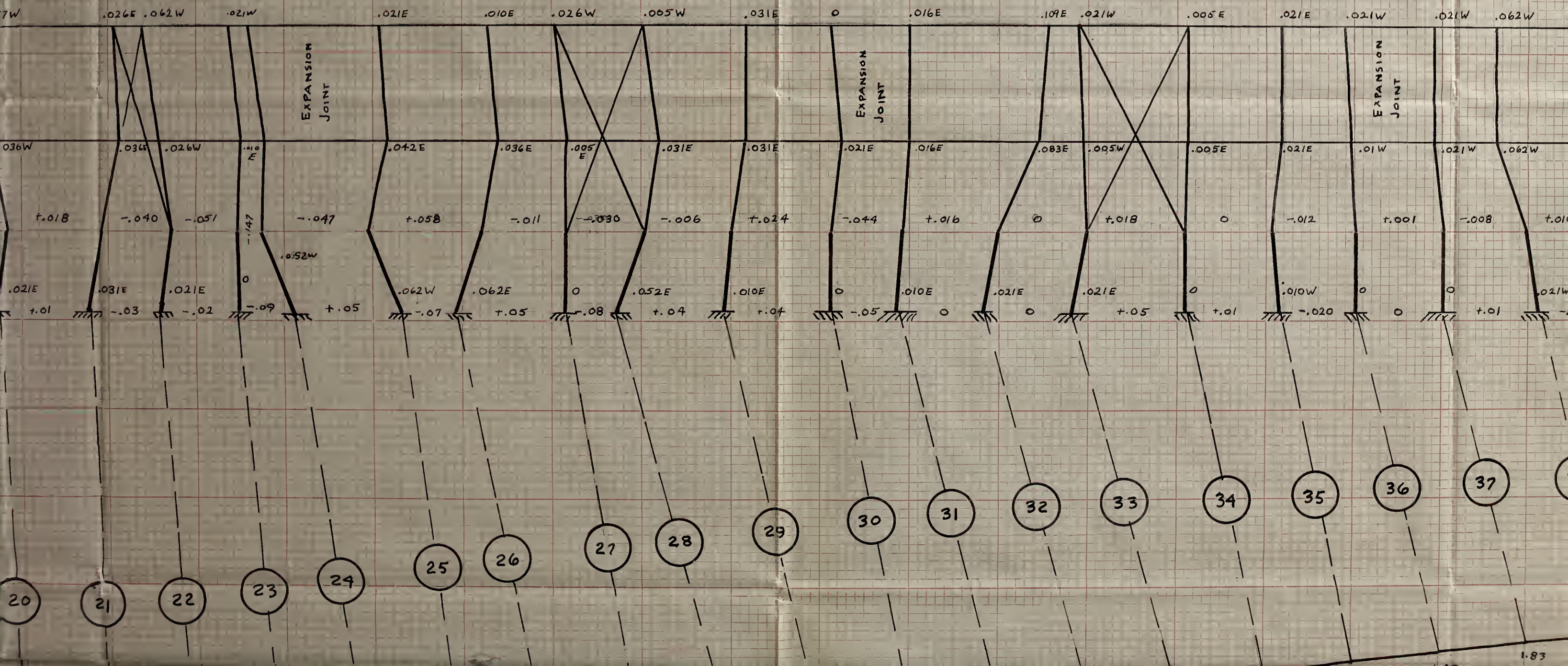














# LEGEND

23'-4" DESIGN DISTANCE BETWEEN COLUMNS 1 TO 48

{ DEVIATION FROM DESIGN DISTANCE BETWEEN COLUMNS  
AT STEEL BASE PLATE — MEASURED

{ DEVIATION FROM DESIGN DISTANCE BETWEEN COLUMNS  
AT GROUND SURFACE — COMPUTED

{ LEAN OF STEEL COLUMN  
MEASURED BETWEEN TOP &  
STEEL BASE PLATE  
Approx. 23'

{ LEAN OF STEEL COLUMN  
MEASURED BETWEEN CRANE  
RAIL BEAM & STEEL BASE  
PLATE Approx. 9'

CONCRETE COLUMN

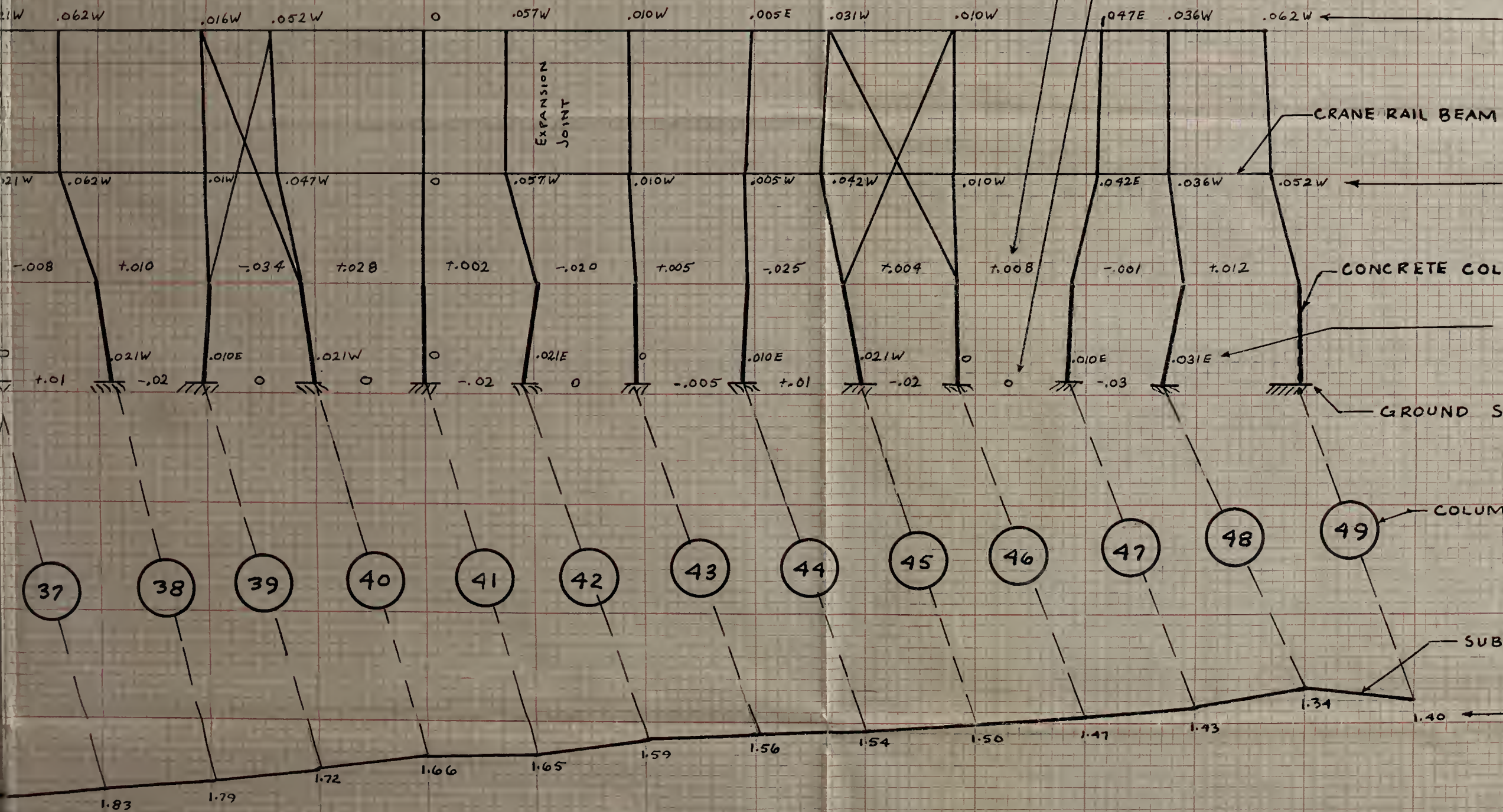
{ LEAN OF CONCRETE COLUMN  
MEASURED BETWEEN TOP &  
7.8' BELOW

GROUND SURFACE

COLUMN NUMBER

SUBSIDENCE CURVE

{ TOTAL SETTLEMENT  
SINCE CONSTRUCTION





SETTLEMENT - FT.

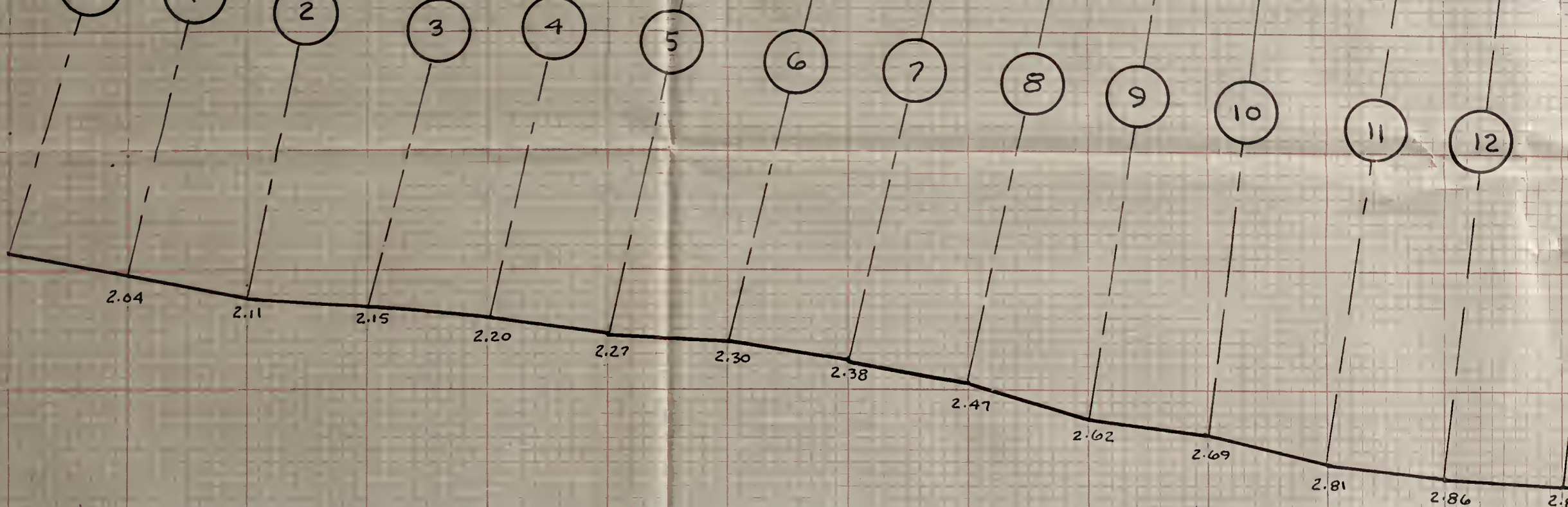
1.0

1.5

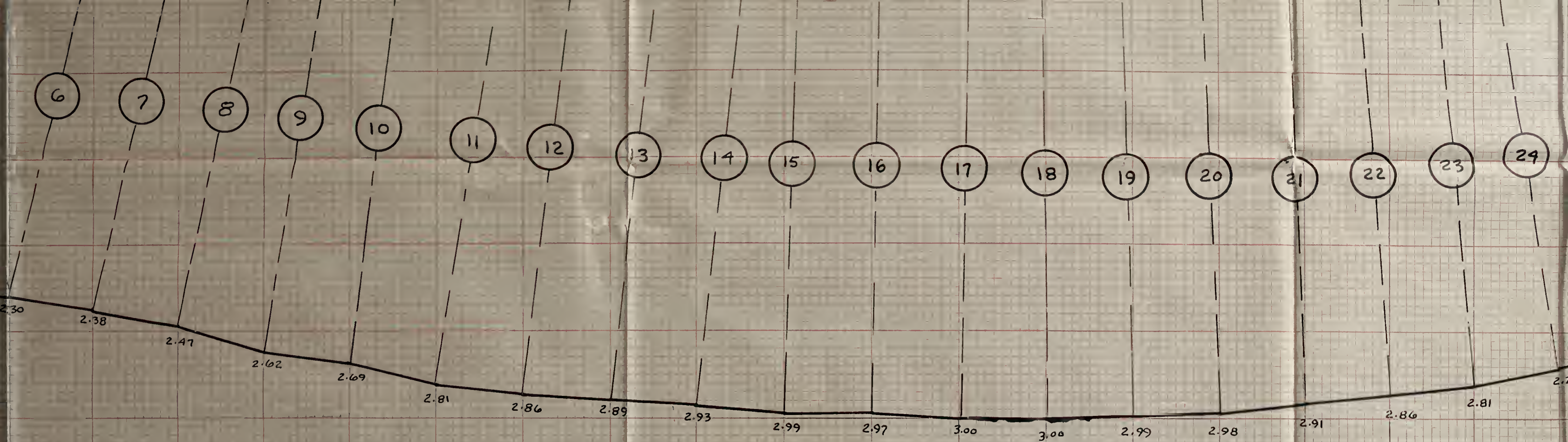
2.0

2.5

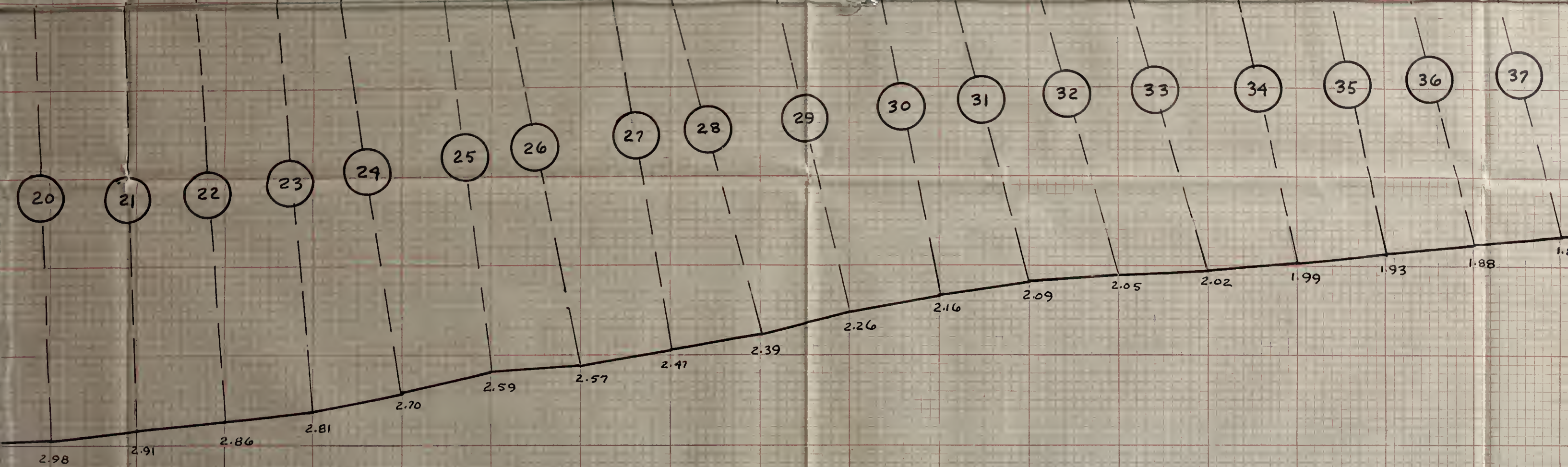
3.0







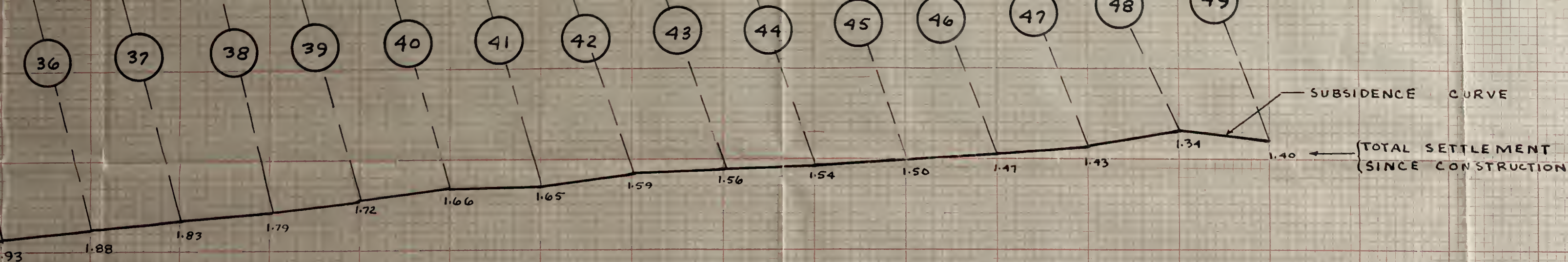




| DISTANCE BETWEEN ENDS OF CRANE RAIL BEAMS<br>MEASURED AT EXPANSION JOINTS |                          |         |  |         |
|---|--------------------------|---------|--|---------|
| DATE  | DEC. 6, 1957<br>POWER ON |         | DEC 13, 1957.<br>POWER OFF<br>TEMPERATURES 10 +<br>15°F LOWER THAN<br>DEC. 6, 1957 |         |
|   | COLUMN                   | OPENING | TEMP °F  | OPENING |
|   | H 6                      | 7/16"   | 53°  | 7/16"   |
|   | H 12                     | 5/16"   | 55°  | 5/16"   |
|   | H 18                     | 1/2"    | 51°  | 1/2"    |
|   | H 24                     | 3/8"    | 51°  | 5/8"    |
|   | H 30                     | 13/16"  | 56°  | 1 5/16" |
|   | H 36                     | 5/8"    | 54°  | 5/8"    |
|   | H 42                     | 1 1/4"  | 55°  | 9/16"   |

SCALES  
 DESIGN CO  
 COLUMN M  
 COLUMN  
 SETTLEM  
 COLUMN





#### SCALES

|                                 |             |
|---------------------------------|-------------|
| DESIGN COLUMN SPACING           | 1" = 23'-4" |
| COLUMN MOVEMENT AND COLUMN LEAN | 1" = 0.20'  |
| SETTLEMENT                      | 1" = 0.5'   |
| COLUMN HEIGHT                   | 1" = 10'    |

#### NOTE

COLUMNS H1 TO H28 SET MAY 1, 1953  
 COLUMNS H29 TO H49 SET MAY 15, 1953

**FIGURE 69**  
**COLUMN LINE H**  
**HORIZONTAL AND VERTICAL**  
**MOVEMENT**  
**FROM**  
**MAY 1953 TO DECEMBER 1957**





NOT TO BE

Foundation Settlement Problems  
at the  
Aluminum Company of Canada Smelter  
Kitimat, British Columbia

by  
Kenneth L. Lee  
April 1958



